Technical Report Documentation Page

1. Report No.	2. Government Accession No.	3. Recipient's Catalog No.
FHWA/RD-86/045	PB88 188313/AS	

4. Title and Subtitle	5. Report Date
WEIGH-IN-MOTION AND RESPONSE STUDY OF FOUR INSERVICE BRIDGES	October 1987
	6. Performing Organization Code

7. Author's)	8. Performing Organization Report No.
J. H. Daniels, J. W. Wilson, B. T. Yen, L. Y. Lai, R. Abbaszadeh	490.3

9. Performing Organization Name and Address	10. Work Unit No. (TRAIS)
Department of Civil Engineering Fritz Engineering Laboratory, Bldg. No. 13 LEHIGH UNIVERSITY Bethlehem, PA 18015	NCP#3D261032 FCP #35K2-112
	11. Contract or Grant No.
	DTFH61-83-C-00091
	13. Type of Report and Period Covered

12. Sponsoring Agency Name and Address	
Federal Highway Administration Office of Engineering and Highway Operations RD & T 6300 Georgetown Pike McLean, VA 22101	Final Report Sept. 1983 – Mar. 1986
	14. Sponsoring Agency Code
	HNR-10

15. Supplementary Notes

FHWA contract manager: Mr. Harold Bosch (HNR-10)

16. Abstract

This report presents the results of a 30-month investigation at Lehigh University during which an FHWA WIM system was redesigned and used to acquire and process simultaneous truck weight plus bridge response data from 19,402 trucks crossing 4 inservice bridges in Pennsylvania. The new system is designated the WIM+RESPONSE system in the report.

The WIM+RESPONSE system is capable of acquiring and processing data to provide information on simultaneous bridge loading and response including GVW and stress range distributions, strain rates, maximum stresses, load distribution, and dynamic effects.

Detailed information is provided in this report on GVW distributions for the four inservice bridges plus stress range distributions, strain rates, and maximum stresses at 16 locations on each of the 4 bridges. Girder stresses are compared with AASHTO design stresses and with stresses from a detailed finite element analysis of the superstructure.

17. Key Words	18. Distribution Statement
Weigh-in-motion; Bridge loading; Stress range; Strain rate; Maximum stress; Stress history; Bridge response; WIM+ RESPONSE system; Bridge redundancy	No restriction. This document is available to the public through the National Technical Information Service, Springfield, Virginia 22161

19. Security Classif. (of this report)	20. Security Classif. (of this page)
Unclassified	Unclassified

Form DOT F 1700.7 (8-72)   Reproduction of completed page authorized

METRIC (SI*) CONVERSION FACTORS

APPROXIMATE CONVERSIONS TO SI UNITS

Symbol	When You Know	Multiply By	To Find	Symbol

LENGTH

Symbol	When You Know	Multiply By	To Find	Symbol
in	inches	2.54	millimetres	mm
ft	feet	0.3048	metres	m
yd	yards	0.914	metres	m
mi	miles	1.61	kilometres	km

AREA

Symbol	When You Know	Multiply By	To Find	Symbol
in²	square inches	645.2	millimetres squared	mm²
ft²	square feet	0.0929	metres squared	m²
yd²	square yards	0.836	metres squared	m²
mi²	square miles	2.59	kilometres squared	km²
ac	acres	0.395	hectares	ha

MASS (weight)

Symbol	When You Know	Multiply By	To Find	Symbol
oz	ounces	28.35	grams	g
lb	pounds	0.454	kilograms	kg
T	short tons (2000 lb)	0.907	megagrams	Mg

VOLUME

Symbol	When You Know	Multiply By	To Find	Symbol
fl oz	fluid ounces	29.57	millilitres	mL
gal	gallons	3.785	litres	L
ft³	cubic feet	0.0328	metres cubed	m³
yd³	cubic yards	0.0765	metres cubed	m³

NOTE: Volumes greater than 1000 L shall be shown in m³.

TEMPERATURE (exact)

Symbol	When You Know	Multiply By	To Find	Symbol
°F	Fahrenheit temperature	5/9 (after subtracting 32)	Celsius temperature	°C

APPROXIMATE CONVERSIONS TO SI UNITS

Symbol	When You Know	Multiply By	To Find	Symbol

LENGTH

Symbol	When You Know	Multiply By	To Find	Symbol
mm	millimetres	0.039	inches	in
m	metres	3.28	feet	ft
m	metres	1.09	yards	yd
km	kilometres	0.621	miles	mi

AREA

Symbol	When You Know	Multiply By	To Find	Symbol
mm²	millimetres squared	0.0016	square inches	in²
m²	metres squared	10.764	square feet	ft²
km²	kilometres squared	0.39	square miles	mi²
ha	hectares (10 000 m²)	2.53	acres	ac

MASS (weight)

Symbol	When You Know	Multiply By	To Find	Symbol
g	grams	0.0353	ounces	oz
kg	kilograms	2.205	pounds	lb
Mg	megagrams (1 000 kg)	1.103	short tons	T

VOLUME

Symbol	When You Know	Multiply By	To Find	Symbol
mL	millilitres	0.034	fluid ounces	fl oz
L	litres	0.264	gallons	gal
m³	metres cubed	35.315	cubic feet	ft³
m³	metres cubed	1.308	cubic yards	yd³

TEMPERATURE (exact)

Symbol	When You Know	Multiply By	To Find	Symbol
°C	Celsius temperature	9/5 (then add 32)	Fahrenheit temperature	°F

```
        °F
°F     32          98.6        212
-40   0  |40   80  120  160  200|
 |----+----+----+----+----+----|
-40  -20   0   20  |40   60  80  100
°C                  37              °C
```
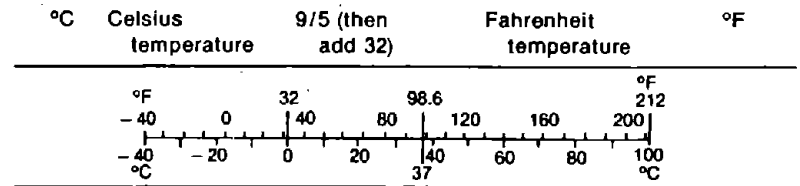
These factors conform to the requirement of FHWA Order 5190.1A.
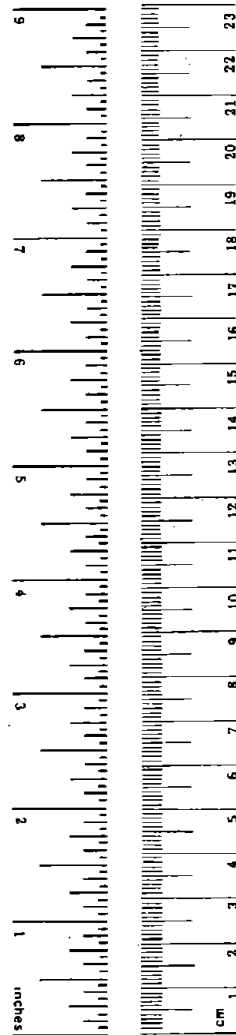
* SI is the symbol for the International System of Measurements

GENERAL DISCLAIMER

This document may have problems that one or more of the following disclaimer statements refer to:

- This document has been reproduced from the best copy furnished by the sponsoring agency. It is being released in the interest of making available as much information as possible.

- This document may contain data which exceeds the sheet parameters. It was furnished in this condition by the sponsoring agency and is the best copy available.

- This document may contain tone-on-tone or color graphs, charts and/or pictures which have been reproduced in black and white.

- The document is paginated as submitted by the original source.

- Portions of this document are not fully legible due to the historical nature of some of the material. However, it is the best reproduction available from the original submission.

TABLE OF CONTENTS

Section

LIST OF FIGURES

vii

LIST OF TABLES

LIST OF ABBREVIATIONS AND SYMBOLS

AASHO	American Association of State Highway Officials
AASHTO	American Association of State Highway and Transportation Officials
ADT	Average daily traffic
ADTT	Average daily truck traffic
ASCE	American Society of Civil Engineers
ASD	Allowable stress design
CB	Citizens Band
cm	centimeter
COTR	Contracting Officer's Technical Representative
D	Dead load
DEC	Digital Equipment Corporation
E	Young's Modulus
EB	East bound
FE	Finite element
FHWA	Federal Highway Administration
ft	feet
GVW	Gross vehicle weight
i	inch
K_{Ic}	Plane strain fracture toughness--slow loading
K_{Id}	Plane strain fracture toughness--dynamic loading
kip	kilopounds
kmp	kilometers per hour
kN	kiloNewtons

ksi	kips per square inch
L	Live load
L+I	Live plus impact load
m	meter
mi/h	miles per hour
MPa	Mega Pascals
N	Number of data points
NB	North bound
NCHRP	National Cooperative Highway Research Program
PA	Pennsylvania
PADOT	Pennsylvania Department of Transportation
psi	pounds per square inch
RMS	Root mean square
s	second
S	Sampling rate or maximum stress
SAP IV	Structural analysis program
S/D	AASHTO load distribution factor
SN	Stress range-vs.-number of cycles
S_r	Stress range
U	Strain Energy
USDOT	United States Department of Transportation
WB	West bound
WIM	Weigh-In-Motion
WIM+RESPONSE	Weigh-In-Motion Plus Response
α	(Defined on page 165)

ε strain

$\dot{\varepsilon}$ strain rate

Δt time interval (defined on page 132)

INTRODUCTION

1. Background

Highway bridges sustain vehicular traffic which varies in weight, overall length, number of axles, axle spacing, speed, and dynamic characteristics. The volume and conditions of traffic such as headway and multiple presence, as well as the correlation of traffic with bridge type, geometry, configuration, and other factors, such as maintenance, determine the integrity and life expectancy of highway bridges and their components.

For any particular bridge the static and dynamic response to a vehicle can be accurately monitored and evaluated if the geometrical and loading characteristics of the vehicle are known. Until recently it has not been possible to determine, to a reasonable degree of accuracy, the characteristics of vehicles crossing a bridge under actual highway conditions. Consequently, expected damages, if any, by vehicular traffic could not be accurately estimated.

Inspection of bridge superstructures throughout the U.S. reveals that some degree of damage does exist. A number of steel bridges have experienced fatigue cracking, some of them even large fractures of steel components (see references 1 to 5). Many other bridges have experienced corrosion damage, buckling of plates and members, connection distress, and undesirable cracking of reinforced and prestressed concrete members. These kinds of damages can be attributed most frequently to high loads, excessive traffic volume, poor maintenance, faulty design, inadequate specifications, or a combination of these.

While great advances have been made, for example, in the areas of fatigue, fracture, and strength of steel bridge components (see references 6 to 10), estimates of the fatigue strength and expected service life of inservice steel bridges have been carried out for only a limited number of cases (see references 11 to 15). Even in these cases, confidence in the estimates is

not high. This is because, although stresses in critical components can be accurately measured as vehicles traverse the bridges, the geometrical and loading characteristics of vehicles crossing the bridges could not be accurately measured but only estimated at the time of the studies.

In recent years significant advances have been made in the development of Weigh-In-Motion (WIM) systems (see references 16 to 20). The WIM system developed for the FHWA by Case Western Reserve University is portable and utilizes an existing bridge to serve as an equivalent static weigh scale to obtain not only Gross Vehicle Weights (GVW) but also axle weights and spacings, as well as speeds of vehicles crossing the bridge at normal highway speeds.[17,18,20] Under FHWA sponsorship three WIM systems were built and used to weigh more than 27,000 trucks in seven states.[19] Since the weighing operation cannot easily be detected by truck drivers, the results are not subject to the usual bias associated with traditional truck weighing methods. Both loadometer surveys and weight data from weigh stations are subject to bias because illegal trucks can easily avoid an operating weigh station with the aid of CB radios. The WIM system data has begun to reveal the true spectrum of truck loads, especially the extent of the high loads which are causing significant bridge damage. The studies reported in reference 19 also indicate that accurate truck weights are obtainable with the WIM system.

Current analysis and design of highway bridges in the U.S. is based on the AASHTO H (M) and HS (MS) truck and lane loads.[21,22] These "standard" AASHTO live loads have remained basically unchanged for over 40 years. The H (M) loadings were introduced in 1924 (see ASCE Transactions, 1924, pp. 1273-1298) and adopted by AASHO in their first edition, 1931. The HS (MS) loadings were introduced in the third edition of AASHO, 1941. These live loads do not represent the majority of modern trucks using today's highway system. In the intervening years the weights of trucks and their frequency of occurence have increased significantly. Many states have responded by raising their design loads, say from HS 20 (MS 18) to HS 25 (MS 22.5). Some states also check their designs by comparing with the heaviest permit vehicles authorized

in their state. With the development of the FHWA WIM system it is now possible to obtain relatively unbiased statistical data on truck speed, configuration, loading, and frequency of occurence to update that data. This information can be used to develop more rational "standard" design trucks for use in bridge design and rating procedures.[23]

Much more can be done, however, with the WIM system. By coupling the WIM system with a system for measuring strains in bridge components, data on bridge response can be achieved at the same time that loading data is being obtained from all the vehicles crossing the bridge with an arbitrary period of time. For an evaluation of bridge response the primary information required is the magnitude and variation of stress in bridge components during passage of vehicles over the bridge. The correlation of gross vehicle weight (GVW), axle weights, and frequency with stress range and induced maximum stress is the foundation of simple bridge design procedures and specifications based on strength and serviceability (such as fatigue) requirements.

This report presents the results of a 30 month research investigation conducted at Lehigh University during which one of the FHWA WIM systems was redesigned and used to obtain simultaneous load and response data from four inservice bridges. The redesigned system is designated the WIM+RESPONSE system throughout this report.

2. Objectives

The overall contract objectives of this investigation are "to determine what bridge response information and truck loading is necessary for a detailed evaluation of structural performance" of bridges and to "develop methods for using weigh-in-motion (WIM) technology to obtain the required data".

Specific objectives included the following:

   o Review existing bridge loading and response information and determine
     the specific needs which will enable an effective evaluation of struc-
     tural performance and remaining service life.

3

o Review weigh-in-motion technology, specifically the FHWA WIM system hardware and software.

o Redesign the FHWA WIM system hardware and software to enable truck loading and bridge response data to be obtained simultaneously from inservice bridges.

o Construct a WIM+RESPONSE system complete with the hardware and software required to acquire and store strain data from inservice bridges and to process that data to obtain simultaneous load and response information.

o Use the WIM+RESPONSE system to acquire and process simultaneous load and response data from several inservice bridges.

o Evaluate the load-response information obtained from the inservice bridges by comparing actual field results with analytically obtained results and with results of analyses based on the AASHTO specifications.

o Documentation of the WIM+RESPONSE system hardware and software and transfer the technology to the FHWA.

3. Scope of Work

Within the project objectives listed on page 1 of this report the following scope of work was accomplished:

o Existing bridge loading and response information was reviewed and needs were determined for steel and concrete bridge superstructures. Those needs are listed and discussed on page 6 of this report.

o The existing FHWA WIM system hardware and software were studied. The WIM system provided to Lehigh by the FHWA on October 17, 1983 was used in July 1984 to weigh 247 trucks crossing the Tilghman Street bridge on Route 309 west of Allentown, PA.[24] An overview of the FHWA WIM system is provided on page 17.

o WIM+RESPONSE system design parameters were developed based on the needs discussed on page 6, the capabilities of the existing WIM system, the project time constraints, and the project financial resources. Valuable input was obtained from the results of a preliminary load-response study conducted during September and October 1984 using the Bartonsville Bridge located on I-80 near Bartonsville, PA.[16,24] In that study a preliminary WIM+RESPONSE system design

4

was used to weigh 329 trucks and, simultaneously, to obtain strain data from three interior girders. The development of the WIM+RESPONSE system final design parameters is presented on page 17.

o Based on these final design parameters the WIM system provided by the FHWA was modified and a prototype WIM+RESPONSE system constructed, complete with hardware and software. The modifications to the WIM system are described on page 17.

o The prototype WIM+RESPONSE system was used to obtain simultaneous load and response data from three inservice steel and one inservice pre-stressed concrete bridge superstructures during the summer of 1985. During 4 weeks of continuous day and night field operation, simultaneous truck weight and bridge response data were obtained from 19,402 trucks crossing the 4 bridges. Descriptions of the field study bridges are provided on page 27.

o Page 60 provides the results of the load-plus-response studies. Details of data processing and a discussion of the field study results are also presented.

o Maximum girder stresses obtained in the field study are compared with the results of finite element analyses of the three-dimensional super-structures on page 136. In addition these actual and analytical girder stresses are compared with stresses computed using the assumptions and procedures of the AASHTO specifications. The chapter concluded with a discussion of the analytical results.

o Conclusions and recommendations are provided on page 168.

o The WIM+RESPONSE hardware and software systems are fully documented in references 25 to 30.

LOAD AND RESPONSE INFORMATION NEEDS

1. Overview of Load and Response Studies

a. Bridge Loading

Current procedures for the analysis and design of highway bridges in the U.S. use the AASHTO H (M) and HS (MS) system of truck and lane loads which represent "standard" single trucks or tractor-and-semitrailer configurations.[21,22] These trucks do not represent the majority of vehicles travelling over highway bridges. Actual vehicles range from small passenger cars to two-, three-and four-axle trucks, to five-axle (eighteen wheel) semitrailers, and to semitrailers and trailers in tandem with more than five axles.

Vehicle factors affecting bridge response include gross vehicle weight (GVW), the number of axles and their spacing, the distribution of GVW among the axles, vehicle speed, overall vehicle length, transverse position of the vehicle (lane), and the dynamic (bounce) characteristics of the axles. Also influencing bridge response are the distances between vehicles in a given lane (headway), the occurence of vehicles in more than one lane (multiple presence), and the dynamic characteristics of the bridge.

A number of studies have been conducted by the FHWA and individual state transportation departments to determine the configuration and weights of vehicles crossing highway bridges. References 16 to 20 and 31 to 34 provide a brief overview of some of the studies conducted over the past twenty years. Typically two approaches have been followed in studies of bridge loading:

(1) Stop-and-Weigh Studies. Vehicles (usually trucks) are stopped and weighed at off-highway operating weigh stations situated at fixed locations along the nation's highways. Alternatively, vehicles are stopped and weighed at random locations along highways using portable axle (wheel) scales. This approach has not been successful in determining the vehicle parameters most affecting bridge response for several reasons. The major problem is that,

6

with the aid of CB radios, most of the very heavy trucks including illegal trucks can easily avoid an operating weigh station. Only a few very heavy trucks are weighed, typically within the first half hour or so after a weigh station opens. Thus the high end of the truck-weight spectrum is missing from the data even though it is known that a significant amount of the structural damage observed in bridges is due to trucks from this part of the spectrum. Another problem is that the dynamic characteristics of a vehicle at rest cannot be measured. In addition the increasing costs of conducting stop-and-weigh operations prohibits their widespread use.

(2) Weigh-In-Motion Studies. In-motion weighing techniques have been developed in the past 10 or 15 years. Reasonably accurate estimates of truck weights, speeds, dynamic characteristics and other information are possible. Basically, three types of weigh-in-motion systems are used: (1) pavement scales embedded in highways and on or off ramps, (2) pavement or platform scales located at off-highway operating weigh stations, and (3) use of existing highway bridges serving as equivalent static weigh scales.

The first two systems have not proved successful for determining most of the vehicle parameters affecting bridge response. The first suffers from a number of problems such as inaccuracies associated with the "bounce" characteristics of the relatively light scale; change in the bounce characteristics of the scale with time; maintenance of the pavement scale, especially in colder climates; and the need to frequently resurface the pavement in the vicinity of the scale. In addition, analytic problems are encountered in computing bridge response using the information obtained from a pavement scale. The second system suffers from some of the above problems plus the major problem associated with stop-and weigh stations, that is, the avoidance of the weigh station by the very heavy trucks.

The third system, although not perfect, is proving to be the most effective means of directly obtaining the vehicle parameters most affecting bridge response primarily because the weighing operation cannot easily be detected by truck drivers and data is obtained while vehicles cross the bridge at normal

7

highway speeds. The FHWA WIM system, for example, can obtain fairly accurate estimates of GVW, axle weight, axle spacing, and speed for individual trucks crossing a bridge in any lane.[19] Ongoing improvements to the system should enable separate truck information to be obtained when multiple vehicles cross the bridge in the same or parallel lanes.

b. Bridge Response

Numerous bridge response studies have been undertaken, primarily during the past twenty years. This span of time coincides with the continuing developments in computer hardware and software which are making it increasingly possible to acquire and process the very large amounts of information associated with realistic bridge response studies. References 1 to 5, and references 11, 13, 14, and 35 to 39 provide a brief overview of some of this work. Typically two approaches have been followed in studies of bridge response.

(1) Analytical Studies. The responses of any bridge superstructure to vehicular loads involves the complex interaction of all elements comprising the superstructure. In a multiple girder bridge, for example, these elements typically include the girders, diaphragms, and deck. In a two-girder bridge they include the girders, floor beams, stringers, diaphragms and/or cross bracing, lateral bracing, and deck.

The AASHTO Bridge Design Specifications and typical office design procedures are outgrowths of the precomputer era when complex structural systems of necessity had to be drastically simplified for routine manual analysis and design. Manual analysis of the simplest superstructure under assumed static loading conditions is extremely difficult. Manual analysis considering the real dynamic loading conditions is virtually impossible to perform.

Actual superstructure stresses and deformations are usually quite different from those calculated in design. In addition, stresses are not calculated for many of the elements comprising the superstructure. Consider, for example, the design of a steel multiple girder bridge. Live load and

8

impact are distributed to a girder in proportion to the assumed design load
intensity ("standard" H (M) or HS (MS) loading) and girder spacing. The re-
sulting design stresses are typically somewhat larger than the measured
stresses under the real vehicular loads. On the other hand stress calcula-
tions are not normally performed for diaphragms or their connections to the
girders. Measured displacement-induced stresses in the vicinity of connec-
tions frequently exceed the specified allowable static and/or fatigue stresses.
This situation is often much worse for two-girder bridges.[5,35] From a
static strength point of view such design procedures have produced rather good
results based on the limited number of strength related failures experienced
to date. However, from a fatigue strength point of view, the level of per-
formance is not so good. Reference 39 points out that approximately half of
the failures reported in a recent survey are attributed to fatigue with most
of the failures related to the connections.

Recent analytical studies of bridge response recognize the need to per-
form more sophisticated computer analyses (usually finite element analyses) of
the superstructure in order to obtain a better estimate of stresses and dis-
placements. Field measurements under controlled loading conditions (usually
test trucks of known axle weights and spacings travelling at crawl speeds or
in fixed locations on the deck) have confirmed the validity of such
analyses.[5,14]

Although useful in bridge response research this approach is not practi-
cal or even possible in the routine evaluation (rating) of existing bridges or
the design of new bridges. Although computer capabilities have increased
enormously over the past decade it is unlikely that the real spectrum of
dynamic loading conditions can be considered in the near future. Even if this
were possible it is not practical to collect traffic data and undertake compli-
cated analyses on a bridge-by-bridge basis to assess existing bridges for damage
by maximum stress or fatigue. For new bridge design, simplified but reasonably
accurate analytical techniques are needed, coupled with statistical information
on current and projected traffic type and volume. In addition new and im-
proved specification provisions are needed which are compatible with these
techniques.

9

(2) Field Studies. An alternate and more direct method of obtaining bridge response information is by measurements of actual strains and displacements of inservice bridges. Bridge response to vehicular loading is a direct result of those loads. The effects of all influencing factors are already included in the response measurements. These factors include all parameters associated with the loading such as vehicle type and volume, lane position, and speed. All parameters associated with the superstructure are also included. These include span length, configuration of girders, floor beams, stringers, diaphragms and cross bracing, lateral bracing, and deck, as well as alignment (tangent or horizontally curved), superelevation , grade, and deck roughness.

A large number of bridge response studies of inservice bridges have been made especially during the past twenty years.[11] Most of these have been stress history studies which generate statistical information on actual maximum stresses and stress ranges at critical details. Although accurate stress history data has been produced in these studies, it was not possible to also obtain simultaneous statistical information on the vehicular loading characteristics which produced the stress history data. All studies, of necessity, were forced to rely on estimates of traffic characteristics from other sources, mainly loadometer surveys conducted on the same or similar traffic routes. This is because, until now, a computer system capable of acquiring, storing, and processing simultaneous load and response information has not been available.

This report presents the results of an investigation in which a WIM+ RESPONSE computer system was designed, built and used in field studies of four inservice bridges to obtain simultaneous load and response data which was used to study and evaluate the behavior of these bridges under the normal traffic conditions.

2. Information Needs

a. Bridge Loading

Improved designs of new bridges and improved evaluations of inservice bridges (operating and inventory ratings), whether for strength or serviceability, are directly dependent upon accurate information on bridge loadings. Some specific needs are presented as follows:

o Accurate statistical information on bridge loading spectra is needed as the foundation for probabilistic based design procedures.[19]

o A complete bridge loading model for strength design or rating requires statistical information on individual truck weights, axle weights, axle spacings, impact levels, truck headway, and multiple presence.[19]

o Serviceability design or rating models require statistical information on individual truck weights, impact levels and frequency of occurence for long spans (main girders) and axle weights, and impact levels and frequency of occurence for short spans (floor beams, stringers, and deck).[11,35]

o Improved specification provisions applicable to redundant versus non-redundant bridges or design procedures to ensure redundancy are dependent upon nonlinear collapse studies of bridges. These studies are dependent upon improved information on bridge loading and dead load to total load ratios.[39]

o Improvements to the "Bridge Formula" require accurate information on the bridge loading spectrum and an improved bridge loading model.[40]

b. Bridge Response

Improved designs of new bridges and evaluations (ratings) of inservice bridges, whether for strength or serviceability, are directly dependent on the ability to accurately predict the response (strains, displacements) of a bridge to the vehicular loads (loading models or loading spectrum). Some

11

specific needs are discussed as follows:

Stress Range. Stress range histograms have been developed using several different counting techniques such as ascending, descending, reservoir, rain-flow, and peak-to-peak.[11] The need for this information is evident from a review of the references already cited, especially references and 35. Although it is recognized that different truck positions generate different magnitudes of stresses at a given point and design procedures do require that "design trucks" be placed at maximum response positions, it is not widely recognized that the stress range histogram for a point on a bridge is not directly proportional to the GVW histogram for the bridge. A review of page 60 of this report will indicate the considerable differences between stress range and GVW histograms. This nonproportionality is due to several factors, such as:

o Not all trucks travel in the positions which produce maximum stress at a point.

o Virtually every truck is considerably different from the "design truck" in axle spacing, number of axles, axle weights, and GVW.

o Actual impact is different from the design impact.

A review of the very limited field data available indicates that a simple analytical procedure to correlate the stress range and GVW histograms for all points of interest on a bridge is not likely to exist. This correlation can best be obtained through field studies of inservice bridges.

Strain Rate. Page 14 of reference 10 discusses the role of strain rate (stress rate or loading rate) in the development of the current AASHTO Bridge Specification fracture control criteria.[14,21] It is pointed out that application of the loading rate (temperature) shift allows K_{Ic} rather than K_{Id} to be the controlling parameter providing for the slow to intermediate loading rates that are experienced in bridges. Correlation of bridge loading with response data will provide definitive information on the correlation between type of bridge (simple span, continuous, number of girders, etc.) bridge

12

loading and expected strain rates in main members and details. Reference 35 discusses the significance of loading rate and crack extension behavior.

A simple analytical procedure to correlate strain or loading rates with GVW histograms for all points of interest on a bridge is not likely to exist. This correlation can best be obtained through field studies of inservice bridges.

Maximum Stress. The correlation between maximum stress and bridge loading is needed for several reasons:

o To obtain the correlation between maximum design stresses in primary members and the actual maximum stresses under actual traffic conditions.

o To obtain the correlation between actual vehicular loading and maximum stresses at details and in members and details for which analytical stresses are not normally available, or very difficult to obtain. Most bridges, although constructed in three-dimensional space, are analyzed and designed as two-dimensional planar structures. The actual stresses induced by considering the actual superstructure configuration which may consist of girders, floor beams, stringers, diaphragms, cross-bracing, lateral bracing, and deck, as well as details, such as floor beam to cantilever bracket tieplates, and all other details and connections actually present in the three-dimensional structure, are not known and not normally calculated.[5]

o Current studies of bridge redundancy as used in the fatigue provisions of the current AASHTO Specification would benefit greatly with data on the correlation of bridge loading and stresses produced as a means of defining load paths.[21,39] This correlation is also needed in the studies to effectively model a three-dimensional bridge for computer aided engineering (CAE) analyses.[36,37]

o Correlation between maximum stress and bridge loading is needed for a better understanding of fracture control.[10,21,35]

Load Distribution. AASHTO criteria on the distribution of live loads have been continuously revised since the first edition in 1931. Many of these criteria are not based on realistic information. A review of the distribution criteria in the 13th Edition[21] indicate that they are not uniform among

13

bridge type. References 38, 41, and 42 report on load distribution studies in the past twenty years for composite box girders and presstressed concrete bridges which were based on more rational and realistic information. Since the late 1960's the NCHRP has made an effort to reduce some of the inequities in load distribution criteria. Reference 43 develops a synthesis of information on the distribution of wheel loads on highway bridges. This reference indicates that a need exists for field studies which will acquire reliable load-response information for the purpose calibrating the various load distribution theories.

Dynamic Effects. From the earliest days, the development of bridge design procedures and specifications have been based on the assumption that a bridge which, in reality, responds dynamically to the dynamic vehicular loads, can be designed for static strength as though the bridge is a static system subjected to static loads but with the live load amplified by an impact factor to account for the influence of the dynamic effects on strength. (Adjustments to allowable stress have also been made to account for frequency of occurence and long span versus short span effects.) Considering only the static strength of a bridge this assumption has served quite well in view of the very low incidence of strength failures of bridges. However, from a serviceability point of view the design of bridges against fatigue, fracture, concrete cracking, and deck deterioration, to name a few factors which are influenced by the long term effects of dynamic loading and response, this assumption has not served well, as evidenced by the increasing number of inservice bridges, both steel and concrete, which are suffering damage and failures attributed to cyclic stress and dynamic effects. Reference 44 states that perhaps the single most important cause of large dynamic response is the presence of roadway unevenness on the bridge deck and approach pavements as well as abrupt discontinuities in levels, as at joints and pot holes.

Stress range and strain rate information obtained from load-response studies of inservice bridges includes the effects of dynamic loading and dynamic response. However, there is a need to perform a larger number of field studies in order to statistically evaluate the effects of vehicular

14

loading, bridge type, and deck roughness on stress range and strain rate. Additional field studies are needed to access the influence of dynamic effects on other bridge design parameters.

3. Information Obtained in this Study

It was not the intent of this study to exhaustively acquire and evaluate load and response data for the purpose of providing definitive solutions to all of the needs discussed in this chapter. Rather the objective was to determine what load and response information is needed for a detailed evaluation of structural performance and to develop methods for using weigh-in-motion technology to obtain the required data.

The prototype WIM+RESPONSE system developed in this investigation and described on page 17 of this report was designed to be able to acquire data related to all of the needs addressed in this chapter. Of necessity, however, the prototype system was designed to acquire response data from a limited number of points on a bridge superstructure. Future improvements to the system would enable it to acquire data from a larger number of points.

Load and response data were obtained from four inservice bridges and evaluated with respect to GVW, stress range, strain rate, and maximum stress needs. Because of the limited capabilities of the prototype WIM+RESPONSE system, evaluation of load distribution and dynamic effects, beyond the dynamic effects included in the stress range and strain rate information, was not possible.

Consideration of load distribution requires a system capable of acquiring sufficient strain data to define the bending moment distribution for all the girders in a cross section of a bridge.[38,41] For example, a five-girder bridge with a minimum of four strain gauges per girder (to obtain a reasonable estimate of the strain distribution in the girder) would require a total of 20 channels of strain response input, exceeding the 16 channels available in the prototype system. Data from all channels would have to be acquired simultaneously for each load event in order to define the load distribution. This

15

requirement is not needed in studying stress range, for example, where the number of strain gauges can exceed the number of available input channels of the response system, since it is not necessary to acquire simultaneous data from all strain gauges for each loading event. The WIM+RESPONSE system could be used in a future load distribution study of four-girder bridges. If somewhat reduced accuracy is acceptable, such as for a pilot study, more girders could be accommodated by using only two or three gauges per girder.

Dynamic effects were considered in this investigation in evaluating stress range and strain rate data. However, other dynamic effects, such as impact are not considered. Conflicting requirements encountered in the design of the prototype WIM+RESPONSE system rendered a study of impact in this investigation somewhat difficult. To obtain accurate truck weight information it is necessary to instrument a bridge that has a relatively smooth deck and smooth transitions at expansion joints and approaches. On the other hand it is desirable to investiage impact for bridges having relatively rough decks and abrupt changes in level at expansion joints and approaches. If load and response information is obtained by instrumenting the same bridge (in the case of continuous spans) or the same span, both conditions can not be met at the same time. It would be possible to weigh trucks using one simple span and obtain response from amother simple span of the same bridge. However, a combination of the two required conditions is not likely to exist in the same bridge unless the rough conditions are artificially created for the response span. This investigation did not explore these possibilities.

PROTOTYPE WIM+RESPONSE SYSTEM

1. Overview of FHWA WIM System

Recognizing the limited success in weighing vehicles using pavement systems, the FHWA launched a series of feasibility studies to recommend alternative weigh-in-motion systems.[45,46,47] The approach described in reference 46 which proposed using strain gauges on main longitudinal bridge girders to weigh vehicles in motion was adopted by FHWA for implementation. A complete description of the design of the resulting FHWA weigh-in-motion (WIM) system and its use to weigh more than 27,000 trucks in seven States are contained in references 19 and 20. The system software users manual is provided in reference 48.

Figure 1 shows the field equipment setup for a typical weighing operation. The FHWA WIM system consists of the following components:

o Two tape switches are placed in the right lane (lane 1) of the approach to the weighing span as shown in the figure. The tape switches themselves are taped down to the pavement. Tape switches can also be placed in the passing lane (lane 2) of a two-lane bridge. The tape switch consists of two metallic strips embedded in a rubber casing. The strips are held out of contact in the normal condition. When a vehicle tire passes over the tape switch the two strips are forced into contact, effectively closing a switch. The tape switch must be held in place by taping it to the pavement. Tape switches can be obtained in a variety of lengths. In this study 5-ft-long (1.52 m) Contraflex 171-1S tape switches were obtained from Tapeswitch Corporation of America, Farmingdale, NY, 11735. Ordinary 2-in (5.08 cm) wire duct tape can be used to secure the tape switches to the deck and was used during the Tilghman Street and Bartonsville preliminary bridge studies (page 21). However, for the main field studies (page 27), 6-in-wide (15.24 cm), Type No. 672, Olive Drab tape, produced by Permacel, New Brunswick, NJ was used. This tape was supplied to Lehigh by FHWA. Tape switch installations are discussed on page 27.

o An optional keypad which can be used to trigger the system and to input data such as the lane in which the truck is travelling and the type of truck. The keypad is not used when the system is in automatic mode and receiving data only from lane 1 or lane 2. It must be used to collect data from both lane 1 and 2.

TAPE
SWITCHES

STRAIN
TRANSDUCERS

KEYPAD
OPERATOR

INSTRUMENTATION
VAN
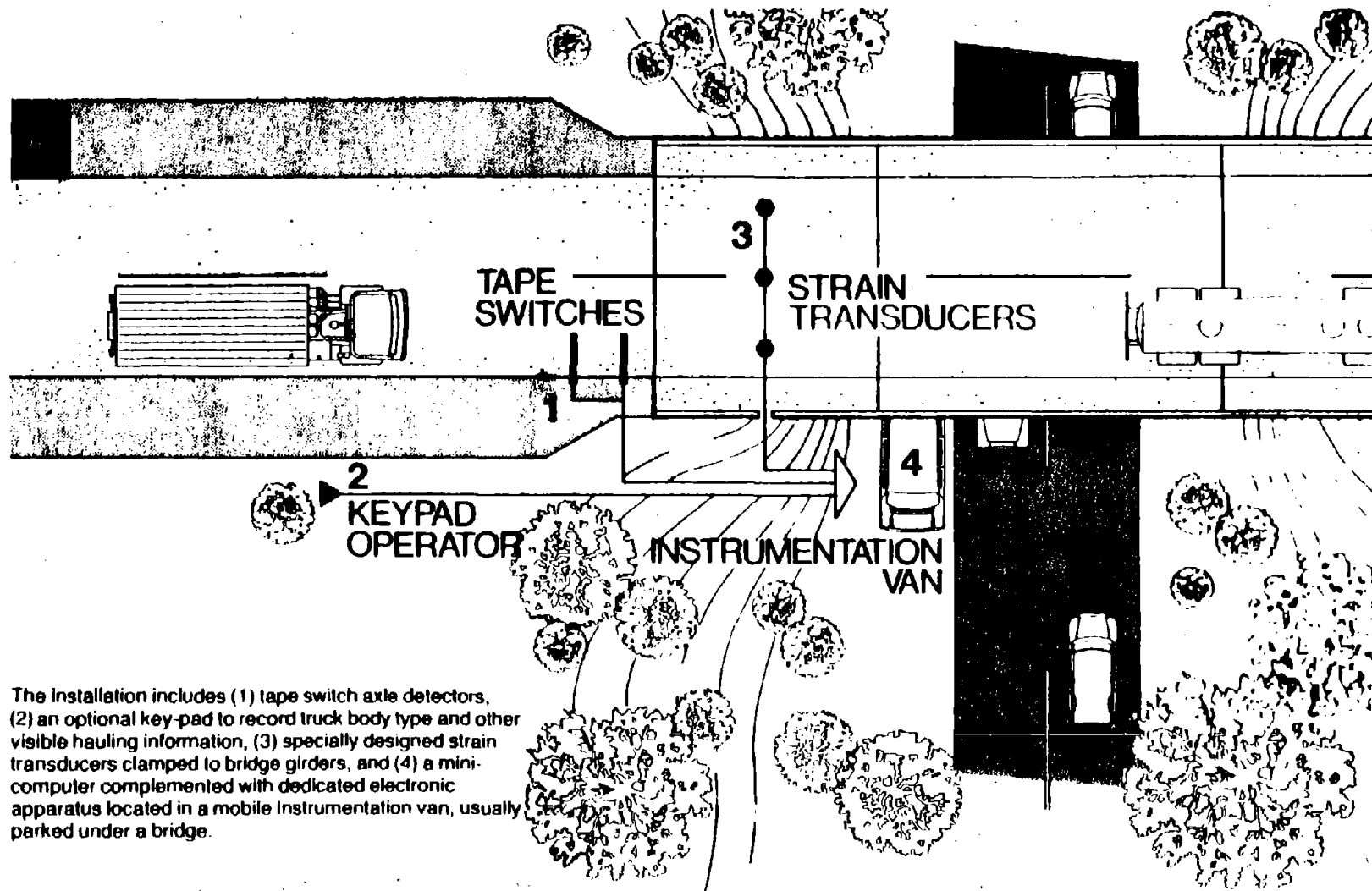
The installation includes (1) tape switch axle detectors,
(2) an optional key-pad to record truck body type and other
visible hauling information, (3) specially designed strain
transducers clamped to bridge girders, and (4) a mini-
computer complemented with dedicated electronic
apparatus located in a mobile instrumentation van, usually
parked under a bridge.

Figure 1. Field equipment setup for a typical WIM truck-weighing operation.

o Strain gauge transducers clamped to the bottom flanges of the girders
of the weigh span. The strain gauge transducers used throughout this
investigation were provided by FHWA (page 21) and are clamp-on devices
developed by Case Western Reserve University during a pile research
project.[17] Small electrical resistance strain gauges are attached at
four stress concentration points of the doughnut shaped aluminum trans-
ducer. The gauges are connected in a full bridge. Each transducer is
identified and its calibration value recorded. The transducer is easily
clamped to the bottom flange of a steel girder or a prestressed concrete
girder. The gauge length is 3 in (7.62 cm). Transducer installations
are shown on page 27.

o An instrumentation van located beneath the weigh span which houses the
weigh-in-motion system consisting of: (1) MINC 11/03 system with mini-
computer (PDP 11) manufactured by Digital Equipment Corporation (DEC);
(2) MINC laboratory modules required for this application which include
two hardware clocks, an analog to digital converter, and a digital in-
put device; (3) Dual floppy disk drive for software and data storage;
(4) a signal conditioning center to collect, condition, and amplify the
strain signals and to condition the keypad and tape switch signals
through a debounce circuit; and (5) a monitor (CRT) to display axle
weights, axle spacing, gross vehicle weight, and vehicle speed as the
data is processed in the field.

Data is acquired by the MINC system from three sources: (1) analog
signals from the strain transducers, (2) "digital" data from the tape switches,
and (3) "digital" signals from the optional keypad. As a vehicle approaches
the weigh span the appropriate vehicle category (box, flat, auto carrier, etc.)
may be input via the keypad if the keypad option is desired. The system then
operates automatically without further input from the keypad operator.

When the steering axle arrives at the first tape switch, which is located
approximately 7 ft (2.13 m) before the beginning of the weigh span, the compu-
ter begins acquiring strain data from the strain transducers. The strain data
is acquired at the rate of 40 to 80 samples per second as selected by the
operator during the input of the site parameters when loading the data acqui-
sition program. The second tape switch is set precisely 6 ft (1.83 m) from the
first tape switch (approximately 1 ft (0.305 m) before the beginning of the
weigh span). The MINC system checks the tape switches several thousand times
per second for axle pulses. Whenever a pulse is detected from either tape
switch the clock is read and the time (timestamp) is stored. The precise

distance between tape switches can be changed at the beginning of the data acquisition program.

All axles of the vehicle have been received when one of the following two contstraints have been met: (1) a limitation of 37 ft (11.28 m) between any two consecutive axles, and/or, (2) a limitation of 65 ft (19.81 m) between the first and the last axle. These distances are changed to equivalent time constraints by dividing by the vehicle velocity. The velocity is obtained from the arrival times of the first axle on each tape switch and the distance between tape switches. Axle spacing is obtained in a similar manner. These constraints can be easily changed at the start of the data acquisition program.

Once the last axle of the vehicle has been timestamped, the program classifies the vehicle as a car or a truck based on the number of axles and the peak strain value during the crossing of the weigh span. A car is arbitrarily defined as any two-axle vehicle with an axle spacing less than 12.1 ft (3.69 m) or any vehicle causing a peak girder strain less than a preset value. The preset strain level is site dependent and on the order of 10 microstrain. The purpose of this constraint is to prevent a car pulling a trailer to be classified as a truck. These constraints are also easily changed at the start of the data acquisition program.

If a vehicle is classified as a car, strain sampling is discontinued. However, the car velocity is stored in a separate file which can be used for velocity statistics if desired.

If the vehicle is classified as a truck, strain acquisition is continued for a predetermined length of time. At the end of this time velocity and axle spacing are then displayed on the CRT and the strain data tape switch activation times, and site information are recorded on a floppy disk. The recording process is programmed to allow the computer to perform other onsite tasks (at the operator's option) such as determining axle weights and gross vehicle weights and simultaneously displaying this information on the CRT.

The length of time that strains are acquired is predetermined at the beginning of the program by designating a "span length". This length is not necessarily the length of the weigh span or the bridge length. The designated "span length" is converted to time by dividing by truck speed. Strain acquisition time will be longer for slower moving trucks and shorter for fast moving trucks. The "span length" selected is a function of the sampling rate and the disk space (buffer length) per truck weighing event. The FHWA WIM system is designed to store 400 truck weighing events (all strain records obtained during the weighing of one truck) per floppy disk. Each floppy disk has a capacity of about 0.5 megabytes. For each truck weighing event the buffer length will accommodate up to 480 strain data records. Additional file space is provided on a floppy disk for storing processed data.

The weigh-in-motion concept is an "inverse" type problem in that the bending moment is measured (input from the strain transducers), but the live loads causing this moment must be calculated. Since data are recorded continuously during truck passage, the axles are "weighed" many times. The axle weights are found by minimizing the least squares difference between the measured strains and the values calculated by the data acquisition program from the vehicle demensions and the influence line for the weigh span (simple span) or bridge (continuous spans). The influence line can be calculated using a suitable structural analysis program or determined in the field using a calibration truck with known axle weights and spacing. The calibration truck can travel over the bridge at normal highway speed a sufficient number of times to ensure a reasonably accurate estimate of the influence line.

Further details on the design, description, and operation of the FHWA WIM system are contained in references 17, 19, 20, 46, and 48.

2. WIM+RESPONSE System Design Parameters

On October 17, 1983 Mr. Harold Bosch, FHWA Contracting Officer's Technical Representative (COTR) delivered one FHWA WIM system to Fritz Engineering Laboratory, Lehigh University. In the approximately nine months that followed

21

the Lehigh research team became familiar with the system hardware and software limitations and with the system operation. In July 1984 the WIM system was used to weigh 247 trucks crossing the Tilghman Street bridge on Route 309 west of Allentown, PA. In September and October of 1984 a preliminary WIM+RESPONSE system design was tested by weighing 329 trucks crossing the Bartonsville bridge on Interstate 80 near Bartonsville, PA, and by simultaneously acquiring and storing data from three strain gauges located on the three interior girders of one of the bridge spans.[16,24]

Based on this experience plus a background of over 15 years' research by Lehigh into the stress history response of over 70 bridges in the U.S. and elsewhere,[6,11,35,49] Lehigh proposed[50] and FHWA agreed to,[51] the following system design parameters on which the FHWA WIM system is to be modified and the prototype WIM+RESPONSE system designed, built, and used to acquire and evaluate load and response data from four inservice bridges (three steel and one prestressed concrete) in Pennsylvania:

o A prototype WIM+RESPONSE system, not a production system, is to be designed and built. Prototype is to mean a system that is complete and capable of obtaining simultaneous load and response data consistent with the information needs discussed on page 6, but of limited capacity and efficiency (proof of concept idea). Production is to mean a system with larger capacity and increased efficiency which evolves from the use and testing of the prototype system by others.

o The prototype WIM+RESPONSE system is to be based on a modification and enhancement of the FHWA WIM system delivered to Lehigh in October, 1983.

o The MINC 11/03 is to be upgraded to a MINC 11/23 since DEC no longer supports the 11/03. This entails, in part, bringing software to the latest version of the operating system and FORTRAN for the 11/23.

o An integrated WIM plus RESPONSE system is to be designed so that load and response data are stored simultaneously on the same mass storage device (floppy disk) since it is important when interpreting both types of data that there are no questions regarding their relationship in time (simultaneous).

o Software developed for data reduction and load-response evaluation (GVW histograms, stress range histograms, etc.) is to be written for processing by the WIM+RESPONSE system and compatible systems.

22

o The WIM+RESPONSE system is to be capable of acquiring and storing up to 16 channels of the simultaneous load and response data. Up to six of these channels are dedicated to WIM data coming from the strain transducers clamped to the main girders of the weigh span. These channels will employ the existing 6-channel WIM strain conditioning center which is part of the FHWA WIM system. These same six channels can provide RESPONSE data from the strain transducers used for the weighing operation plus additional strain transducers mounted elsewhere on the bridge, if less than six are used in the weighing operation. A new 10-channel strain conditioning center will be provided to simultaneously obtain additional channels of RESPONSE data from up to 10 strain gauges mounted anywhere on the bridge. The strain conditioning centers for both the WIM and RESPONSE data require continuous manual balancing during field studies to ensure close to zero strain at all gauges prior to a truck crossing the bridge. Automatic balancing conditioners are available but are not used in this system. Consideration should be given to automatic balancing when designing improvements to the WIM+RESPONSE system.

o The dual floppy disk drives which are part of the FHWA WIM system will be incorporated into the WIM+RESPONSE system for storing load and response data. Although a new higher capacity data storage device such as magnetic tape or hard disk is desirable, neither of these were considered efficient nor practical for use with the prototype system. Previous experience in using magnetic tape storage during the Lehigh stress history stories indicated that it could not be efficiently used with the WIM+RESPONSE system. Use of hard disks in field operations where the disk drives would be handled roughly and subjected to dusty conditions is not considered practical. However, both of these options should be reevaluated based on the state of the art when designing improvements to the WIM+RESPONSE system.

o The FHWA WIM system is designed to store 400 truck weighing events per floppy disk, each event consisting of 480 strain data records as explained on page 17. Also explained was the fact that to obtain reasonably accurate axle weights data acquisition may terminate before or after the truck crosses the weigh span. The design parameters for the WIM+RESPONSE system, however, are somewhat different. The buffer length must be increased to accommodate an increase in the number of data channels from 6 to 16. In addition, to obtain a complete record of response for a point on the bridge the truck must not only cross the weigh span but also the response spans (if different from the weigh span) and sampling should continue for a sufficient time to allow residual vibrations of the weigh and response spans to dissipate after the truck has passed. The WIM+RESPONSE system was therefore designed to achieve a compromise between storing as many truck weight plus response events per floppy disk and accommodating as long a span or bridge as possible. The system was finally designed to store 110 truck weight-plus-response events per floppy disk. A buffer length of 2,000 strain data records was also selected. At a sampling rate of 40 samples per second per channel, a truck speed of 55 mph (88 kph), and with one

23

second allowed for residual vibrations to dissipate, a maximum bridge length of about 170 ft (51.8 m) can be accommodated. For example, one simple span up to 170 ft (51.8 m) can be used to obtain both weight and response data. Two consecutive simple spans with a total length up to 170 ft (51.8 m) can be used with one span providing weight data and both spans providing response data. A series of continuous spans or a combination of simple and continuous spans with a total length up to 170 ft (51.8 m) can also be used. In this case, one span will be used for weight data, while response data can be obtained from all spans.

o The WIM+RESPONSE system is capable of obtaining simultaneous load plus response data from more than 16 gauges. While truck weight data is being obtained from the weigh span the remaining response channels can be changed periodically to other groups of gauges. In this way simultaneous truck weight plus bridge response information can be obtained from a large number of locations on the bridge.

3. Modification of FHWA WIM System

To achieve the prototype WIM+RESPONSE system capabilities described on page 21 the FHWA WIM hardware system delivered to Lehigh in October 1983 was modified extensively. The components needed to make this modification are listed in table 1. Also shown in the table are additional capabilities achieved with each component and the reasons for selecting each component. Additional software is described in the Software Reference Manual (see reference 29).

4. WIM+RESPONSE System Documentation

o WIM+RESPONSE System Overview (reference 25). This document is intended for administrative personnel and planners from FHWA and State Departments of Transportation. It contains a brief synopsis of what the WIM+RESPONSE System is and what it can be used for.

o WIM+RESPONSE Training Guide (reference 26). This document is intended for those technicians who need an introductory guide on how to operate the WIM+RESPONSE System. It contains detailed descriptions, including numerous pictures, on the various phase of operation of the WIM+RESPONSE System.

o WIM+RESPONSE System Users Guide (reference 27). This document is intended for technical personnel who need information on how to operate the WIM+RESPONSE System.

o <u>WIM+RESPONSE Hardware Reference Manual</u> (reference 28). This document is intended to provide technical personnel with the characteristics and basic information on the use of all equipment (hardware) associated with the WIM+RESPONSE System.

o <u>WIM+RESPONSE Software Reference Manual</u> (reference 29). This document is intended to provide technical personnel with the details on how to execute, operate, and modify the software which was developed at Lehigh University for the WIM+RESPONSE System.

o <u>WIM+RESPONSE Appendixes</u> (reference 30). This document is intended to provide information on field tips and notes from the experiences of the Lehigh University and FHWA researchers.

Table 1. Modifications to FHWA WIM system.

	Component	Additional Capabilities	Reasons
A.	CPU		
1.	Memory Board--DEC (MSV-11-LK)	256 kbytes	Increased memory for data processing
2.	11/23 CPU and Memory Management-- DEC (KDF-11-AA)	Upgrade to MINC 11/23 System	Increased efficiency and throughput
3.	Operating System, Version 5.1--DEC (QJ018-HX)	Current OS for 11/23	Present versions of OS for WIM no longer supported by DEC
B.	MASS STORAGE		
1.	Two new floppy disk drives--DEC	Return to functional operating state	WIM system failure in March, 1984. Hard disk technology not suitable for field conditions
2.	New Circuit Boards--DEC	Needed replacement	WIM System failure in May, 1984
C.	HARDCOPY DEVICE		
1.	Portable Graphics Printer--DEC (LA-50)	Local hardcopy of tabular or graphical data from CRT	Compatible with DEC, VT-125 CRT
D.	TERMINAL/CRT		
1.	Graphics CRT--DEC (VT-125)	Graphics capabilities not available on VT-100	Upgrades VT-100 to VT-125. Permits graphical displays on CRT
E.	SIGNAL CONDITIONERS		
1.	Vishay Ten Channels (No. 2120)	10 additional channels for data acquisition	Compatible with present system. Includes power supply and cabinet.

FIELD STUDY BRIDGES

1. Bridge Selection Criteria

Prior to March 1985, the Pennsylvania Department of Transportation (PADOT) District 5-0 was asked by Lehigh to provide a listing of steel and concrete bridges having potential for the field study together with maps showing their locations. This request produced a listing of over 100 bridges, all within District 5-0. This list was reduced to less than 50 steel and concrete bridges located on routes having a significant ADTT (Average Daily Truck Traffic). The objective was to obtain data from a minimum of about 3,000 to 4,000 trucks crossing each field study bridge within a 5-day (24 hours per day) data acquisition period (600 to 800 ADTT). Between March and July 1985, site inspections were made at about 30 bridges. All are within 100 mi (160 km) of Lehigh University; 26 are within 50 mi (80 km). Of these, four bridges (three steel and one prestressed concrete) were selected for the field study and included in the work plan presented to and verbally approved by Mr. Harold Bosch, COTR, FHWA.[52]

The following criteria were used to select the four bridges which are described on page 29:

o The four bridges are to be located within PADOT District 5-0. Most of the over 70 bridges on which stress history studies were conducted by Lehigh over the past 15 years were located in District 5-0. During this time a high degree of cooperation was developed between Lehigh and District 5-0 engineers. This cooperation was considered a desirable asset in conducting the field studies.

o Of all the bridges inspected, the four most suitable bridges nearest to Lehigh University are to be selected. Not only are financial resources conserved, but previous stress history study experience has shown that field studies are more efficiently organized and executed if travel time to and from the bridges is kept to a minimum. Within the University environment much of the field study work is performed by graduate students and these students have class schedules to meet as well as other research obligations throughout the year.

o The field studies are to be conducted between May and October, preferably during June, July, and August. The air temperatures should be

higher than 40 to 50 degrees Fahrenheit (4.4 to 10 degrees Celsius) and the relative humidity fairly low so that strain gauging of the bridges can be accomplished without difficulty. Also graduate student help is more readily available outside of the regular academic semester (late August through mid-May).

o Right or skewed bridges are acceptable. Although right bridges result in more accurage axle weights,[19] it is desirable to include both right and skewed bridges in the response data.

o About ½ to 1 mi (0.8 to 1.6 km) of reasonably level approach is required for nearly constant traffic speed over the weigh span so that accurate axle weight and spacing can be obtained.

o About ½-mi (0.8 km) site distance is required for traffic control and personnel safety during installation of the tape switches on the bridge approach at the start of the operation as well as replacement of tape switches during the operation and removal of tape switches at completion.

o Smooth roadway surface in the vicinity of the tape switches is required to avoid wheels bouncing and skipping over the tape switches.

o Relatively smooth deck on the weigh span is needed to avoid significant impact loading which would affect the WIM data. (This criterion conflicts with the desirability for a rough deck which would enhance the RESPONSE data.)

o Steel girder superstructures are to include some interesting welded, bolted, or riveted details and stiffeners or diaphragms which might yield potentially high displacement induced stress ranges.

o For concrete bridges, prestressed concrete I-girders or reinforced concrete T-girders are preferred. Other configurations, such as slab bridges or box girders would make it difficult or impossible with the current WIM system instrumentation to obtain weight data.

o Accessibility of the girders from below the bridge is required, within a reasonable height. Installation of the strain gauge transducers and strain gauges is more difficult if the bridge is quite high or over water.

o A reasonably low level of traffic on the roadway below the bridge and good site distances are needed for personnel safety during installation of the strain gauge transducers and strain gauges.

o A suitable off-roadway location for the instruments van below the bridge is required for personnel safety especially during night time operations.

o Availability of an electrical power source is required, located within about 400 ft (122 m) of the instruments van. Experience obtained at the Tilghman Street and Bartonsville bridges indicated that for continuous week long data collection the portable power supply resulted in too many power interruptions (to add gasoline and oil and to change oil) and was fairly noisy.

o In conformance with the WIM+RESPONSE system design parameters, specifically item 16, page 22, the appropriate span or bridge length is limited to a maximum of 170 ft (51.8 m).

o Since a maximum of six strain gauge transducers are available for truck weight data, the weigh span superstructure is limited to a maximum of six interior girders.

2. Description and Instrumentation

a. EB Route 22 over 19th Street

Bridge: East bound (EB) two lanes of PA Route 22 (part of Interstate 78) crossing over 19th Street in Allentown, PA. Two lane bridge with four, right, simple, steel girder spans:

Span 1: 45 ft-10   (13.97 m)
Span 2: 84 ft-10   (25.61 m)
Span 3: 125 ft-10   (38.11 m)
Span 4: 35 ft-10   (10.92 m)

Weigh Span: Span 2

Response Span: Span 2

Span 2 Superstructure: Figure 2 shows a partial cross section through the fascia and first interior girders. Span 2 consists of five multiple, riveted built-up steel plate girders, with a newly constructed 8½-in (21.59 cm) composite concrete deck. Girders are spaced at 8 ft-0 (2.44 m). The deck width is 32 ft-6 (9.91 m) curb-to-curb.

29

Instrumentation: Figure 3 shows the locations of the strain gauge trans-
ducers and strain gauges on span 2 of the EB bridge. All strain gauges are
¼-in (0.64 cm) electrical resistance gauges. In the figure, the transducers
are numbered 1 to 6. Weight and response data were obtained from transducers
1, 2, and 3. Transducers 4, 5, and 6 were used for response data. The strain
gauges, which are used for response data, are numbered 7 to 16. The trans-
ducers and strain gauges in cross sections 1 and 2 are mounted on the under-
side of the bottom flanges and are positioned 1½ in (3.81 cm) from the edge of
the plate. The locations of sections 1 and 2 were established so that the
transducers and strain gauges would fall midway between the outside line of
rivets which are at 6-in (15.24 cm) spacing. Sections 1 and 2 were also
located within the region of maximum bending moments produced by most trucks.
All transducers and strain gauges on the girders are oriented to measure
strains in the longitudinal direction of the girders. Strain gauges on the
diaphragm members are oriented to measure strain in the direction of the
members and are located midway between connections.

ADTT: The estimated average daily truck traffic (ADTT) is 2,000 to 3,000
on peak days. PADOT also estimates 40,000 to 60,000 average daily traffic
(ADT) with possibly 80,000 ADT on peak days. Due to reconstruction of Route
22, 10 mi (16 km) east of the bridge during the field study, the ADTT was
expected to be somewhat lower than the PADOT estimate.

Data Sample: Weight and response data were obtained from 4,680 trucks
crossing the span in both lanes during the 5-day period, June 18 through 22,
1985.

Bridge Photos: Figures 4 and 5 are aerial views of Route 22 looking east.
The EB bridge (and WB bridge—see page 37) are situated at the far (distant)
end of the segment of Route 22 shown in the figures. The city of Allentown is
mostly under the aircraft wing. The city of Bethlehem is in the distance,
mostly to the left of the wing. The Allentown-Bethlehem-Easton (ABE) Airport
is just beyond the far end of the segment of Route 22 shown in figure 4.
(ABE air traffic controllers would not permit low level aerial photography

closer to the bridge since it is located on the approach to, and about 4 mi (6.4 km) from, Runway 6.) Figures 6 through 9 show various views of the EB bridge. The approach to the bridge is shown in figure 6. Figure 7 shows a view looking east over the bridge with span 1 in the foreground. The truck shown in figure 7 is in lane 2 and about to enter span 3. Figure 8 shows a truck crossing the EB bridge in lane 1; the rear of the truck is on span 1 and the front is on span 2. Figure 9 shows the tape switches in lanes 1 and 2 of span 1. The joint between spans 1 and 2 is visible to the right of the figure.

Additional Remarks: In addition to the criteria listed on page 27, additional factors involved in the selection of the EB bridge are as follows:

  o Route 22 has a relatively high ADTT. A large percentage of the heavier trucks are travelling to New York City, (from New York City for the WB bridge--page 37) located about 90 mi east of the bridge.

  o The weight and response data can be compared with the adjacent WB bridge (page 37) where the significant variable is expected to be span length.

  o The original EB bridge was constructed in 1951 and had a noncomposite 8-in (20.32 cm) concrete deck. A new 8½-in (21.59 cm) composite concrete deck was constructed in 1983-84. No modifications were made to the steel girders. The response behavior of the fascia girders is of interest because of the new design provisions for exterior girders introduced with the 1957 AASHTO Specification, 7th Edition.

Location: The EB bridge on Route 22 over 19th Street is located at point A shown in figure 166 of the Appendix.

31
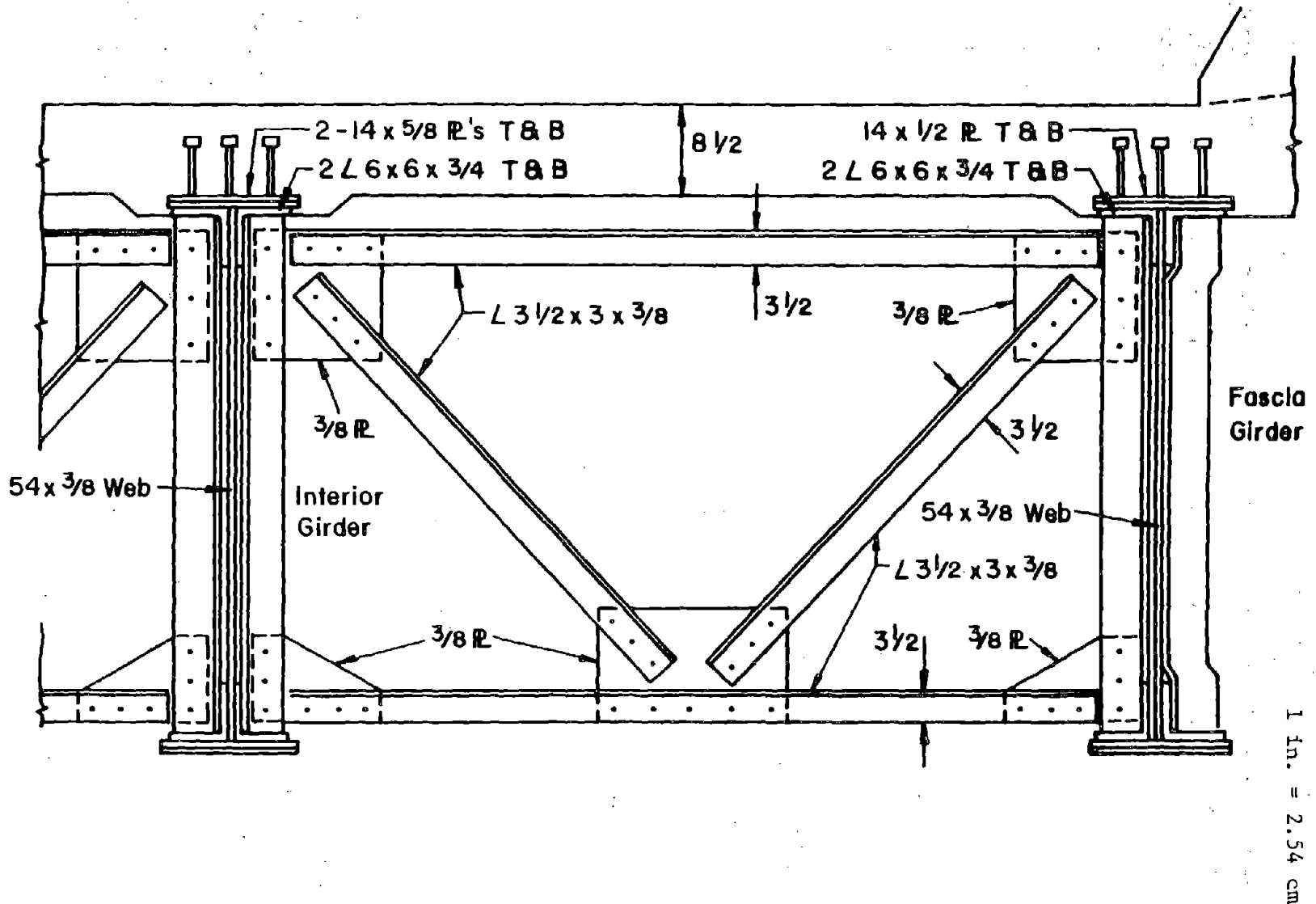
Figure 2. Partial cross section through fascia and first interior girders.

2-14 x 5/8 ℞'s T&B
2 ∟ 6 x 6 x 3/4 T&B

14 x 1/2 ℞ T&B
2 ∟ 6 x 6 x 3/4 T&B

8 1/2

∟ 3 1/2 x 3 x 3/8

3 1/2

3/8 ℞

3/8 ℞

Fascia
Girder

3 1/2

54 x 3/8 Web

Interior
Girder

54 x 3/8 Web

∟ 3 1/2 x 3 x 3/8

3/8 ℞

3 1/2

3/8 ℞

32

1 in. = 2.54 cm

TRAFFIC DIRECTION

1 ft. = 0.3048 m

2'-1"

6'-6"

6'-11"

42'-5"

42'-5"

84'-10"

Section ①—①

15 3 2 1 8

Section ②—②

16 6 4 5 7

Section ③—③

11,12 9,10

13,14

3"

9,11,13

10
12
14

3½"

1½"

Figure 3. Locations of transducers and strain gauges.

33

Figure 4. Aerial view of Route 22 looking east.

Figure 5. Aerial view of Route 22 looking ENE.
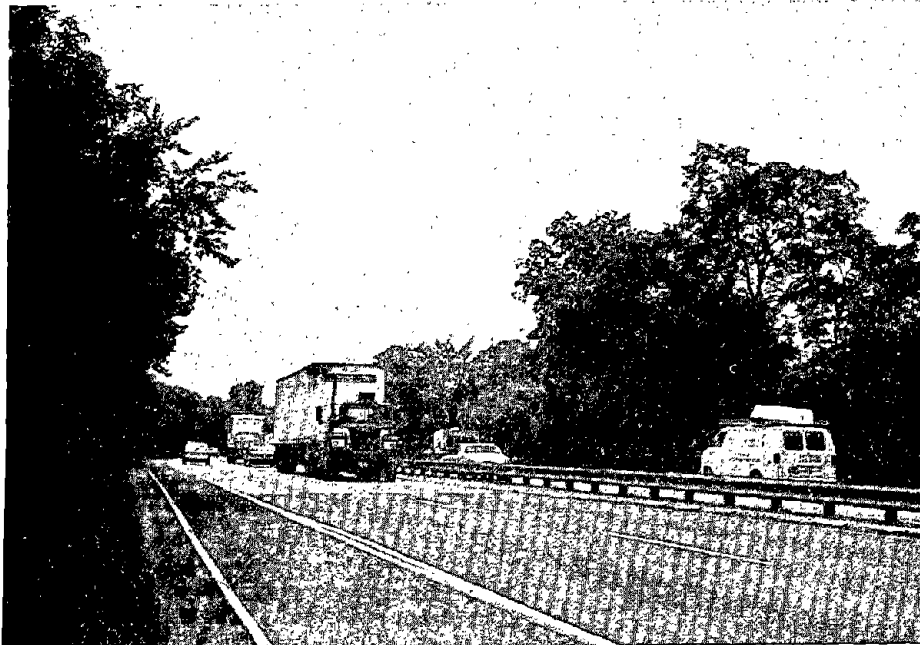
Figure 6. Approach to the EB Bridge.

Figure 7. Looking east over the EB Bridge.
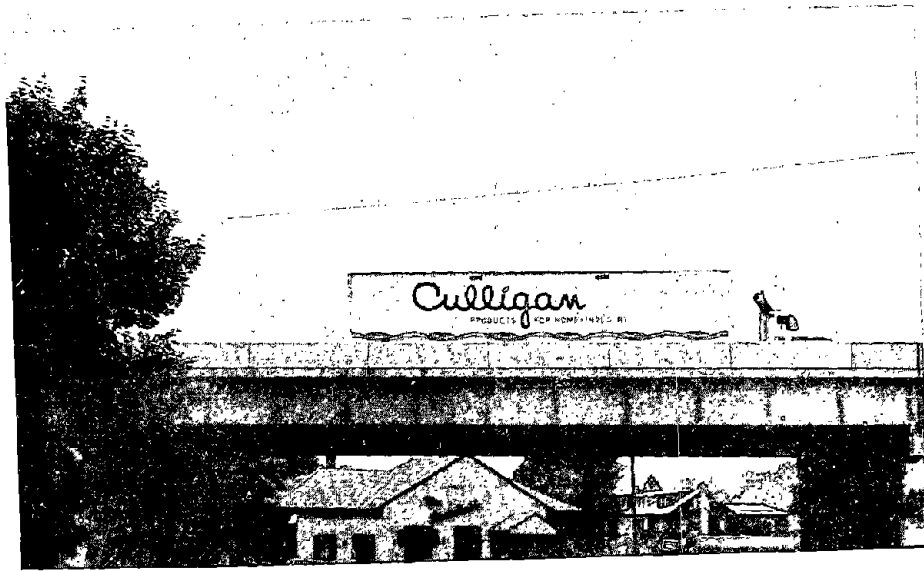
Figure 8. Truck crossing spans 1 and 2 in lane 1.
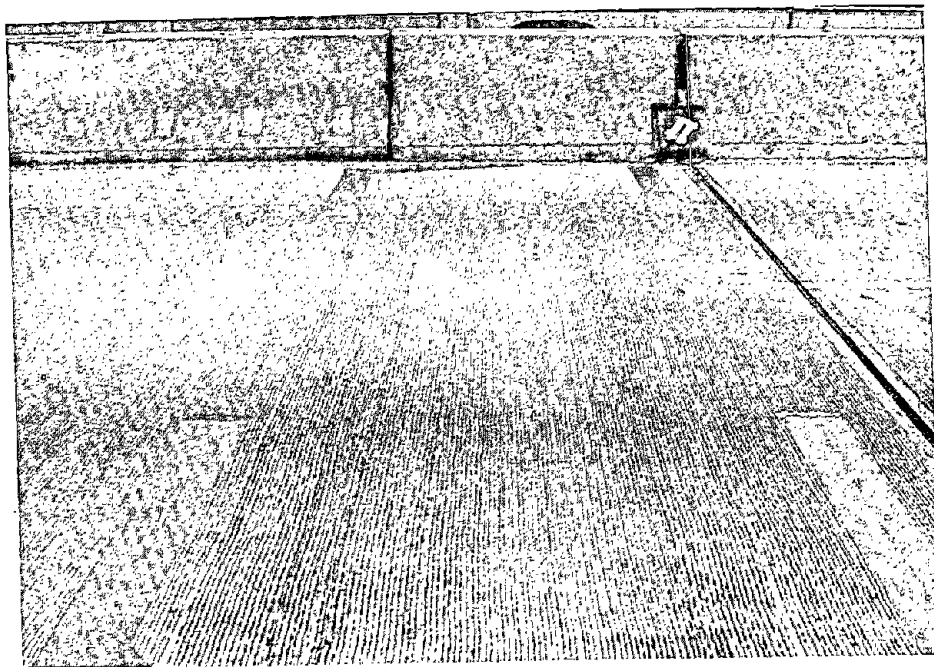
Figure 9. Tape switches in lanes 1 and 2 of span 1.

36

b. WB Route 22 over 19th Street

Bridge: West Bound (WB) two lanes of PA Route 22 (part of Interstate 78) crossing over 19th Street in Allentown, PA. Two-lane bridge with four, right, simple, steel girder spans:

Span 1: 35 ft-10   (10.92 m)
Span 2: 125 ft-10   (38.11 m)
Span 3: 84 ft-10   (25.61 m)
Span 4: 45 ft-10   (13.97 m)

(Note: The EB (page 29) and WB bridges are parallel, adjacent structures. For purpose of this report, span 1 of each bridge is the first span encountered by a truck crossing the bridge.)

Weigh Span: Span 2

Response Span: Span 2

Span 2 Superstructure: Figure 10 shows a partial cross section through the fascia and first interior girders. Span 2 consists of 5 multiple, riveted, built-up, steel plate girders, with a newly constructed 8½-in (21.59 cm) composite concrete deck. Girders are spaced at 8 ft-0 (2.44 m). The deck width is 32 ft-6 (9.91 m) curb-to-curb.

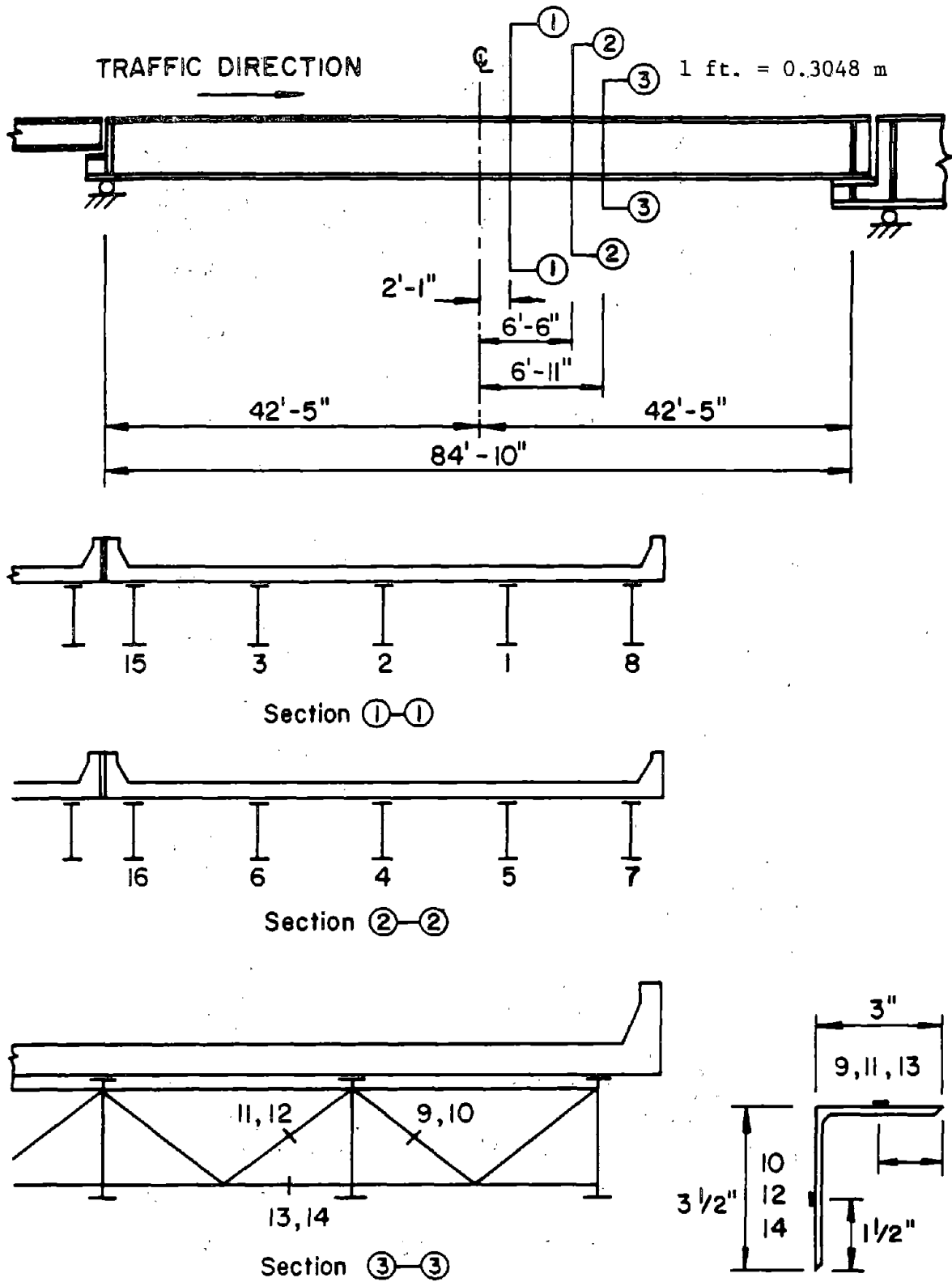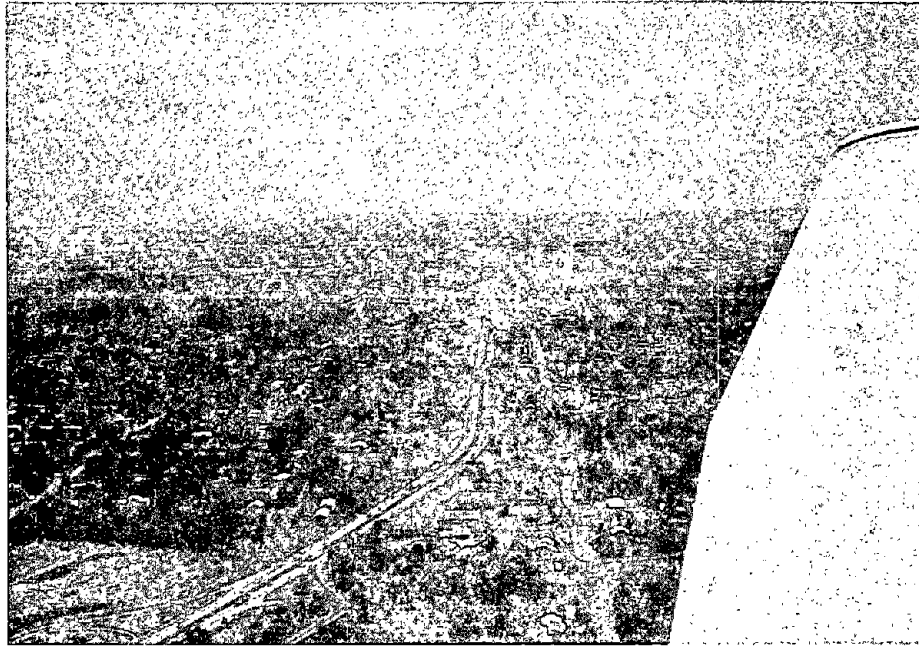Instrumentation: Figure 11 shows the locations of the strain gauge transducers and strain gauges on span 2 of the WB bridge. All strain gauges are ¼-in (0.64 cm) electrical resistance gauges. In the figure the transducers are numbered 1 through 6. Weight and response data were obtained from transducers 1, 2, and 3. Transducers 4, 5, and 6 were used for response data. The strain gauges, which are used for response data, are numbered 7 through 16. The transducers and strain gauges in sections 1 and 3 are mounted on the underside of the bottom flanges and are positioned 1½ in (3.81 cm) from the edge of the plate. The locations of sections 1 and 3 were established so that

37

the transducers and strain gauges would fall midway between the outside line
of rivets which are at a 6-in (15.24 cm) spacing. Sections 1 and 3 are also
located within the region of maximum bending moments produced by most trucks.
All transducers and strain gauges on the girders are oriented to measure
strains in the longitudinal direction of the girders. Strain gauges on the
diaphragm members are oriented to measure strain in the direction of the
members and are located midway between connections.

ADTT: (Same as for the EB bridge--page 29)

Data Sample: Weight and response data were obtained from 7,112 trucks
crossing the span in both lanes during the 6-day period, June 24 through 29,
1985.

Bridge Photos: Figures 12 through 15 show various views of the WB bridge.
(See figures 4 and 5 for aerial views of Route 22 on which the WB bridge is
located.) The approach to the bridge is shown in figure 12. Figure 13 shows
a view looking west over the bridge with span 1 in the foreground. The truck
in lane 1 is on span 2. The figure also shows the tape switches in lanes 1
and 2 of span 2. Figure 14 shows a truck in lane 1 crossing span 2. Figure
15 shows a view looking west during the instrumentation of span 2, which
employed a PADOT lift truck, the platform of which is shown in the figure.

Additional Remarks: (Same as for the EB bridge--page 29)

Location: The WB bridge on Route 22 over 19th Street is located at point
B shown in figure 166 of the Appendix.

18 x ¾ ℞ T&B   18 x ½ ℞ T&B

2 L 8x6x ¾ T&B   2 L 8x6x¾ T&B

8½"

L3½ x3x ⅜

3½"

3/8" ℞   ⅜℞

3½"

Interior
Girder

90x ½ Web ℞

Fascia
Girder

90 x ½ Web ℞

L 3½ x3 x ⅜

3½

⅜ ℞   L3½ x3x ⅜   ⅜ ℞
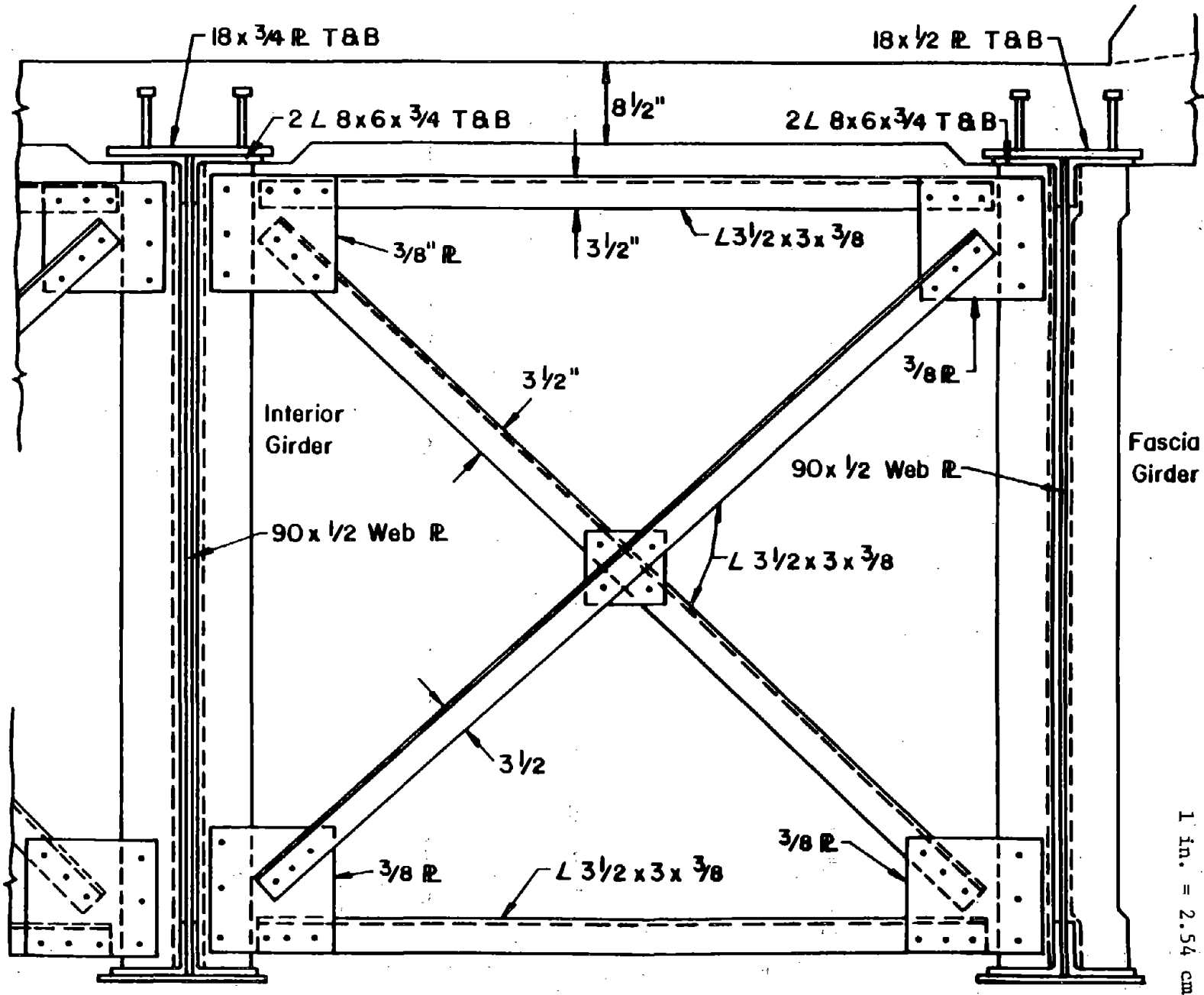
1 in. = 2.54 cm

39

Figure 10. Partial cross section through fascia and first interior girders.

TRAFFIC DIRECTION

1 ft. = 0.3048 m

3'-6"

5'-9"

7'-6"

62'-6"   62'-6"

125'-0"

7   3   2   1   15

Section ①—①

3"

9,11,13

9,10

1¼"

13,14

10
12   1½"
14

11,12

3½"

Section ②—②

8   4   5   6   16

Section ③—③

Figure 11. Locations of transducers and strain gauges.

40

Figure 12.   Approach to the WB Bridge.

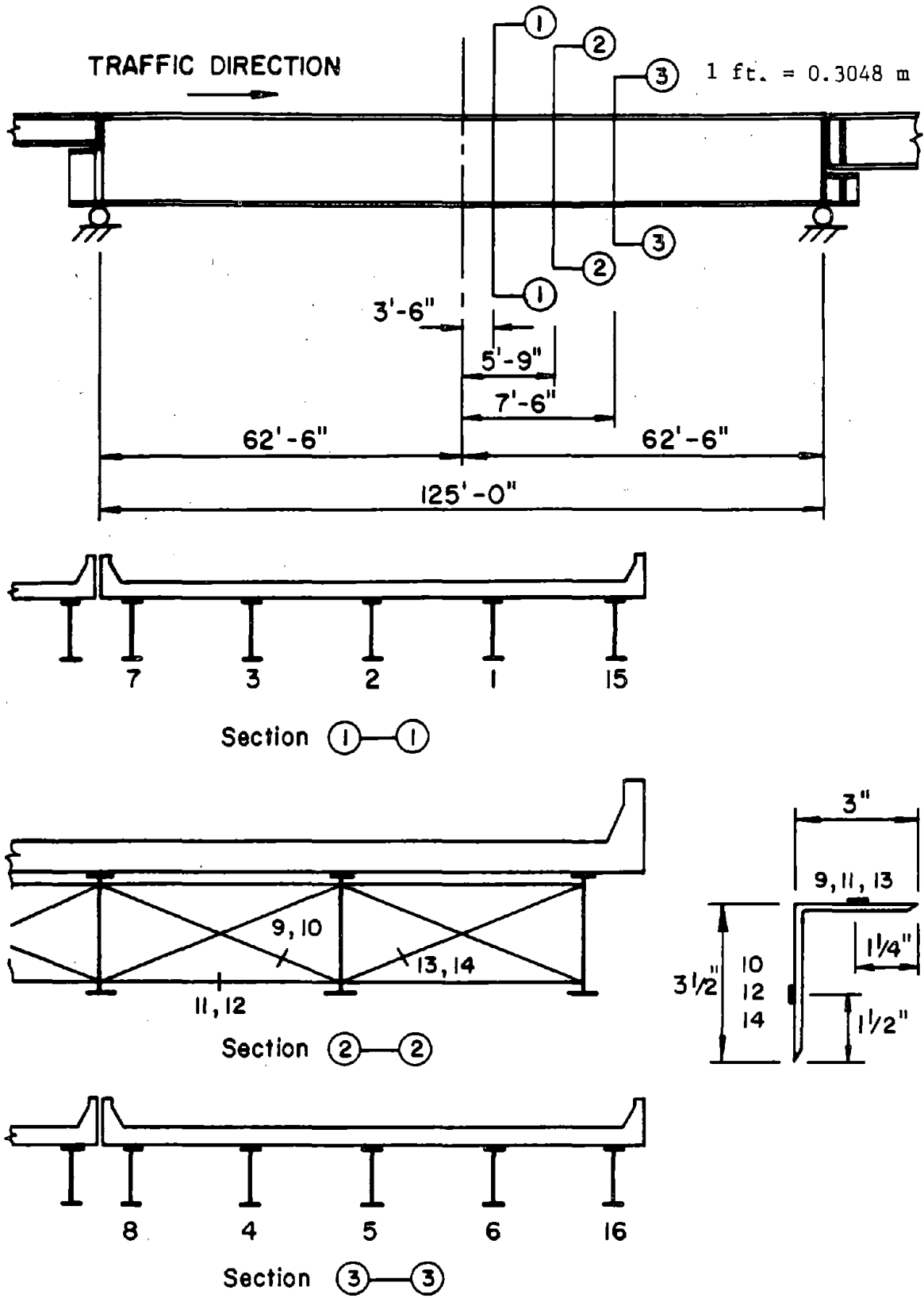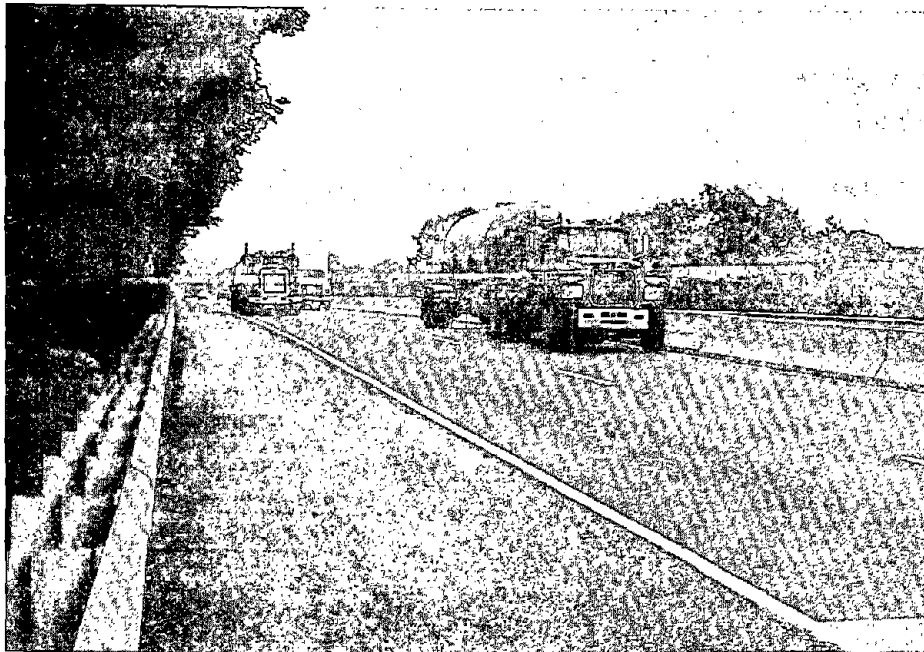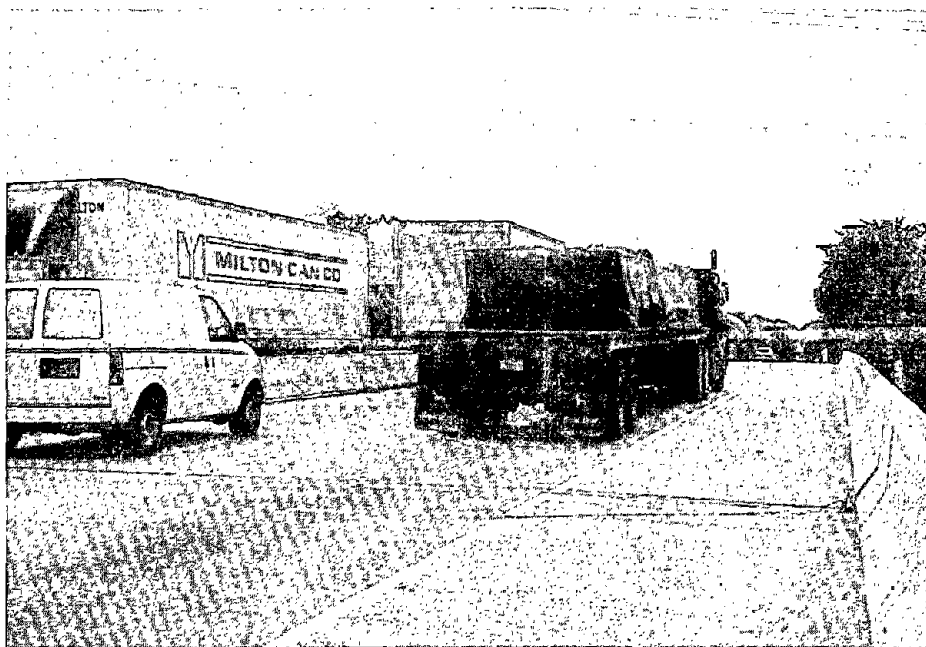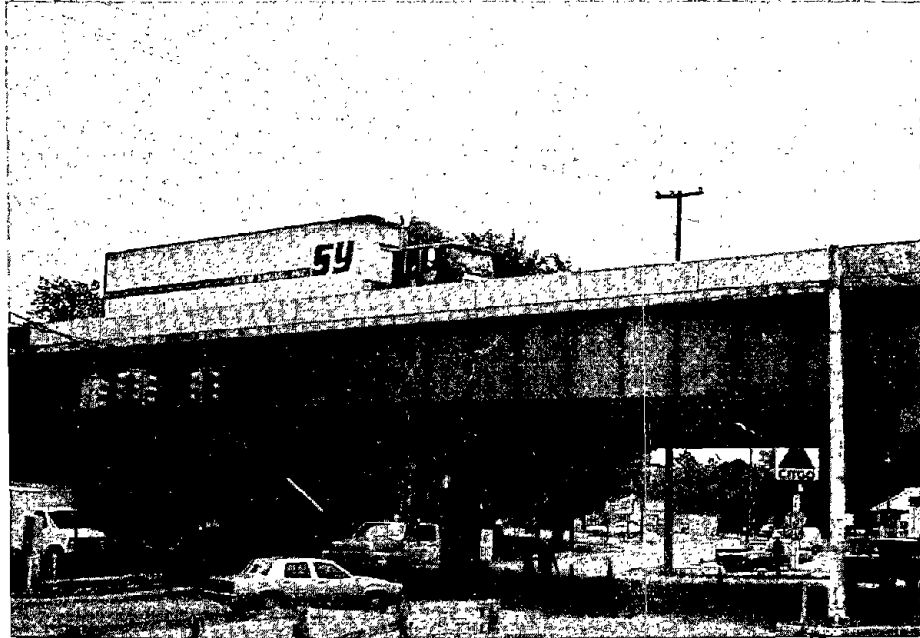Figure 13.   Looking west over the WB Bridge.

41

Figure 14.   Truck crossing WB Bridge in lane 1.

Figure 15.   Instrumentation of span 2 from PADOT lift truck.

42

c. NB Route 33 Over Van Buren Road

Bridge: North Bound (NB) two lanes of PA Route 33 over Van Buren Road, located 1 mi (1.6 km)·north of PA Route 248 and about 10 mi (16 km) NE of Bethlehem, PA. Two-lane bridge with three, skew, simple, steel girder spans:

Span 1:	39 ft-7 5/8	(12.08 m)	53° 29 ft 06 in skew
Span 2:	108 ft-3	(32.99 m)	53° 29 ft 06 in skew
Span 3:	39 ft-7 5/8	(12.08 m)	53° 29 ft 06 in skew

Weigh Span: Span 1

Response Spans: Spans 1 and 2

Span 1 Superstructure: Figure 16 shows a partial plan of the super-structure containing the span 1 girders. Span 1 consists of six, multiple, hot rolled W33 x 130 steel girders with an 8½-in (21.59 cm) non-composite concrete deck. Girder spacing is 7 ft-4 (2.24 m). The deck width is 40 ft-0 in (12.19 m) curb-to-curb.

Span 2 Superstructure: Figure 16 also shows the span 2 girders and a partial cross section through the fascia and first two interior girders. Span 2 consists of six, multiple, welded, steel plate girders with an 8½-in (21.59 cm) composite concrete deck. Girder spacing is 7 ft-4 (2.24 m). The deck width is 40 ft-0 (12.19 m) curb-to-curb.

Instrumentation: Figure 16 also shows the locations of the strain gauge transducers and strain gauges on spans 1 and 2. All strain gauges are ¼-in (0.64 cm) electrical resistance gauges. In the figure the transducers are numbered 1 through 6. Weight and response data were obtained from transducers 1 through 4. Transducers 5 and 6 were used for response data. The strain gauges, which are used for response data, are numbered 7 through 16. The transducers on span 1 are mounted on the bottom of the bottom flanges of the steel girders, at midspan, and oriented to measure strains in the longitudinal

43

direction of the girders. Strain gauge 7 is mounted below the web and ½ in (1.27 cm) from the end of the bevelled flange splice. Strain gauges 8 and 11 are mounted to measure vertical strains (membrane strain) on the webs of the fascia and first interior girder. The gauges are located just below the end of a fillet weld joining the diaphragm connection plate (transverse web stiffener) to the web, which terminates at the cope. These strain gauges are designed to measure displacement induced strains which often occur in these locations when the connection plate is not welded to the bottom flange. Strain gauges 9, 10, 12, and 13 are mounted on the diaphragm members and are oriented to measure strain in the direction of the member. They are placed midway between connections. Strain gauges 14, 15, and 16 are located on the underside of the bottom flanges of the plate girders, directly under the web, and oriented to measure strains in the longitudinal direction of the girders. These three gauges are located 2 ft-4 (0.71 m) from midspan which is the maximum moment location for an HS 20 (MS 18) truck.

ADTT: PADOT estimated ADTT is 1,000.

Data Sample: Weight and response data were obtained from 3,626 trucks crossing spans 1 and 2 in both lanes during the 6 day period July 22 through 27, 1985.


Bridge Photos: Figures 17 and 18 are aerial views of the PA Route 33 which show the NB and SB bridges crossing Van Buren Road. Figure 17 is a view looking SW towards Bethlehem, PA (about 10 mi (16 km) away). The NB bridge is the left most bridge of the pair of bridges situated to the left of the large buildings. The NB bridge is in the foreground of figure 18 which is looking about NNW. Van Buren Road, situated north-south passes under the bridge. The instruments van can be seen in figure 18 parked under the left end of span 2 (see also figure 21). Figures 19 through 23 show various views of the NB bridge. Figure 19 shows the approach to the NB bridge. Figure 20 shows a view looking NE over the bridge with span 1 in the foreground. The tractor of the truck in lane 2 is on span 1. The figure also shows the skew angle and the tape switches on the approach pavement. The tape switches are perpendicular to

the bridge centerline. Span 2 and the instruments van which is parked off Van Buren Road are shown in figure 21. Figure 22 is a view looking NE from the abutment end of span 1. Span 1 is the foreground; span 2 is beyond the pier. Another view of the tape switches in lanes 1 and 2 of pavement approach to span 1 is shown in figure 23. The data acquisitions setup in the instruments van is shown in figure 24. Part of the MINC 11/23 system, containing the PDP 11 computer and dual drive, can be seen in the lower right hand corner of the figure. The VT-125 graphics CRT and keyboard are to the left of the MINC 11/23. To the left of the VT-125 are the two signal conditioning units. The lower unit (next to Mr. L. Y. Lai's hand) contains the six Vishay signal conditioners which are connected to the six strain gauge transducers mounted on span 1. The upper unit contains the 10 Vishay signal conditioners which are connected to the 10 strain gauges mounted on span 2.

Additional Remarks: In addition to the criteria listed on page 27, additional factors involved in the selection of the NB bridge over Van Buren Road are as follows:

o This bridge is the nearest suitable welded steel girder bridge to Lehigh University, meeting the criteria of page 27 including the requirement for a reasonably high ADTT route travelled by a significant percentage of heavy trucks. Route 33 is one of the major connecting links between Interstates 78 and 80 and carries significant truck traffic to and from New York City.

o Weight and response data obtained from the NB bridge over Van Buren Road can be compared with data obtained from the NB bridge over State Park Road (page 51) both of which are located on the NB lanes of PA Route 33, where the significant variable is bridge girder construction (steel versus prestressed concrete).

o The bridge was constructed in 1969.

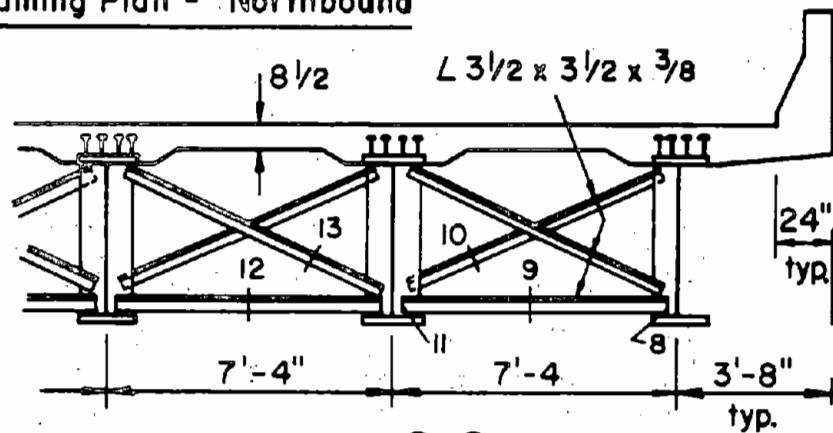Location: The NB bridge on Route 33 over Van Buren Road is located at point C of figure 166 in the Appendix.
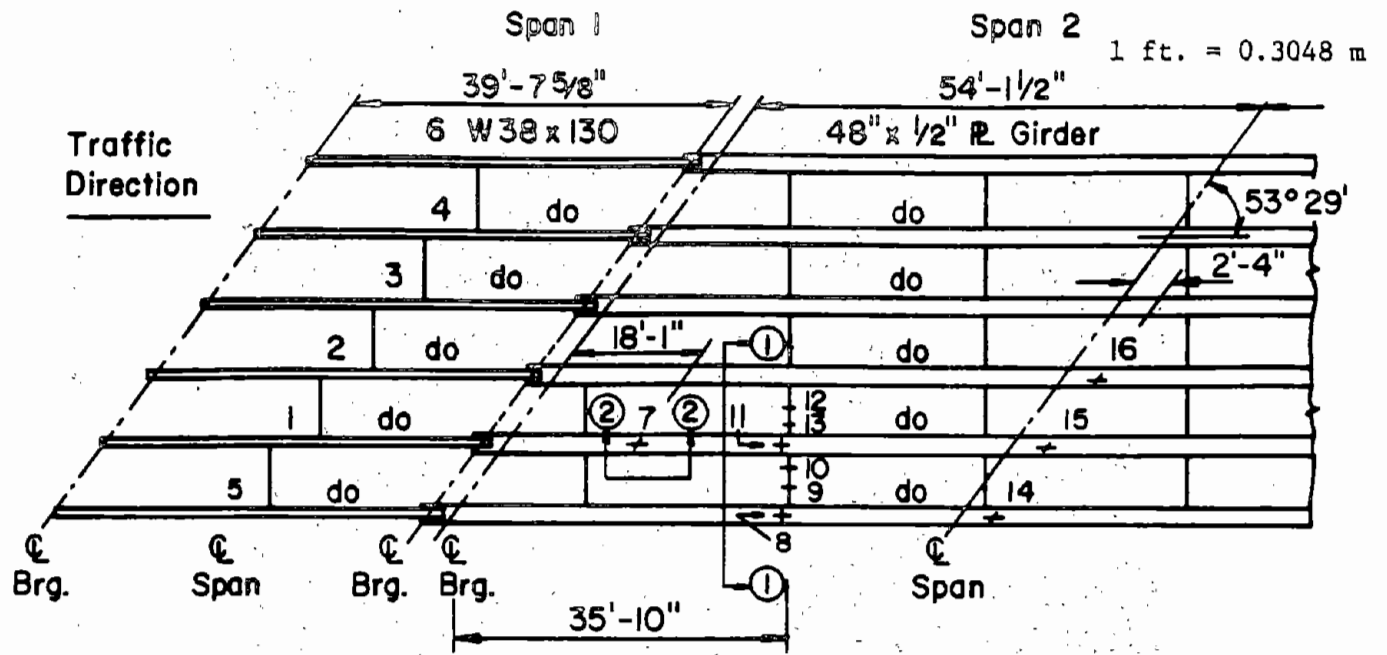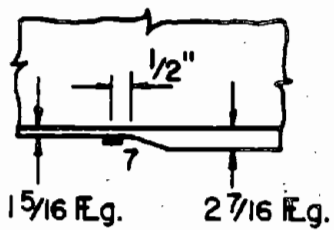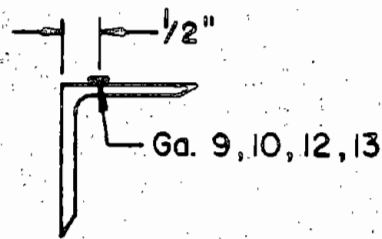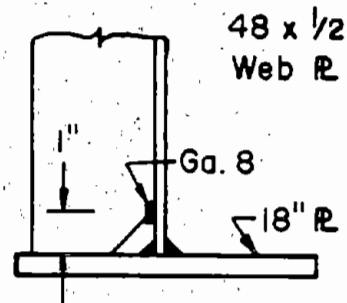
Figure 16. Partial plan and cross section of superstructure showing locations of transducers and strain gauges.

46

Figure 17. Aerial view of Route 33 looking southwest.

Figure 18. Aerial view of bridges over Van Buren Road.

Figure 19. Approach to the NB Bridge.

Figure 20. Looking northeast over the NB Bridge.

48

Figure 21. Instruments van parked under span 2.

Figure 22. Looking northeast from span 1 abutment.

Figure 23.   Tape switches on pavement approach to span 1.

Figure 24.   Data acquisition setup in instruments van.

d. NB Route 33 Over State Park Road

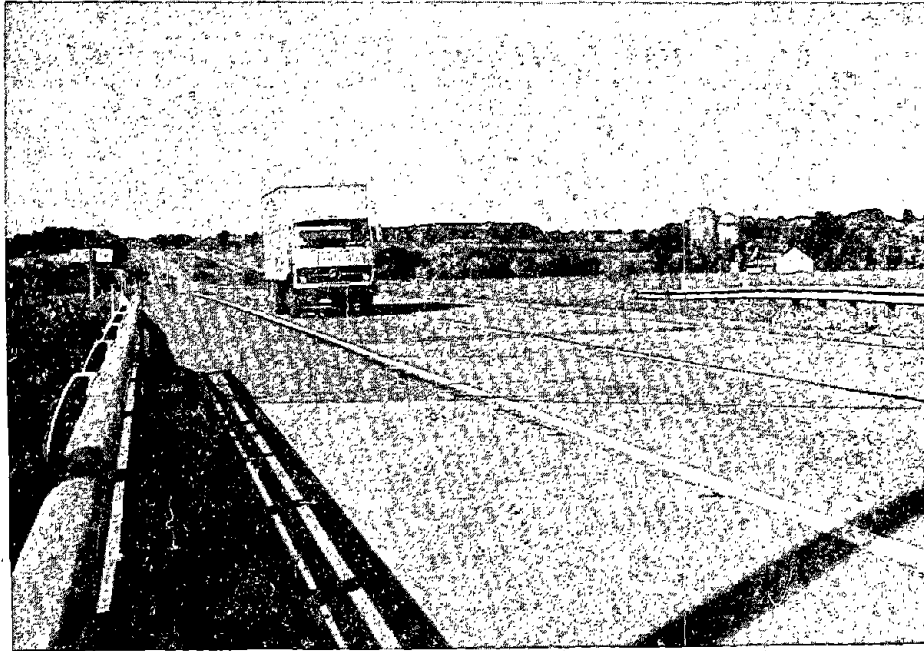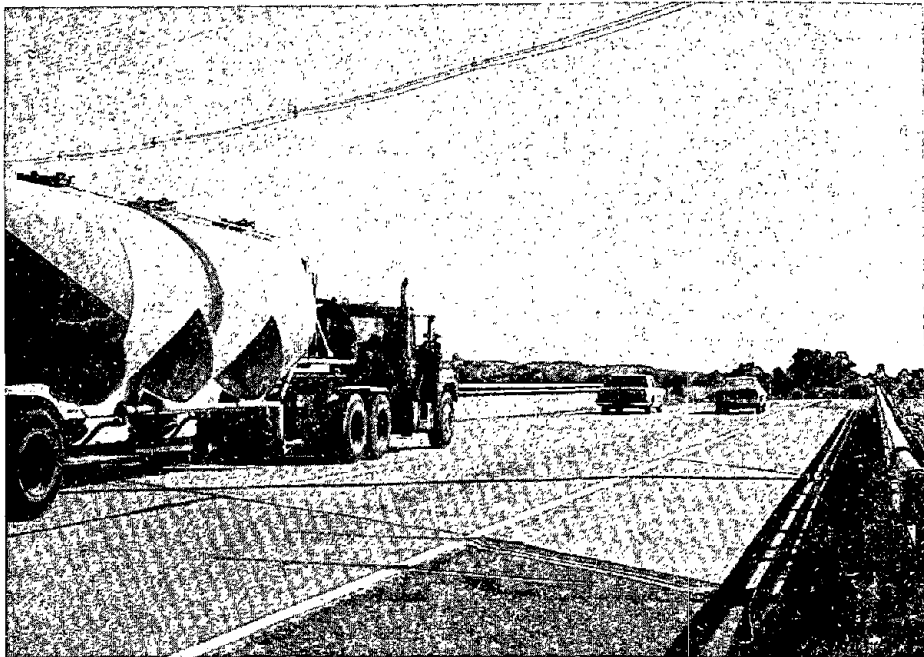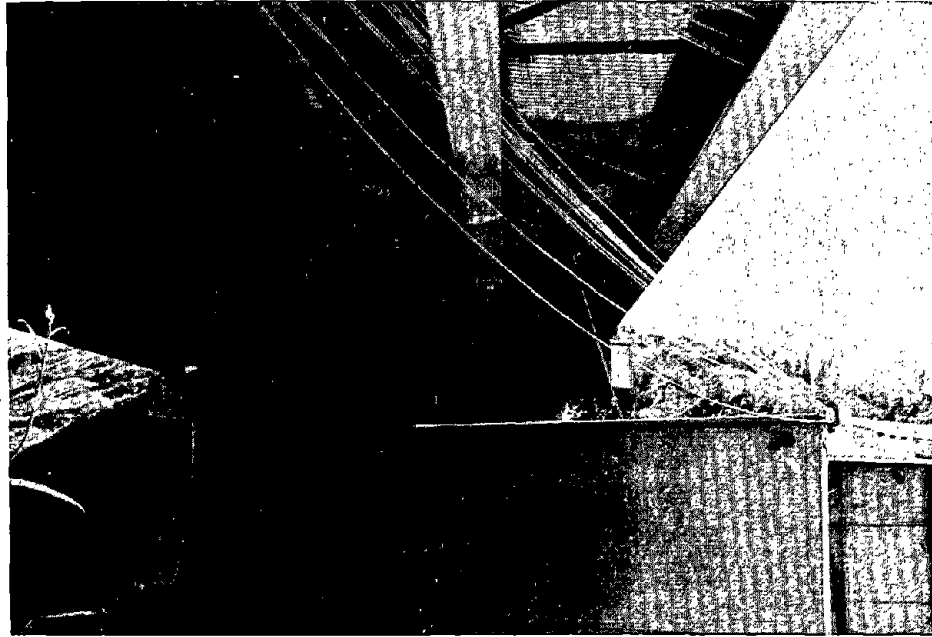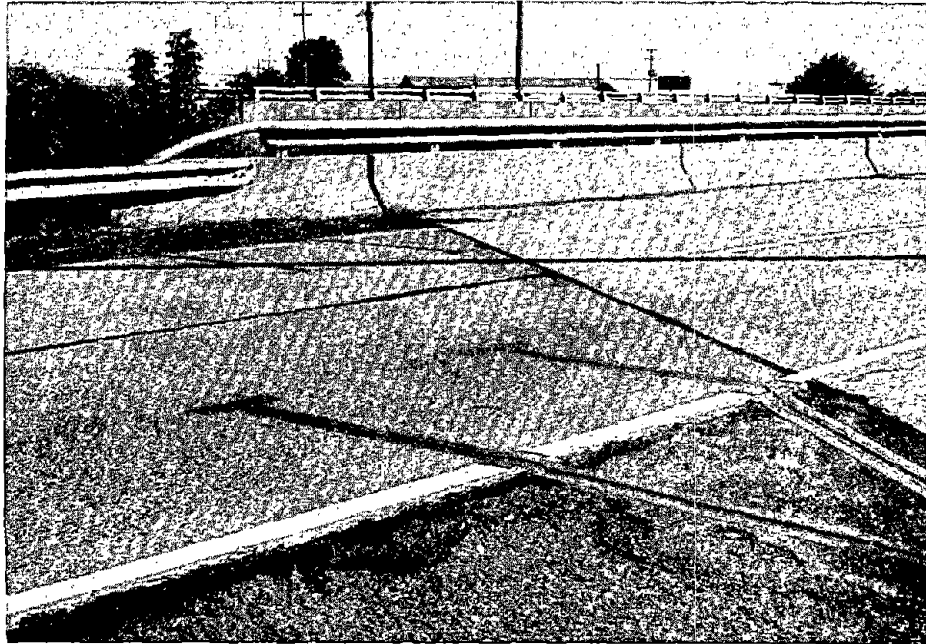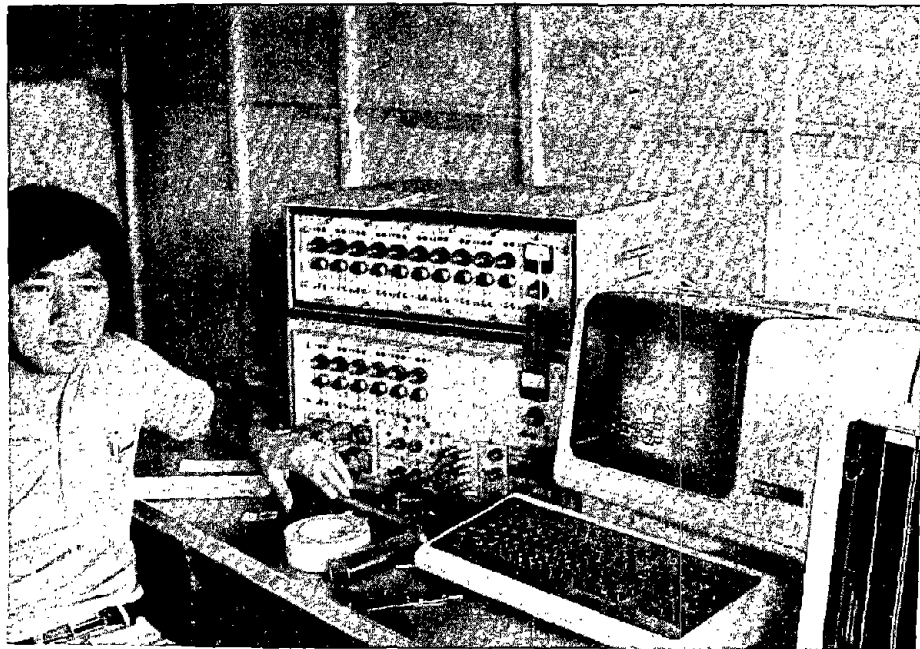Bridge: North Bound (NB) two lanes of PA Route 33 over Van Buren Road, located two mi (3.2 km) north of the Belfast exit on Route 33 and about 4 mi (6.4 km) north of the NB Route 33 bridge over Van Buren Road (page 43). Two-lane bridge with three, skew, simple, prestressed concrete I-girder spans:

Span 1:   28 ft-0   (8.53 m) 48° 46 ft 55 in skew
Span 2:   66 ft-3½   (20.21 m) 48° 46 ft 55 in skew
Span 3:   28 ft-0   (8.53 m) 48° 46 ft 55 in skew

Weigh Span: Span 2

Response Spans: Spans 2 and 3

Span 2 Superstructure: Figure 25 shows a partial plan of the super-structure and cross section of the span 2 girders. Span 2 consists of six, multiple, prestressed I-girders with an 8-in (20.32 cm) composite concrete deck. The prestressed girders are PADOT Type 24 in/45 in (0.61 m/ 1.14 m).[53] Girder spacing is 7 ft-4 (2.24 m). the deck width is 40 ft-0 (12.19 m) curb-to-curb.

Span 3 Superstructure: Figure 25 also shows the span 3 girders. Span 3 consists of six, multiple, prestressed I-girders with an 8-in (20.32 cm) composite concrete deck. The prestressed girders are PADOT Type 20 in/30 in (0.51 m/0.76 m).[53] Girder spacing is 7 ft-4 (2.24 m). The deck width is 40 ft-0 (12.19 m) curb-to-curb.

Instrumentation: Figure 25 also shows the locations of the strain gauge transducers and strain gauges on spans 2 and 3. All strain gauges are 5 in (12.70 cm) electrical resistance gauges. In the figure the transducers are numbered 1 through 6. Weight and response data were obtained from trans-ducers 1 through 4 (on span 2). Transducers 5 and 6 (on span 3) were used for response data. The strain gauges, which are used for response data, are

51

numbered 7 through 16. The transducers on spans 2 and 3 are mounted on the sides of the bottom flanges of the prestressed I-girders, about 2 in (5.08 cm) from the bottom surface of the girder, and at midspan. All transducers are oriented to measure strains in the longitudinal direction of the girders. Strain gauges 7 and 8 and 13 through 16 are mounted on the underside of the prestressed girders midway between the two edges. They are also oriented to measure strains in the longitudinal direction of the girders. The remaining 4 strain gauges numbered 9 through 12 are mounted horizontally on a diaphragm in span 2 as shown in figure 25.

ADTT: PADOT estimated ADTT is 1,000.

Data Sample: Weight and response dtat were obtained from 3,984 trucks crossing spans 2 and 3 in both lanes during the 8-day period, August 12 through 19, 1985.
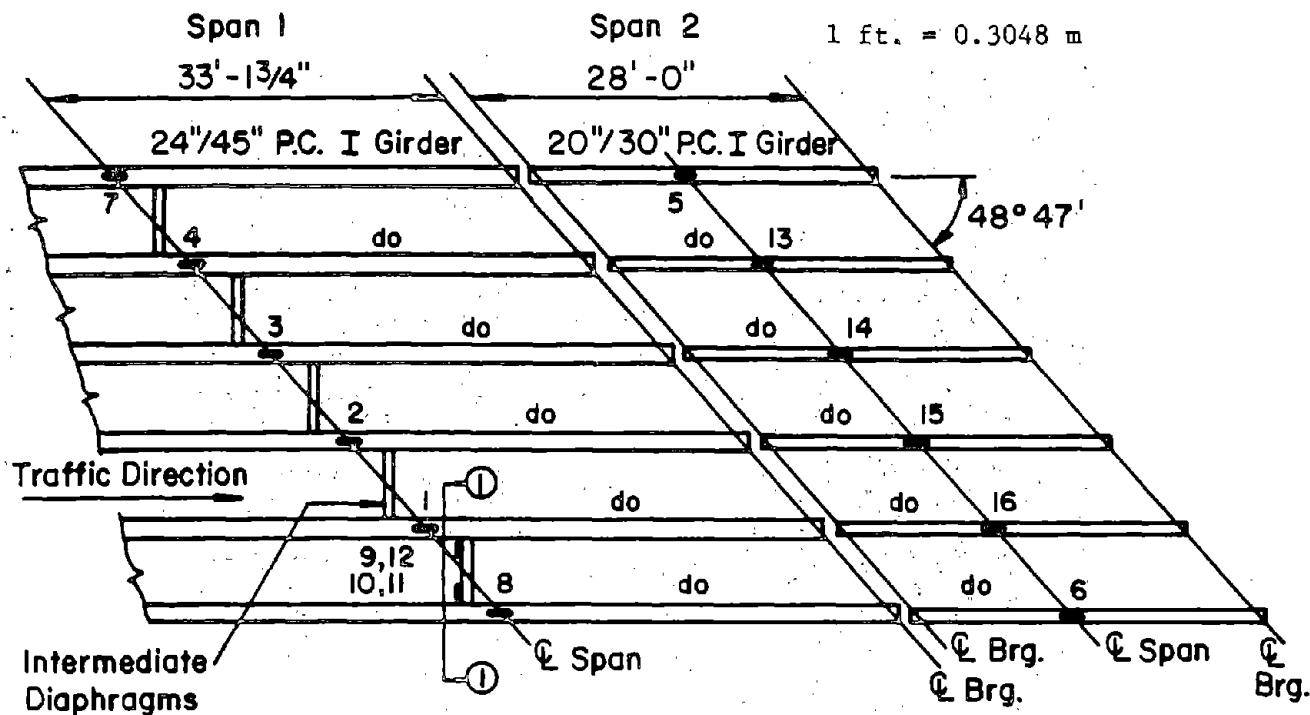
Bridge Photos: Figures 26 and 27 are aerial views of PA Route 33 which show the NB and SB bridges crossing State Park Road. Figure 26 is a view looking north. The NB bridge over State Park Road is located about midway between the two bends in the highway which can be seen near the top of the figure. Figure 27 is a view looking approximately east and shows State Park Road passing under the bridge. The NB bridge is the farther east of the two bridges shown in the figure. Figures 28 to 35 show various views of the NB bridge. The approach to the bridge is shown in figure 28. The tractor of the truck shown in lane 1 is mostly on span 3. The rear axles of the trailer are on span 2. Figure 29 also shows a truck in lane 1 crossing spans 2 and 3. The tape switches are mounted in lanes 1 and 2 of span 1 and are visible in the figure at the far end of span 1 (span in the foreground). Instrumentation of span 2 from the PADOT lift truck is shown in figure 30. Span 3 is to the right. Figure 31 shows the long clamps that are used to mount a transducer on the side of a prestressed I-girder. A transducer and the two clamps holding it to the side of a prestressed I-girder are shown in figure 32. For installation on prestressed girders, long adjustable clamps are used to accommodate bottom flange widths up to 27 in (0.69 m). For steel girders small

52

2-in (3.08 cm) clamps are used which span the flange thickness. In this case the transducer can be mounted on the top or bottom surface of a steel flange. Figure 33 shows the transducers and strain gauges on span 2. The nearest transducer is transducer number 1 (figure 25). The strain gauge on the girder at the top of the figure is gauge number 8. The instrumented diaphragm is between gauge 8 and transducer 1. Transducer number 5 and strain gauges 13 and 14 on span 3 are shown in figure 34. The four strain gauges on the diaphragm are shown in figure 35.

Additional Remarks: In addition to the criteria listed on page 27, additional factors involved in the selection of the NB bridge over State Park Road are as follows:

o This bridge is the nearest suitable prestressed concrete I-girder bridge to Lehigh University, meeting the criteria if page 27 including the requirement for a reasonably high ADTT route travelled by a significant percentage of heavy trucks.

o Weight and response data obtained from the Van Buren Road and State Park Road Bridges can be compared.

o The bridge was constructed in 1968.

Location: The NB bridge on Route 33 over State Park Road is located 4 mi (3.2 km) north of point C in figure 166 of the Appendix.

Span 1
33'-1¾"

Span 2
28'-0"

1 ft. = 0.3048 m

24"/45" P.C. I Girder

20"/30" P.C. I Girder

48°47'

7

4   do   5

3   do   do   13

2   do   do   14

Traffic Direction   do   do   15

1   do   do   16

9,12
10,11   8   do   do   6

₵ Span   ₵ Brg.   ₵ Span   ₵ Brg.

Intermediate
Diaphragms   ₵ Brg.   Brg.

Framing Plan – North Bound

Intermediate
Diaphragm   8"   9"   6"   6"

2"

9   10

12   11   6"   24"
typ.

2"

4"

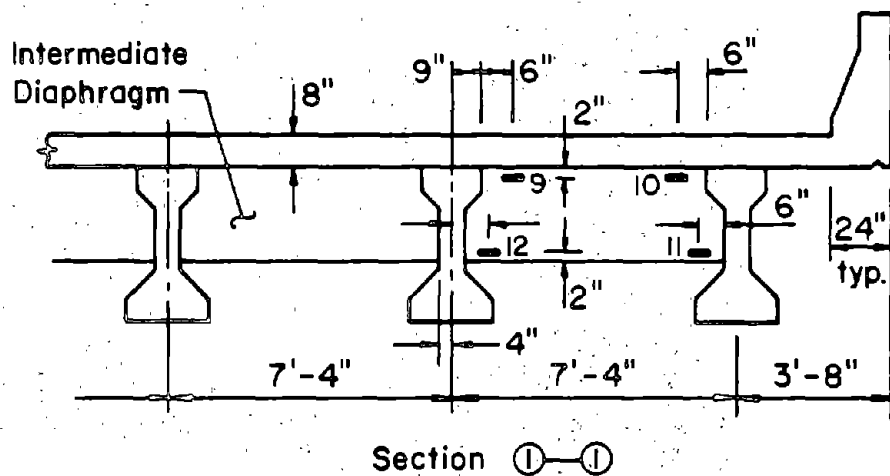7'-4"   7'-4"   3'-8"

Section ①—①

Figure 25.   Partial plan and cross section of superstructure showing locations
of transducers and strain gauges.

54

Figure 26. Aerial view of Route 33 looking north.

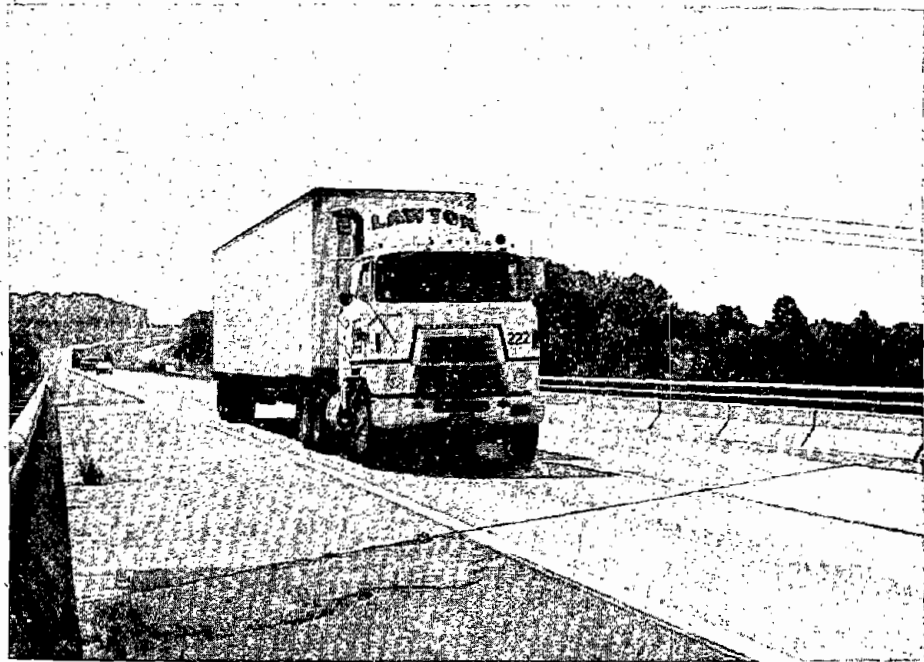Figure 27. Aerial view of bridges over State Park Road.

Figure 28. Approach to the NB Bridge.

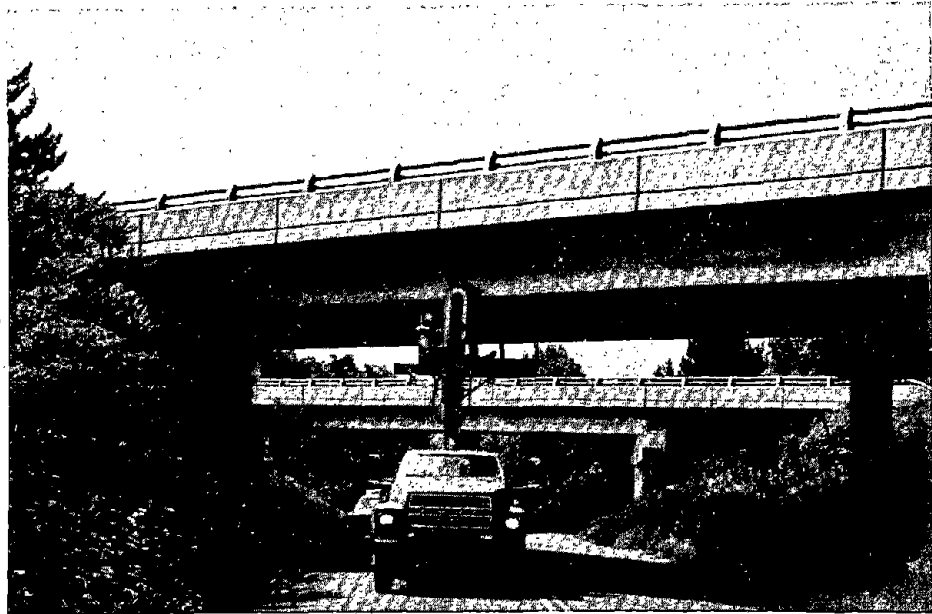Figure 29. Looking north over the NB Bridge.

Figure 30. Instrumenting span 2 from PADOT life truck.
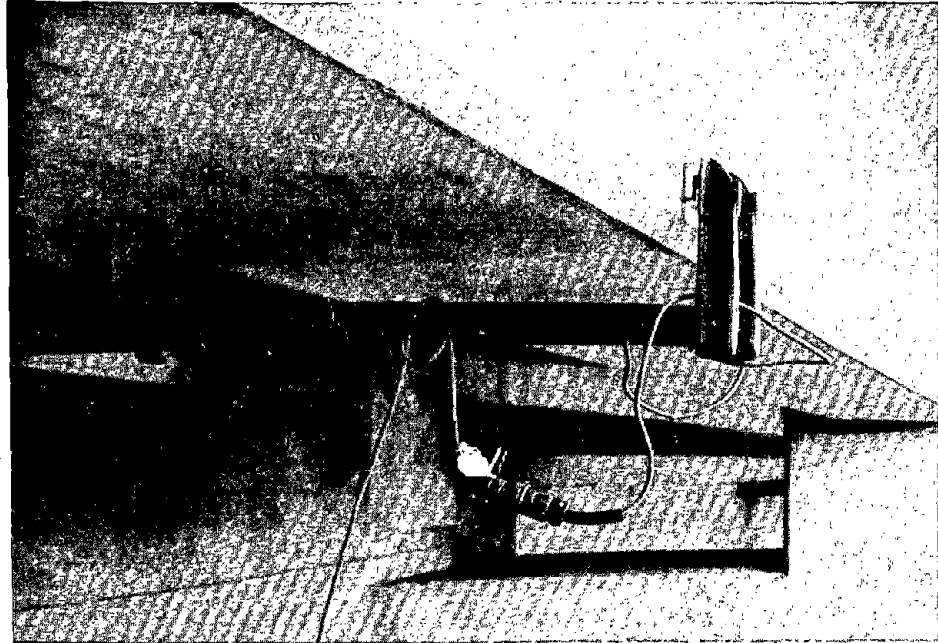

Figure 31. Method of clamping transducers to the prestressed concrete I-girder (span 3).
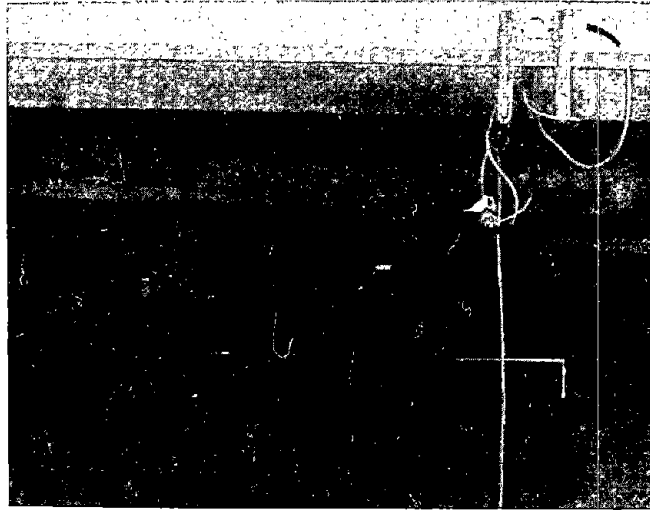
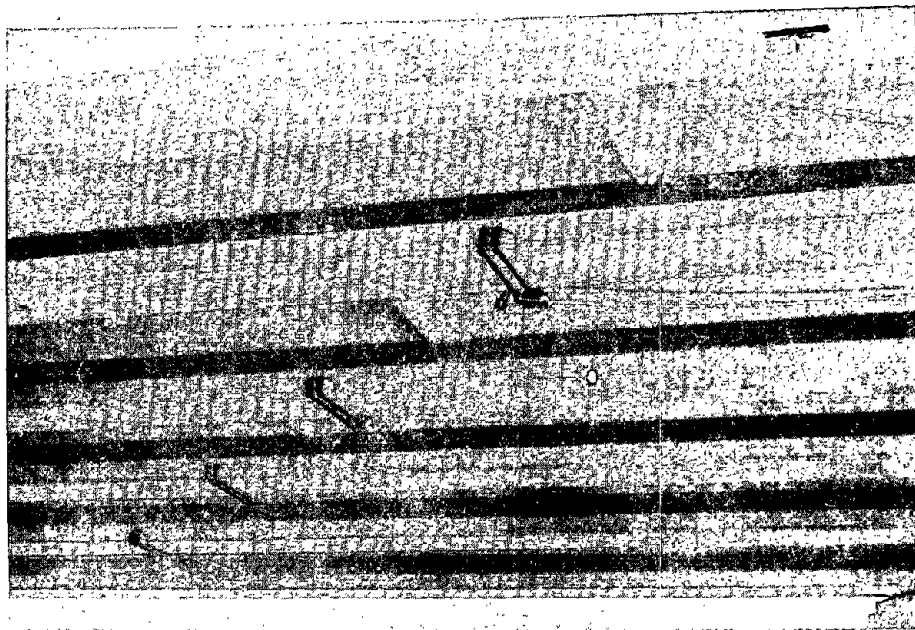Figure 32. View of transducer between two clamps.

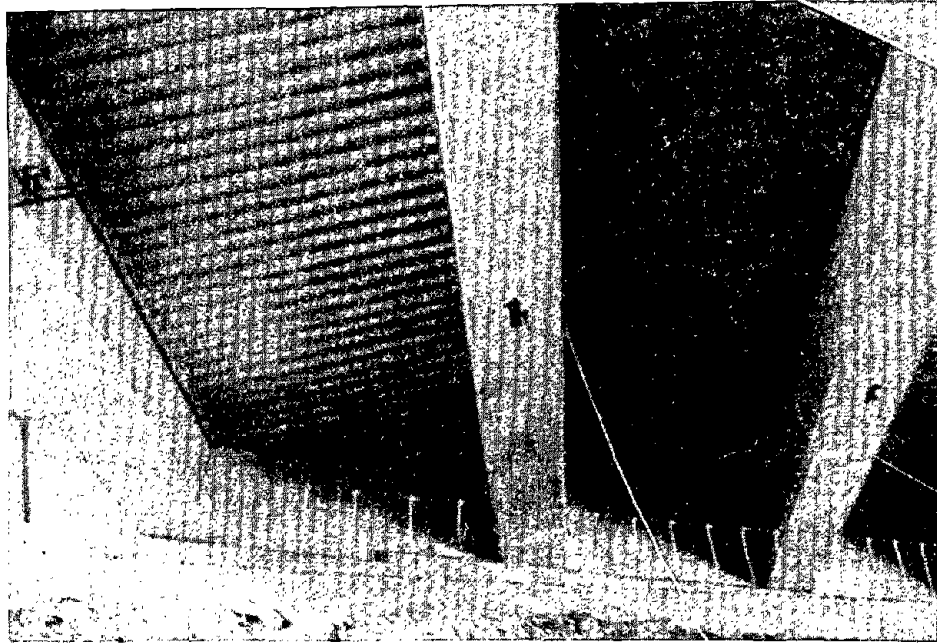Figure 33. Transducers and strain gauges on span 2.

58

Figure 34.   Transducers and strain gauges on span 3.
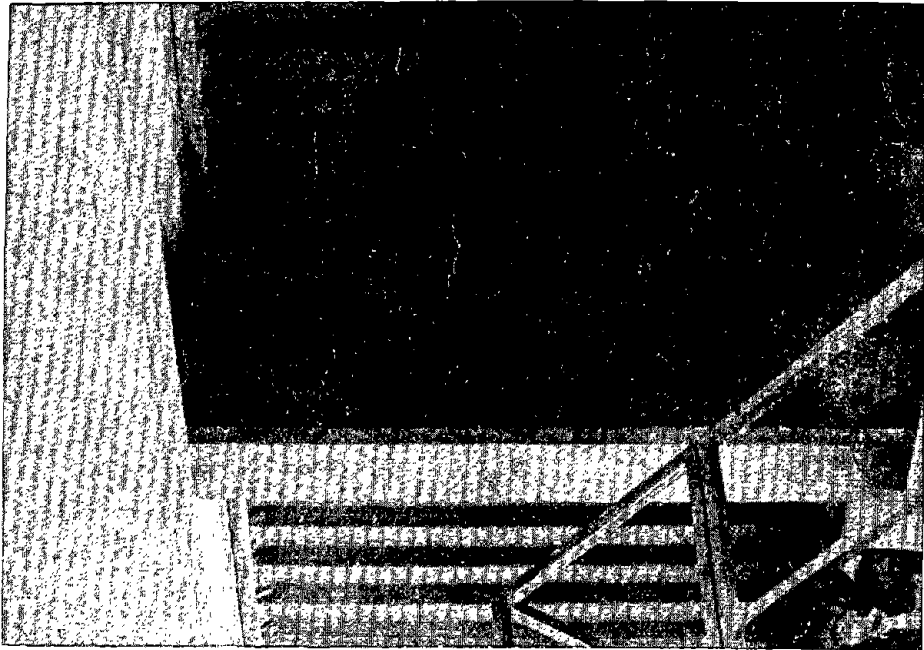

Figure 35.   Strain gauges on the diaphragm.

59

RESULTS OF FIELD STUDY

1. <u>Data Processing</u>

All data acquired in the field studies were processed in Fritz Labora-
tory by the WIM+RESPONSE System MINC 11/23 computer after completion of the
field studies. All figures contained in this chapter were first displayed on
the VT-125 Graphics CRT, then plotted using the LA-50 portable graphics
printer. The computer programs used to process the data are described in
detail in reference 29. The source codes of the programs are contained in
the Master Program Library (MPL) for the system.[29]

To obtain reasonably accurate axle and gross weights with the WIM+RESPONSE
System only one truck at a time should be weighed (single truck events). The
simultaneous presence of other heavy vehicles results in erroneous weigh data.
Cars have a negligible effect on the data. On the other hand it is desirable
to obtain some response data when more than one heavy truck is crossing the
bridge at the same time in order to sample maximum values of response. Since
the system acquires simultaneous weight and response data, both conditions can-
not be met at the same time. It is necessary to exclude the multiple truck
weight data from the data base used to compute GVW distribution.

When the keypad option is selected this is easily accomplished in one of
two ways: (1) the operator can make a separate note of the multiple truck
events so that the corresponding erroneous weight data are excluded when pro-
cessing to obtain the GVW distribution, or (2) the single truck and multiple
truck events can be stored on separate disks. When the automatic mode is
selected, separation of the weight data is made more difficult. It was
observed in the field however that data produced by a multiple truck event
frequently resulted in negative or unusually high or low values of one or more
axle weights being displayed. Based on this observation the weight data was
screened, prior to processing for GVW distribution, using the following
arbitrary (but reasonable and consistent) criteria. A multiple truck
weighing event is assumed to occur if: (1) the steering axle weight is less

60

than zero or greater than 20 kips (88.96 kN) and, (2) any other axle weight is less than zero or greater than 40 kips (177.92 kN). These criteria are consistent in that for most heavy trucks having two wheels on the steering axle and four wheels on the other axles the wheel load limits are the same. It is also reasonable to limit axle weights, rather than GVW, so that data from actual very heavy single trucks is not eliminated. For example, the choice of upper limits make it possible for data from an 18-wheel truck having a GVW of 180 kips (800.64 kN) to be included in the weight data base. The above criteria do not guarantee that all multiple truck events are excluded from the single truck event weight data, which may account for some of the very high truck weights which were computed.

The GVW histograms were generated using single trucks in lanes 1 and 2. The stress range histograms were generated using the reservoir (modified rain-flow) cycle counting method.[54] Strain rate is computed as the positive slope of the chord joining consecutive valleys and peaks of the strain-vs.-time curve. Although only the maximum strain rate may be of primary interest, strain rate histograms are provided for completeness of presentation of the field study results. The maximum stress vs. GVW relationships shown in this chapter were processed only for single trucks in lane 1. The maximum stress is computed from the maximum strain recorded at the gauge during the single truck event.

2. EB Route 22 Over 19th Street

a. GVW Distribution

The gross vehicle weight (GVW distribution computed for 4,239 trucks in lanes 1 and 2 is shown in figure 36. The maximum value of GVW is 147.4 kips (655.6 kN).

61

b. Stress Range Distribution

   Figures 37 through 49 show the stress range distributions for 13 of the
16 gauges computed by the reservoir cycle counting method using data from all
4,680 trucks in lanes 1 and 2. Data suitable for computing stress ranges was
not available from transducer 6 and train gauges 9 and 10. The stress range
histograms were computed using all cycles (no lower cutoff) of the strain-vs.-
time response curve for each single and multiple truck event. Note that for
figures 44 through 47 the scale of the vertical axis is different from the
remaining figures. The maximum computed stress range is provided below each
figure. Also provided are the Miners and RMS equivalent stress ranges.[6]

c. Strain Rate Distribution

   Figures 50 through 56 show strain rate distributions computed for 6 of
the 16 gauges using data from all 4,680 trucks in lanes 1 and 2. The six
gauges were selected to provide representative strain rates for the main
girders and diaphragm members. The strain rate histograms were computed using
all cycles (no threshold) of the strain-vs.-time response curve for each
single and multiple truck event. The maximum computed strain rate is provided
below each figure.

d. Maximum Stress vs. GVW

   Figures 57 through 63 show the relationships between maximum stress (S)
and GVW for 7 of the 16 gauges, computed using data from 2,861 single trucks
in lane 1 only. The seven gauges were selected to provide representative
maximum stress-vs.-GVW relationships for the main girders and diaphragm
members. In addition the absolute maximum stress is also provided below each
figure. Also provided are the equation of the linear regression line in psi
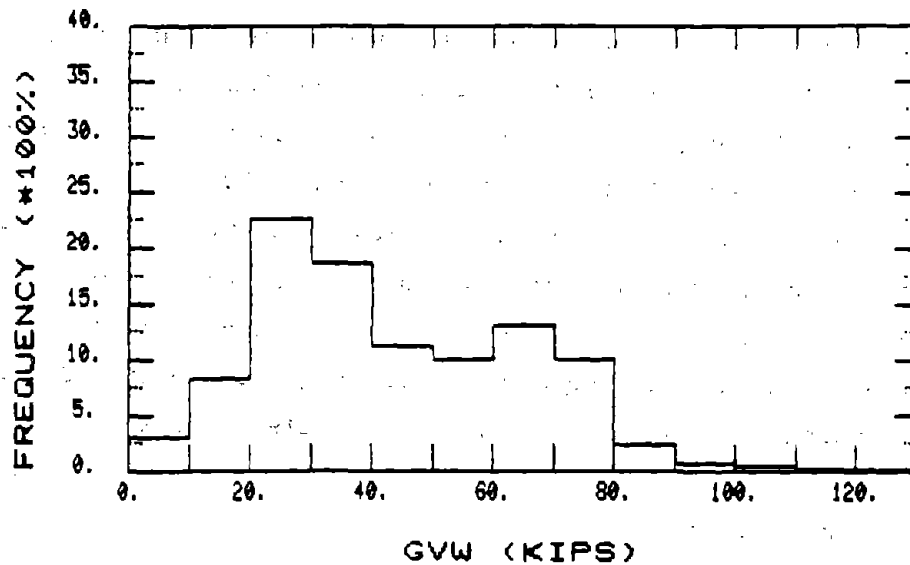and kip units and the sample correlation coefficient.

62

Figure 36. GVW distribution: max. GVW - 147.4 kips (655.6 kN): EB Route 22
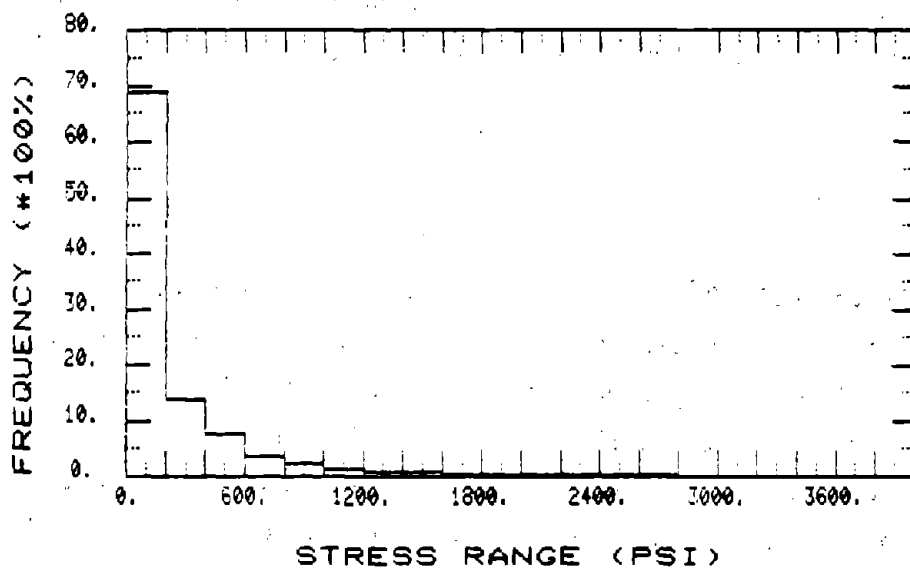over 19th Street.

Figure 37. S_r distribution--gauge 1: max. S_r = 5.8 ksi (40.0 MPa): miner
S_r = 0.66 ksi (4.6 MPa): RMS S_r = 0.45 ksi (3.1 MPa): EB Route
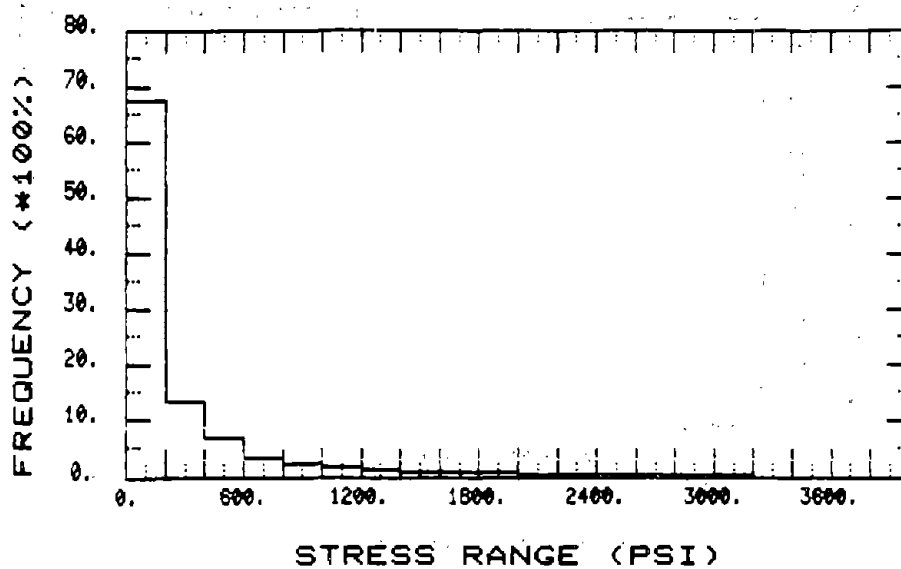22 over 19th Street.

Figure 38. S_r distribution--gauge 2: max. S_r = 5.6 ksi (38.6 MPa): miner S_r = 0.78 ksi (5.4 MPa): RMS S_r = 0.53 ksi (3.7 MPa): EB Route 22 over 19th Street.
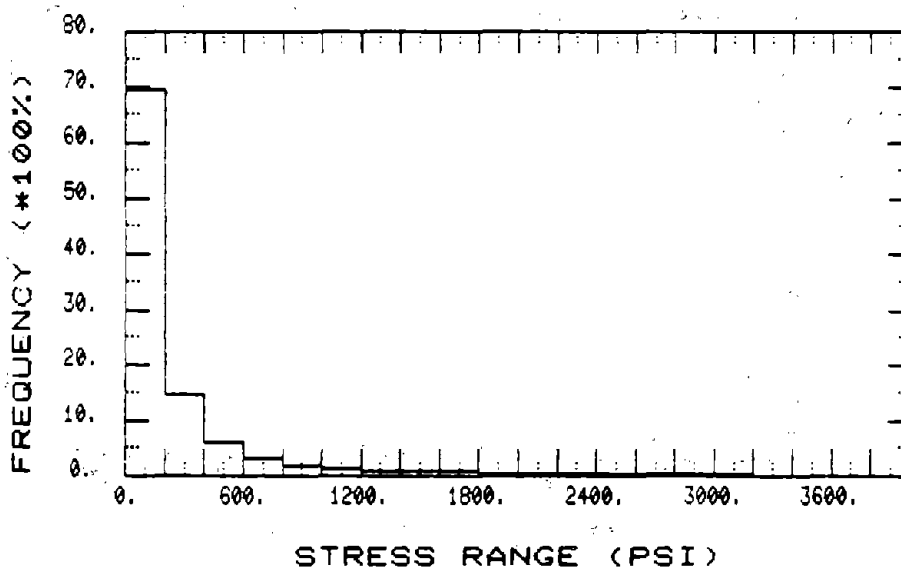

Figure 39. S_r distribution--gauge 3: max. S_r = 5.4 ksi (37.2 MPa): miner S_r = 0.73 ksi (5.0 MPa): RMS S_r = 0.48 ksi (3.3 MPa): EB Route 22 over 19th Street.
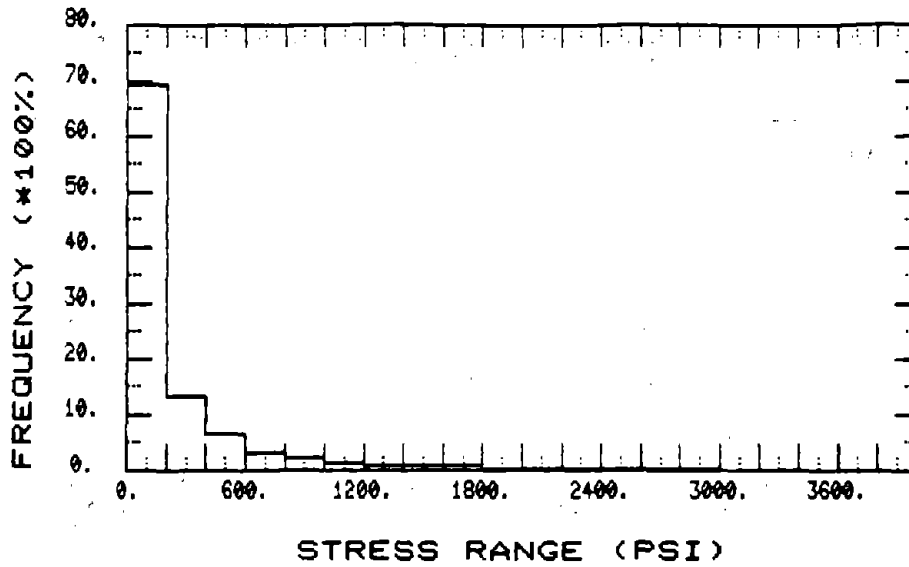
Figure 40. S_r distribution--gauge 4: max. S_r = 6.2 ksi (42.7 MPa): miner S_r = 0.72 ksi (5.0 MPa): RMS S_r = 0.48 ksi (3.3 MPa): EB Route 22 over 19th Street.
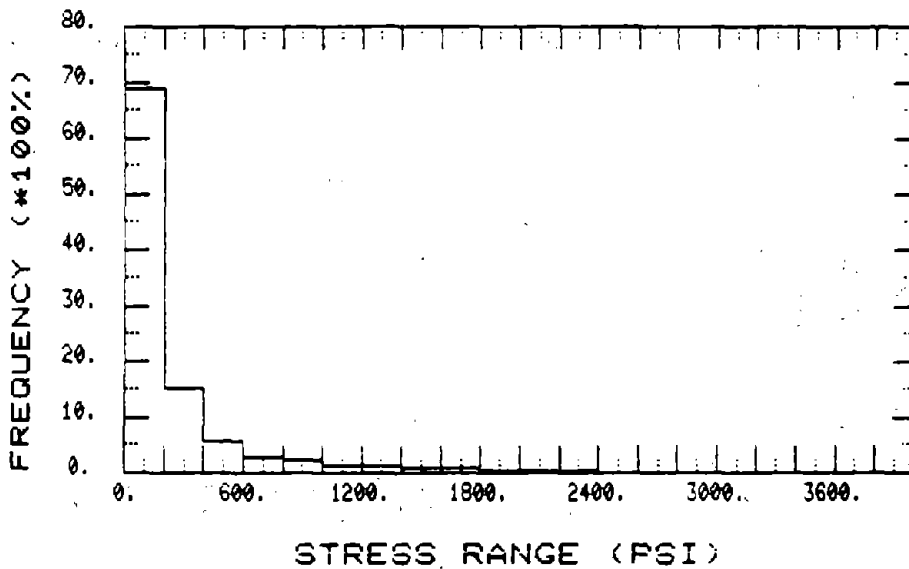

Figure 41. S_r distribution--gauge 5: max. S_r = 5.2 ksi (35.9 MPa): miner S_r = 0.63 ksi (4.3 MPa): RMS S_r = 0.44 ksi (3.0 MPa): EB Route 22 over 19th Street.
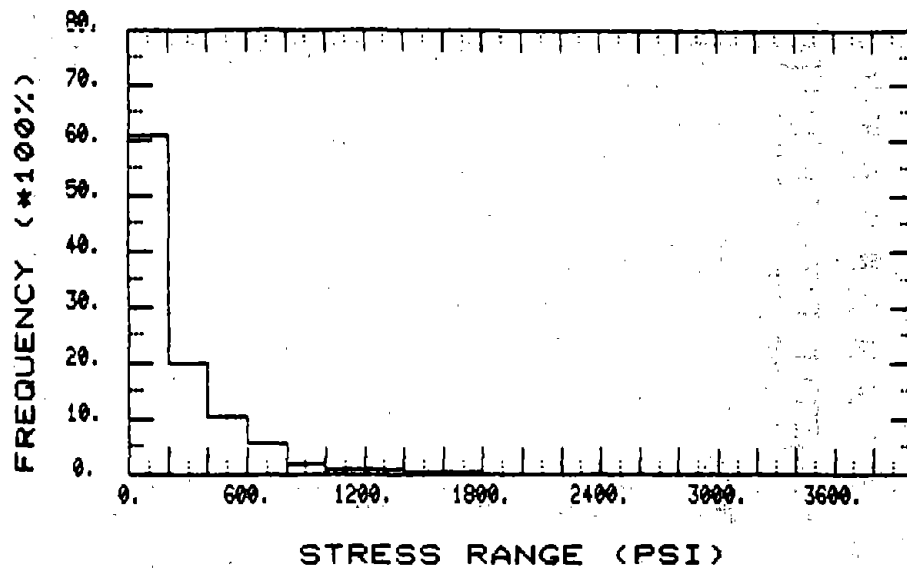
Figure 42. S_r distribution--gauge 7: max. S_r = 3.8 ksi (26.2 MPa): miner
S_r = 0.46 ksi (3.2 MPa): RMS S_r = 0.36 ksi (2.5 MPa): EB Route
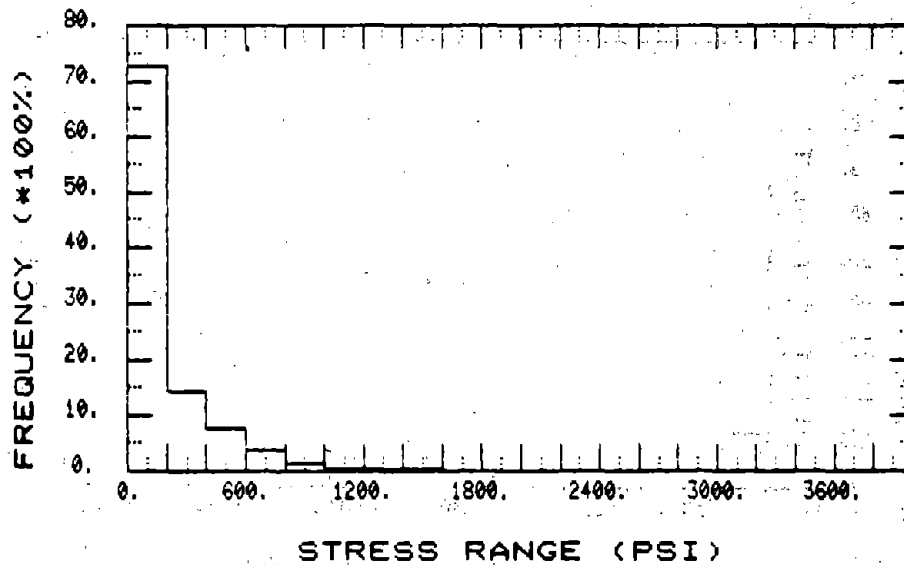22 over 19th Street.

Figure 43. S_r distribution--gauge 8: max. S_r = 3.4 ksi (23.4 MPa): miner
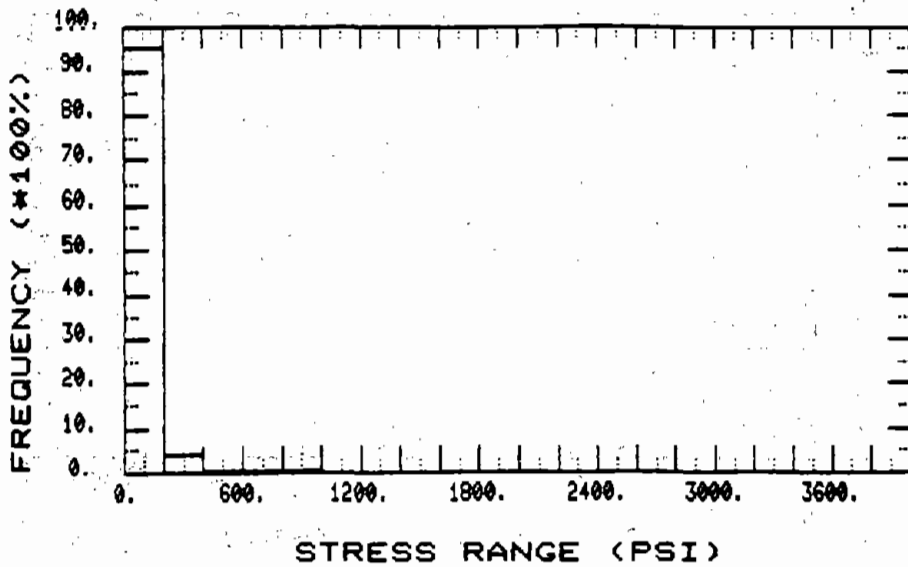S_r = 0.38 ksi (2.6 MPa): RMS S_r = 0.28 ksi (1.9 MPa): EB Route
22 over 19th Street.

66

Figure 44. S_r distribution--gauge 11: max. S_r = 3.8 ksi (26.2 MPa): miner S_r = 0.18 ksi (1.2 MPa): RMS S_r = 0.13 ksi (0.9 MPa): EB Route 22 over 19th Street.
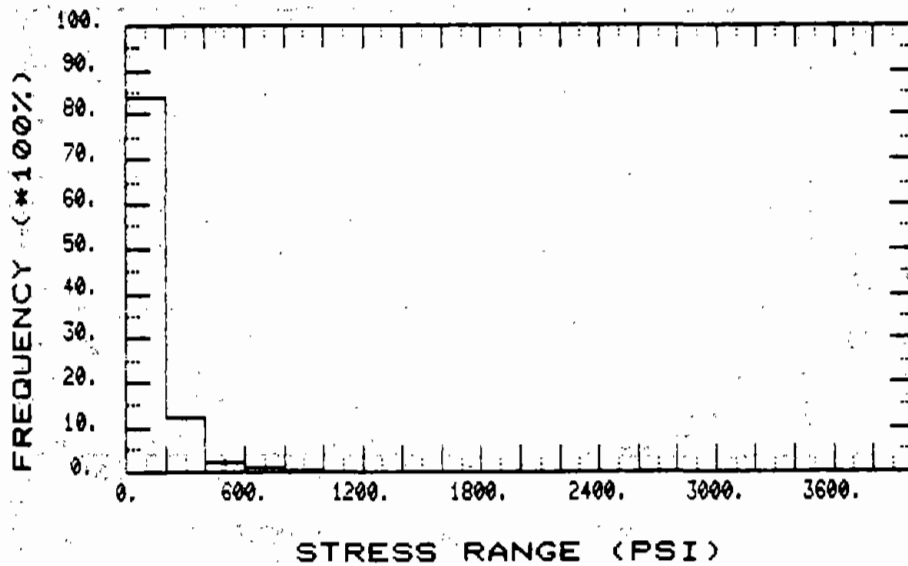

Figure 45. S_r distribution--gauge 12: max. S_r = 4.2 ksi (29.0 MPa): miner S_r = 0.27 ksi (1.9 MPa): RMS S_r = 0.19 ksi (1.3 MPa): EB Route 22 over 19th Street.
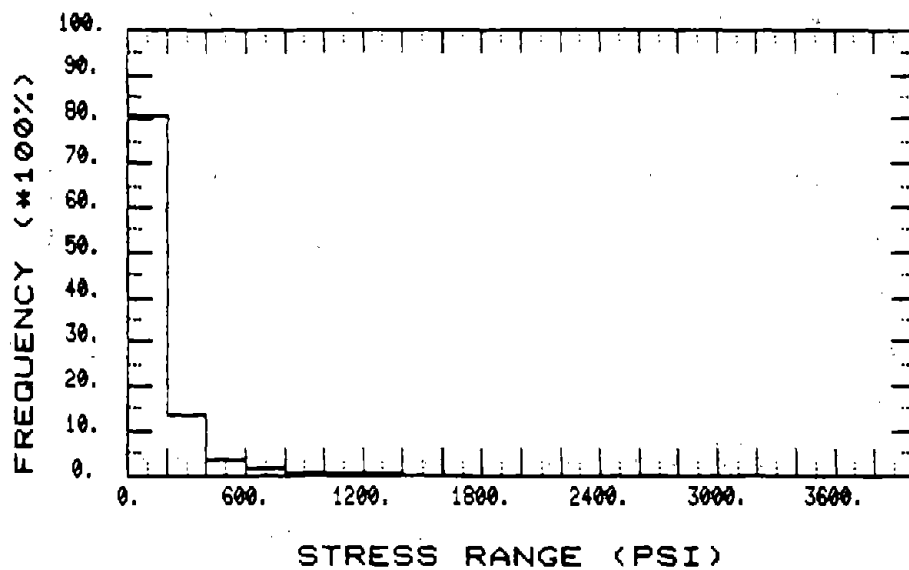
67

Figure 46. S_r distribution--gauge 13. max. S_r = 2.0 ksi (13.8 MPa): miner S_r = 0.29 ksi (2.0 MPa): RMS S_r = 0.22 ksi (1.5 MPa): EB Route 22 over 19th Street
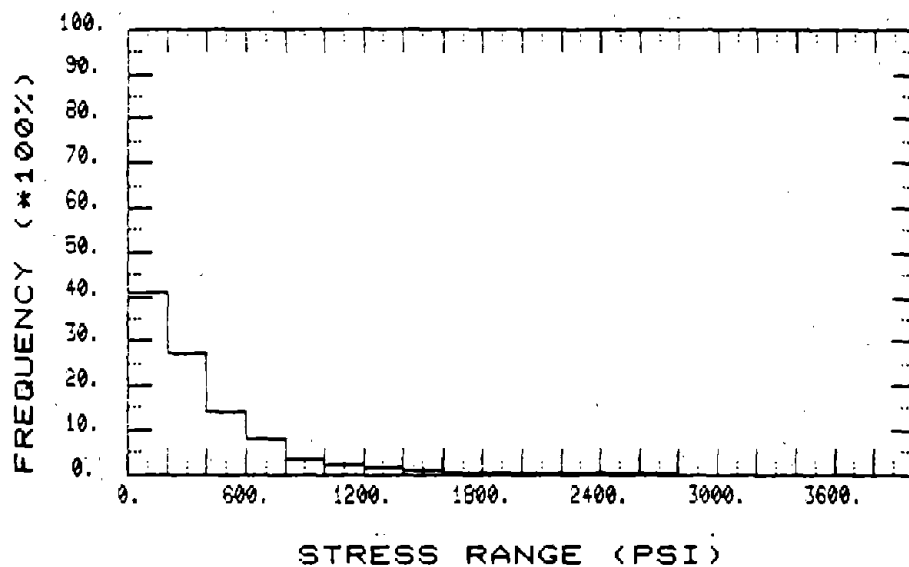

Figure 47. S_r distribution--gauge 14: max. S_r = 5.6 ksi (38.6 MPa): miner S_r = 0.75 ksi (5.2 MPa): RMS S_r = 0.55 ksi (3.8 MPa): EB Route 22 over 19th Street.
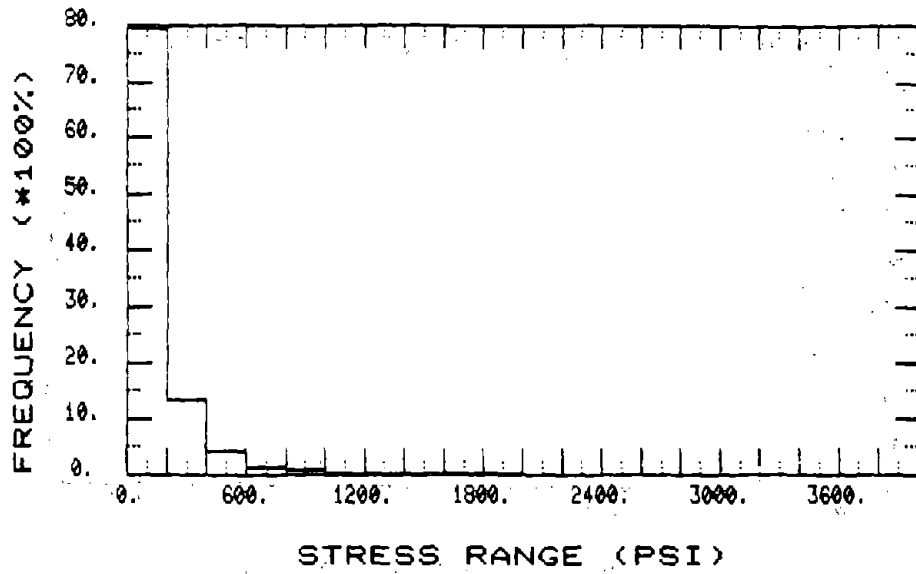
Figure 48. S_r distribution--gauge 15: max. S_r = 3.2 ksi (22.1 MPa): miner S_r = 0.40 ksi (2.8 MPa): RMS S_r = 0.26 ksi (1.8 MPa): EB Route 22 over 19th Street.
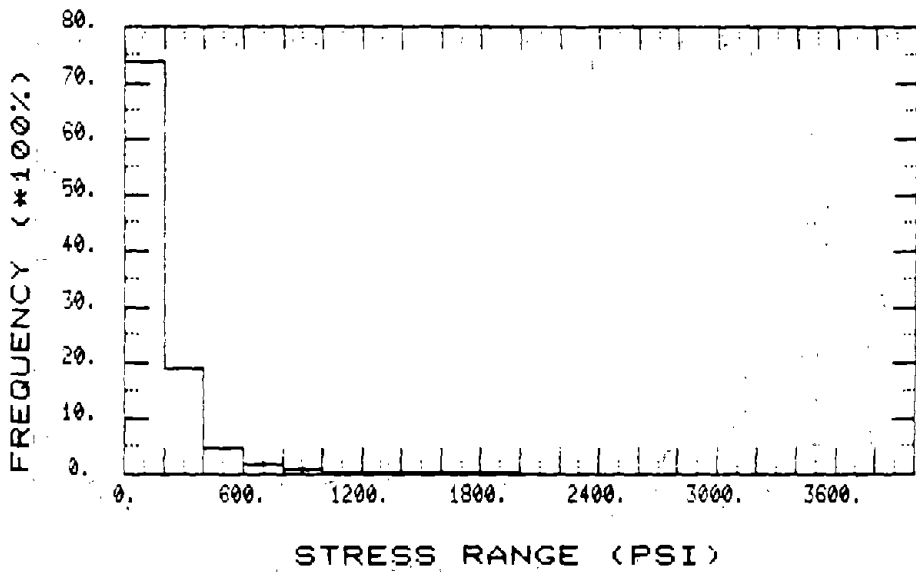

Figure 49. S_r distribution--gauge 16: max. S_r = 2.8 ksi (19.3 MPa): miner S_r = 0.37 ksi (2.6 MPa): RMS S_r = 0.26 ksi (1.8 MPa): EB Route 22 over 19th Street.
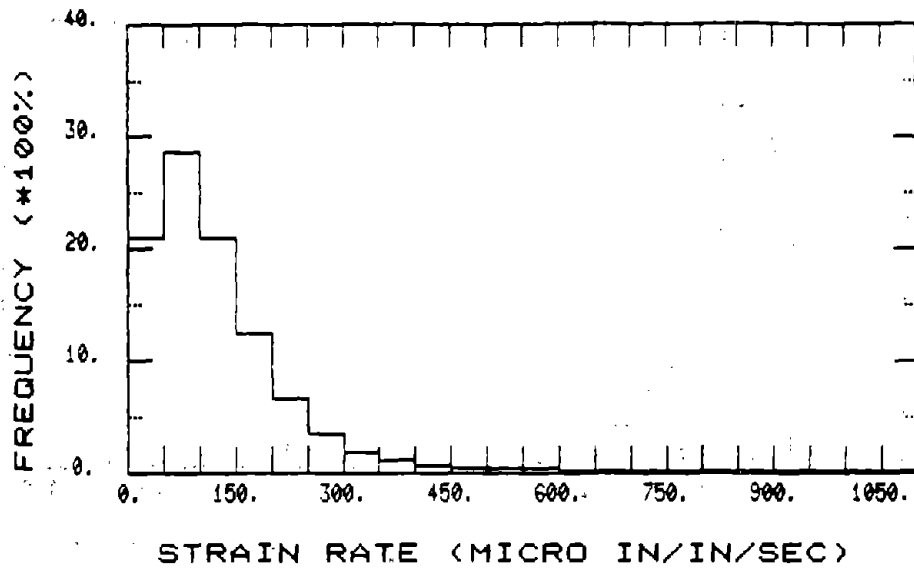
69

Figure 50.   <u>Strain rate distribution--gauge 1</u>: max. strain rate = 6,458 micro
in/in/s (6,458 micro m/m/s): EB Route 22 over 19th Street.

Figure 51.   <u>Strain rate distribution--gauge 2</u>: max. strain rate = 5,766 micro
in/in/s (5,766 micro m/m/s): EB Route 22 over 19th Street.

Figure 52. Strain rate distribution—gauge 3: max. strain rate = 4,216 micro in/in/s (4,216 micro m/m/s): EB Route 22 over 19th Street.

Figure 53. Strain rate distribution—gauge 8: max. strain rate = 3,375 micro in/in/s (3,375 micro m/m/s): EB Route 22 over 19th Street.

Figure 54.   Strain rate distribution--gauge 12:   max. strain rate = 4,187 micro
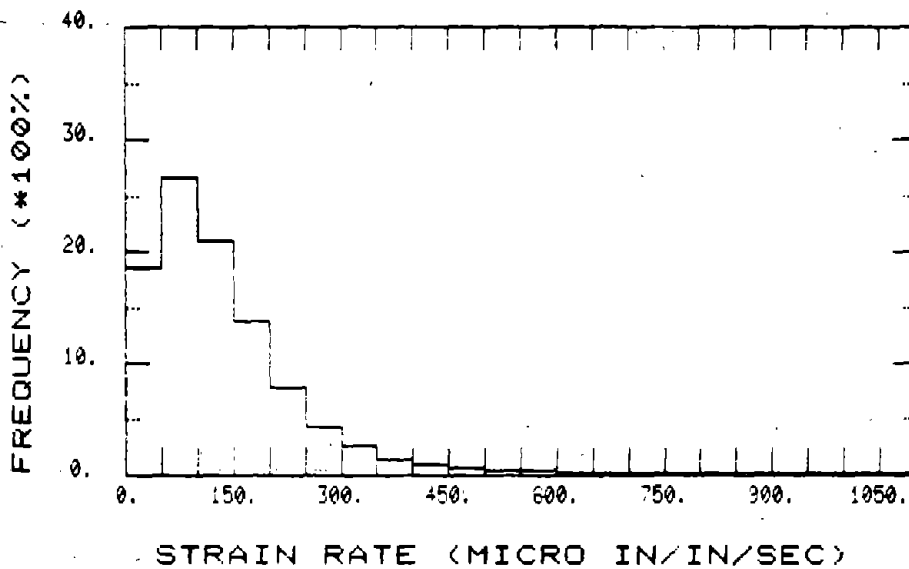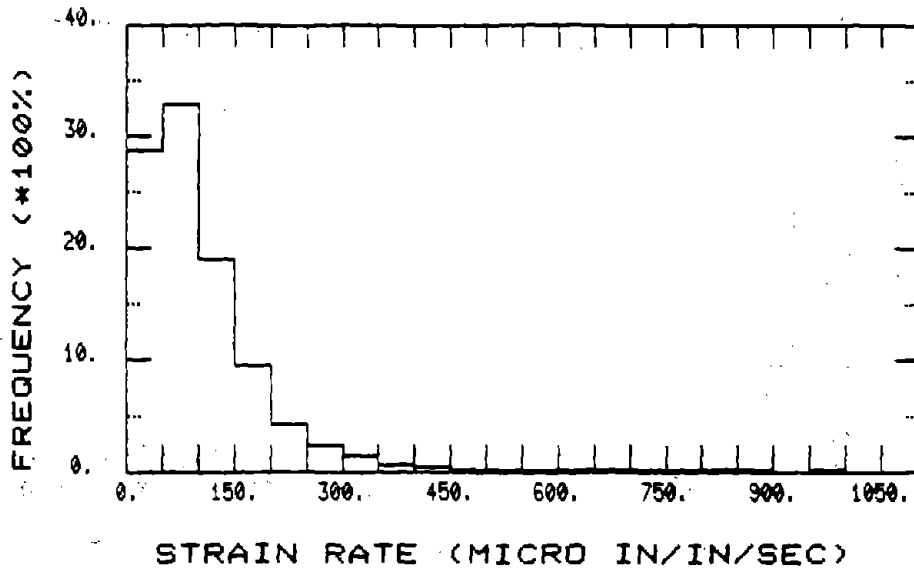in/in/s (4,187 micro m/m/s):   EB Route 22 over 19th Street.

Figure 55.   Strain rate distribution--gauge 14:   max. strain rate = 5,000 micro
in/in/s (5,000 micro m/m/s):   EB Route 22 over 19th Street.
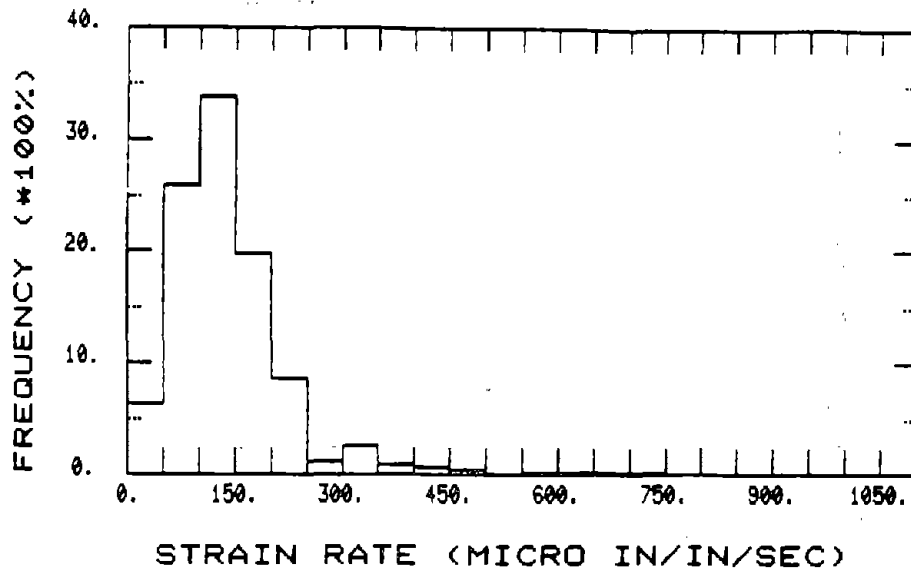
Figure 56. Strain rate distribution—gauge 15: max. strain rate = 1,700 micro in/in/s (1,700 micro m/m/s): EB Route 22 over 19th Street.
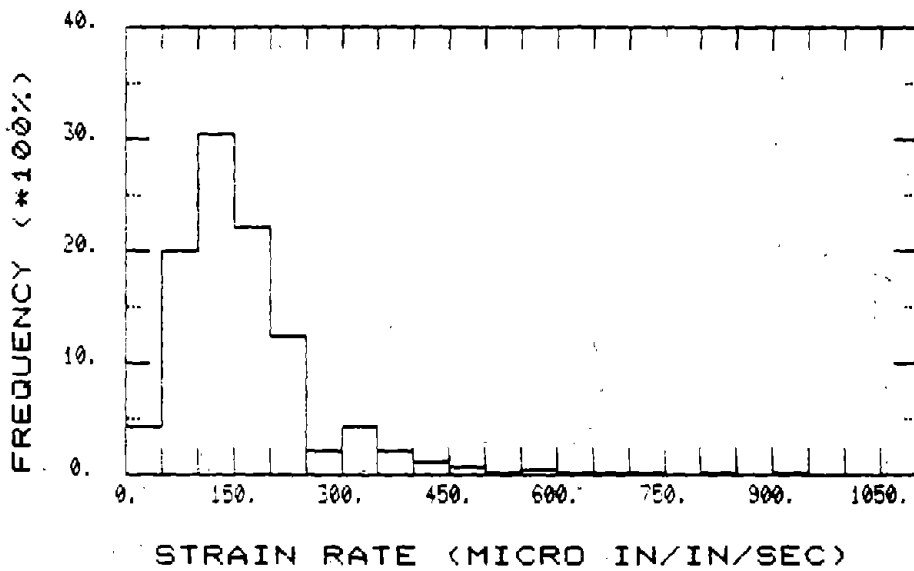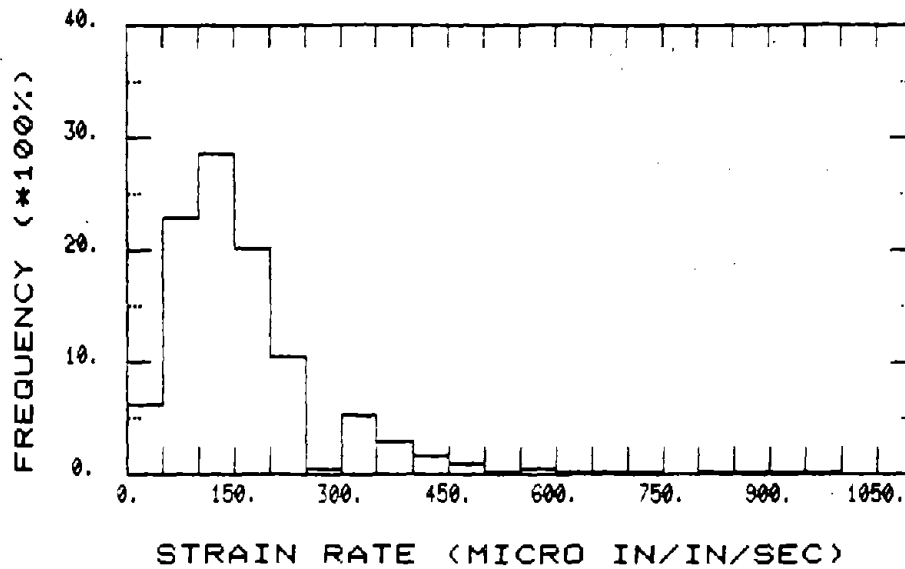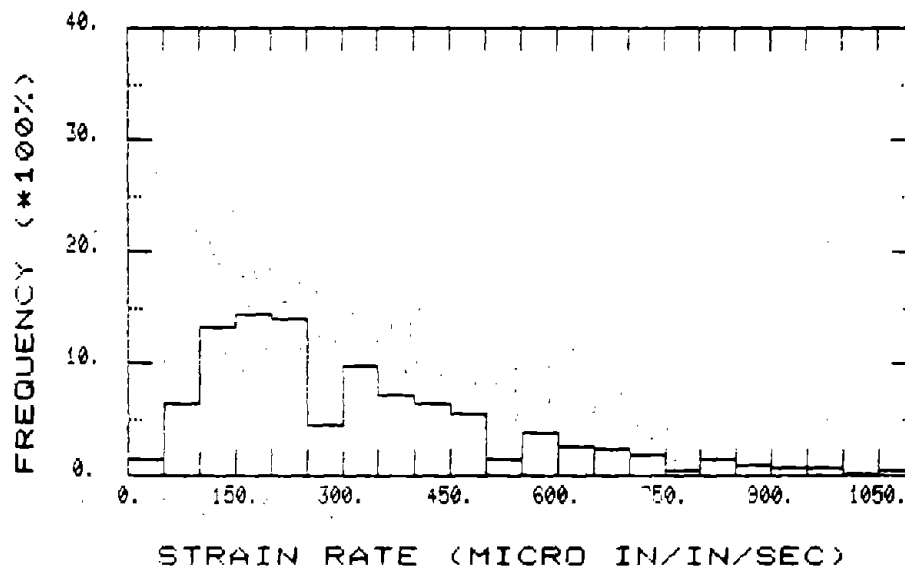

Figure 57. Max. stress (S) vs. GVW—gauge 1: absolute max. stress = 7.6 ksi (52.4 MPa): equation of linear regression line, S (psi) = 303.5 + 22.9 GVW (kips): correlation coefficient = 0.827: EB Route 22 over 19th Street.

73

Figure 58.   Max. stress (s) vs. GVW--gauge 2:   absolute max. stress = 5.3 ksi
(36.5 MPa):   equation of linear regression line, S (psi) = 382.1 +
28.1 GVW (kips):   correlation coefficient = 0.892:   EB Route 22
over 19th Street.
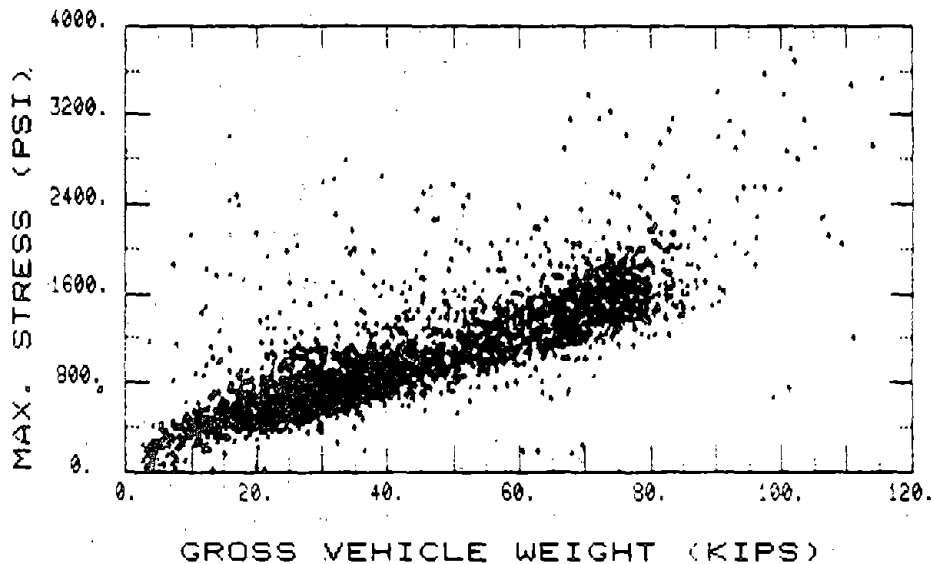
Figure 59.   Max. stress (S) vs. GVW--gauge 3:   absolute max. stress = 9.4 ksi
(64.8 MPa):   equation of linear regression line, S (psi) = 188.7 +
19.3 GVW (kips):   correlation coefficient = 0.778:   EB Route 22
over 19th Street.

74
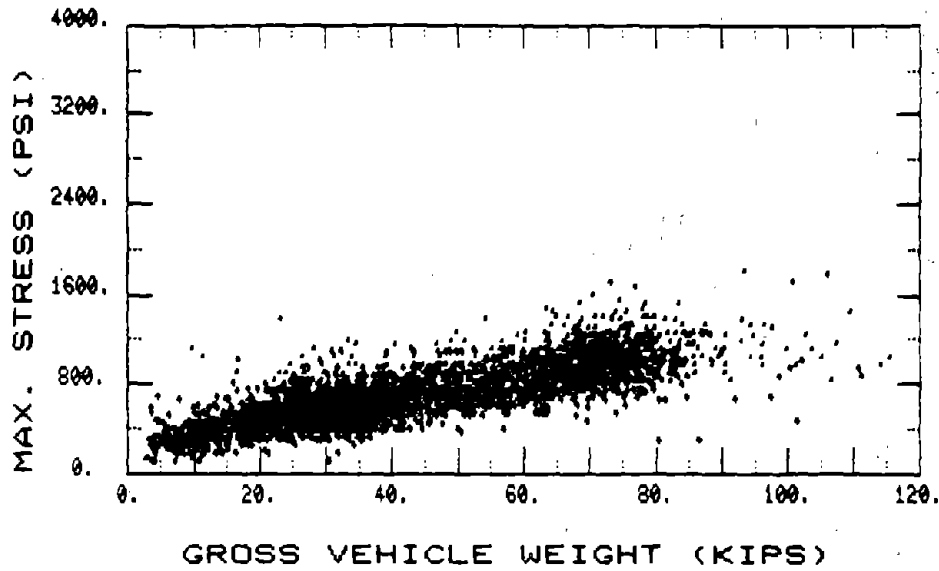
Figure 60. Max. stress (S) vs. GVW--gauge 8: absolute max. stress = 1.8 ksi
(12.4 MPa): equation of linear regression line, S (psi) = 268.6 +
9.8 GVW (kips): correlation coefficient = 0.806: EB Route 22 over
19th Street.
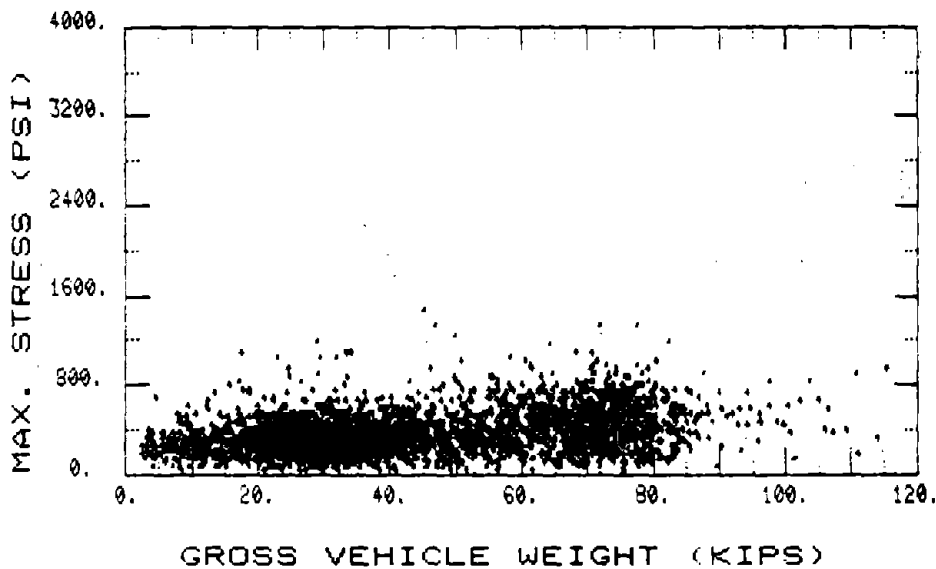
Figure 61. Max. stress (S) vs. GVW--gauge 12: absolute max. stress = 1.5 ksi
(10.3 MPa): equation of linear regression line, S (psi) = 228.9 +
2.9 GVW (kips): correlation coefficient = 0.330: EB Route 22 over
19th Street.
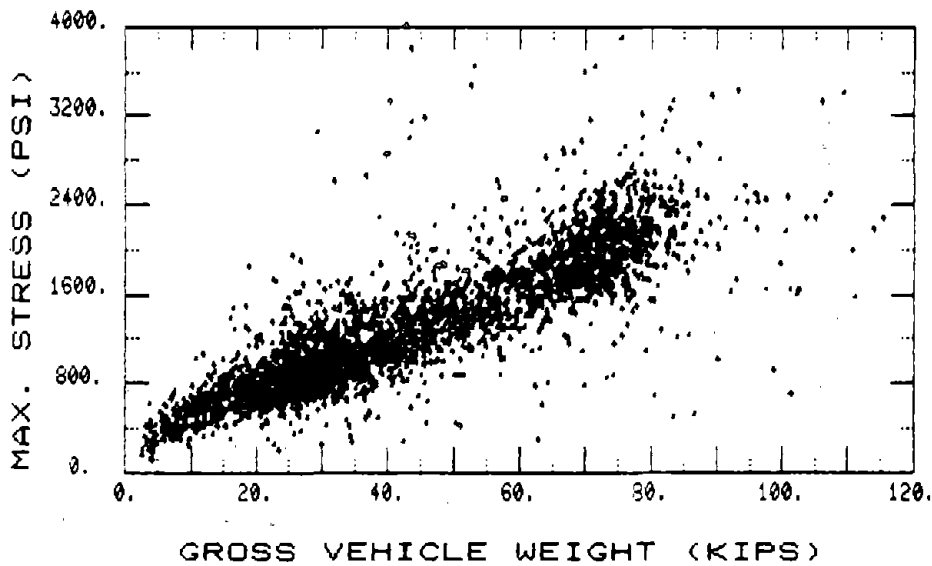
Figure 62. <u>Max. stress (S) vs. GVW--gauge 14</u>: absolute max. stress = 4.4 ksi (30.3 MPa): equation of linear regression line, S (psi) = 781.4 + 22.4 GVW (kips): correlation coefficient = 0.751: EB Route 22 over 19th Street.
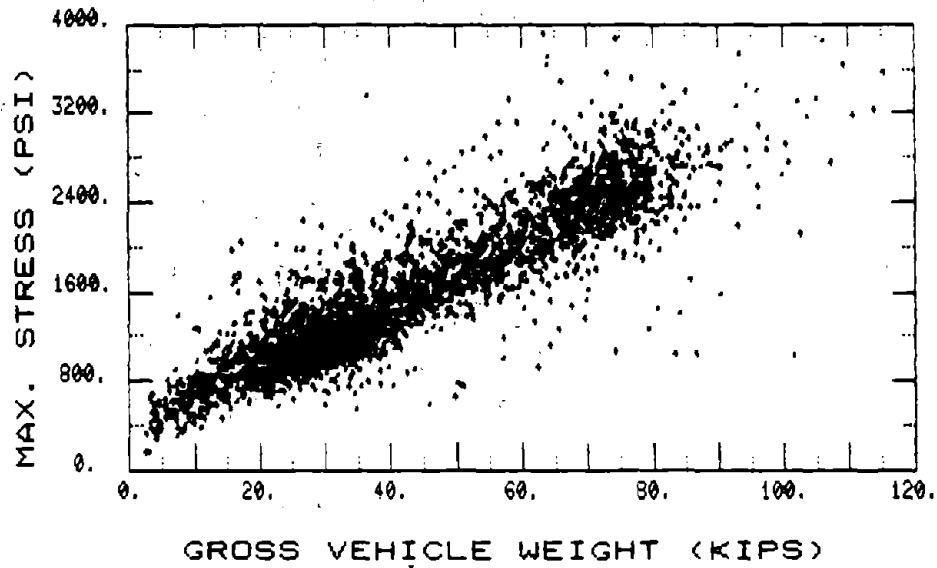

Figure 63. <u>Max. stress (S) vs. GVW--gauge 15</u>: absolute max. stress = 2.8 ksi (19.3 MPa): equation of linear regression line, S (psi) = 166.5 + 5.7 GVW (kips): correlation coefficient = 0.467: EB Route 22 over 19th Street
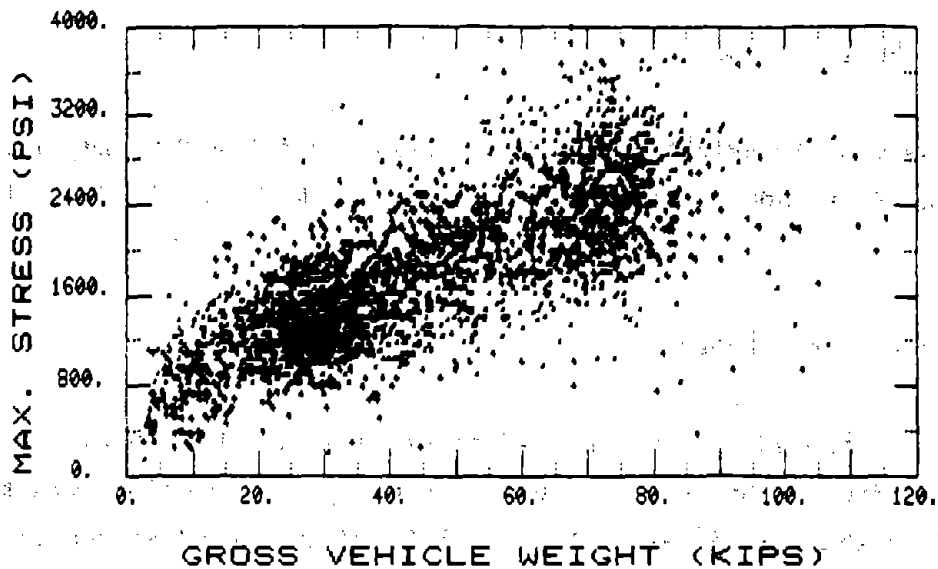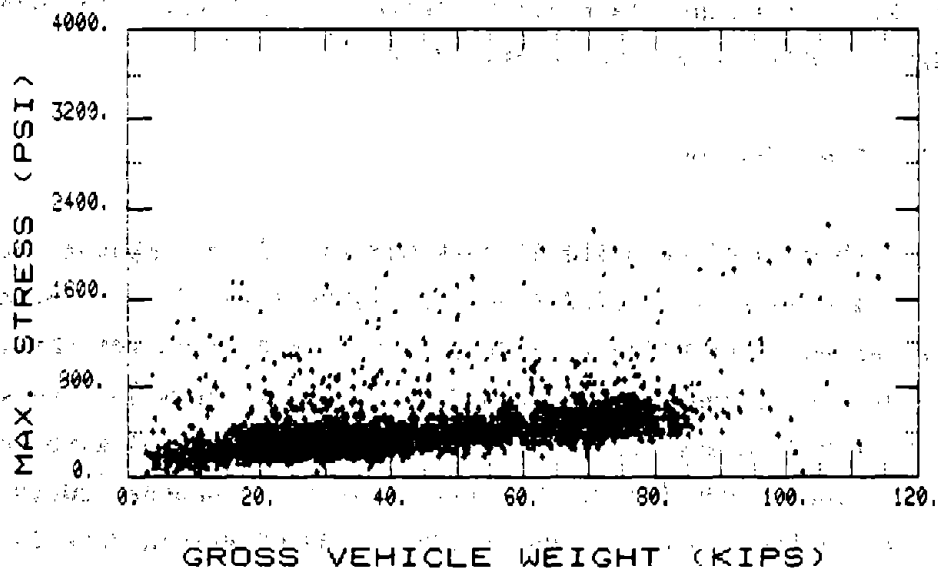
76

3. WB Route 22 Over 19th Street

a. GVW Distribution

The gross vehicle weight distribution computed for 5,116 single trucks in lanes 1 and 2 is shown in figure 64. The maximum value of GVW is 160 kips (711.7 kN).

b. Stress Range Distribution

Figures 65 through 79 show the stress range distributions for 15 of the 16 gauges computed by the reservior cycle counting method using data from 6,782 trucks in lanes 1 and 2. Data suitable for computing stress ranges were not available from transducer 6. Data from 330 trucks (3 disks) could not be used for response analysis. The stress range histograms were computed using all cycles (no threshold) of the strain vs.-time response curve for each single and multiple truck event. Note that for figures 74 through 77 the scale of the vertical axis is different from the remaining figures. The maximum computed stress range is provided below each figure. Also provided are the Miners and RMS equivalent stress ranges.[6]

c. Strain Rate Distribution

Figures 80 through 87 show strain rate distributions computed for 8 of the 16 gauges using data from 6,782 trucks in lanes 1 and 2. The eight guages were selected to provided representative strain rates for the main girders and diaphragm members. As explained above data from 330 trucks could not be used for response analysis. The strain rate histograms were computed using all cycles (no threshold) of the strain-vs.-time response curve for each single and multiple truck event. The maximum computed strain rate is provided below each figure. The large strain rate shown in figure 87 is due to a spike (see figure 139).

d. Maximum Stress vs. GVW

Figures 88 through 95 show the relationships between maximum stress (S) and GVW for 8 of the 16 gauges computed using data from 2,970 single trucks in lane 1 only. The eight gauges were selected to provide representative maximum stress-vs.-GVW relationships for the main girders and diaphragm members. In addition the absolute maximum stress is provided below each figure. Also provided are the equation of the linear regression line in psi and kip units and the sample correlation coefficient.
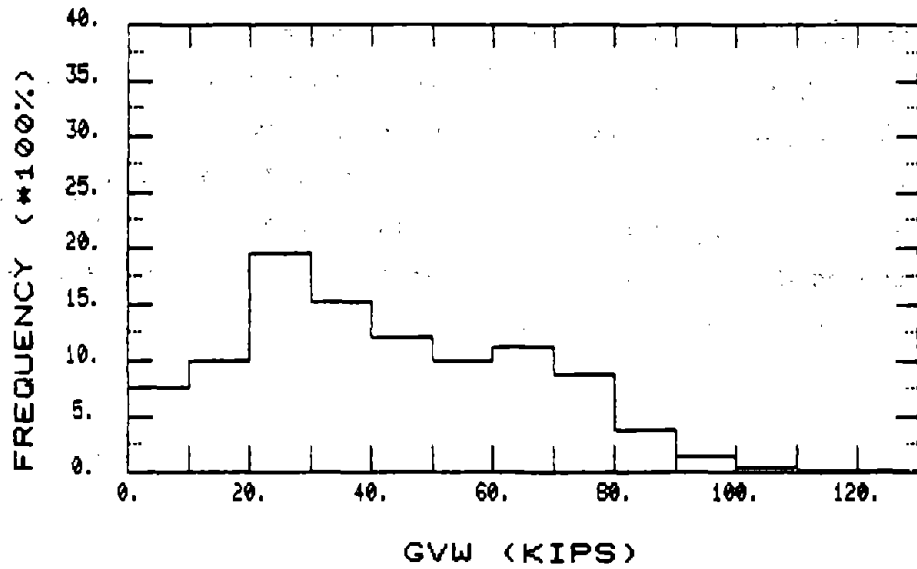
Figure 64. GVW distribution: max. GVW = 160 kips (711.7 kN): WB Route 22 over 19th Street.
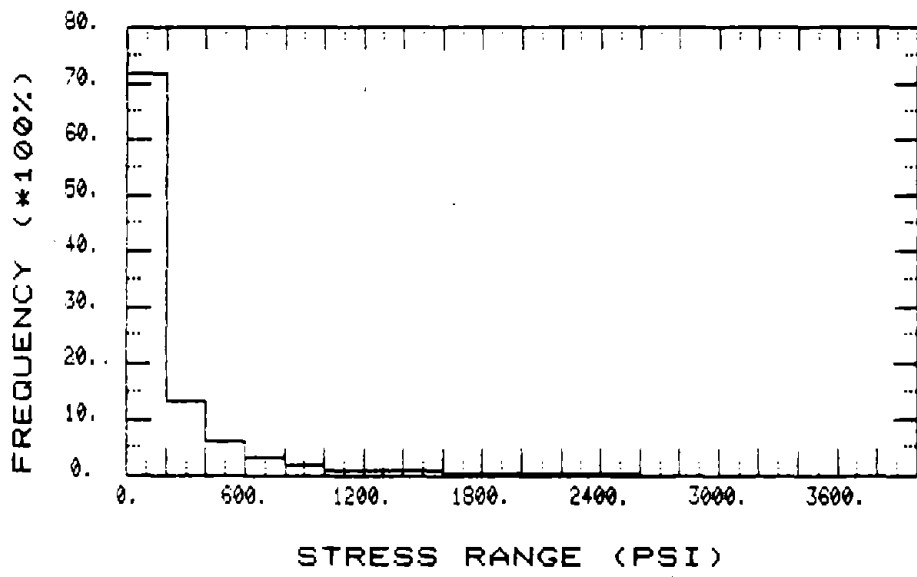
Figure 65. S_r distribution--gauge 1: max. S_r = 5.8 ksi (40.0 MPa): miner S_r = 0.61 ksi (4.2 MPa): RMS S_r = 0.41 ksi (2.8 MPa): WB Route 22 over 19th Street.
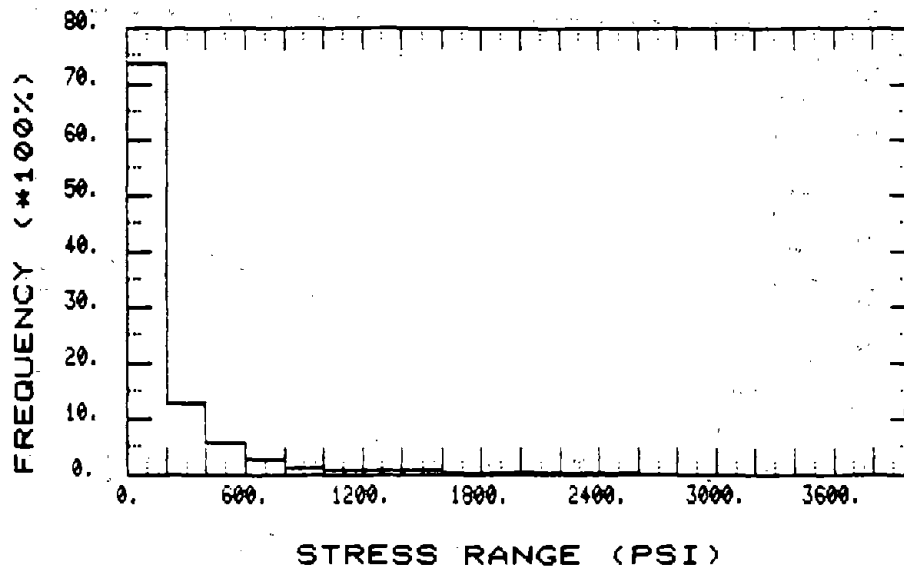
Figure 66. S_r distribution--gauge 2: max. S_r = 6.2 ksi (42.7 MPa): miner S_r = 0.61 ksi (4.2 MPa): RMS S_r = 0.40 ksi (2.8 MPa): WB Route 22 over 19th Street.
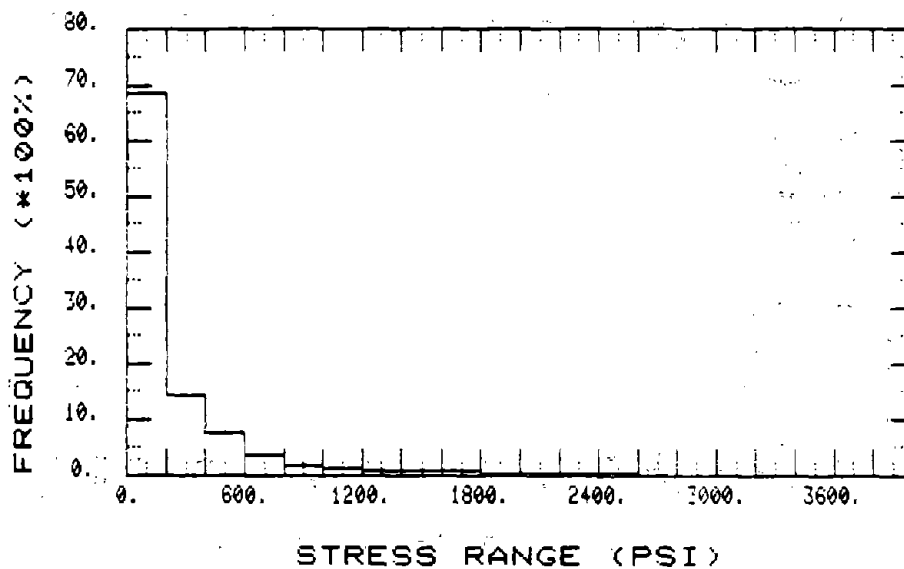
Figure 67. S_r distribution--gauge 3: max. S_r = 5.0 ksi (34.5 MPa): miner S_r = 0.64 ksi (4.4 MPa): RMS S_r = 0.43 ksi (3.0 MPa): WB Route 22 over 19th Street.

Figure 68. S$_r$ distribution--gauge 4: max. S$_r$ = 5.60 ksi (38.6 MPa): miner
S$_r$ = 0.64 ksi (4.4 MPa): RMS S$_r$ = 0.44 ksi (3.0 MPa): WB Route
22 over 19th Street.
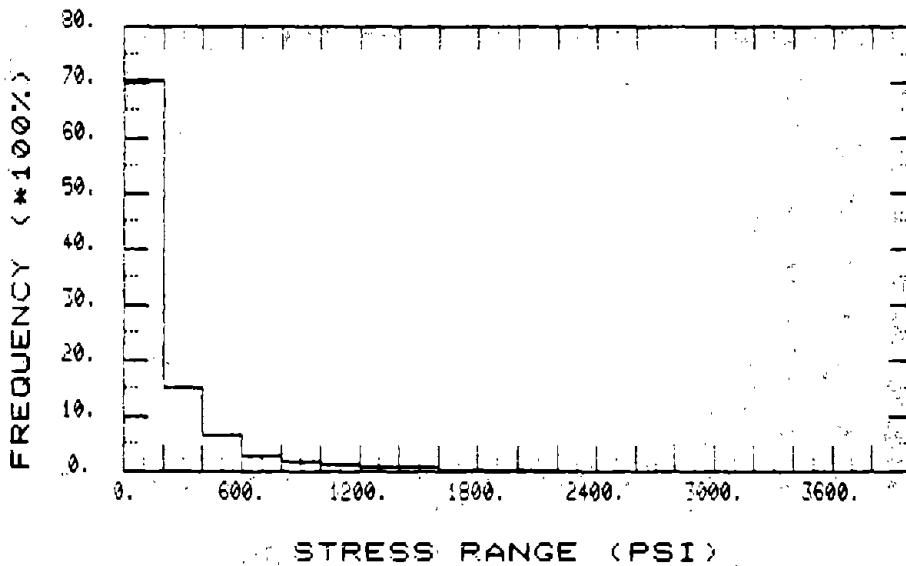
Figure 69. S$_r$ distribution--gauge 5: max. S$_r$ = 3.80 ksi (26.2 MPa): miner
S$_r$ = 0.52 ksi (3.6 MPa): RMS S$_r$ = 0.37 ksi (2.6 MPa): WB Route
22 over 19th Street.

81
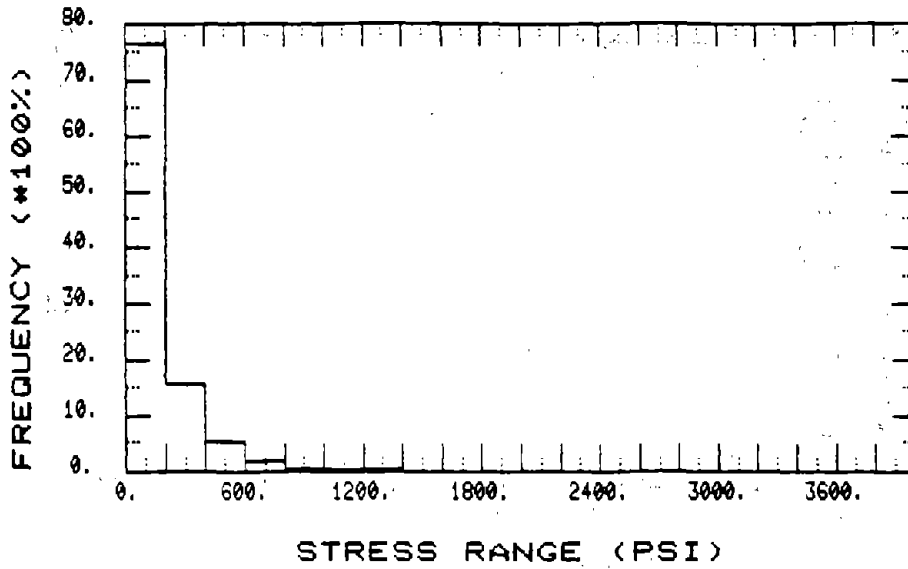
Figure 70. S_r distribution--gauge 7: max. S_r = 3.2 ksi (22.1 MPa): miner S_r = 0.34 ksi (2.3 MPa): RMS S_r = 0.24 ksi (1.7 MPa): WB Route 22 over 19th Street.
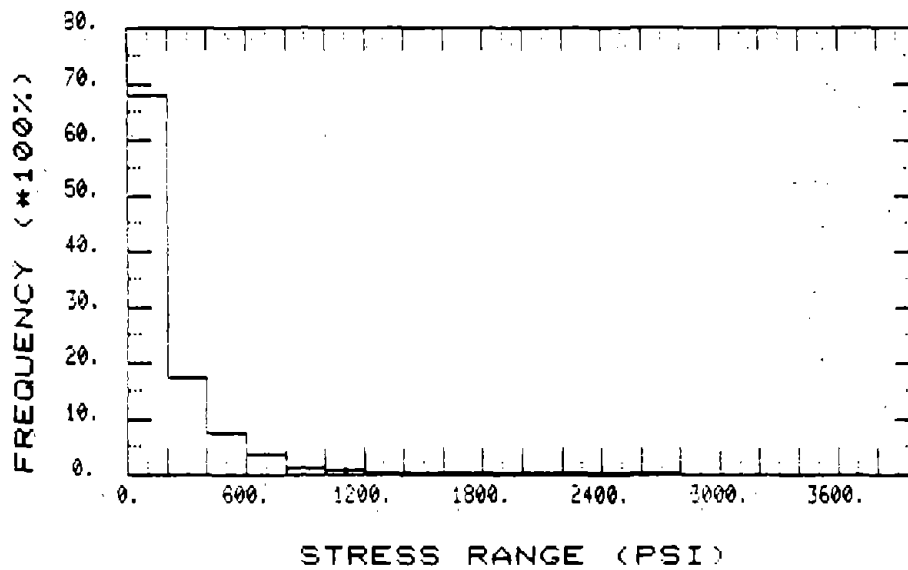
Figure 71. S_r distribution--gauge 8: max. S_r = 6.2 ksi (42.7 MPa): miner S_r = 0.59 ksi (4.1 MPa): RMS S_r = 0.38 ksi (2.6 MPa): WB Route 22 over 19th Street.
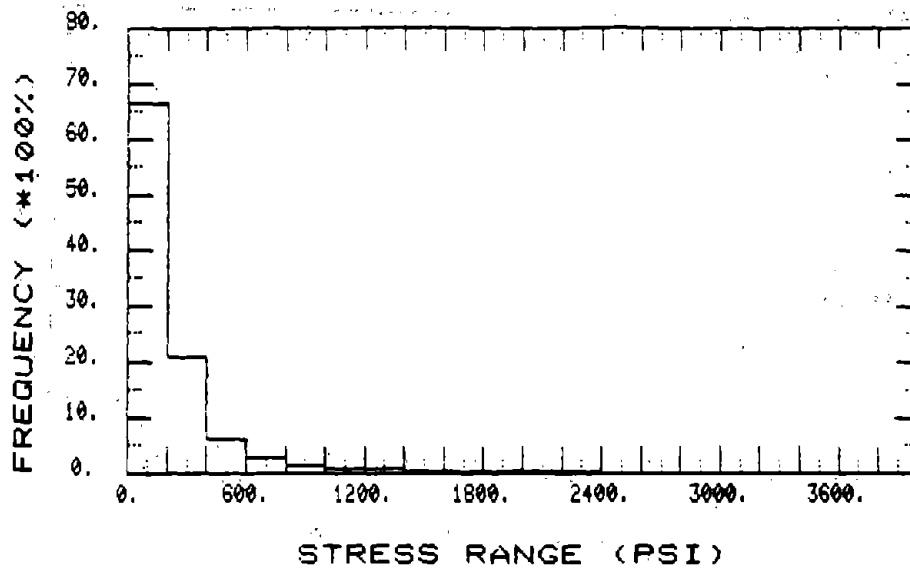
Figure 72. S_r distribution--gauge 9: max. S_r = 4.0 ksi (27.6 MPa): miner S_r = 0.54 ksi (3.7 MPa): RMS S_r = 0.36 ksi (2.5 MPa): WB Route 22 over 19th Street.
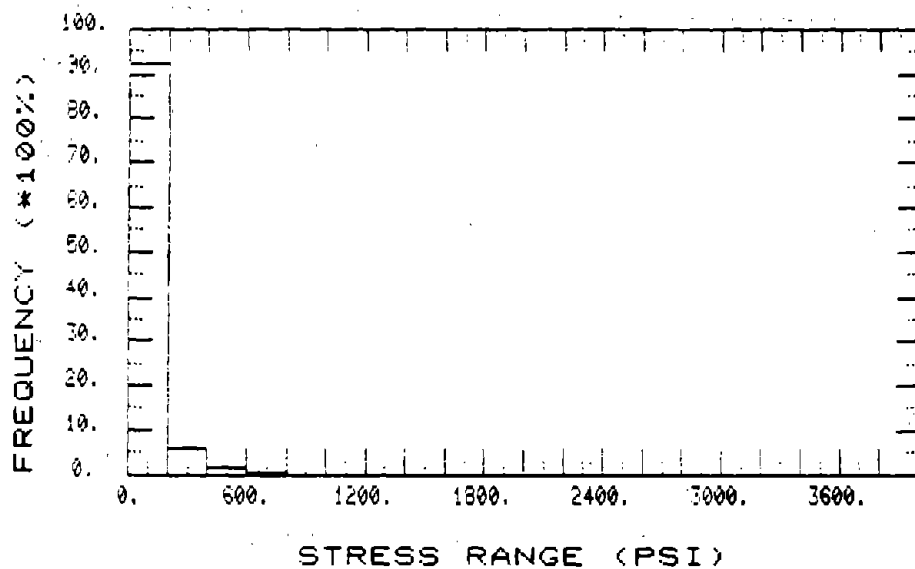

Figure 73. S_r distribution--gauge 10: max. S_r = 2.4 ksi (16.5 MPa): miner S_r = 0.19 ksi (1.3 MPa): RMS S_r = 0.15 ksi (1.0 MPa): WB Route 22 over 19th Street.
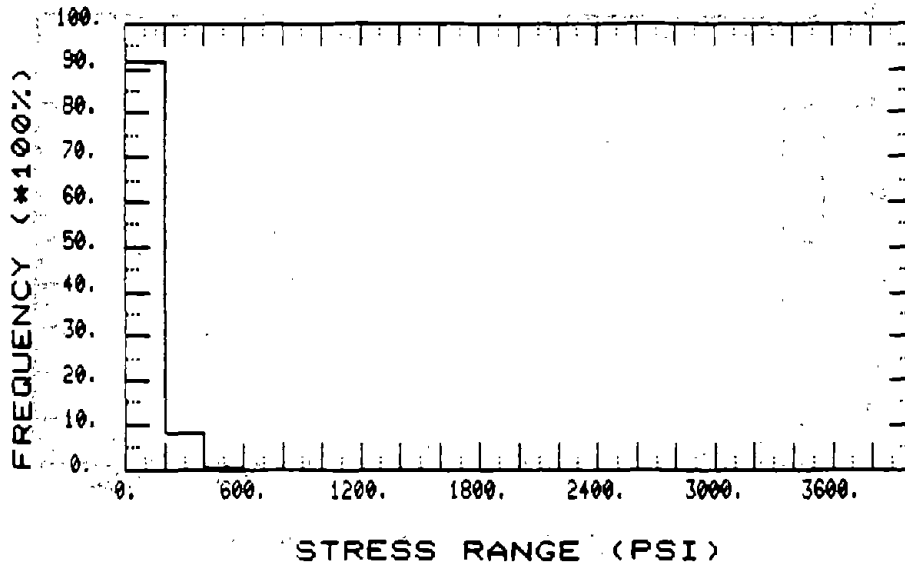
Figure 74. S_r distribution--gauge 11: max. S_r = 2.2 ksi (15.2 MPa): miner S_r = 0.16 ksi (1.1 MPa): RMS S_r = 0.13 ksi (0.9 MPa): WB Route 22 over 19th Street.
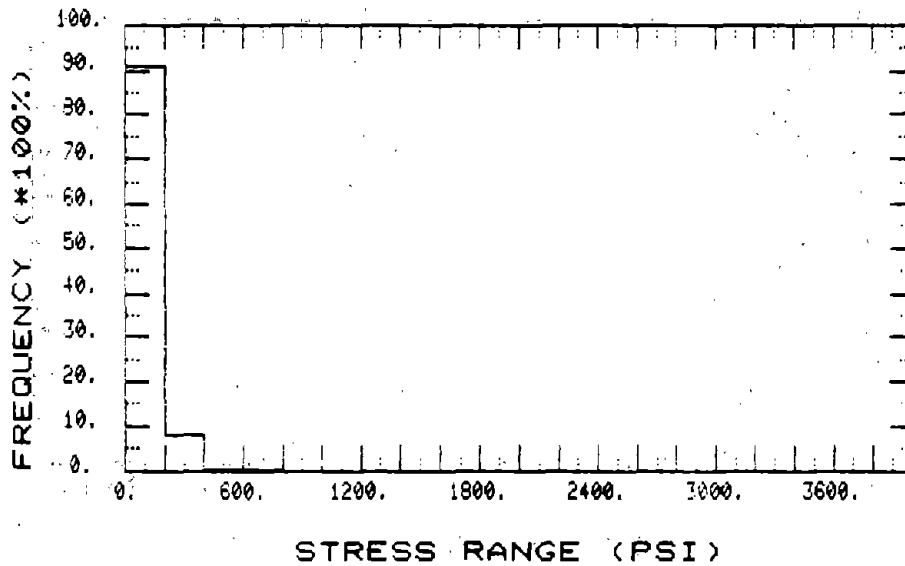

Figure 75. S_r distribution--gauge 12: max. S_r = 1.6 ksi (11.0 MPa): miner S_r = 0.16 ksi (1.1 MPa): RMS S_r = 0.14 ksi (1.0 MPa): WB Route 22 over 19th Street.

84
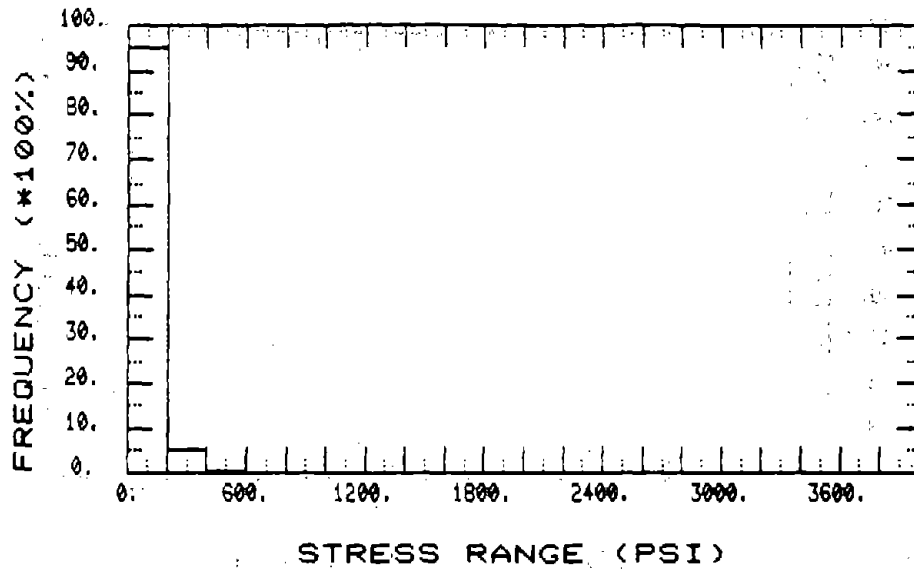
Figure 76. S_r distribution--gauge 13: max. S_r = 2.0 ksi (13.8 MPa): miner S_r = 0.14 ksi (1.0 MPa): RMS S_r = 0.12 ksi (0.8 MPa): WB Route 22 over 19th Street.
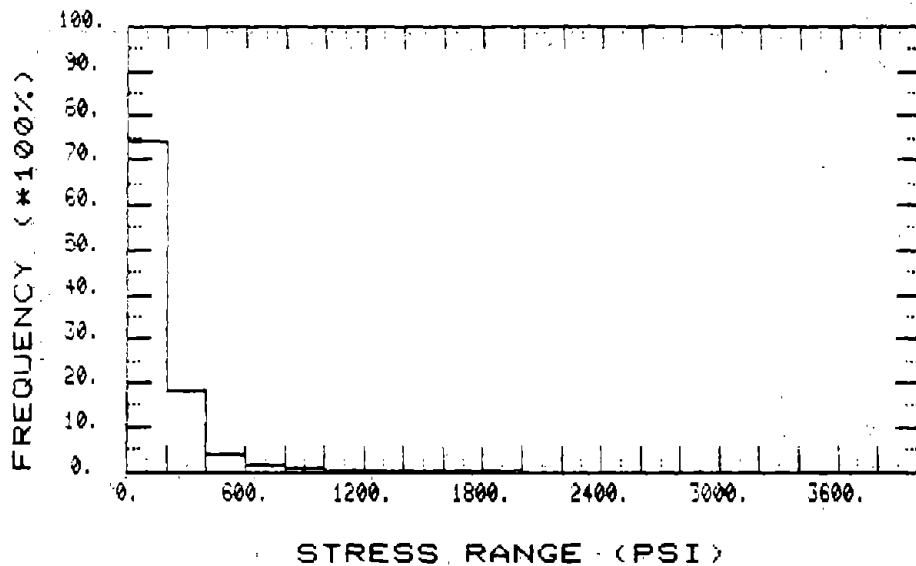
Figure 77. S_r distribution--gauge 14: max. S_r = 2.8 ksi (19.3 MPa): miner S_r = 0.40 ksi (2.8 MPa): RMS S_r = 0.28 ksi (1.9 MPa): WB Route 22 over 19th Street.
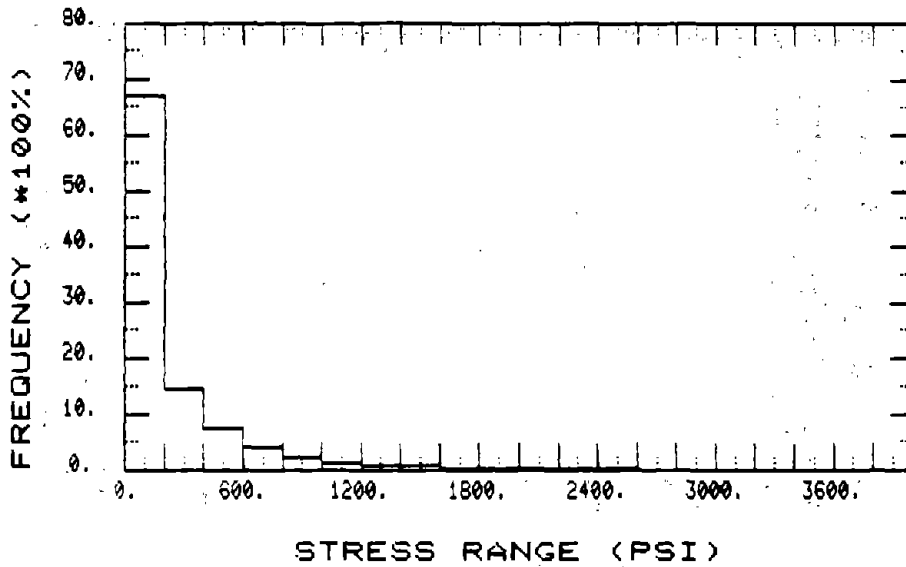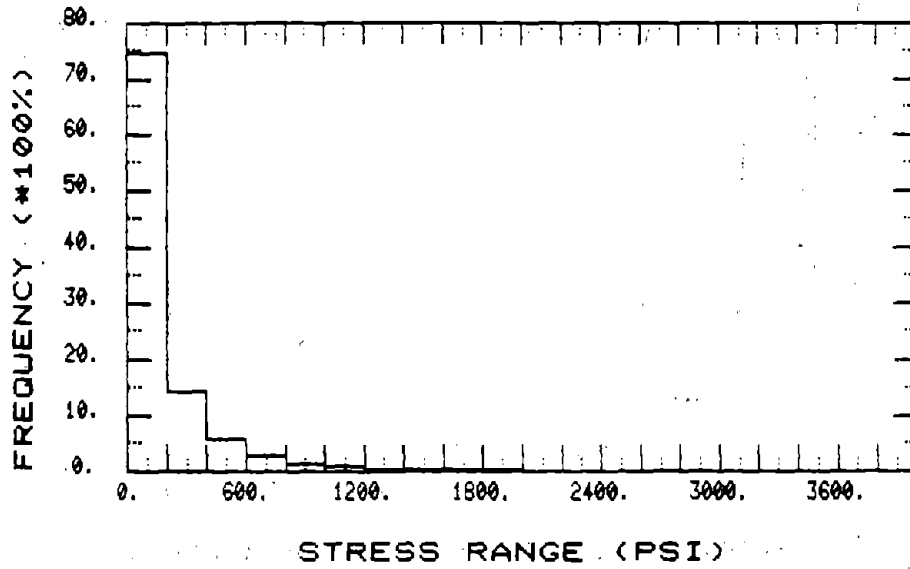
Figure 78. S_r distribution--gauge 15: max. S_r = 6.2 ksi (42.7 MPa): miner $\dot{S}_r$ = 0.41 ksi (2.8 MPa): RMS S_r = 0.29 ksi (2.0 MPa): WB Route 22 over 19th Street.
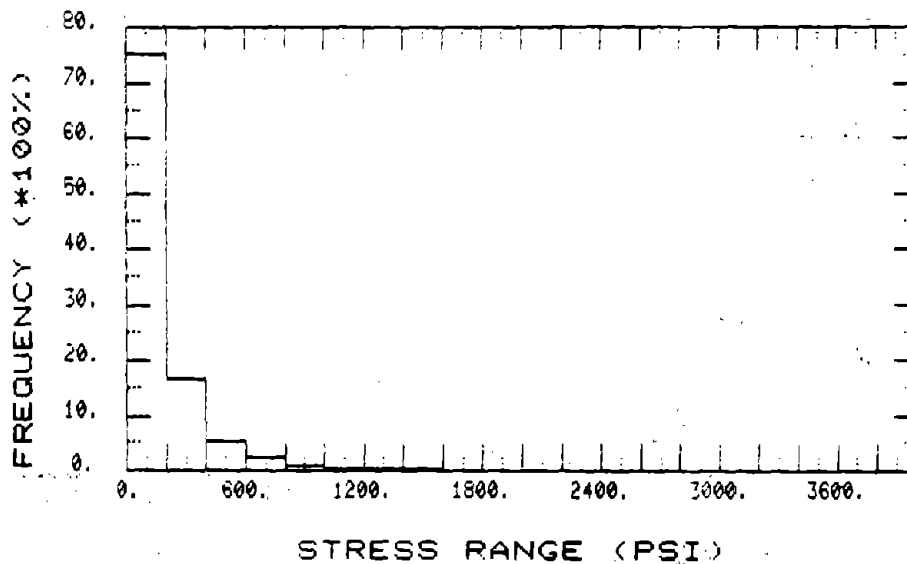
Figure 79. S_r distribution--gauge 16: max. S_r = 5.0 ksi (34.5 MPa): miner S_r = 0.38 ksi (2.6 MPa): RMS S_r = 0.26 ksi (1.8 MPa): WB Route 22 over 19th Street.

86
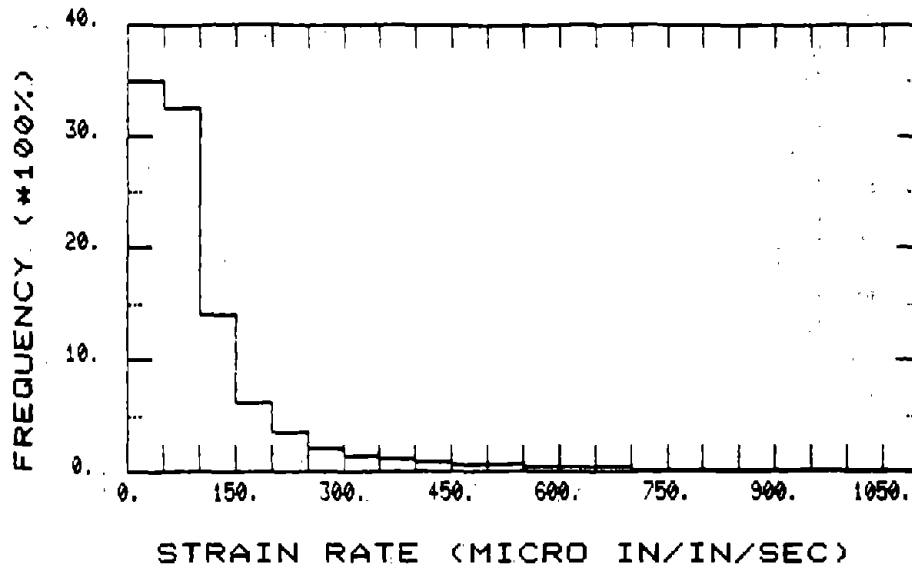
Figure 80. Strain rate distribution--gauge 1: max. strain rate = 8,017 micro in/in/s (8,017 micro m/m/s): WB Route 22 over 19th Street.
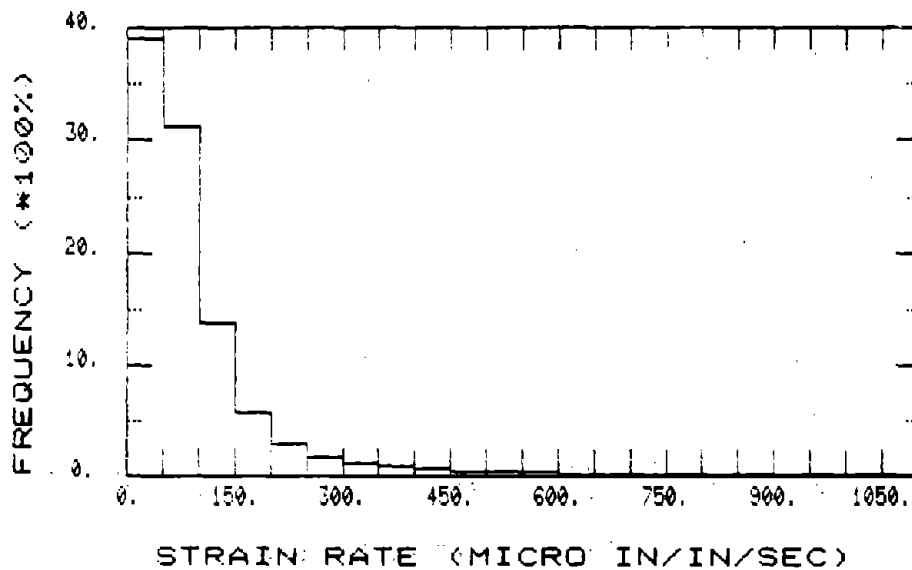
Figure 81. Strain rate distribution--gauge 2: max. strain rate = 7,718 micro in/in/s (7,718 micro m/m/s): WB Route 22 over 19th Street.
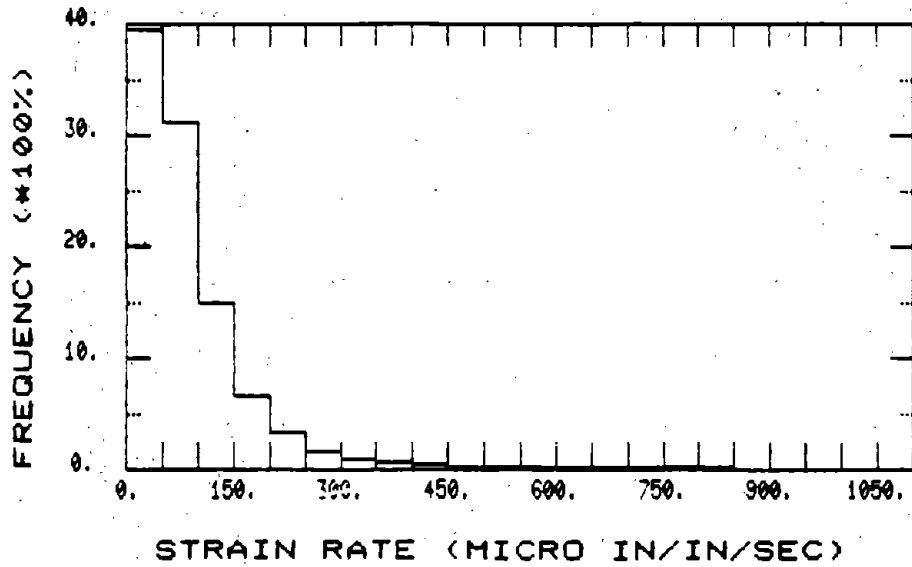
Figure 82. Strain rate distribution—gauge 3: max. strain rate = 3,007 micro in/in/s (3,007 micro m/m/s): WB Route 22 over 19th Street.
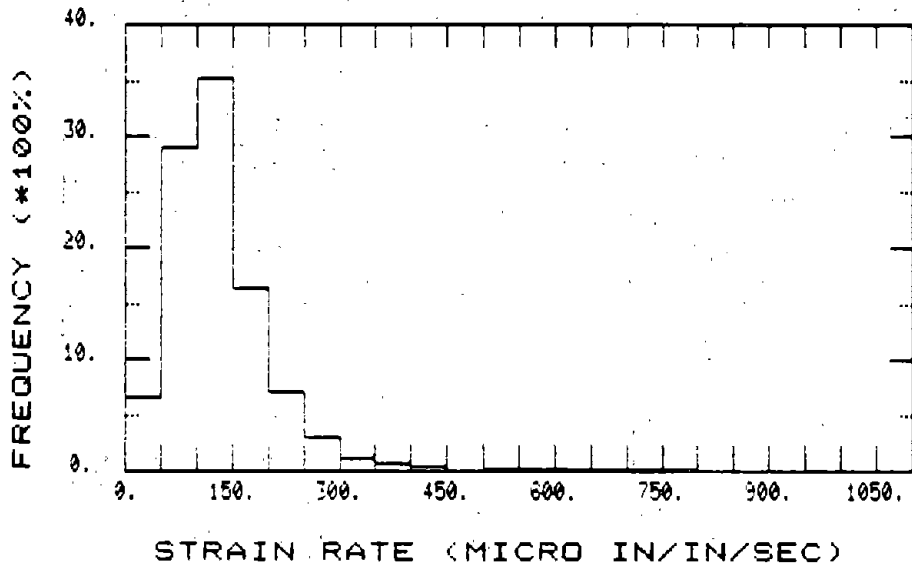
Figure 83. Strain rate distribution—gauge 7: max. strain rate = 4,218 micro in/in/s (4,218 micro m/m/s): WB Route 22 over 19th Street.
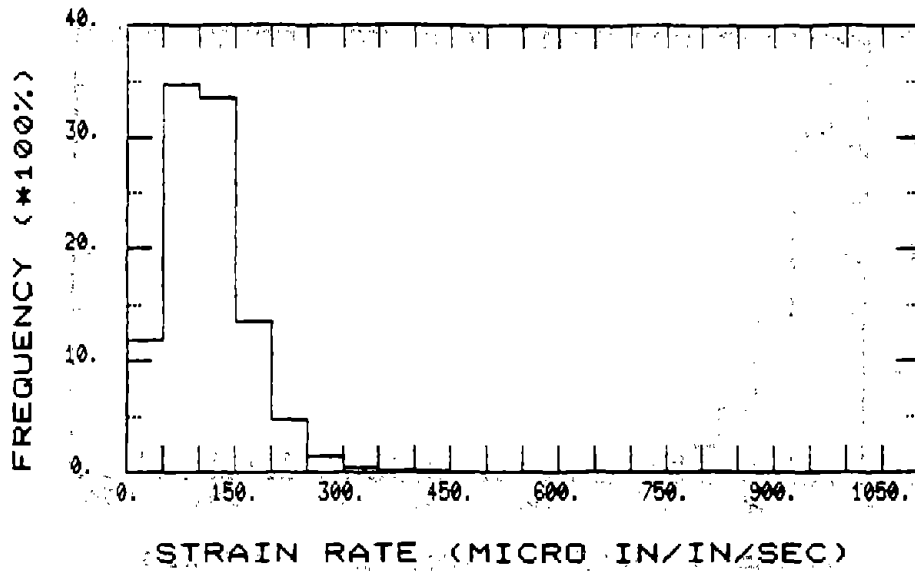
Figure 84.   Strain rate distribution--gauge 10:   max. strain rate = 800 micro
             in/in/s (800 micro m/m/s):   WB Route 22 over 19th Street.
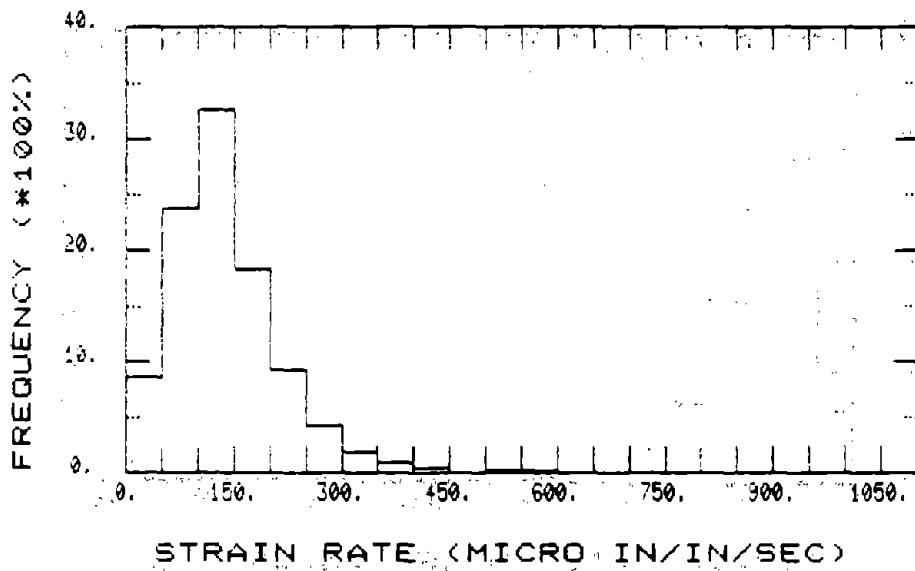
Figure 85.   Strain rate distribution--gauge 12:   max. strain rate = 2,400 micro
             in/in/s (2,400 micro m/m/s):   WB Route 22 over 19th Street.

89
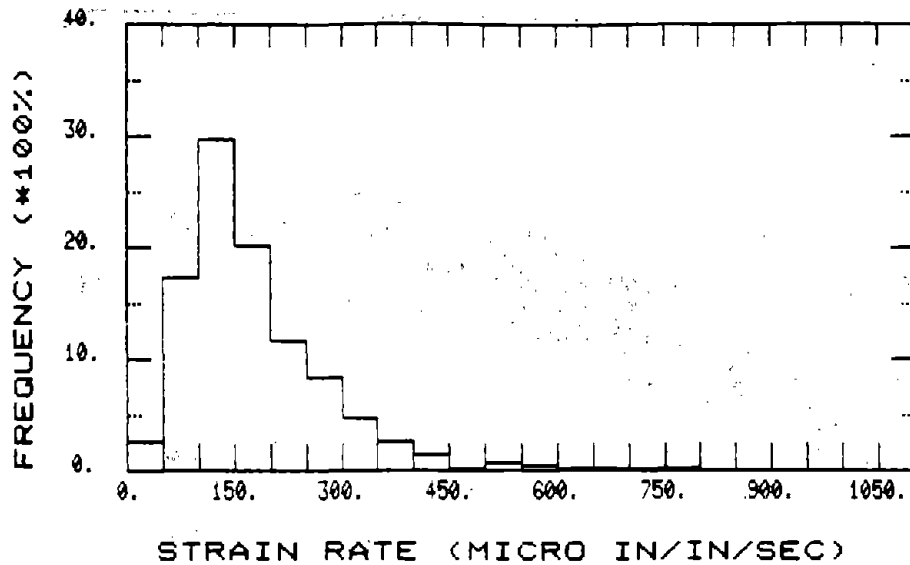
Figure 86.   Strain rate distribution--gauge 14:   max. strain rate = 2,850 micro
in/in/s (2,850 micro m/m/s):   WB Route 22 over 19th Street.
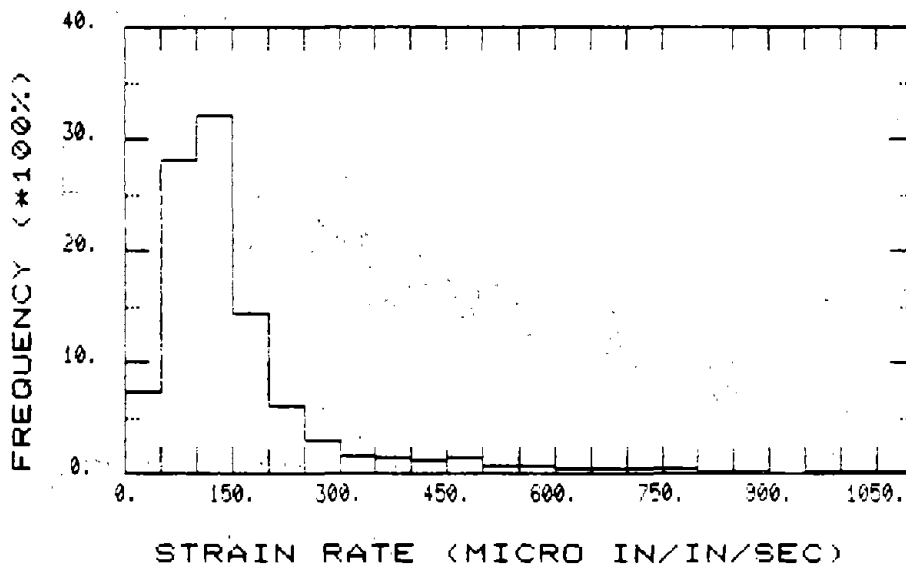
Figure 87.   Strain rate distribution--gauge 15:   max. strain rate = 60,494
micro in/in/s (60,494 micro m/m/s):   WB Route 22 over 19th Street.
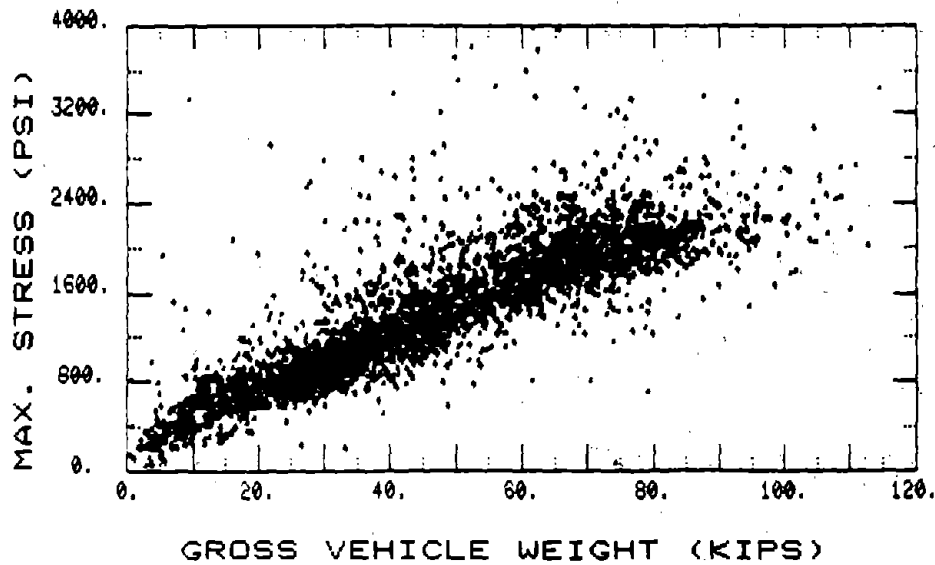
Figure 88. Max. stress (S) vs. GVW--gauge 1: absolute max. stress = 9.9 ksi (68.3 MPa): equation of linear regression line, S (psi) = 320 + 22.9 GVW (kips): correlation coefficient = 0.731: WB Route 22 over 19th Street.
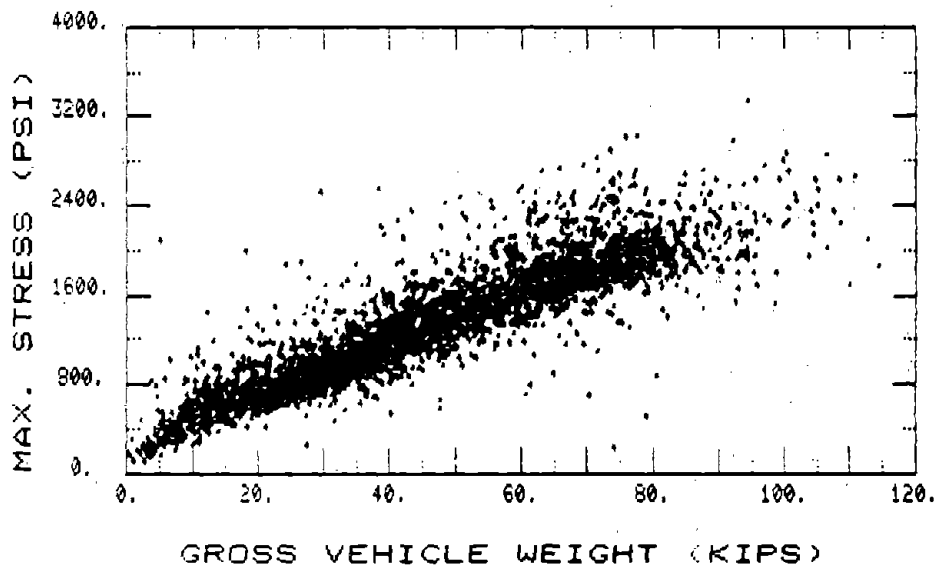
Figure 89. Max. stress (S) vs. GVW--gauge 2: absolute max. stress = 3.2 ksi (22.1 MPa): equation of linear regression line, S (psi) = 323 + 20.7 GVW (kips): correlation coefficient = 8.895: WB Route 22 over 19th Street.
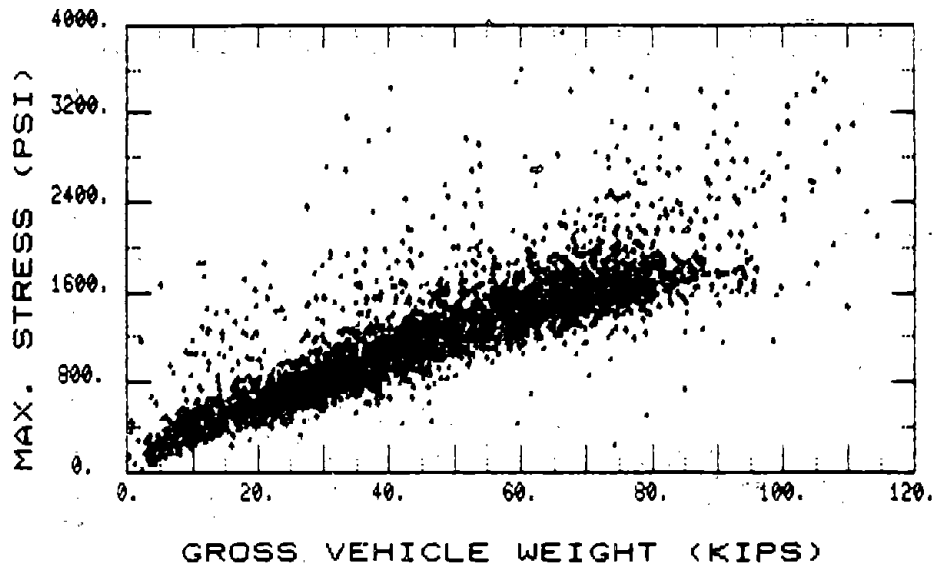
Figure 90. Max. stress (S) vs. GVW--gauge 3: absolute max. stress = 6.6 ksi
(45.5 MPa): equation of linear regression line, S (psi) = 260.4 +
20.4 GVW (kips): correlation coefficient = 0.808: WB Route 22
over 19th Street.
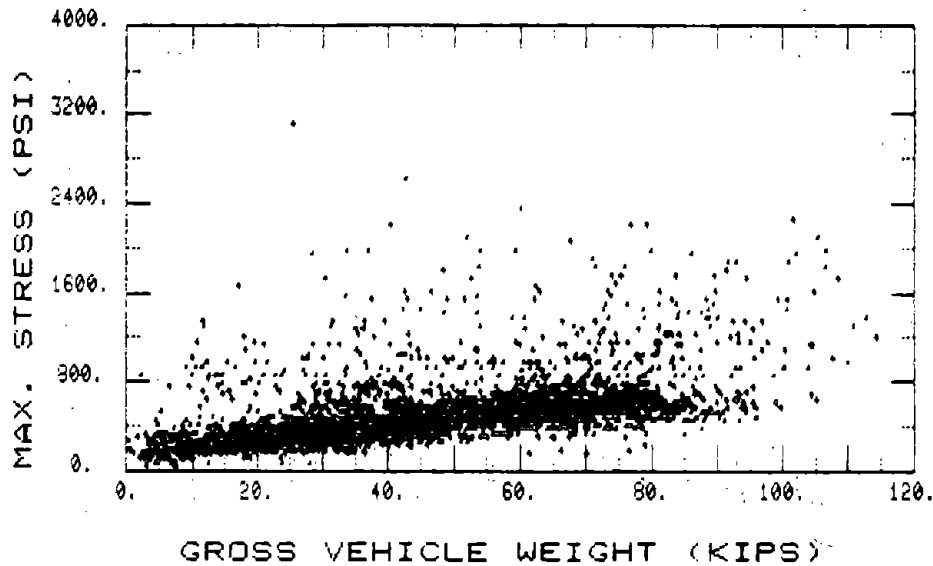
Figure 91. Max. stress (S) vs. GVW--gauge 4: absolute max. stress = 3.1 ksi
(21.4 MPa): equation of linear regression line, S (psi) = 187.7 +
7.05 GVW (kips): correlation coefficient = 0.526: WB Route 22 over
19th Street

92
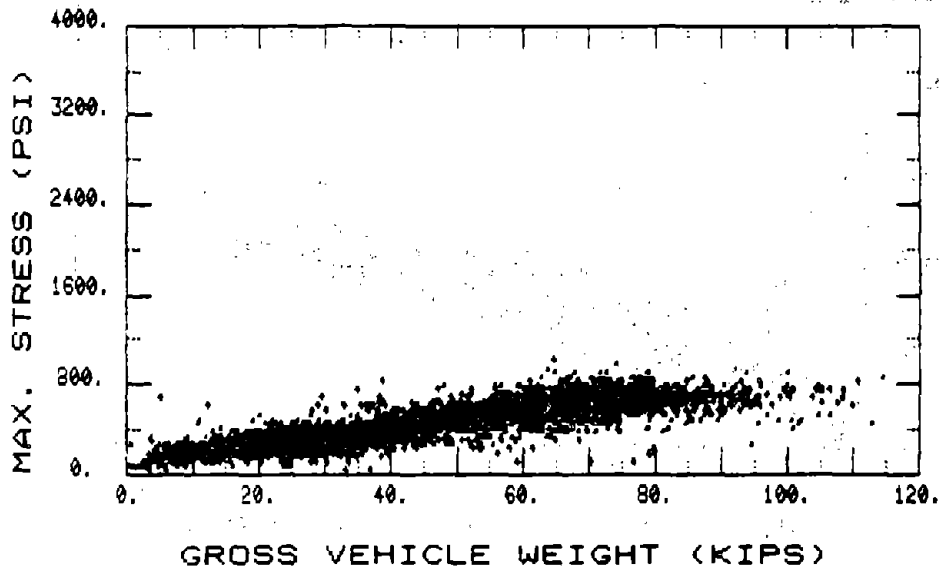
Figure 92. Max. stress (S) vs. GVW--gauge 10: absolute max. stress = 1.0 ksi (6.9 MPa): equation of linear regression line, S (psi) = 132.9 + 6.55 GVW (kips): correlation coefficient = 0.822: WB Route 22 over 19th Street.
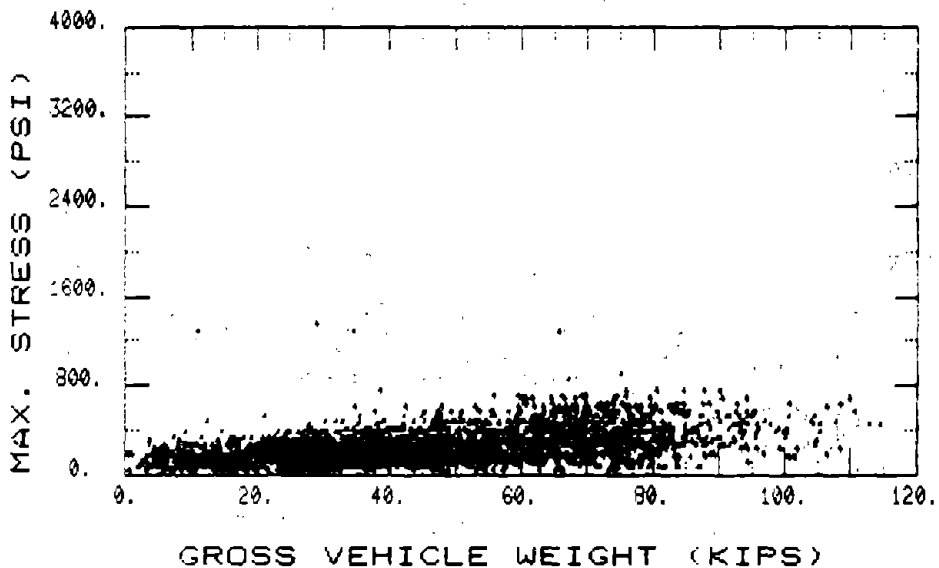
Figure 93. Max. stress (S) vs. GVW--gauge 11: absolute max. stress = 1.4 ksi (9.7 MPa): equation of linear regression line, S (psi) = 96.7 + 3.27 GVW (kips): correlation coefficient = 0.501: WB Route 22 over 19th Street.

93
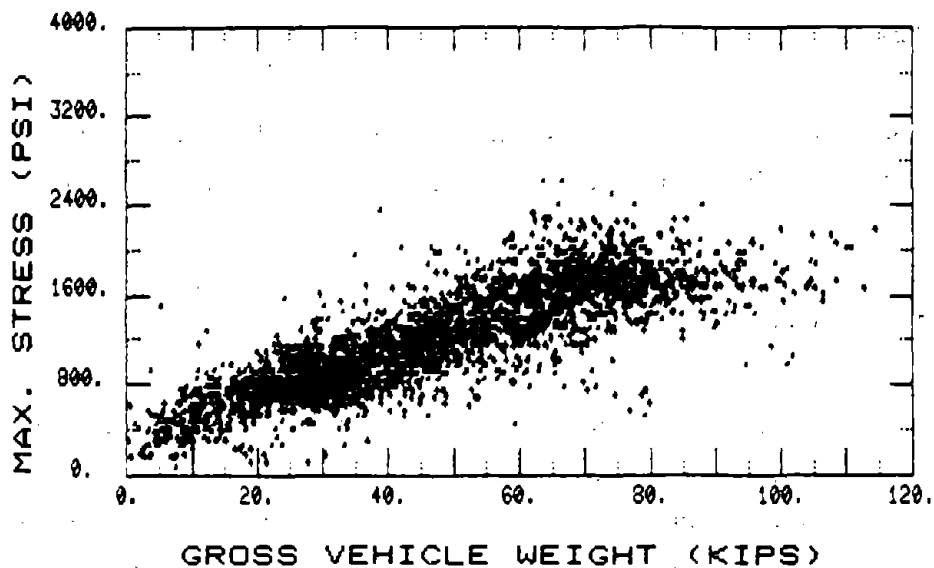
Figure 94. Max. stress (S) vs. GVW—gauge 14: absolute max. stress = 2.6 ksi (17.9 MPa): equation of linear regression line, S (psi) = 385.8 + 17.06 GVW (kips): correlation coefficient = 0.835: WB Route 22 over 19th Street.
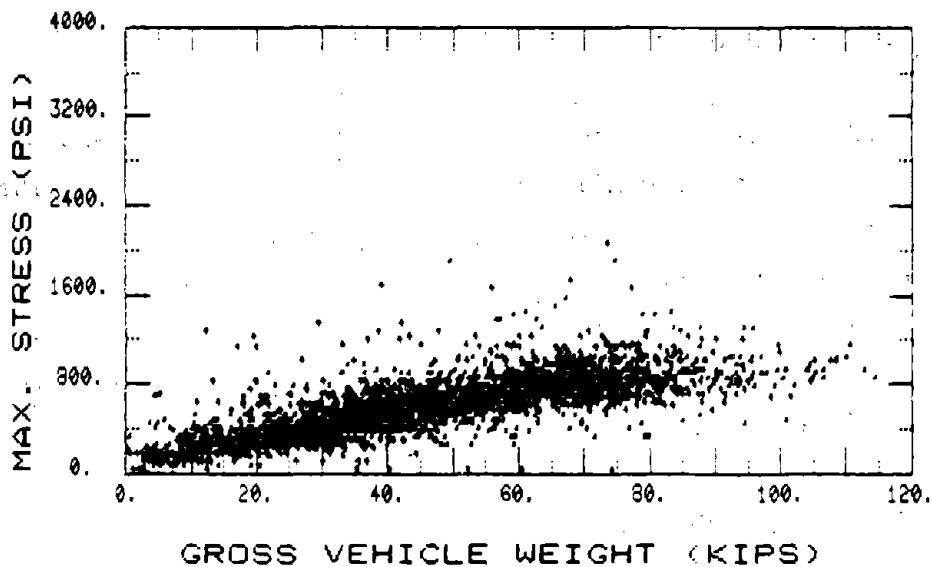
Figure 95. Max. stress (S) vs. GVW—gauge 15. absolute max. stress = 5.1 ksi (35.2 MPa): equation of linear regression line, S (psi) = 175.8 + 8.96 GVW (kips): correlation coefficient = 0.729: WB Route 22 Over 19th Street.

94

4. NB Route 33 Over Van Buren Road

a. GVW Distribution

The gross vehicle weight distribution computed for 3,255 single trucks in lanes 1 and 2 is shown in figure 96. The maximum value of GVW is 150 kips (667.2 kN).

b. Stress Range Distribution

Figures 97 through 109 show the stress range distributions for 13 of the 16 gauges computed by the reservoir cycle counting method using data from all 3,626 trucks in lanes 1 and 2. Data suitable for computing stress ranges were not available from strain gauges 9, 10, and 12. The stress range histograms were computed using all cycles (no threshold) of the strain-vs.-time response curve for each single and multiple truck event. The maximum computed stress range is provided below each figure. Also provided are the Miners and RMS equivalent stress range.[6]

c. Strain Rate Distribution

Figures 110 through 121 show strain rate distributions computed for 12 of the 16 gauges using data from all 3,626 trucks in lanes 1 and 2. The 12 gauges were selected to provide representative strain rates for the main girders of spans 1 and 2, and diaphragm members. The strain rate histograms were computed using all cycles (no threshold) of the strain-vs.-time response curve for each single and multiple truck event. The maximum computed strain rate is provided below each figure.

d. Maximum Stress vs. GVW

Figures 122 through 129 show the relationships between maximum stress (S) and GVW for 8 of the 16 gauges computed using data from 2,856 single trucks in lane 1 only. The eight gauges were selected to provide representative maximum

stress-vs.-GVW relationships for the main girders of spans 1 and 2, and dia-
phragm members. In addition the absolute maximum stress is provided below
each figure. Also provided are the equation of the linear regression line in
psi and kip units and the sample correlation coefficient.
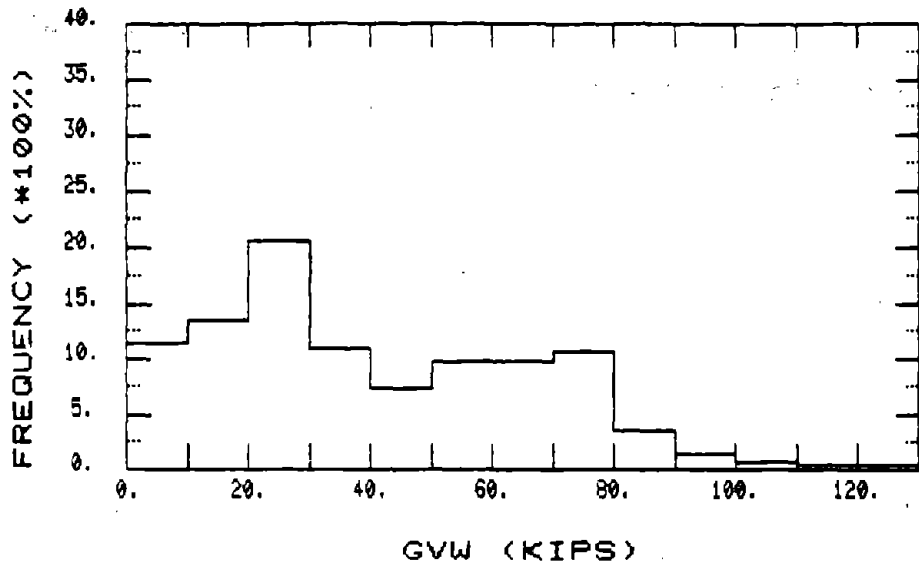
Figure 96. GVW distribution: max. GVW = 150 kips (667.2 kN): NB Route 33 over Van Buren Road.
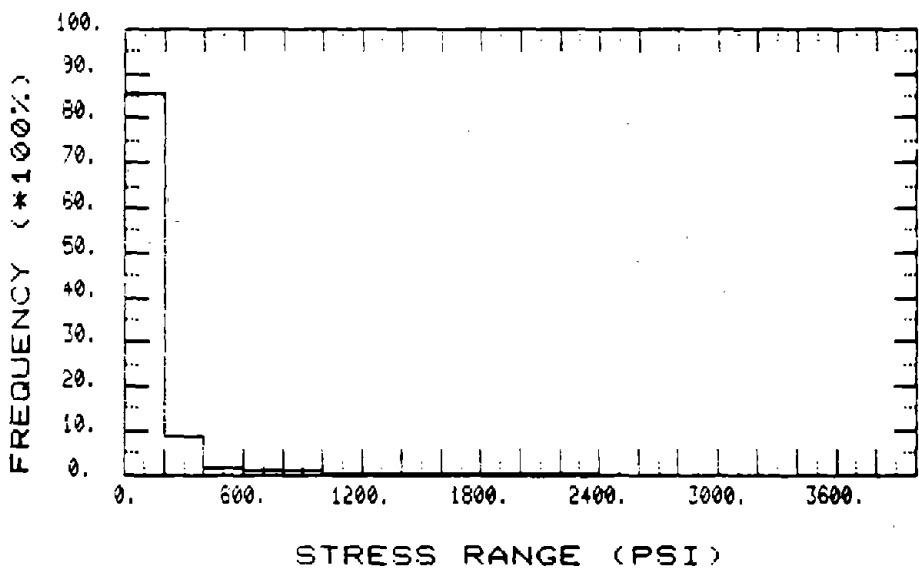
Figure 97. S_r distribution--gauge 1: max. S_r = 6.2 ksi (42.7 MPa): miner S_r = 0.52 ksi (3.6 MPa): RMS S_r = 0.32 ksi (2.2 MPa): NB Route 33 over Van Buren Road.
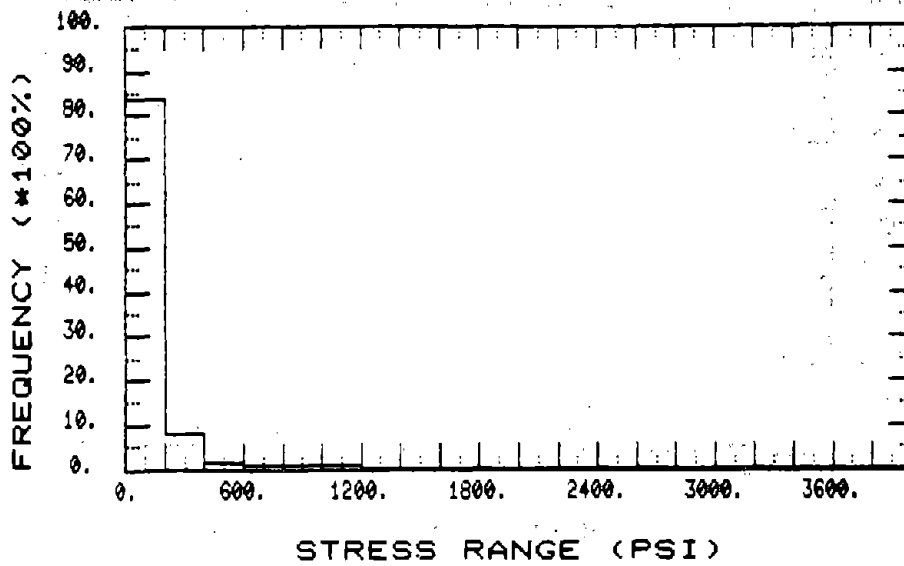
Figure 98. S_r distribution--gauge 2: max. S_r = 6.2 ksi (42.7 MPa): miner S_r = 0.85 ksi (5.9 MPa): RMS S_r = 0.51 ksi (3.5 MPa): NB Route 33 over Van Buren Road.
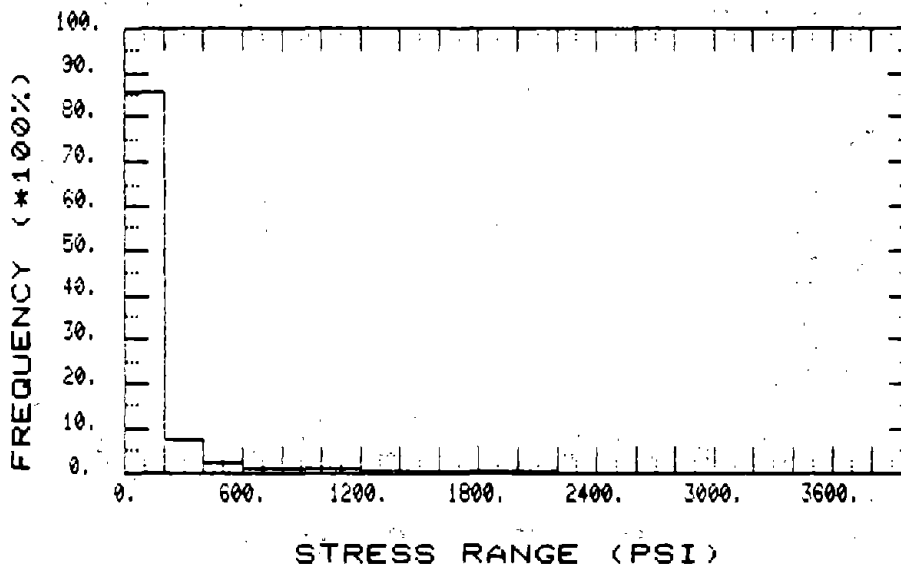
Figure 99. S_r distribution--gauge 3: max. S_r = 3.8 ksi (26.2 MPa): miner S_r = 0.53 ksi (3.7 MPa): RMS S_r = 0.32 ksi (2.2 MPa): NB Route 33 over Van Buren Road.
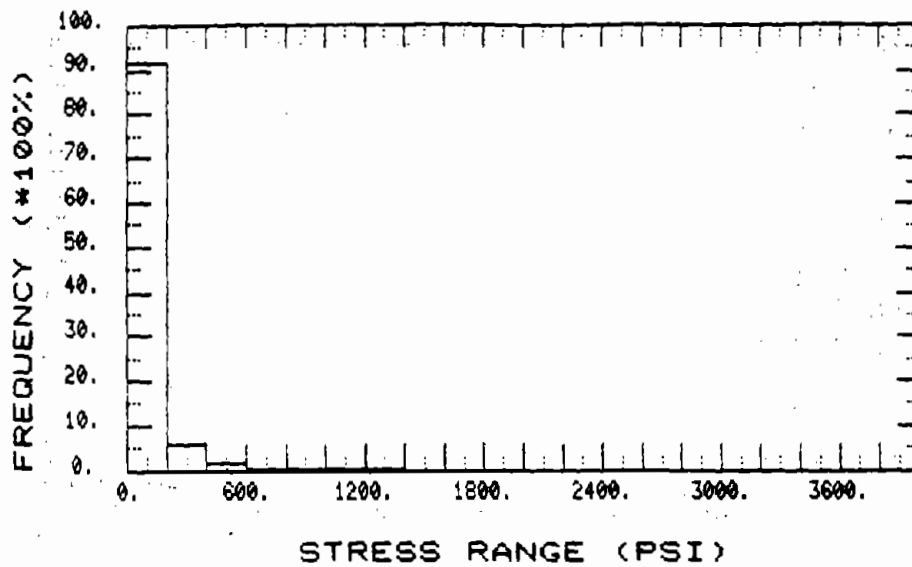
Figure 100: S_r distribution--gauge 4: max. S_r = 3.2 ksi (22.1 MPa): miner S_r = 0.32 ksi (2.2 MPa): RMS S_r = 0.19 ksi (1.3 MPa): NB Route 33 over Van Buren Road.
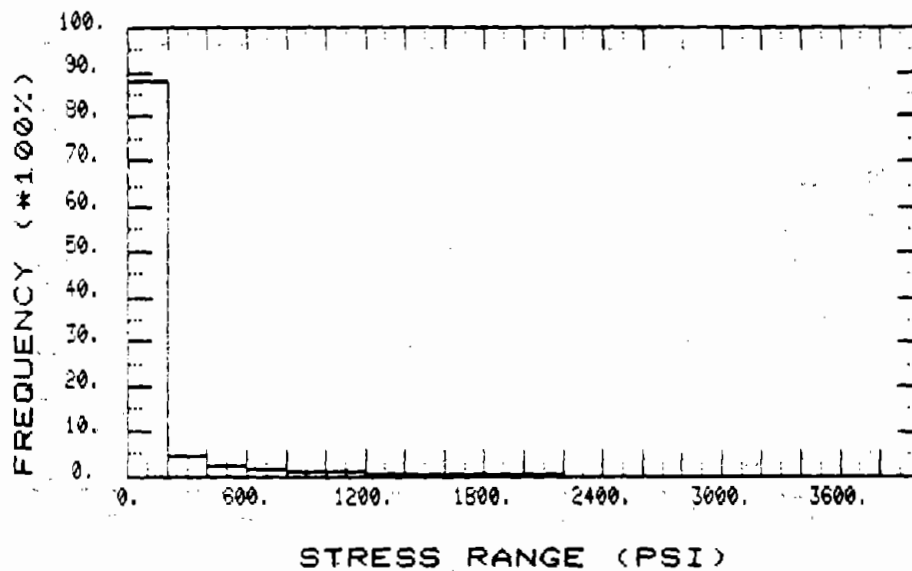
Figure 101: S_r distribution--gauge 5: max. S_r = 3.2 ksi (22.1 MPa): miner S_r = 0.58 ksi (4.0 MPa): RMS S_r = 0.36 ksi (2.5 MPa): NB Route 33 over Van Buren Road.

99
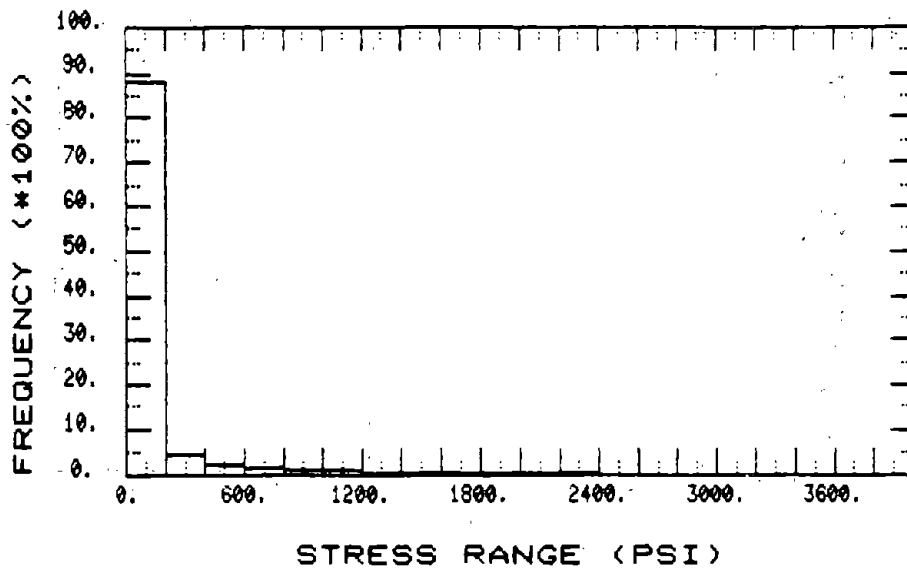
Figure 102. S_r distribution--gauge 6: max. S_r = 3.6 ksi (24.8 MPa): miner S_r = 0.50 ksi (3.4 MPa): RMS S_r = 0.31 ksi (2.1 MPa): NB Route 33 over Van Buren Road.
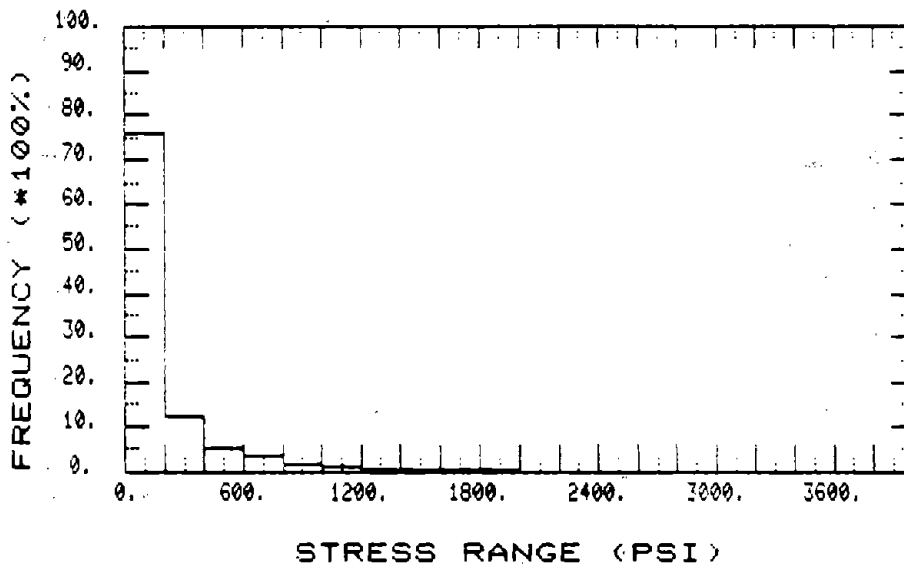
Figure 103. S_r distribution--gauge 7: max. S_r = 3.2 ksi (22.1 MPa): miner S_r = 0.42 ksi (2.9 MPa): RMS S_r = 0.30 ksi (2.1 MPa): NB Route 33 over Van Buren Road.

100
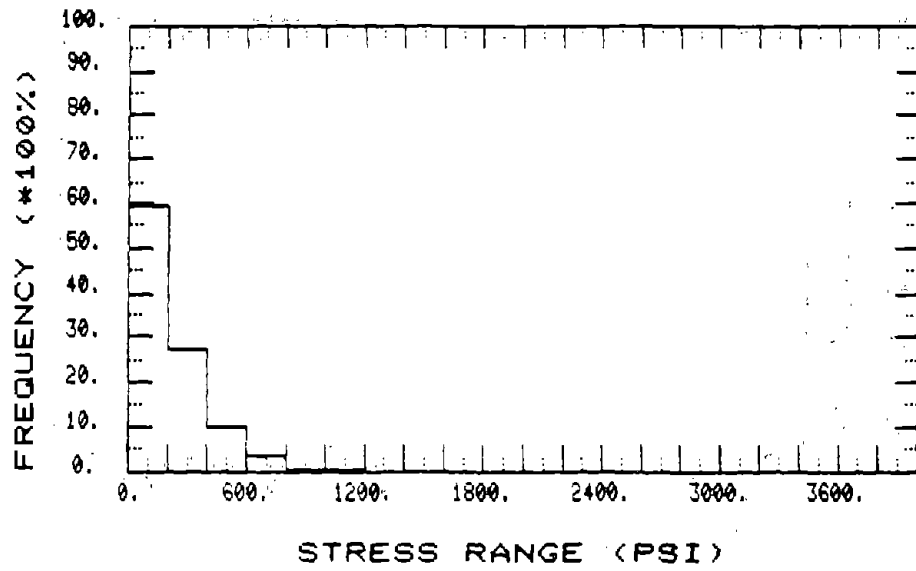
Figure 104. S_r distribution--gauge 8: max. S_r = 5.2 ksi (35.9 MPa): miner S_r = 0.37 ksi (2.6 MPa): RMS S_r = 0.29 ksi (2.0 MPa): NB Route 33 over Van Buren Road
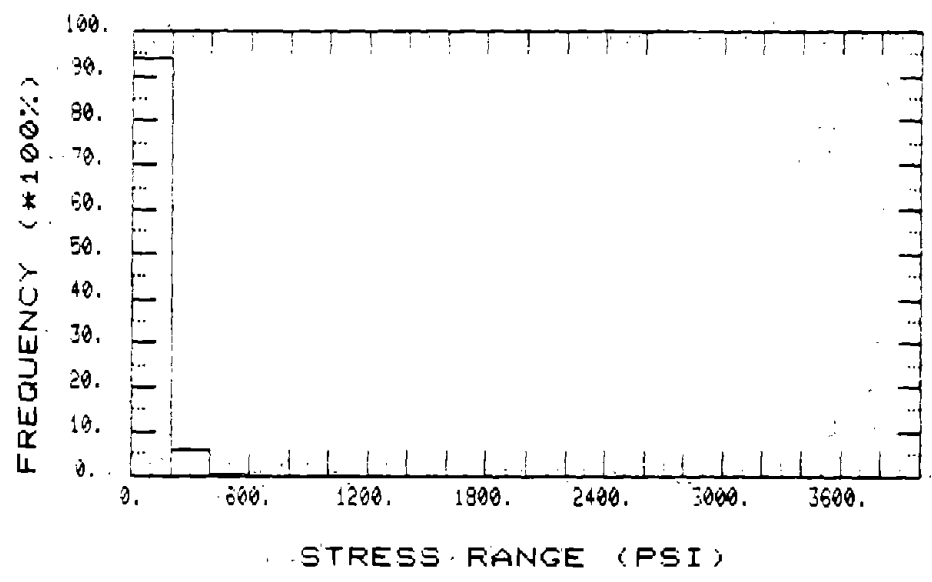
Figure 105. S_r distribution--gauge 11: max. S_r = 1.4 ksi (9.7 MPa): miner S_r = 0.14 ksi (1.0 MPa): RMS S_r = 0.12 ksi (0.8 MPa): NB Route 33 over Van Buren Road.

101
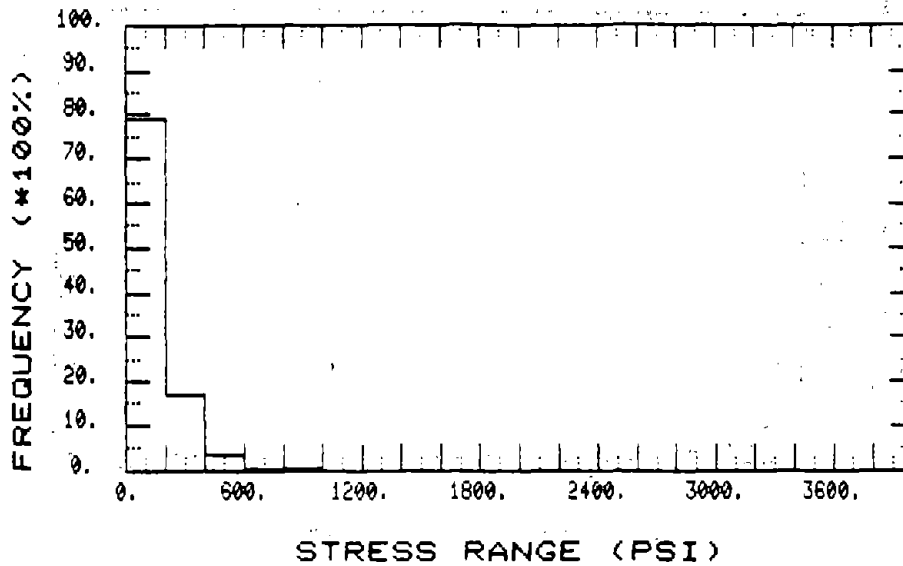
Figure 106. S_r distribution--gauge 13: max. S_r = 2.2 ksi (15.2 MPa): miner S_r = 0.24 ksi (1.7 MPa): RMS S_r = 0.19 ksi (1.3 MPa): NB Route 33 over Van Buren Road.
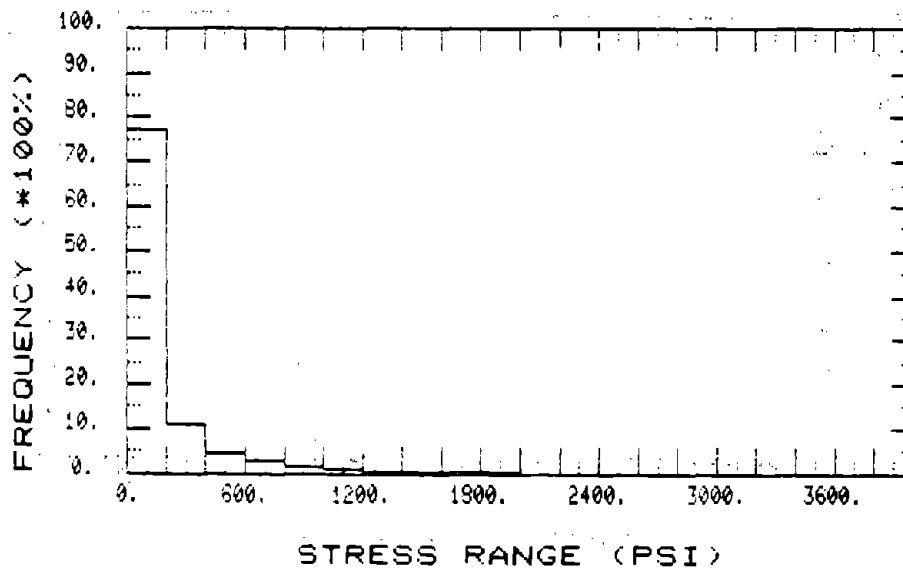
Figure 107. S_r distribution--gauge 14: max. S_r = 5.8 ksi (40.0 MPa): miner S_r = 0.45 ksi (3.1 MPa): RMS S_r = 0.31 ksi (2.1 MPa): NB Route 33 over Van Buren Road.

102
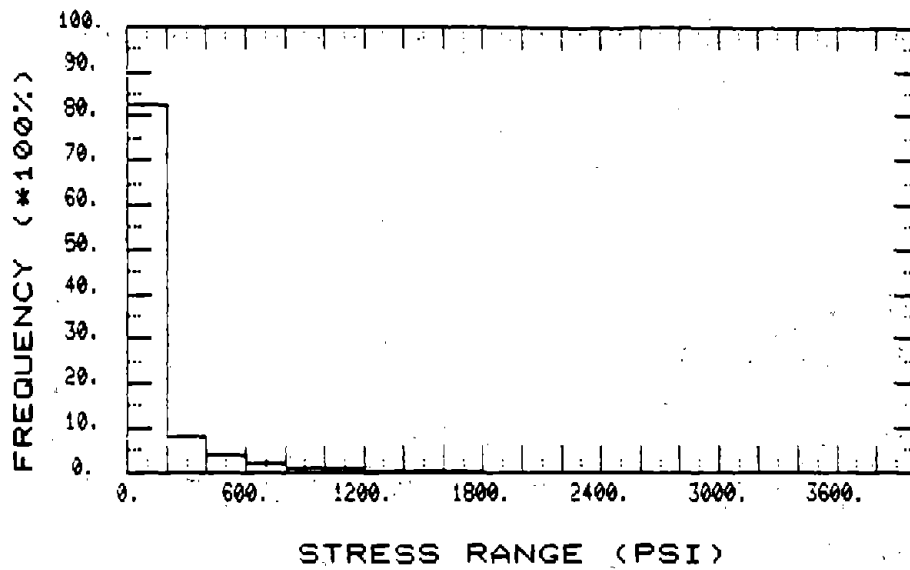
Figure 108. S_r distribution--gauge 15: max. S_r = 2.6 ksi (17.9 MPa): miner S_r^* = 0.41 ksi (2.8 MPa): RMS S_r = 0.28 ksi (1.9 MPa): NB Route 33 over Van Buren Road.
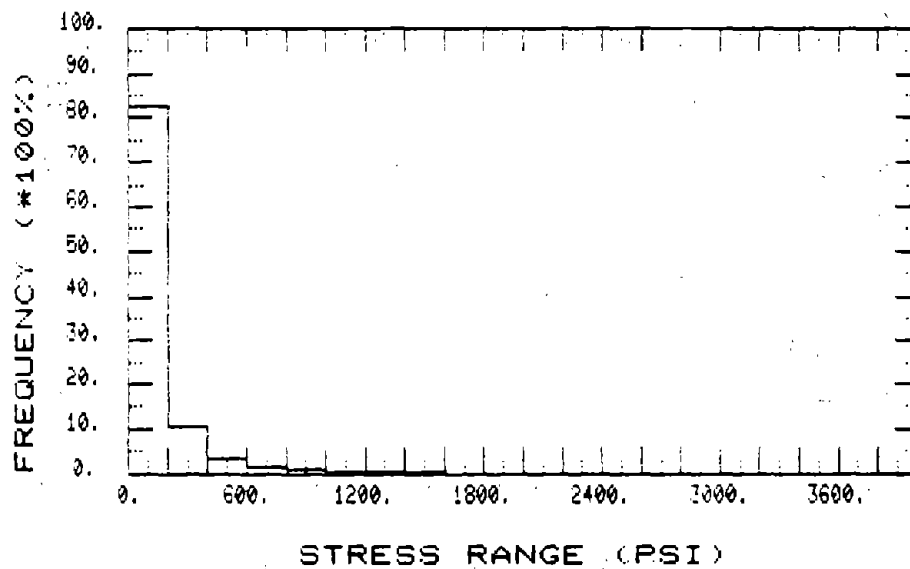
Figure 109. S_r distribution--gauge 16: max. S_r = 2.0 ksi (13.8 MPa): miner S_r = 0.33 ksi (2.3 MPa): RMS S_r = 0.23 ksi (1.6 MPa): NB Route 33 over Van Buren Road.
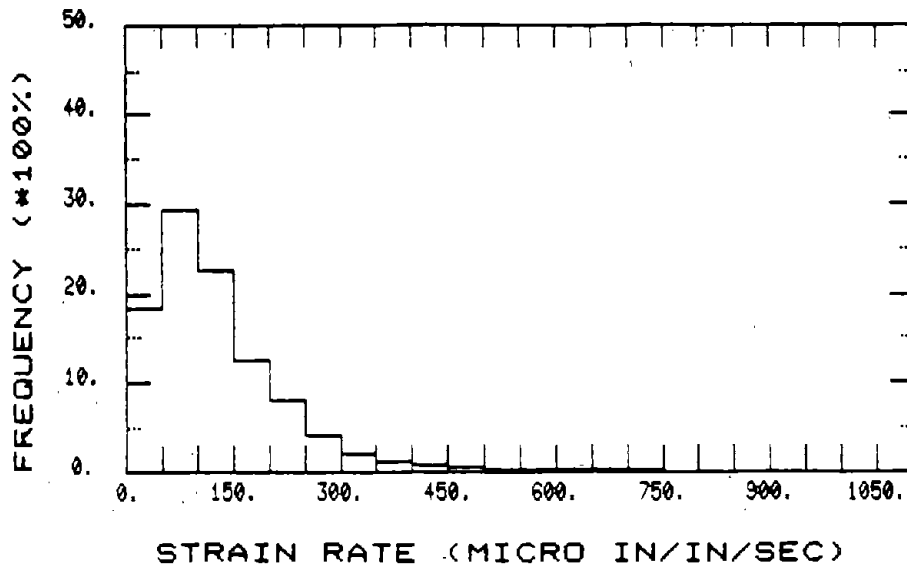
Figure 110. Strain ratedistribution--gauge 1: max. strain rate = 2,850 micro
in/in/s (2,850 micro m/m/s): NB Route 33 over Van Buren Road.
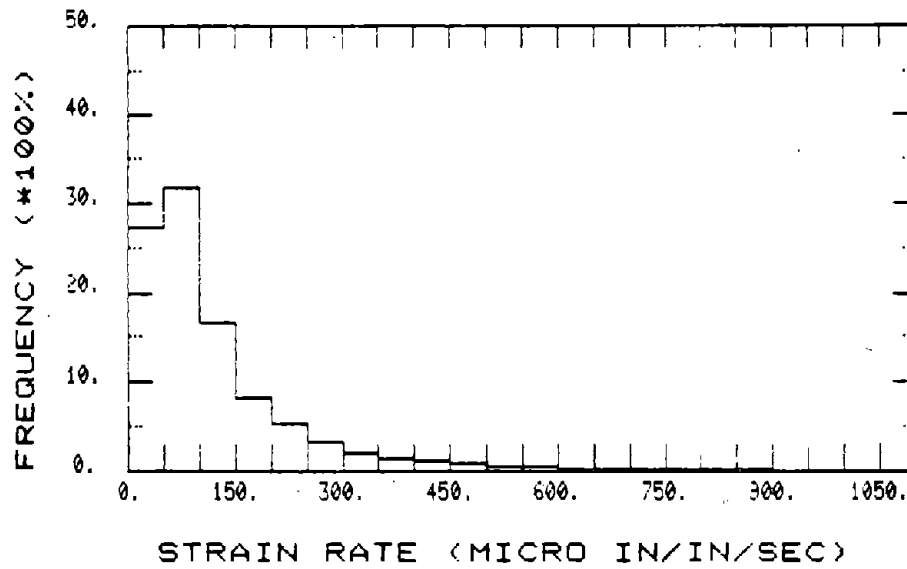
Figure 111. Strain rate distribuiton--gauge 2: max. strain rate= 8,640 micro
in/in/s (8,640 micro m/m/s): NB Route 33 over Van Buren Road.
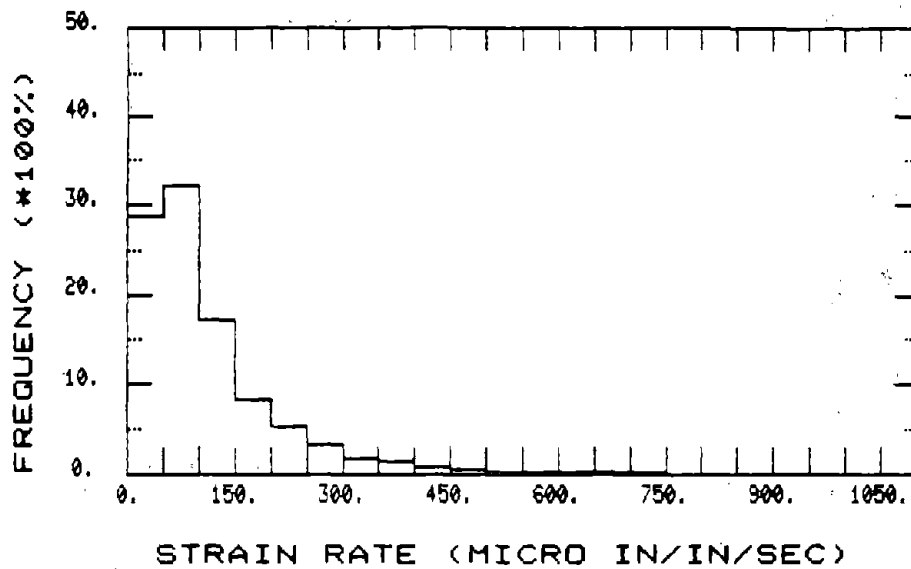
Figure 112. Strain rate distribution—gauge 3: max. strain rate = 1,950 micro in/in/s (1,950 micro m/m/s): NB Route 33 over Van Buren Road.
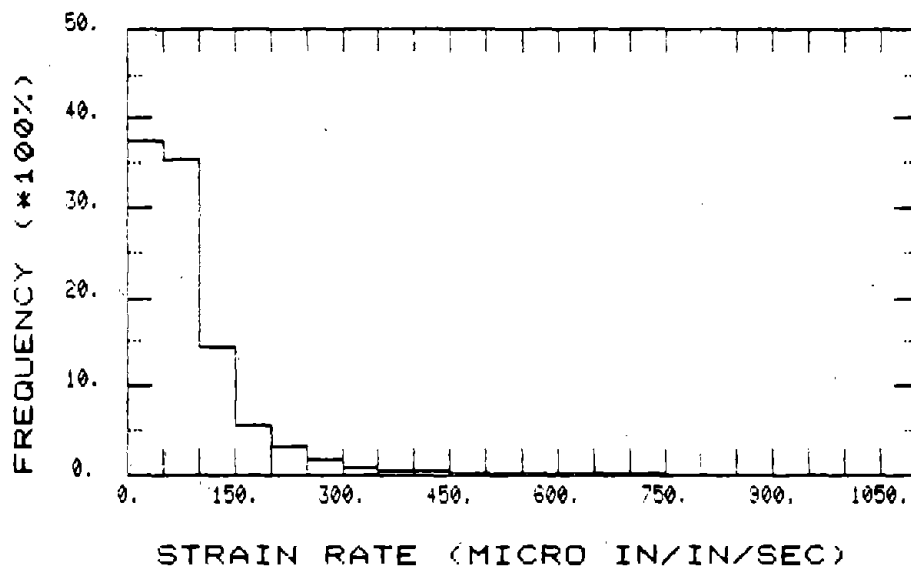
Figure 113. Strain rate distribution—gauge 4: max. strain rate = 1,900 micro in/in/s (1,900 micro m/m/s): NB Route 33 over Van Buren Road.
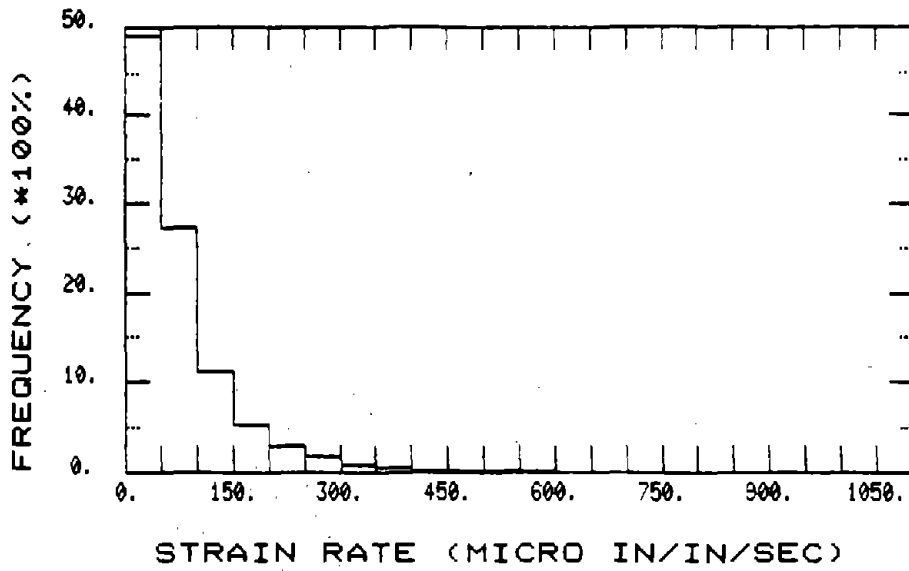
Figure 114. Strain rate distribution--gauge 5: max. strain rate = 2,600 micro in/in/s (2,600 micro m/m/s): NB Route 33 over Van Buren Road.
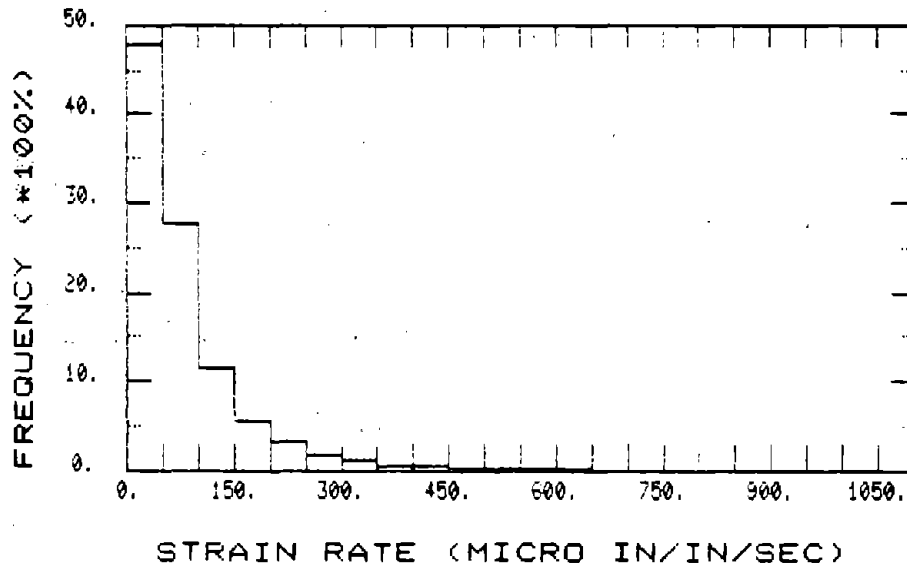
Figure 115. Strain rate distribution--gauge 6: max. strain rate = 3,300 micro in/in/s (3,300 micro m/m/s): NB Route 33 over Van Buren Road.
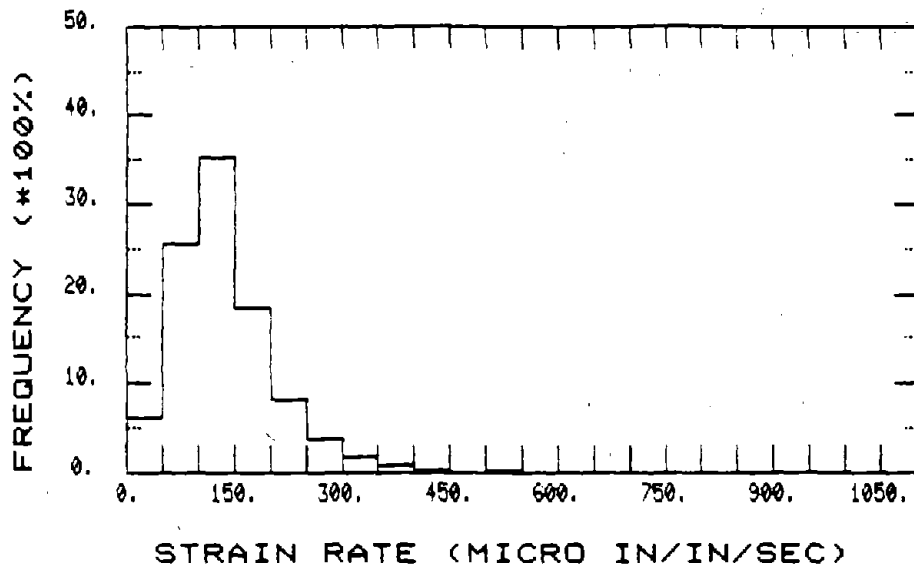
Figure 116.　Strain rate distribution--gauge 7:　max. strain rate = 1,600 micro in/in/s (1,600 micro m/m/s):　NB Route 33 over Van Buren Road.
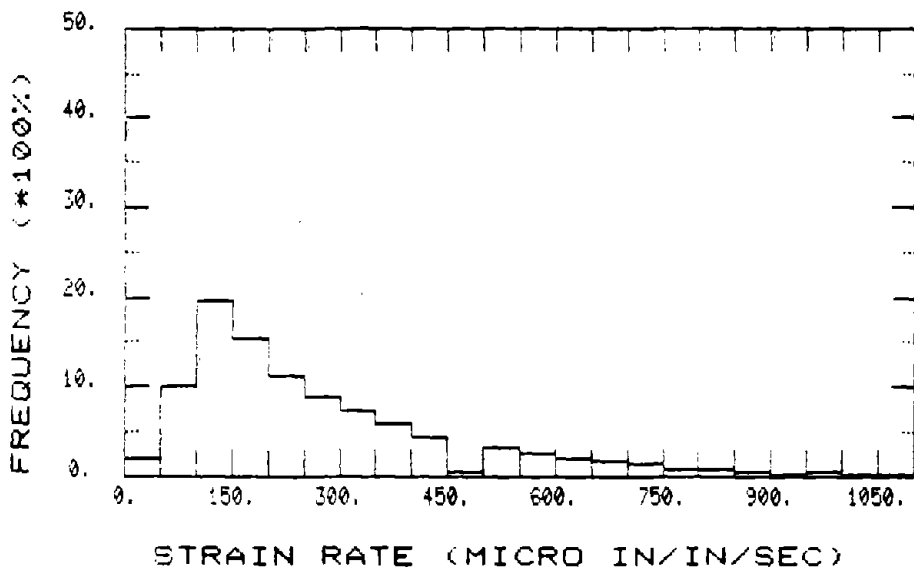
Figure 117.　Strain rate distribution--gauge 8:　max. strain rate = 6,918 micro in/in/s (6,918 micro m/m/s):　NB Route 33 over Van Buren Road.

107
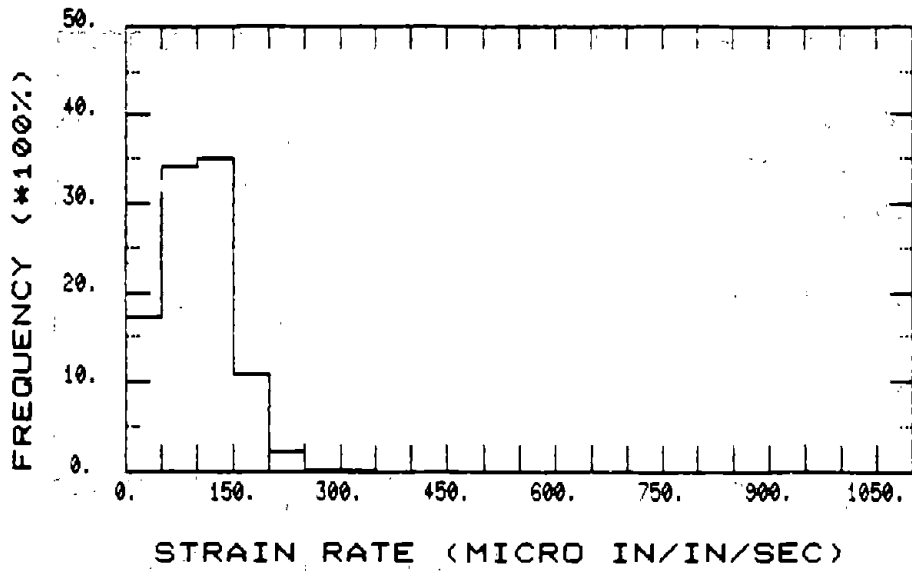
Figure 118. Strain rate distribution—gauge 11: max. strain rate = 4,725 micro
in/in/s (4,725 micro m/m/s): NB Route 33 over Van Buren Road.
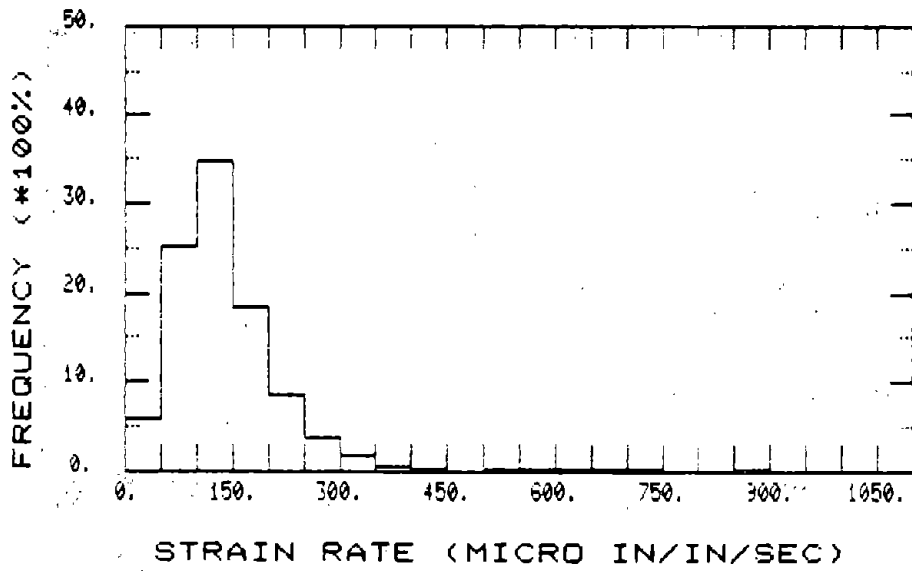
Figure 119. Strain rate distribution—gauge 14: max. strain rate = 6,421 micro
in/in/s (6,421 micro m/m/s): NB Route 33 over Van Buren Road.
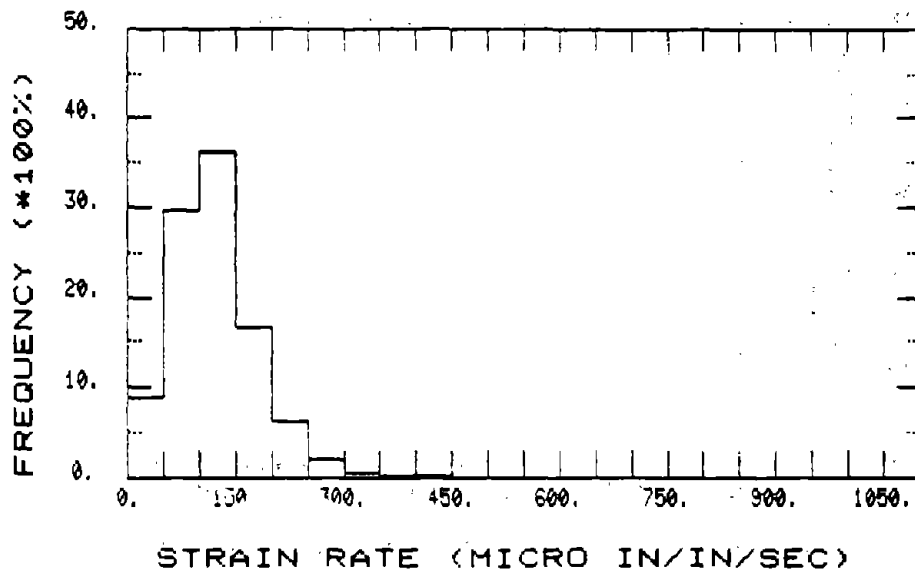
Figure 120. Strain rate distribution--gauge 15:   max. strain rate = 3,937 micro
in/in/s (3,937 micro m/m/s): NB Route 33 over Van Buren Road.
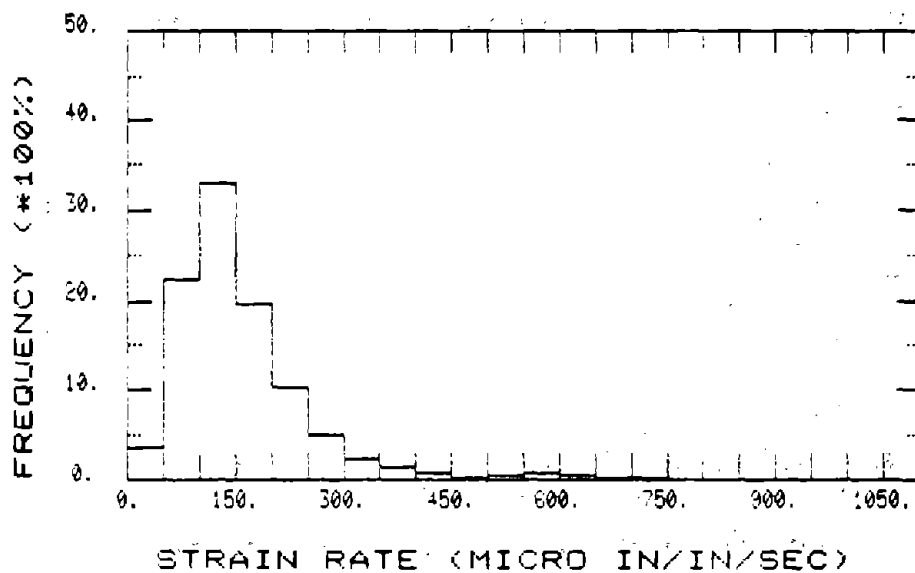
Figure 121. Strain rate distribution--gauge 16:   max. strain rate = 3,262 micro
in/in/s (3,262 micro m/m/s): NB Route 33 over Van Buren Road.
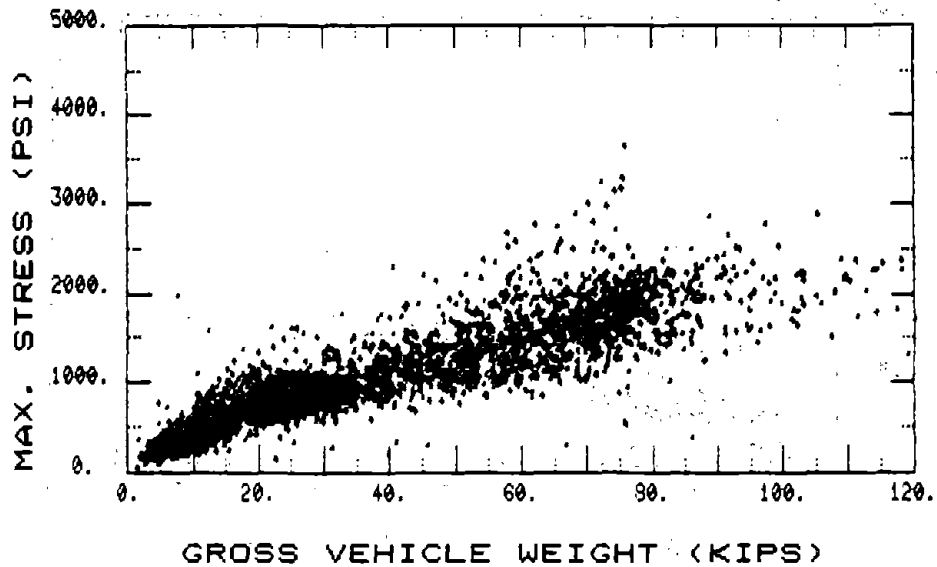
Figure 122. Max. stress vs. GVW--gauge 1: absolute max. stress = 9.9 ksi (68.3 MPa): equation of linear regression line, S (psi) = 333.42 + 18.68 GVW (kips): correlation coefficient = 0.8338: NB Route 33 over Van Buren Road
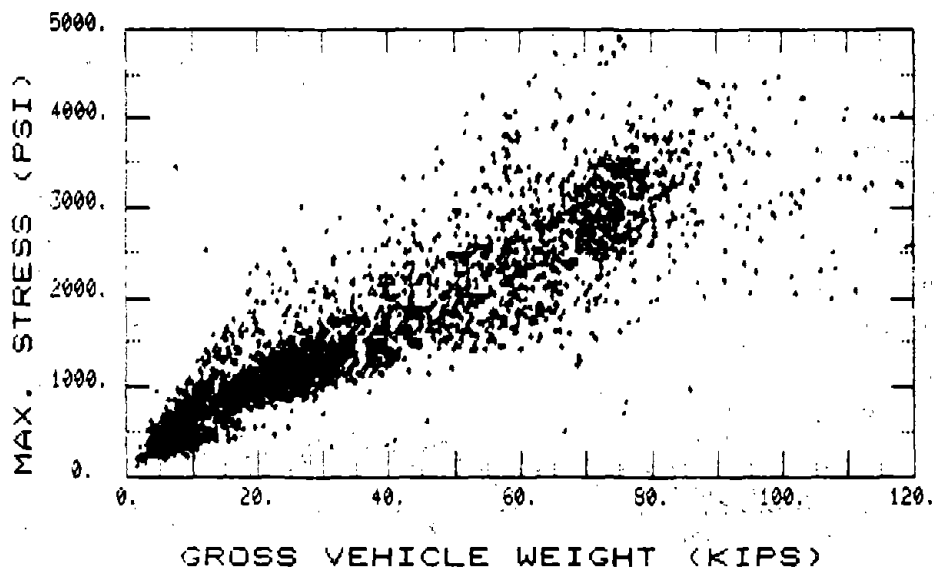
Figure 123. Max. stress vs. GVW--gauge 2: absolute max. stress = 5.5 ksi (37.9 MPa): equation of linear regression line, S (psi) = 403.31 + 33.17 GVW (kips): correlation coefficient = 0.8803: NB Route 33 over Van Buren Road.
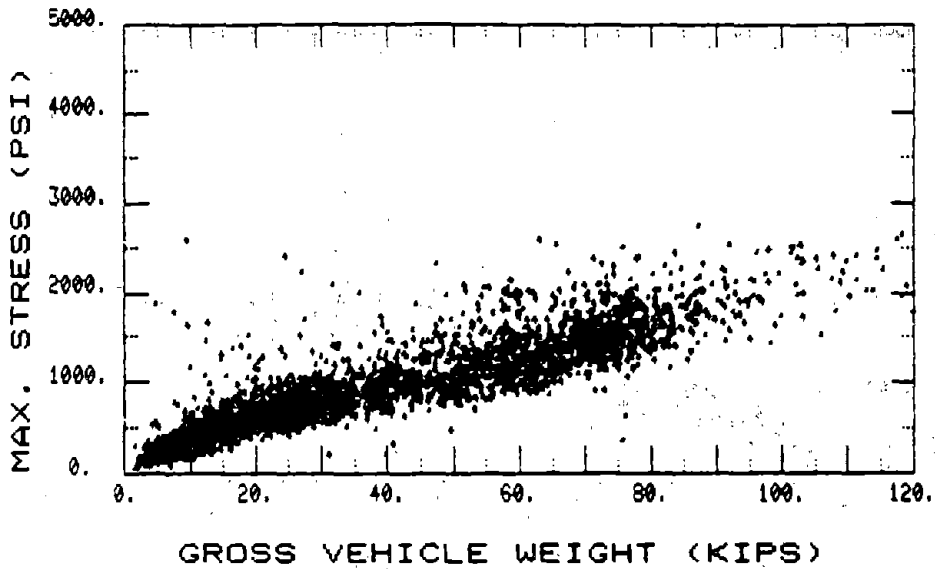
Figure 124. Max. stress vs. GVW--gauge 3: absolute max. stress = 3.0 ksi
(20.7 MPa): equation of linear regression line, S (psi) = 241.2
+ 17.76 GVW (kips): correlation coefficient = 0.8947: NB Route
33 over Van Buren Road.
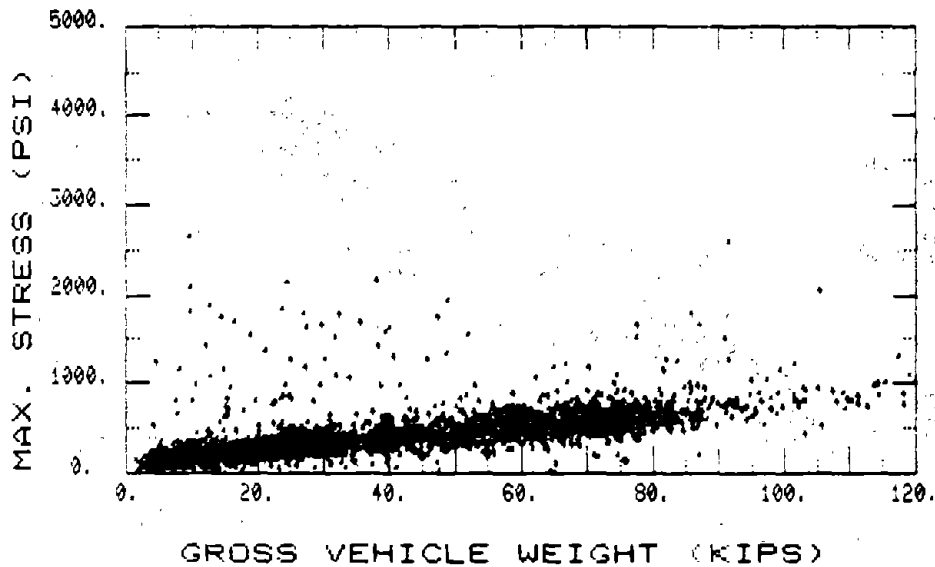
Figure 125. Max. stress vs. GVW--gauge 4: absolute max. stress = 2.6 ksi
(17.9 MPa): equation of linear regression line, S (psi) = 147.61
+ 6.35 GVW (kips): correlation coefficient = 0.6445: NB Route
33 over Van Buren Road.

111
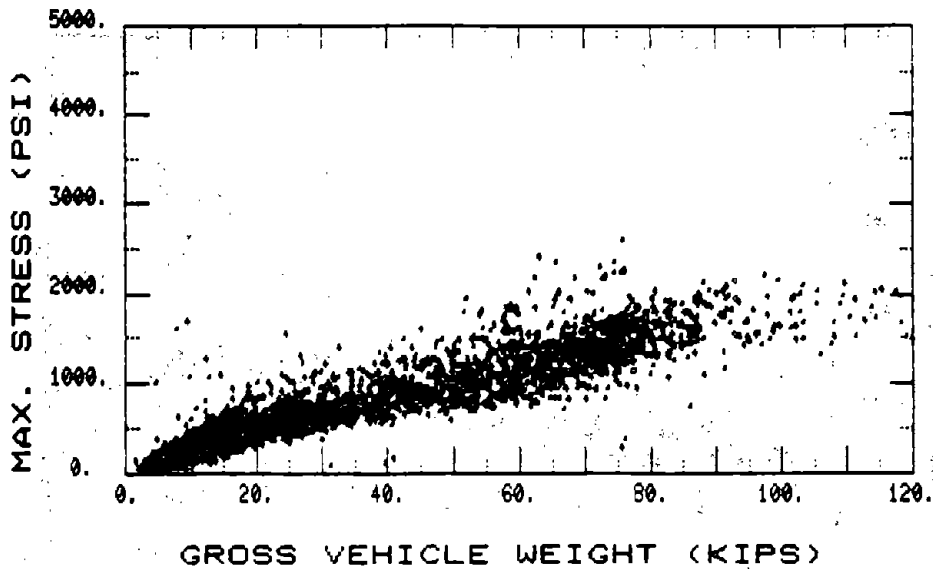
Figure 126. Max. stress vs. GVW--gauge 5: absolute max. stress = 2.61 ksi (17.9 MPa): equation of linear regression line, S (psi) = 161.9 + 16.84 GVW (kips): correlation coefficient = 0.9037: NB Route 33 over Van Buren Road.
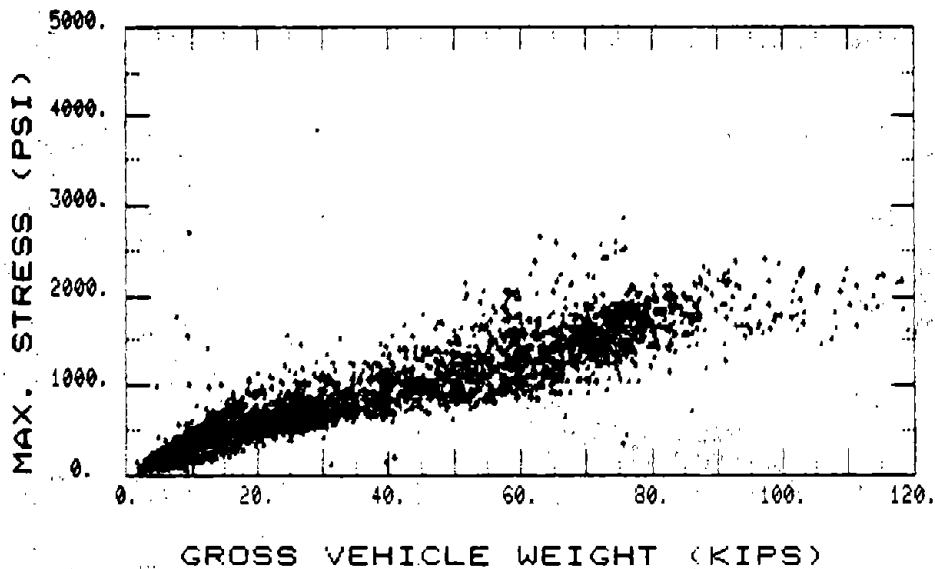
Figure 127. Max. stress vs. GVW--gauge 6: absolute max. stress = 2.9 ksi (20.0 MPa): equation of linear regression line, S (psi) = 187.54 + 18.41 GVW (kips): correlation coefficient = 0.9045: NB Route 33 over Van Buren Road.

112
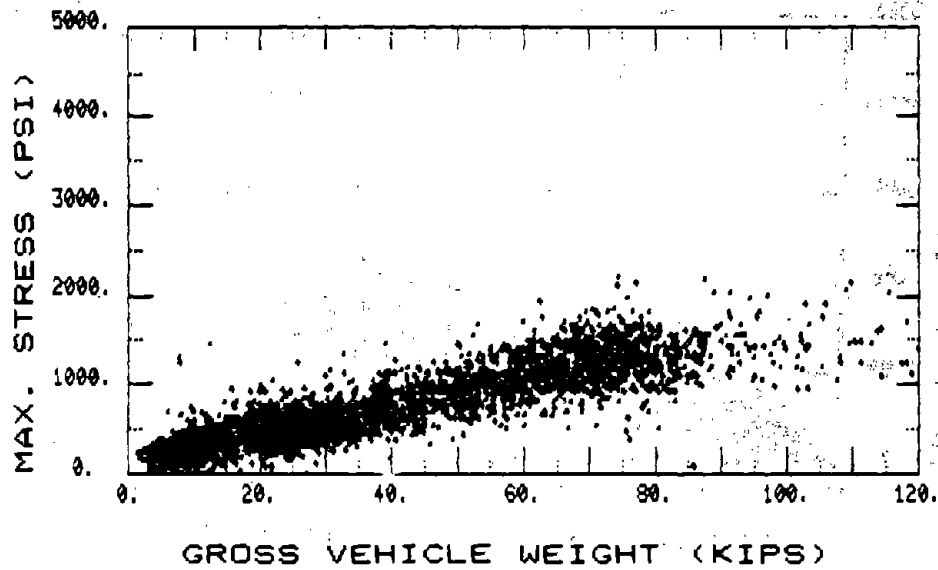
Figure 128. Max. stress vs. GVW--gauge 14: absolute max. stress = 2.4 ksi (16.5 MPa): equation of linear regression line, S (psi) = 159.26 + 14.39 GVW (kips): correlation coefficient = 0.8777: NB Route 33 over Van Buren Road.
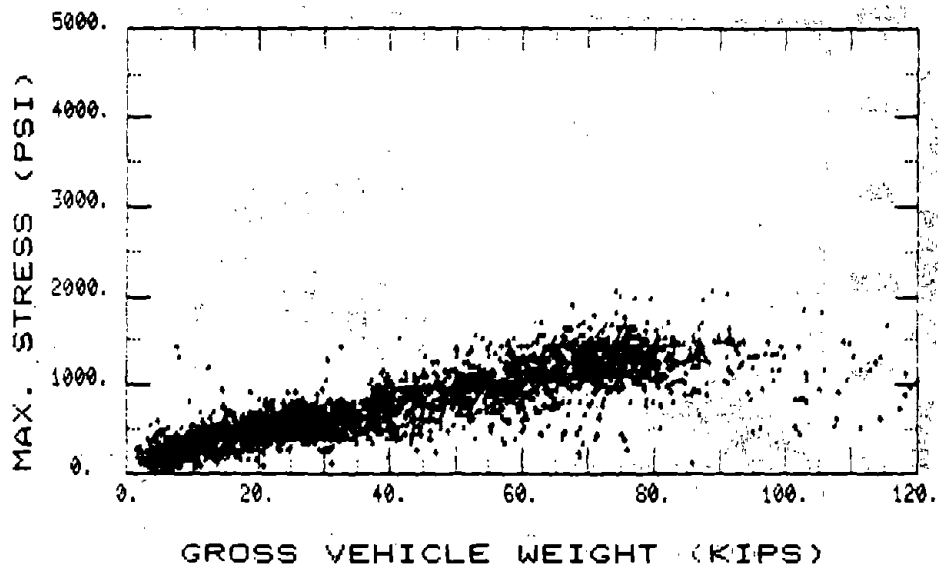
Figure 129. Max. stress vs. GVW--gauge 15: absolute max. stress = 2.1 ksi (14.5 MPa): equation of linear regression line, S (psi) = 219.92 + 12.53 GVW (kips): correlation coefficient = 0.840: NB Route 33 over Van Buren Road.

113

5. NB Route 33 Over State Park Road

a. GVW Distribution

The gross vehicle weight distribution computed for 3,188 single trucks in lanes 1 and 2 is shown in figure 130. The maximum value of GVW is 150 kips (667.2 kN).

b. Maximum Stress vs. GVW

Figures 131 through 135 show the relationships between maximum stress (S) and GVW for 5 of the 16 gauges computed using data from 2,861 single trucks in lane 1 only. The five gauges were selected to provide representative maximum stress vs.-GVW relationships for the main girders of spans 2 and 3. Data from the diaphragm gauges could not be processed to show maximum stress-vs.-GVW relationships. In addition the absolute maximum stress is provided below each figure. Also provided are the equation of the linear regression line in psi and kip units and the sample correlation coefficient. The conversion of all strain data to stress assumes a value of Young's Modulus for the prestressed girders of 4,500 ksi (31,028 MPa).
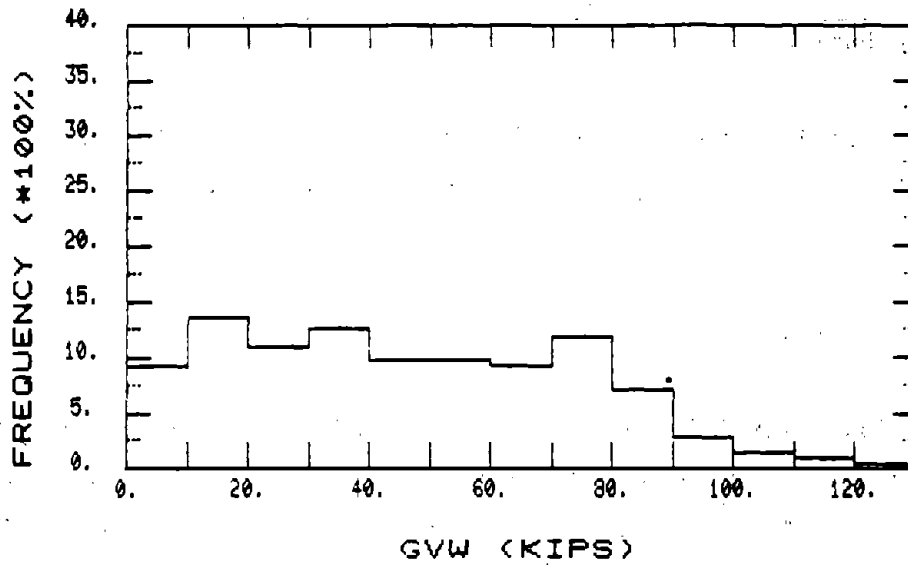
Figure 130. GVW distribution: max. GVW = 150 kips (667.2 kN): NB Route 33 over State Park Road.
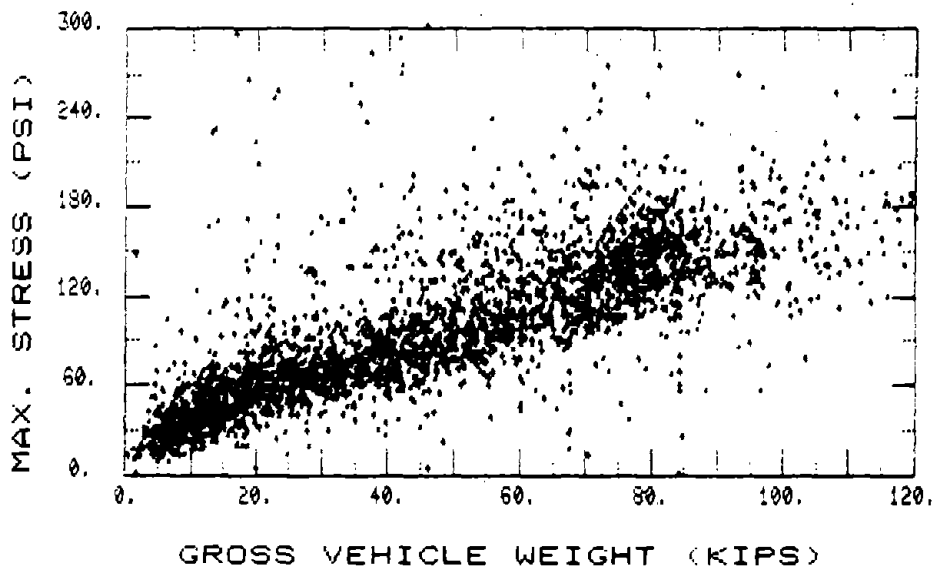
Figure 131. Max. stress vs. GVW—gauge 1: absolute max. stress = 1.13 ksi (7.8 MPa): equation of linear regression line, S (psi) = 36.80 + 1.34 GVW (kips): NB Route 33 over State Park Road.

115
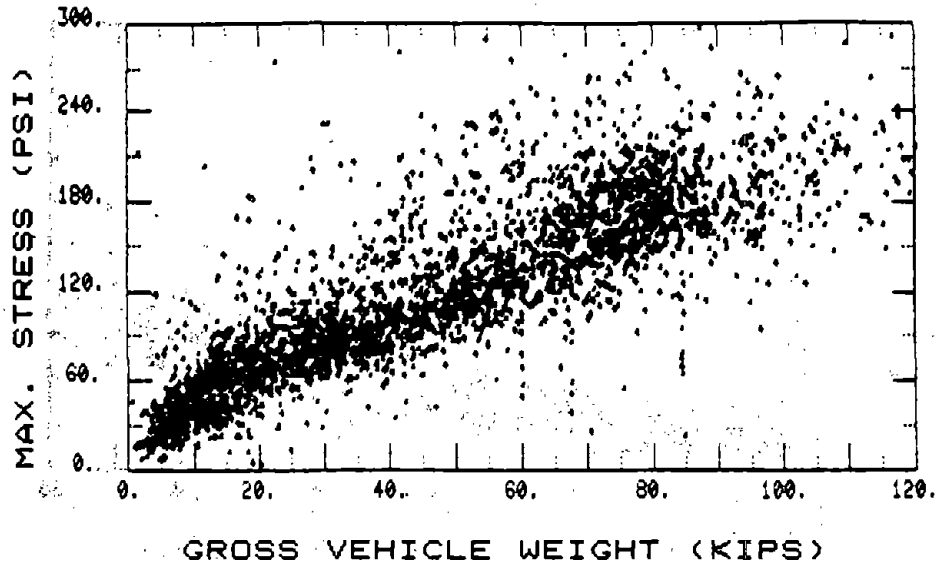
Figure 132. Max. stress vs. GVW--gauge 2: absolute max. stress = 0.37 ksi (2.6 MPa): equation of linear regression line, S (psi) = 39.34 + 1.68 GVW (kips): correlation coefficient = 0.830: NB Route 33 over State Park Road.
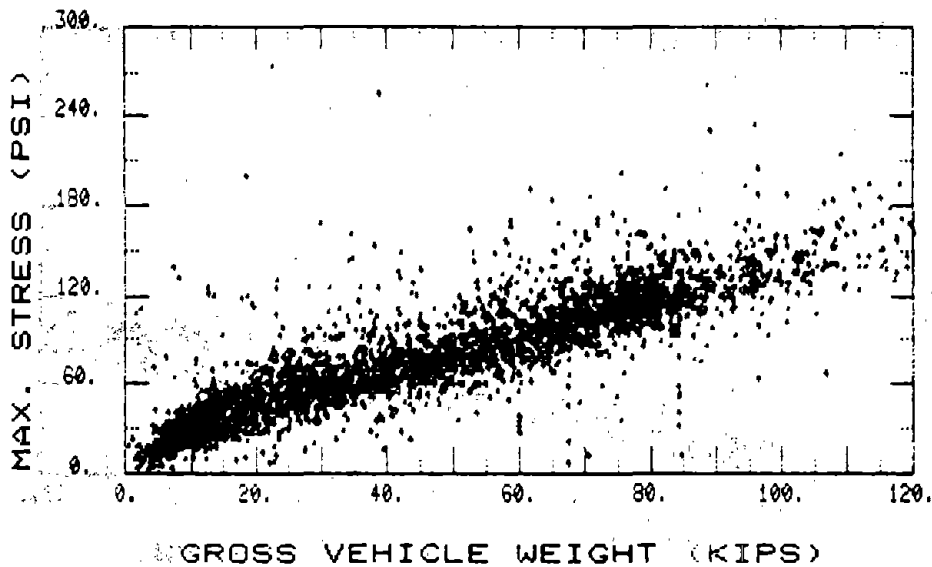
Figure 133. Max. stress vs. GVW--gauge 3: absolute max. stress = 0.27 ksi (1.9 MPa): equation of linear regression line, S (psi) = 22.4 + 1.19 GVW (kips): correlation coefficient = 0.861: NB Route 33 over State Park Road.

116
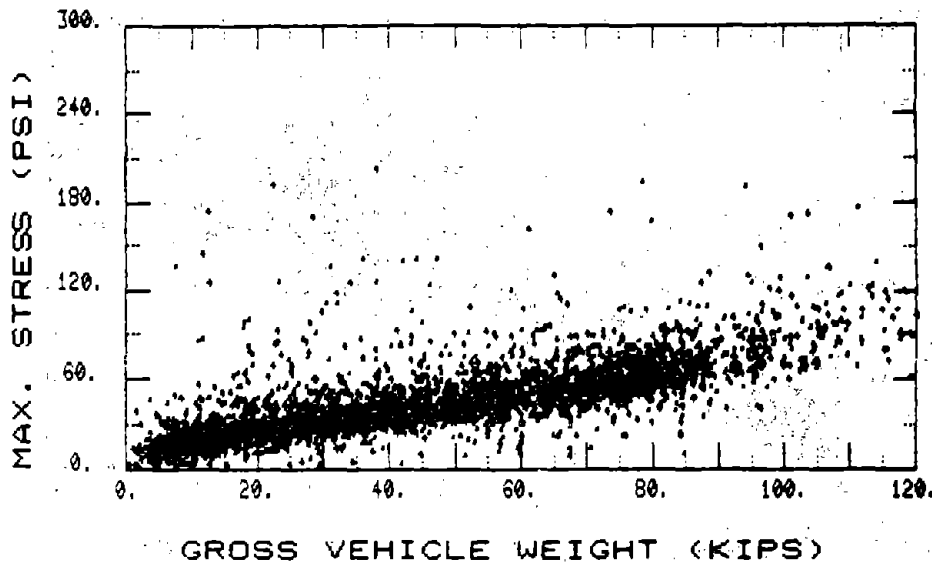
Figure 134. Max. stress vs. GVW--gauge 4: absolute max. stress = 0.25 ksi (1.7 MPa): equation of linear regression line, S (psi) = 14.18 + 0.678 GVW (kips): correlation coefficient = 0.733: NB Route 33 over State Park Road.
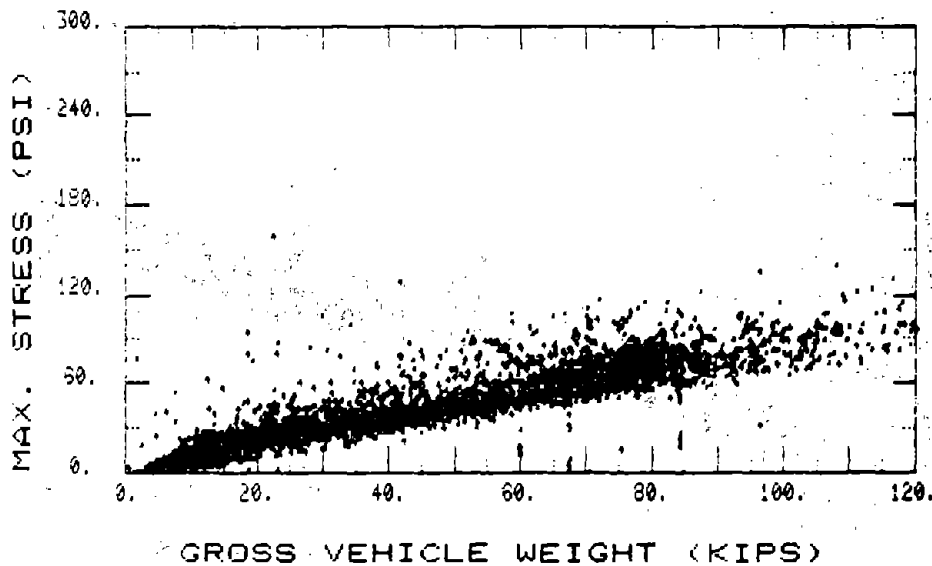
Figure 135. Max. stress vs. GVW--gauge 6: absolute max. stress = 0.16 ksi (1.1 MPa): equation of linear regression line, S (psi) = 5.35 + 0.83 GVW (kips): correlation coefficient = 0.888: NB Route 33 over State Park Road.

117

6. Discussion of Field Study Results

a. GVW Distribution

The GVW distribution for each of the four field study bridges is shown in figures 36, 64, 96, and 130. The distributions shown in these figures can be compared with those obtained in other investigations. Figure 136 for example shows the GVW distribution from the 1970 FHWA Nationwide Loadometer Survey. The results of this survey were used to develop stress cycles for design against fatigue damage of steel bridges,[6] which are incorporated into the AASHTO Specifications.[21] Figure 137 is taken from reference 19. That report presents truck weight data obtained for over 27,000 trucks crossing 33 bridges in seven States using the FHWA WIM system. Figure 137 shows the resulting GVW distribution for all trucks at all bridge sites. GVW distributions are also presented in reference 19 for many other situations, such as all trucks, all bridge sites, for each of the seven States, all trucks, all bridge sites, for interstate bridges only, and other combinations.

The GVW distributions obtained in this field study closely resemble the distributions shown in figures 136 and 137. Characteristic of these distributions is the presence of two peak values of frequency, the first at about 25 kips (111.2 kN) GVW, the second at about 70 kips (311.4 kN) GVW. The first peak corresponds to a relatively high percentage of heavy small trucks (3 axles), the second to a relatively high percentage of heavy large trucks (5 or more axles).[19] The GVW distribution in figure 130 does not show the characteristic two peaks. However, this distribution is not unlike some of those shown in reference 19 which were obtained on individual state or interstate routes. The GVW distribution will be dependent on the particular mix of trucks crossing the bridge during the weigh period. As the period is lengthened and as data from other sites are included the tendency is towards the characteristic distributions shown in figures 136 and 137.

Of particular interest is the GVW distribution corresponding to the higher values of gross vehicle weight, since most damage to bridges (and pavements)

118

corresponds to vehicles in this GVW range.[6,35] Table 2 shows a comparison
of truck percentages in the high GVW distribution range obtained in this study
with those obtained in reference 19 for all trucks, all sites, and with those
obtained in the 1970 FHWA Nationwide Loadometer Survey. The 1970 survey was
conducted before the computerized WIM system was available and relied on static
weigh scales. The relatively small percentage of trucks above 73.28 kips (326
kn) GVW obtained in the 1970 FHWA survey could be due to three reasons: (1)
gross vehicle weights may not have been so high in 1970 as they are today; (2)
heavy, illegal trucks could have avoided the weigh scales; and (3) the U.S.
Congress enacted legislation permitting an increase in the maximum GVW for
interstate routes from 73.28 kips (326 kN) to 80 kips (355.8 kN) shortly after
the 55 mph (88 km/hr) speed limit was adopted in December 1973.

Table 2 – Comparison of Truck Percentages
in the High GVW Distribution Range

	Percent of GVW Exceeding – kips (kN)				
Source	73.28 (326)	80 (355.8)	90 (400.3)	120 (533.8)	Max. GVW kips (kN)
1970 FHWA Loadometer Survey -- figure 136	5.2	0.5	0.1	-	100 (445)
Reference 19 -- figure 137	12.8	5.9	1.4	-	120 (534)
EB Route 22 -- figure 36	10.9	4.2	1.7	0.2	147 (656)
WB Route 22 -- figure 64	11.9	6.2	2.7	0.1	160 (712)
NB Route 33 - Van Buren Road -- figure 96	14.4	7.0	3.5	0.5	150 (667)
NB Route 33 - State Park Road -- figure 130	20.9	12.9	5.7	0.5	150 (667)

The study reported in reference 19 reflects 1981 truck data which likely ac-
counts for the increase in the percentage of trucks above 73.28 kips (326 kN)
GVW at that time. However, that study and the present field study conducted
in 1985 indicate that a significant number of trucks exceed 80 kips (355.8 kN)
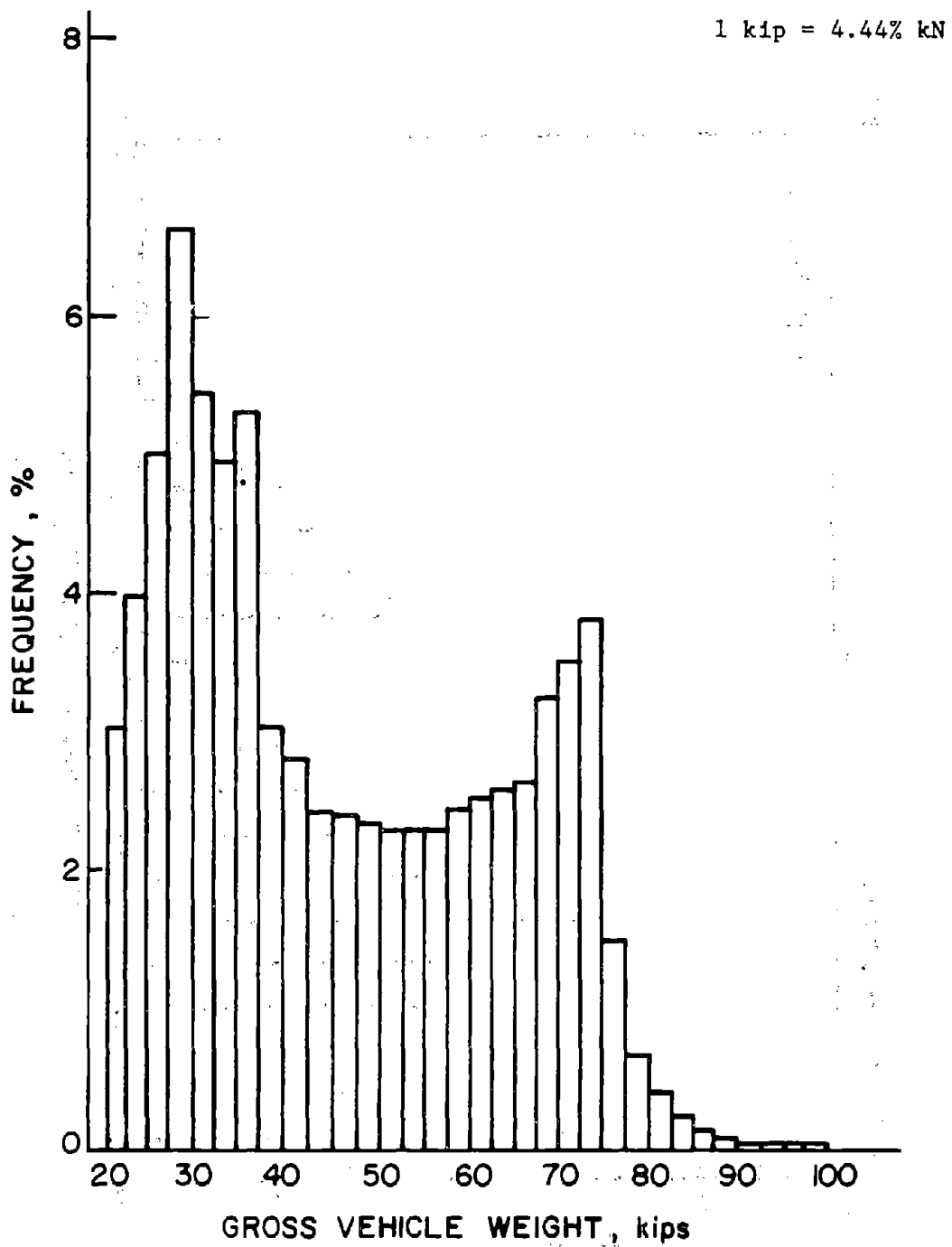
Figure 136.   1970 FHWA Nationwide Loadometer Survey

All Sites, All Trucks

1 kip = 4.448 kN

27519 Trucks
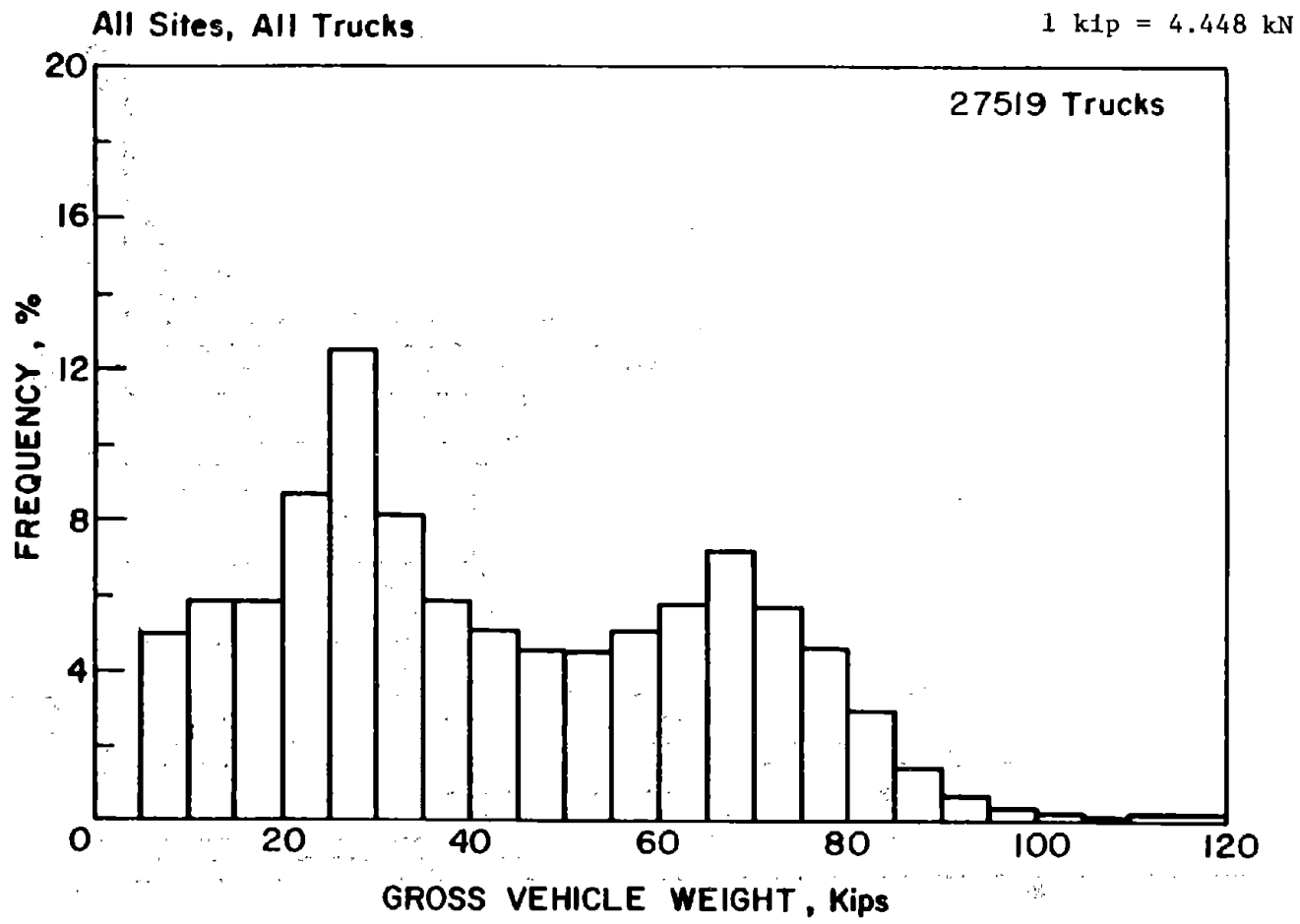
Figure 137. GVW distribution—all sites—all trucks (1981).

(From reference 19)

GVW. Also the maximum GVW has increased during the 1980's. It should be pointed out that a few of the extremely high values of measured GVW obtained in this study may be due to the presence of more than one truck on the weigh span even though the truck weight data was carefully screened (page 60) to eliminate this possibility.

b. Stress Range Distribution

The stress range distributions computed for the three steel field study bridges are typical of those obtained from stress history studies of steel bridges (see references 11, 35, 55, and 56). Fatigue analyses of details subjected to variable amplitude loading, such as those found in highway bridges, can be made directly from measured stress range distributions and are based on the Strange Range vs. Cycle Life (SN) relationships developed at Fritz Engineering Laboratory,[6] and incorporated into the AASHTO Specifications.[21] Reference 55 indicates that fatigue life is a function of two parameters, the effective stress range (Miner or RMS),[6] and maximum stress range. Three different situations are encountered:

1. Effective Stress Range $>$ Constant Amplitude Fatigue Limit
2. Effective Stress Range $<$ Constant Amplitude Fatigue Limit
   Maximum Stress Range $>$ Constant Amplitude Fatigue Limit
3. Effective Stress Range $<$ Constant Amplitude Fatigue Limit
   Maximum Stress Range $<$ Constant Amplitude Fatigue Limit

For case 1, the effective stress range is used as the equivalent constant amplitude stress range to determine fatigue life from the constant amplitude SN curves. Figure 138 shows the constant amplitude SN curves on which the allowable fatigue stresses of the AASHTO specifications are based.[21] If, for example, the effective (Miner) stress range at a category E detail is 10 ksi (68.95 MPa) the fatigue life is 10^6 cycles (refer to figure 138).

For case 2, the effective stress range must be used in conjunction with a straight line extension of the sloping portion of the SN curve in figure 138

to determine fatigue life.[55] An example of case 2 is shown in the figure for a category E detail. The assumed stress range distribution shown in the figure has a maximum stress range of about 14 ksi (96.5 MPa) exceeding the fatigue limit of 5 ksi (34.5 MPa). The effective Miner stress range is about 2.4 ksi (16.6 MPa). As shown in the figure the fatigue life of the category E detail is 7×10^7 cycles.

For case 3 since all of the stress range spectrum is below the constant amplitude fatigue limit, none of the stress ranges should be damaging and no fatigue crack propogation is expected.

Fatigue analyses using stress range distributions from 2 of the gauges on the NB Route 33 Bridge over Van Buren Road will illustrate the above:

    o For gauge 2 on span 1 (figure 16), the maximum stress range is 6.2 ksi (42.7 MPa) and the effective Miner stress range is 0.85 ksi (5.9 MPa) (figure 98). If a category E detail existed near gauge 2, such as the end of a welded cover plate, case 2 exists and the fatigue life is determined from an extension of the sloping category E line as shown in figure 138 corresponding to the effective stress range of 0.85 ksi (in this case, well off the figure to the right). If a category B detail exists near gauge 2, such as a flange to web fillet weld, case 3 applies and no fatigue crack propogation is expected.

    o For gauge 15 on span 2 (figure 16), the maximum stress range is 2.6 ksi (17.9 MPa) and the effective Miner stress range is 0.41 ksi (2.8 MPa) (figure 108). Therefore case 3 applies to all categories of details which could exist in the vicinity of this gauge.

c. Maximum Stress Range and Maximum Stress

The following observations regarding the maximum stress range and maximum stress should be kept in mind when studying the stress range distributions and maximum stress vs. GVW information presented in this chapter.

    o The values of maximum stress range and maximum stress recorded at a particular gauge location during the field study are not necessarily both produced by the same truck crossing the bridge.

123
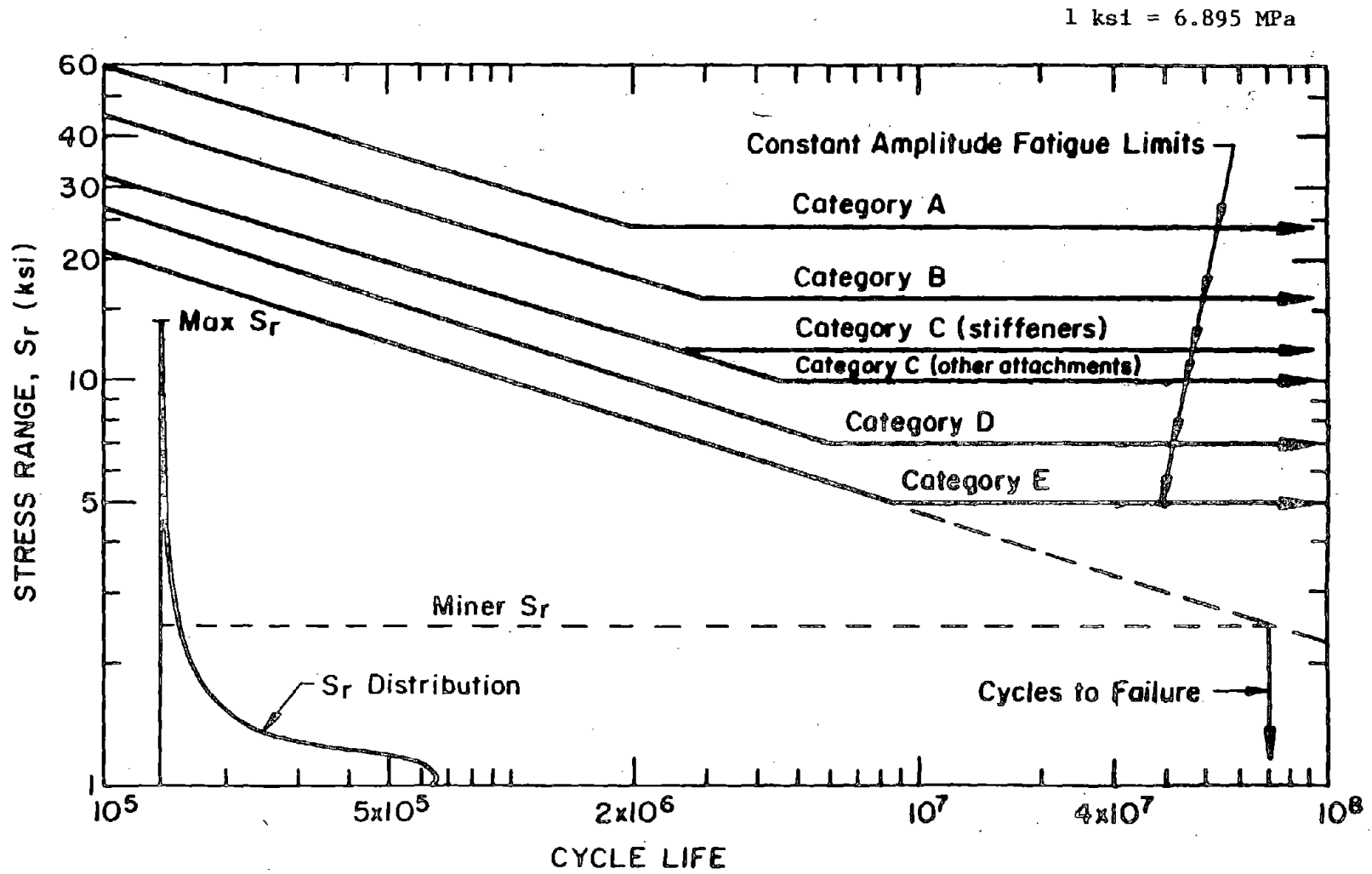
Figure 138.   Design stress range (SN) curves--categories A to E.

o Continuous manual balancing of the strain conditioning centers is re-
  quired, as explained on page 21, to ensure zero strain at each gauge
  location prior to a truck crossing the bridge. During times of rapidly
  increasing or decreasing temperatures, such as during mornings and
  evenings, all 16 strain conditioners have to be manually balanced (by
  rotating a control knob) quite frequently, as often as three or four
  times a minute to prevent "zero drift". Occasionally a truck would
  cross the bridge before all strain conditioners could be balanced.
  Improper balancing of the strain conditioners does not affect the
  recorded values of stress range since stress range is a function of
  the difference between strains not the absolute strain. However,
  maximum stress is a function of absolute strain and accuracy requires
  proper balancing. The recorded values of maximum stress therefore
  are as accurate as humanly possible but some values may be a bit too
  high or too low.

o Occasionally the maximum value of stress range and the maximum value
  of stress which is recorded at any particular gauge location can be
  significantly in error due to a problem unrelated to the design or
  operation of the WIM+RESPONSE system itself. It has frequently been
  observed during this and previous stress history studies that unusually
  high values of strain can result from electrical noise introduced by
  external sources, even though care is taken to sheild cables and ground
  the system to eliminate most external interference. It has been
  observed that an erroneous spike in the strain-time response curve can
  occur if a strong radio transmitter is activated near the bridge. High
  powered CB transmitters in trucks or radio transmissions from low flying
  aircraft overhead are two such sources of interference. Both the EB and
  WB bridges on Route 22 over 19th Street are located about 4 mi (6.4 km)
  from the ABE Airport and on the approach to Runway 6. Aircraft on the
  approach to this runway cross almost directly over these bridges at an
  elevation of about 1,500 ft (457 m). The NB bridges on Route 33 over
  Van Buren Road and State Park Road are about 2 mi (3.22 km) either side
  of the approach to Runway 24 and about 10 mi (16.1 km) from the ABE
  Airport. Aircraft on IFR approaches pass between these bridges at about
  2,800 ft (853 m) elevation. Although aircarft transmitters can be a
  source of interference at all four bridges, CB transmitters in trucks
  probably account for more frequent interference. This source of inter-
  ference cannot be avoided, unfortunately, at any bridge location.
  Figure 139 shows a typical spike which occured in the response curve for
  strain gauge transducer number 1 of the WB bridge on PA Route 22 over
  19th Street (figure 11). A sharp increase in strain gauge voltage (which
  is converted to strain) occurs during the passage of truck No. 27, disk
  No. 34. The response curve for the same truck but at strain gauge trans-
  ducer number 4 of the same bridge (figure 11) which is shown in figure
  140 does not contain a spike. The infrequent occurrence of spikes should
  not significantly affect the resulting value of truck weight because of
  the statistical sampling and averaging of strains from several trans-
  ducers. However, occasional spikes can have a pronounced effect on a
  few of the maximum stress ranges and maximum stresses recorded at a

125
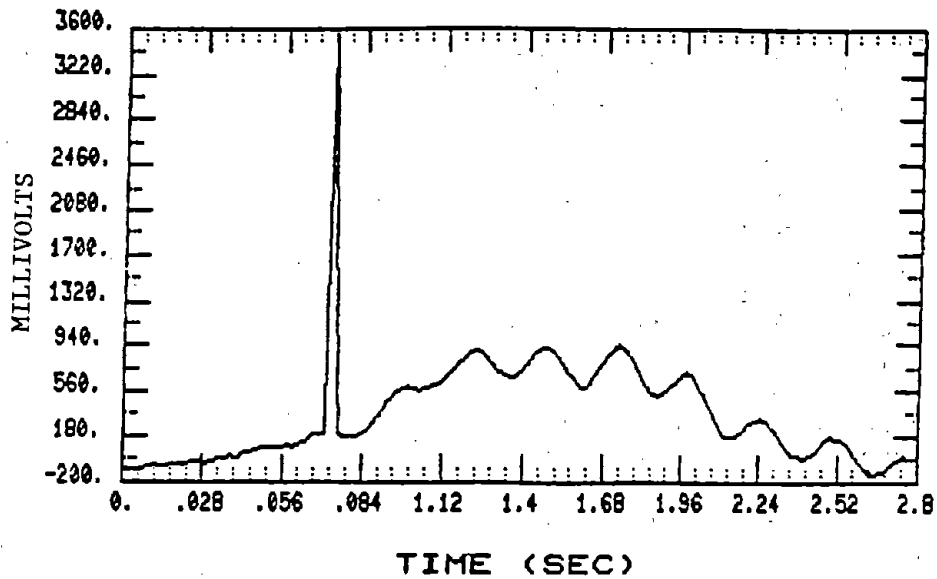
Figure 139. Typical voltage--time trace at a gauge location due to passage of one vehicle.
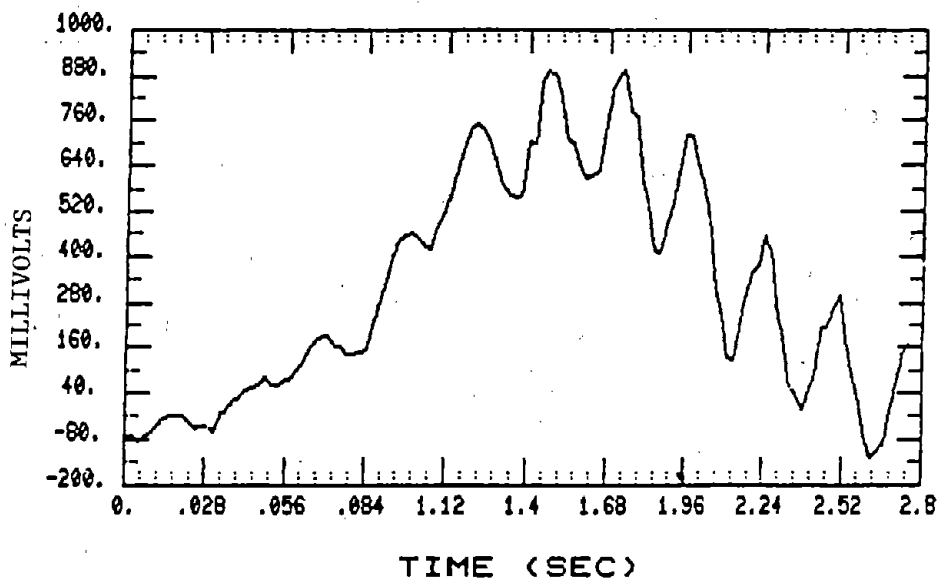
Figure 140. Typical voltage--time trace at a gauge location due to a multiple truck event.

126

transducer or gauge. Outside electrical interference can be minimized
by care taken in shielding and grounding the electrical cables and
system equipments, but it is difficult to eleminate it altogether.
Improvements in the design of the WIM+RESPONSE system might consider
suitable methods of eliminating these spikes when processing the
RESPONSE data.

o Stress history studies indicate that the peak values of maximum stress
range at a gauge location usually exceed the peak values of maximum
stress range at a gauge location usually exceed the peak values of max-
imum stress. This is because stress range is computed as the algebraic
difference between the maximum and minimum stress whereas the absolute
maximum stress is the difference between the maximum positive stress
and zero or maximum negative stress and zero. Thus, if both positive
and negative stresses exist, the maximum stress range will be larger
than the absolute maximum stress. However, if different trucks produce
the maximum stress range and maximum stress this relationship may not
always be true. As a general rule, however, for a reasonably large
truck sample, if the peak value of maximum stress is significantly
larger than the peak value of maximum stress range, the presence of a
spike in one or more response curves is suspected.

o For fatigue analyses under variable amplitude stress range it is impor-
tant to determine the maximum stress range for the spectrum, as dis-
cussed on page 122. If a spike is suspected the maximum stress range
may be taken either from the stress range distribution plot or from a
listing of maximum stress ranges, disregarding the value associated with
the spike. For example, since a spike is present in the response curve
for strain gauge transducer number 1 of the WB bridge on Route 22 over
19th Street, figure 139, the maximum stress range might be obtained in-
stead from figure 65. In that figure the maximum stress range appears
to be 2.6 ksi (17.9 MPa). However, since the frequency of occurence of
the larger stress ranges is so small it is possible that the real
maximum stress range is somewhat larger than 2.6 ksi (17.9 MPa) and does
not appear in the figure. In this case a listing of stress ranges larger
than 2.6 ksi (17.9 MPa) should reveal the correct value. On the other
hand, for strain gauge transducer number 4, on the same bridge, no spike
is suspected, and none occurred as shown in figure 140. Thus the maxi-
mum stress range of 5.6 ksi (38.6 MPa) is the correct value. Note that
this value is somewhat larger than the 2.2 ksi (15.2 MPa) which appears
to be the maximum in figure 69.

d. Stress Range vs. GVW

Fatigue damage of steel bridge details is related primarily to the fre-
quency of stress ranges to which the details are subjected.[6] The stress
cycle provisions of the 1983 AASHTO specifications (reference 21--article 10.3.2)

for main (longitudinal) members are based on one maximum stress range per truck event and an assumed linear relationship between maximum stress range and GVW (see references 6,35,57,58,59). The concept of one maximum stress range per truck event for main members has been criticized because it implies that the remaining numerous smaller stress ranges produce no damage. As mentioned on page 122 this is not the situation for cases 1 and 2 discussed in that article.

The assumption of a linear relationship between the maximum stress range and GVW, although easy to apply, has not been rigorously investigated. The following illustrates the use of the data obtained from this field study to study the validity of this relationship. Figures 141 and 142 show the relationship between maximum stress range and GVW which was obtained at one gauge location on a main (longitudinal) girder for each of two bridges. Figure 141 shows this relationship for strain gauge transducer number 1 on the EB bridge on PA Route 22 over 19th Street (figure 3). Figure 142 shows the relationship for strain gauge transducer number 1 on the NB bridge on PA Route 33 over Van Buren Road (figure 16). Only one maximum stress range is plotted for each truck GVW event. Only trucks travelling in lane 1 are included for each bridge (2,861 trucks for the EB bridge and 2,856 trucks for the NB bridge).

Even though the relationships shown in figures 141 and 142 are not conclusive and are valid only for two gauge locations the following observations can be made:

o Although two span lengths are involved in two different bridges on different traffic routes (84 ft-10 (28.9 m) EB span 2 and and 39 ft-7 5/8 (12.08 m) NB span 1) the two figures look quite similar. The two linear regression line equations representing the data are almost the same as are the correlation coefficients.

o The rate of increase in maximum stress range is less than the rate of increase in GVW. For the EB bridge a doubling of GVW from 40 to 80 kips (117.9 to 355.8 kN) is accompanied by a stress range increase from 0.61 to 1.00 ksi (4.21 to 6.895 MPa) a ratio of 1.64. For the NB bridge a doubling of GVW from 40 to 80 kips (117.9 to 355.8 kN) is accompanied by a stress range increase from 0.54 to 0.86 ksi (3.72 to 5.93 MPa) a ratio of 1.59. Thus the maximum stress range increases at a lower rate than the GVW.

128
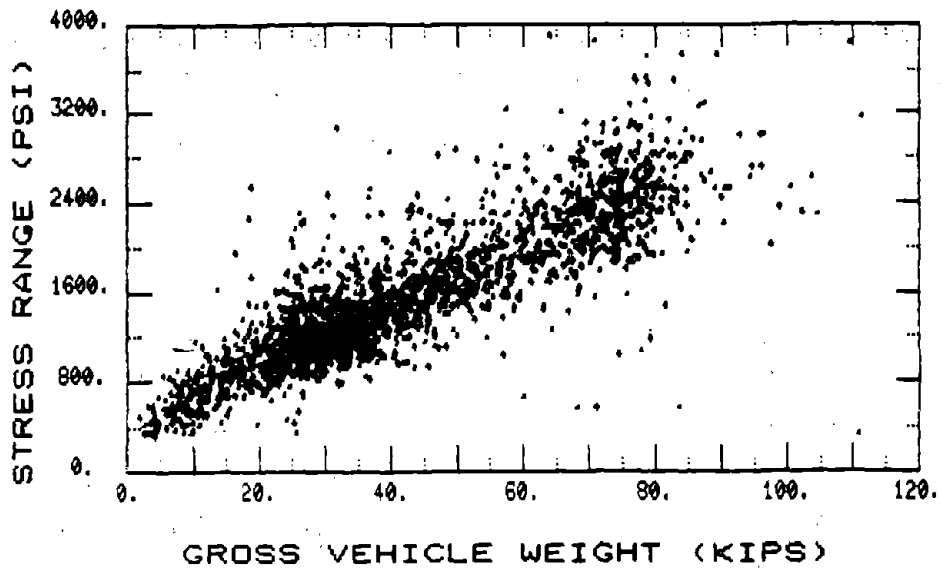
Figure 141. Stress range vs. GVW--strain gauge transducer no. 1--EB Bridge on PA Route 22 over 19th Street: max. S_r = 5.07 ksi: equation of linear regression line S_r (ksi) = 506.73 + 25.11 GVW (kips): correlation coefficient = 0.843.
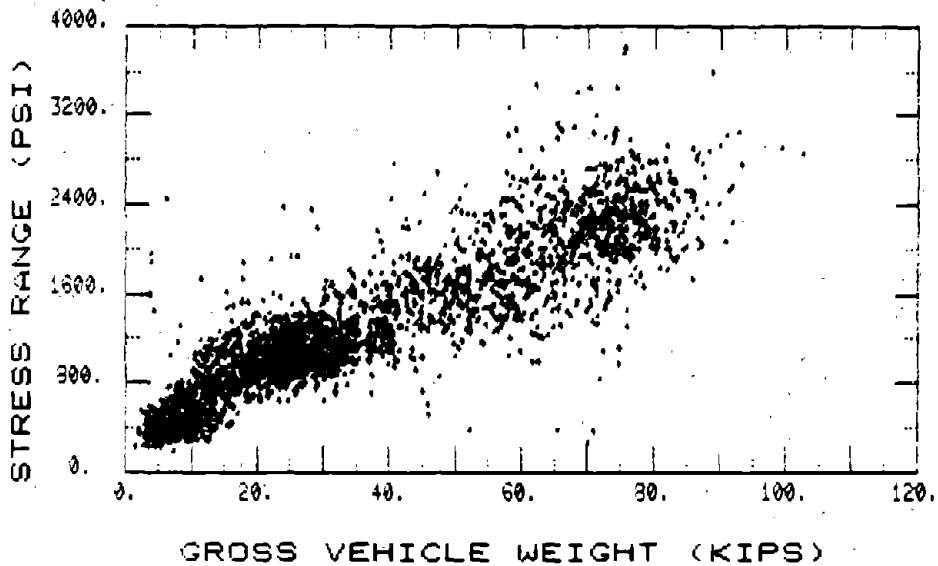
Figure 142. Stress range vs. GVW--strain gauge transducer no. 1--NB Bridge on PA Route 33 over Van Buren Road: max. S_r = 4.17 ksi: equation of linear regression line S_r (ksi) = 417.72 + 24.53 GVW (kips): correlation coefficient = 0.884.

129

e. Stress Range vs. Strain Rate

Fracture toughness of metals, K_{Ic}, is known to be dependent on strain rate.[60] Higher strain rates often produce lower fracture toughness and, hence, greater crack sensitivity. It is therefore reasonable to assume that the sensitivity of details to unstable crack growth will be significantly influenced by high stress ranges in combination with high strain rates. An example of the use of the WIM+RESPONSE data obtained in this investigation to explore this combination is presented in the following.

Figures 143 and 144 show the relationships between stress range and strain rate for two gauge lolations. Figure 143 corresponds to strain gauge transducer number 1 on the EB bridge on PA Route 22 over 19th Street (figure 3). Figure 144 corresponds to strain gauge transducer number 1 on the NB bridge on PA Route 33 over Van Buren Road (figure 16). These are the same two gauges used in figures 141 and 142. Data from 110 trucks on disk No. 27 were used in figure 143. Data from 110 trucks on disk No. 2 were used in figure 144. Each of these disks contained the absolute maximum strain rate that was recorded for the bridge during the field study. Stress range was computed using the ascending method; that is, one stress range count is the algebraic difference in stress from the bottom of a given cycle to the next peak of the same cycle. Strain rate is computed as the positive average slope from the bottom of a given cycle to the next peak of the same cycle. A zero threshold was used in computing both stress range and strain rate.

It is observed that the plotted points in figures 143 and 144 all lie along discrete straight line trajectories. For a given sampling rate, the slope of each trajectory is a function of the number of strain data samples included between the bottom of a given cycle and the next peak of the same cycle. The following derivation should clarify this relationship.

The solid curve in figure 145 (a) represents a typical analog strain vs. time curve produced by a strain gauge as a vehicle crosses the bridge. The analog curve is converted to digital information by the system analog-to-
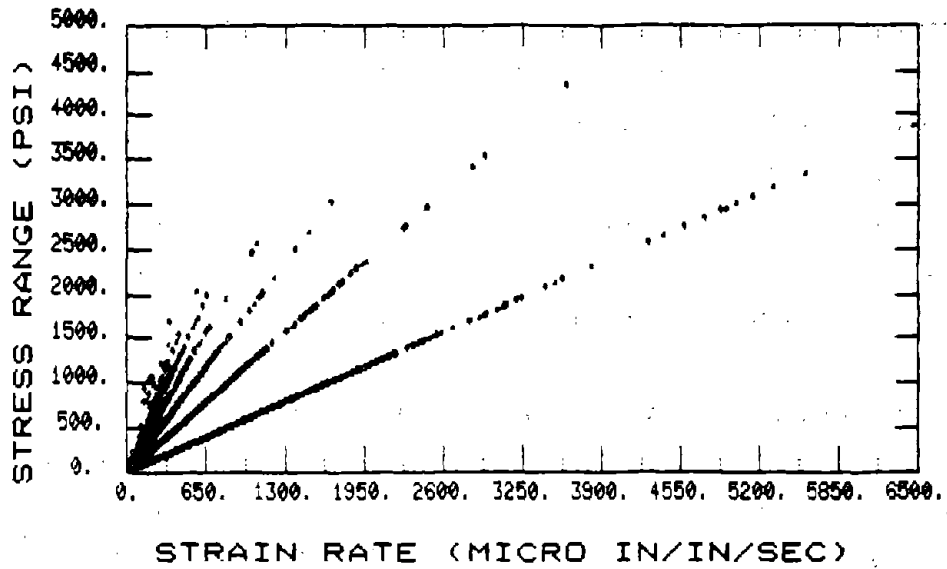
Figure 143. Stress range-vs.-strain rate--strain gauge transducer no. 1--EB
Bridge on PA Route 22 over 19th Street.
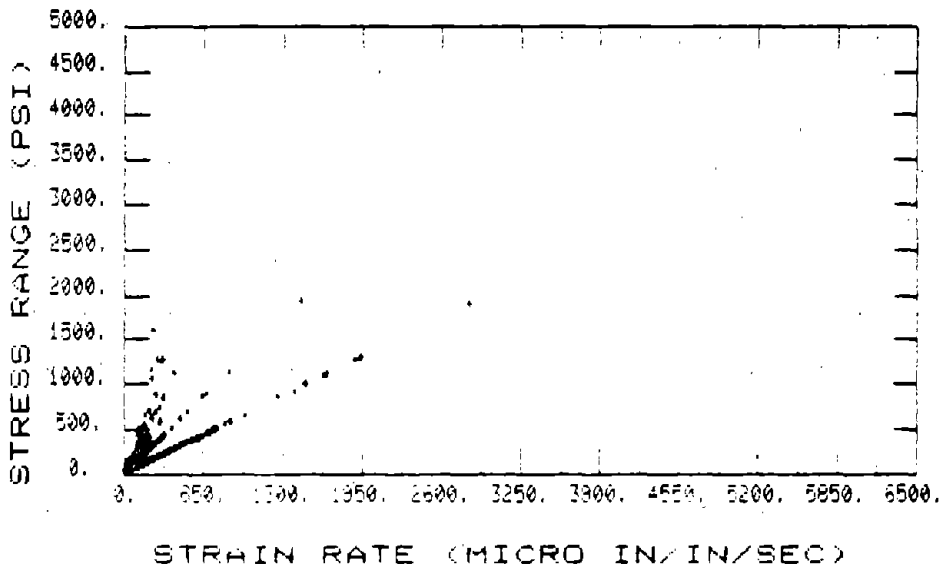
Figure 144. Stress range-vs.-strain rate--strain gauge transducer no. 1--NB
Bridge on PA Route 33 over Van Buren Road.

131

digital converter (page 17). The sampling rate is specified by the operator at the beginning of the data acquisition program. For example, the sampling rates for the field study bridges are as follows:

EB Route 22 over 19th Street   - 50 samples/s

WB Route 22 over 19th Street   - 45 samples/s

NB Route 33 over Van Buren Road   - 45 samples/s

NB Route 33 over State Park Road   - 40 samples/s

The discrete points along the solid curve in figure 145 (a) represents the digital input values of strain (strain data points used by the response system) which are spaced at equal time intervals, Δt, where

$$\Delta t = \frac{1}{S} \tag{1}$$

and S is the sampling rate. The slope of the dashed line in the figure is computed strain rate, $\dot{\varepsilon}$, given by

$$\dot{\varepsilon} = \frac{\varepsilon}{t} \tag{2}$$

where ε is the strain range and t is the time interval between the bottom and the peak of the cycle shown, and

$$t = \frac{N-1}{S} \tag{3}$$

where N is the number of data points between the bottom and the peak of the cycle. Note that digital data points may not correspond to the exact bottom and peak of the analog curve. For computation purposes ε and t are computed for the local minimum and maximum values of the data points in the vicinty of the bottom and peak.

Since the stress range, S_r , is $\tag{4}$

$$S_r = E\varepsilon$$
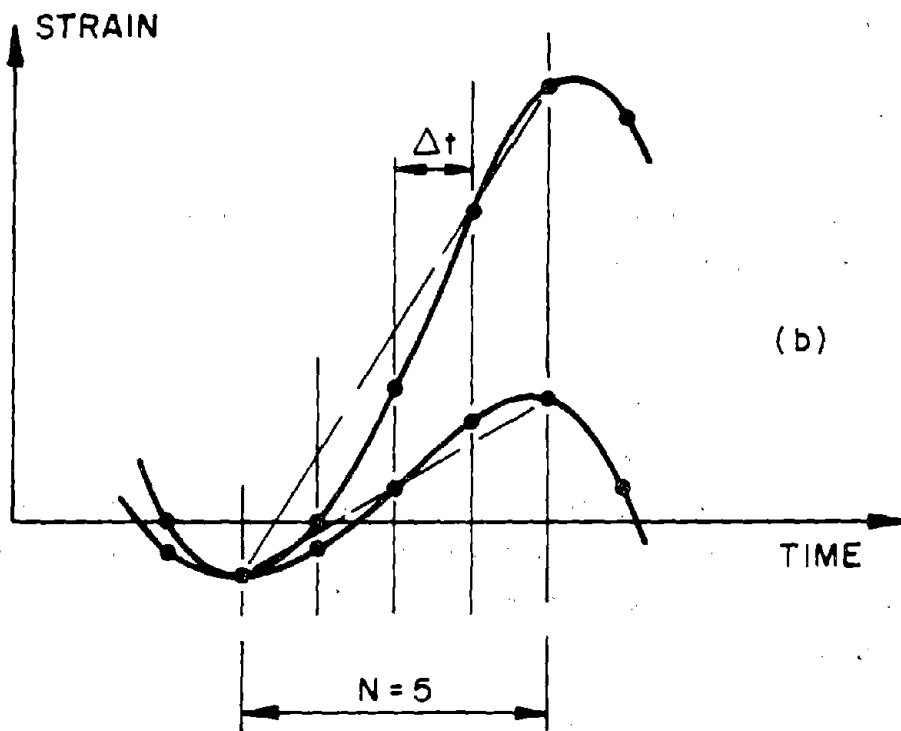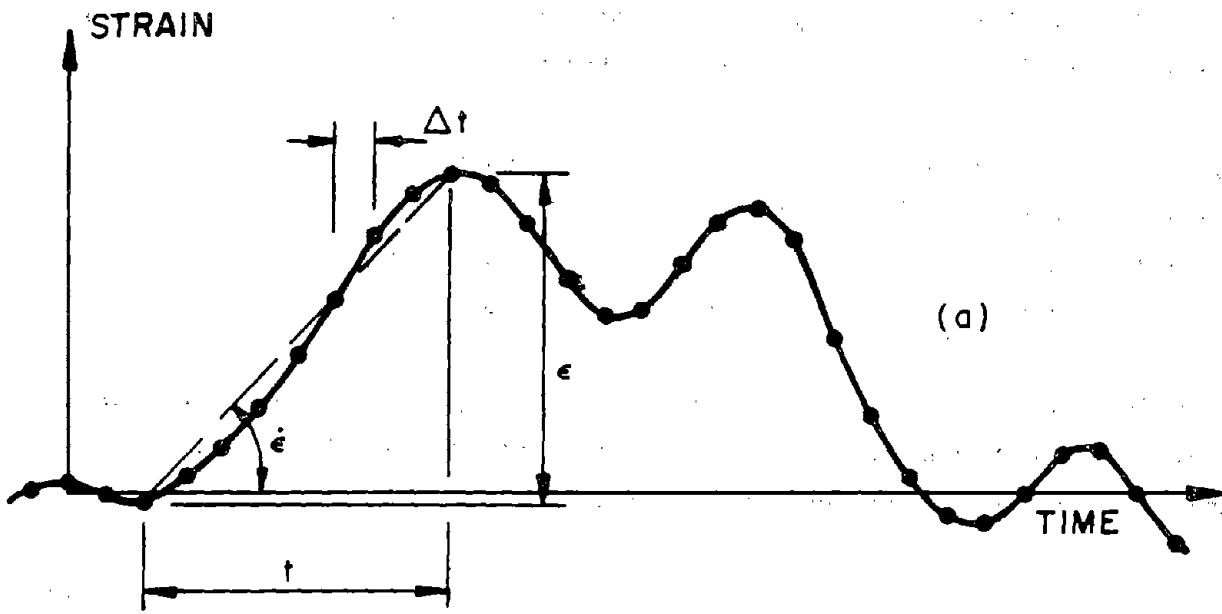
Figure 145. Digital representation of typical analog strain-vs.-time curves.

where E is Young's Modulus, then the slope of a given trajectory in figures
143 and 1-4 is determined by

$$\frac{S_r}{\dot{\varepsilon}} = \frac{E}{S} \ (N - 1) \tag{5}$$

Consider, for example, the trajectory in figure 143 having the smallest
slope. The maximum recorded strain rate is 6,458 micro in/in/s (6,458 micro
m/m/in) and is shown in figure 143 as the point of the extreme right end of
the trajectory. The corresponding stress range is 3,875 psi (26.718 kPA).
For a sampling rate of 50 and E - 30 x 10^6 psi (206.9 kPa), then N = 2. Thus
each point along this trajectory corresponds to all strain vs.-time curves for
the entire 110 truck sample which have cycles with digital data points only at
(or near) the bottom of a cycle and at (or near) the peak of the same cycle
and none between. The time interval between the bottom and next peak of all
these cycles will be 1/50 = 0.02 seconds.

The trajectory in figure 143 having the next largest slope corresponds
to N = 3. In this case all points on this trajectory correspond to cycles
with digital data points at (or near) the bottom and next peak plus one be-
tween, and so on.

Figure 145 (b) shows cycles from two different strain-vs.-time curves.
The two cycles have the same value of N but different values of strain range.
The data points for each of these cycles will plot on the same stress range-
vs.-strain rate trajectory. That trajectory has a slope corresponding to N =
5.

It is evident that as the sampling rate increases, the number of data
points and the number of trajectories will increase. For example, for a samp-
ling rate of 100, additional trajectories would appear in figure 143 and these
would fall between the trajectories shown in the figure. The N value would
also change with N = 2 corresponding again to the trajectory having the
smallest slope.

The data points at the upper ends of all the trajectories define an envelop which provides the relationship between high stress range and corresponding strain rate for a particular location on a bridge. Figures 143 and 144 both indicate that the highest strain rates are not associated with the highest stress range. In each figure the maximum observed strain rate is the data point at the end of the trajectory with the smallest slope (N = 2). Also in each case the corresponding stress range is smaller than the maximum observed (or plotted) stress range.

If, for example, the envelope in figure 143 were constructed of straight line segments between the extreme data point on each trajectory, the maximum stress range and corresponding strain rate would be about 4.3 ksi (29.7 MPa) and 3,580 micro in/in/s (3,580 micro m/m/s). The maximum strain rate of 6,458 micro in/in/s (6,458 micro m/m/s) occurs with the stress range of about 3.9 ksi (26.7 MPa).

In figure 144 the maximum stress range of about 1.9 ksi (13.1 MPa) is accompanied by a strain rate of about 1,430 micro in/in/s (1,430 micro m/m/s). However, at about this same or slightly smaller stress range, strain rates up to the maximum recorded 2,850 micro in/in/s (2,850 mirco m/m/s) were obtained.

RESULTS OF ANALYTICAL STUDIES

1. Description of Analytical Studies

Girder live-load-plus-impact stresses were computed for all four bridges
using the provisions of the 1983 AASHTO Specifications, 13th Edition. Live-
load-plus-impact stresses in the fascia girders of the EB and WB bridges on
PA Route 22 over 19th Street were also computed using the provisions of the
pre-1957 AASHO Specifications. Since the fascia girders of the EB and WB
bridges were originally designed about 1951 and not modified during the 1983-
84 retrofit, except for the addition of shear connectors, it is of interest to
compare the two sets of stresses. Stresses computed by the pre-1957 provisions
assume a noncomposite concrete deck which is consistent with the construction
of the original 1951 bridges. Prior to 1957 live-load-plus-impact was dis-
tributed to the fascia girders assuming the deck to act as a simple span be-
tween the fascia and first interior girders. The 1957 AASHTO specification,
7th Edition, and subsequent specifications require, in addition, the use of
S/D distribution factors similar to those used for interior girders.

Finite element live-load-plus-impact analyses of each of the three steel
girder bridges were performed on the CYBER 730 Computer located at Lehigh
University. For the EB and WB steel bridges on PA Route 22 over 19th Street
and for the NB steel bridge on PA Route 33 over Van Buren Road only span 2 of
each bridge was analyzed. A finite element analysis of the NB prestressed
concrete bridge on PA Route 33 over State Park Road was not performed.

For each of the steel bridge spans the complete three-dimensional super-
structure was modelled for finite element analysis using the SAP IV program.[61]
Beam elements are used to model the diaphragm members including the web connec-
tion plates (transverse web stiffener), and the bottom flanges of the girders.
Truss elements are used to model the transverse web stiffeners between the
diaphragms and the top flanges of the girders. Plane stress elements are used
to model the girder webs. Plate bending elements are used to model the concrete
deck. Complete interaction between the concrete deck and steel girders is

136

assumed. Beam elements are also used to model the discontinuous concrete
barriers along the edges of the deck.

2. EB Route 22 Over 19th Street

Figures 146 through 150 compare girder live-load-plus-impact flexural
steel stresses computed in accordance with the AASHTO specifications with
flexural stresses obtained from finite element analyses. AASHTO HS 20 (MS 18)
truck loading is used throughout. The girder spacing and deck width are pro-
vided on page 29.

In each figure, values of girder stresses shown as points on the upper
two solid lines (points are located directly below each girder) are computed
in accordance with the 1983 AASHTO specifications assuming both composite and
noncomposite construction. The original 1951 design was noncomposite. The
new 1983-84 deck was made composite. The pre-1957 AASHO specifications are
also used to calculate the fascia girder stresses which are the points located
on the dashed lines.

Values of girder stresses located on the lower solid line were obtained
from finite element analyses of the actual composite superstructures. In these
analyses either one or two design traffic lanes of HS 20 (MS 18) trucks were
used and placed in the transverse locations shown at the top of each figure.
The arrows represent a line of HS 20 (MS 18) wheel loads. the position of each
AASHTO truck on the span is shown at the bottom of each figure. The arrow
indicates the direction of travel for the trucks.

Figure 151 compares girder stresses resulting from the field study with
live load plus impact stresses computed from a finite element analysis of the
composite superstructure. Points on the solid line labelled "Field Study" are
the maximum girder stresses measured at section 1 of figure 3 as the calibra-
tion truck travelled across the span on a typical run in lane 1 as shown at
the top of the figure. The transverse position of the truck in lane 1 is
unknown. The longitudinal position of the truck corresponding to each maximum
girder stress is also unknown. However, a single truck location would not likely

137

produce simultaneous maximum stress in each girder at section 1. It was observed that the maximum girder stresses at sections 1 and 3 of figure 3 which were obtained during a typical run of the calibration truck were not significantly different.

Points on the solid line of figure 151 labelled "Finite Element--Composite" are the girder stresses calculated at section 1 of figure 3 in a finite element analysis of the composite span with a single calibration truck in the center of lane 1 as shown at the top of the figure. In the analysis the 27 kip (120.1 kN) axle of the truck is positioned at section 1 as shown at the bottom of the figure. The calibration truck was selected for the analysis (and comparison with the field study results) since the axle spacings were accurately measured and the axle weights were obtained from a static weighing of each axle. Girder stresses computed for AASHTO HS 20 (MS 18) trucks, as discussed above, are also shown in the figures for comparison.

Similarly, points on the solid line labelled "Finite Element--Composite" of figure 152 are the girder live-load-plus-impact stresses calculated at section 1 of figure 3 in a finite element analysis of the composite span but with calibration trucks in the center of lanes 1 and 2 as shown at the top of the figure. The position of each truck on the span is shown at the bottom of the figure. No field study results are available for this case. Girder stresses computed for HS 20 (MS 18) trucks are also shown for comparison.

36" 36"

STRESS
ksi

10

8

AASHTO Non-Composite

AASHTO Composite

6

4

Finite Element - Composite

2

0

32   32   8^k

2'-4"

84'-10"
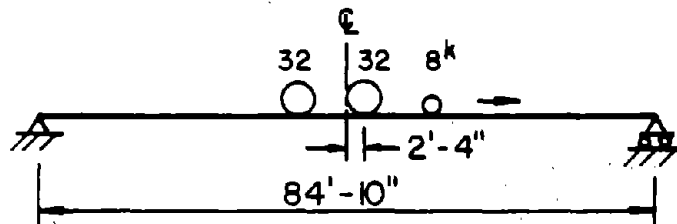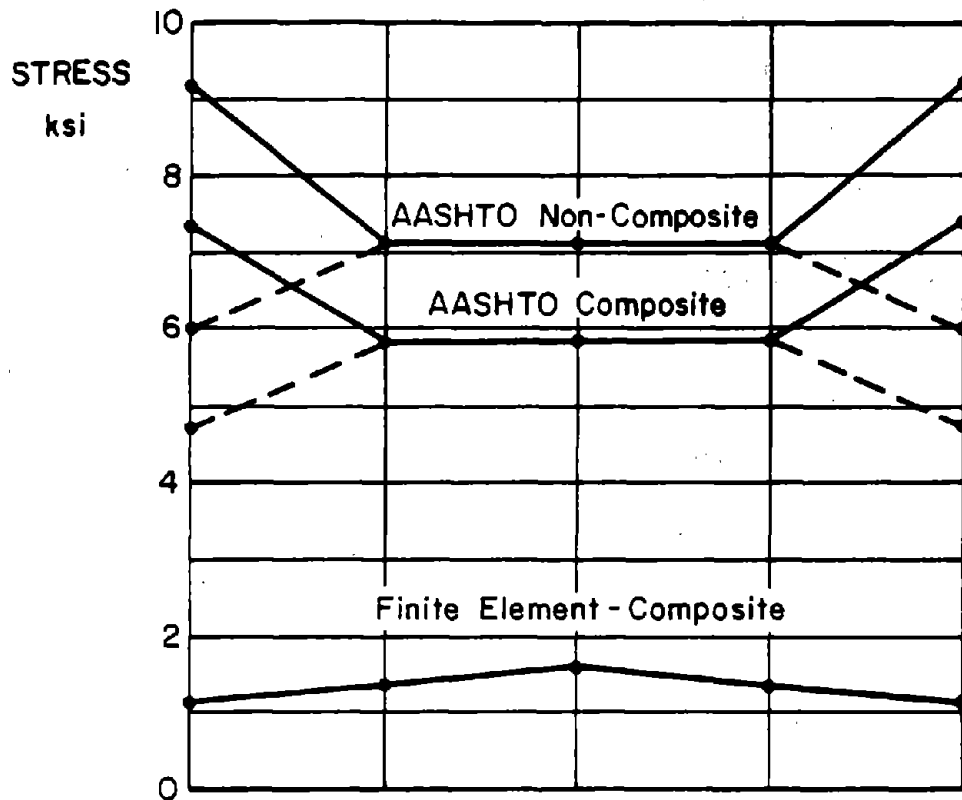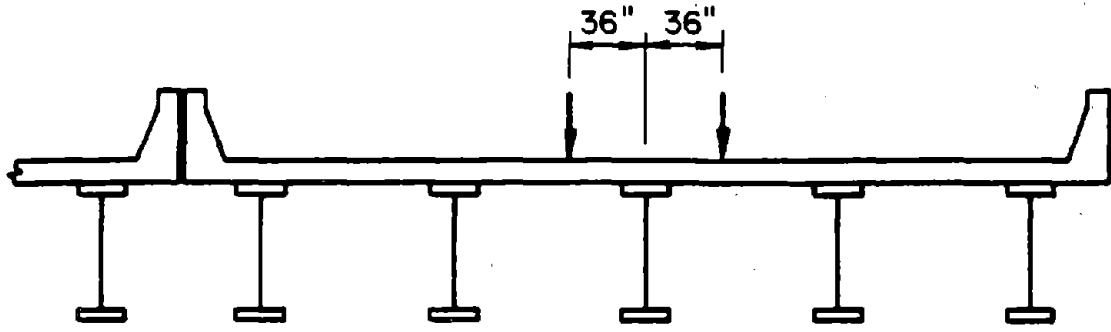
Axle Spacing : 14'-14'

Figure 146. Comparison of girder flexural stresses-span 2 EB Route 22 over 19th Street--AASHTO HS 20 (MS 18) vs. FE analysis.

1 ft. = 0.3048 m

Figure 147. Comparison of girder flexural stresses—span 2 EB Route 22 over 19th Street—AASHTO HS 20 (MS 18) vs. FE analysis.

140

1 ft. = 0.3048 m

Figure 148. Comparison of girder flexural stresses-span 2 EB Route 22 over 19th Street--AASHTO HS 20 (MS 18) vs. FE analysis.

141

1 ft. = 0.3048 m

Figure 149. Comparison of girder flexural stresses--span 2 EB Route 22 over 19th Street--AASHTO HS 20 (MS 18) vs. FE analysis.

142

1 ft. = 0.3048 m

Figure 150. Comparison of girder flexural stresses--span 2 EB Route 22 over 19th Street--AASHTO HS 20 (MS 18) vs. FE analysis.

143

Figure 151. Comparison of girder flexural stresses--span 2 EB Route 22 over 19th Street--AASHTO HS 20 (MS 18) vs. FE analysis.

144

1 ft. = 0.3048 m

Figure 152. Comparison of girder flexural stresses--span 2 EB Route 22 over 19th Street--AASHTO HS 20 (MS 18) vs. FE analysis.

145

3. WB Route 22 Over 19th Street

Figures 153 through 157 compare girder live-load-plus-impact flexural steel stresses computed in accordance with the AASHTO specifications with flexural stresses obtained from finite element analysis. AASHTO HS 20 (MS 18) truck loading is used throughout. The girder spacing and deck width are proviced on page 37. These figures are similar to figures 146 through 150. The discussion of those figures on page 137 also applies to figures 153 through 157.

Figure 158 compares girder live-load-plus-impact stresses resulting from the field study with live-load-plus-impact stresses computed from the finite element analysis of the composite superstructure. Points on the solid line labelled "Field Study" are the maximum girder stresses measured at section 1 of figure 11 as a random heavy truck travelled across the span in lane 1 as shown at the top of the figure. The random truck selected is truck No. 64, disk No. 11. The transverse position of the truck in lane 1 is unknown. The longitudinal position of the truck corresponding to each maximum girder stress is also unknown. As before, however, a single truck location would not likely produce simultaneous maximum stress in each girder at section 1.

Points on the solid line of figure 158 labelled "Finite Element--Composite" are the girder live-load-plus-impact stresses calculated at section 1 of figure 11 in a finite element analysis of the composite span with truck No. 64, disk No. 11 in the center of lane 1 as shown at the top of the figure. In the analysis the two 16.7 kip (74.28 kN) axles of the truck are positioned either side of section 1 which is 3 ft-6 (1.07 m) from the span centerline (figure 11). The random truck was selected in this case because the calibration truck used during the WB field study was somewhat smaller and larger analytical live load stresses were desired. Girder stresses computed for AASHTO HS 20 (MS 18) trucks are also shown in the figure for comparison.

Similarly, points on the solid line labelled "Finite Element--Composite" of figure 159 are the girder live-load-plus-impact stresses calculated at section

146

1 of figure 11 in a finite element analysis of the composite span but with a
random truck in the center of lanes 1 and 2 as shown at the top of the figure.
Each truck is assumed to be truck No. 64, disk No. 11 as before. The position
of each truck on the span is shown at the bottom of the figure. No field
study results are available for this case. Girder stresses computed for HS 20
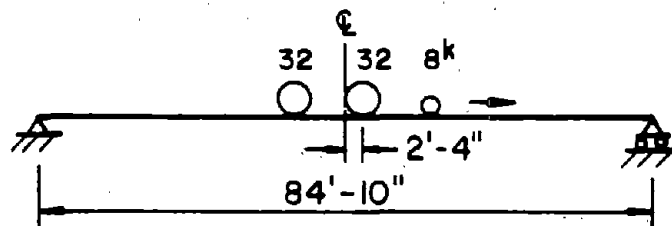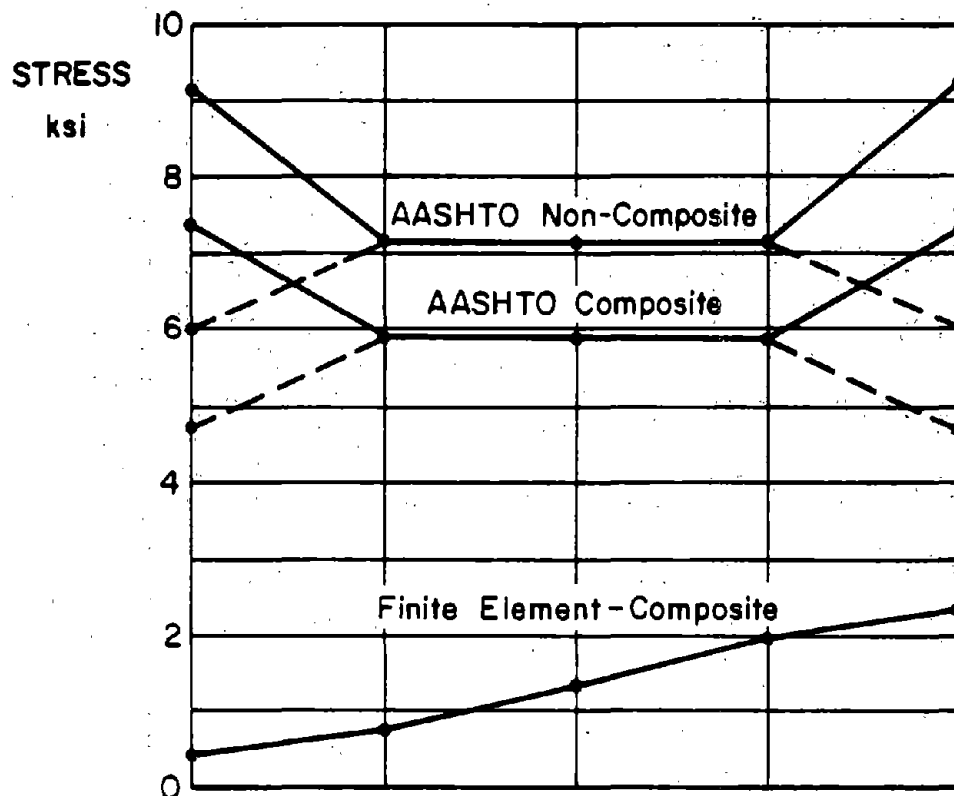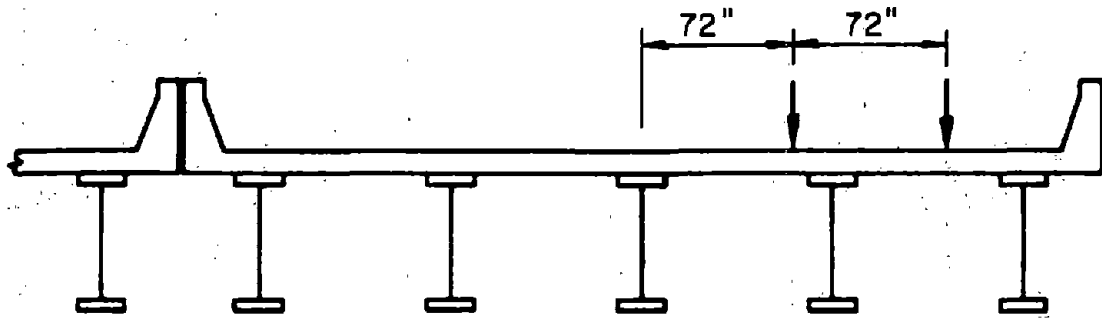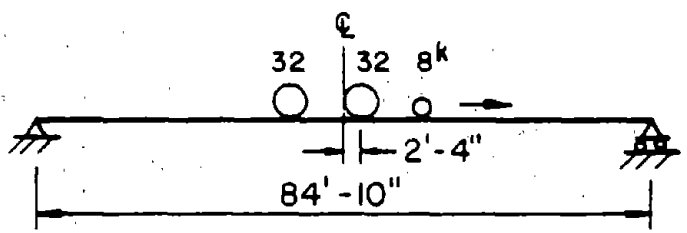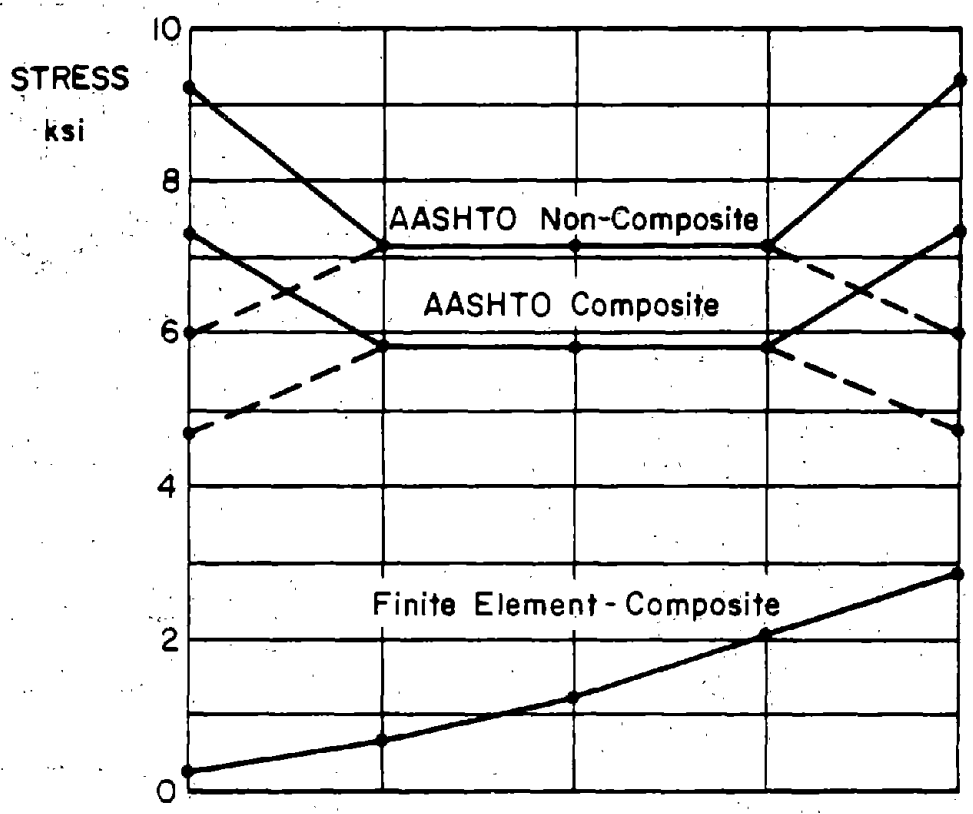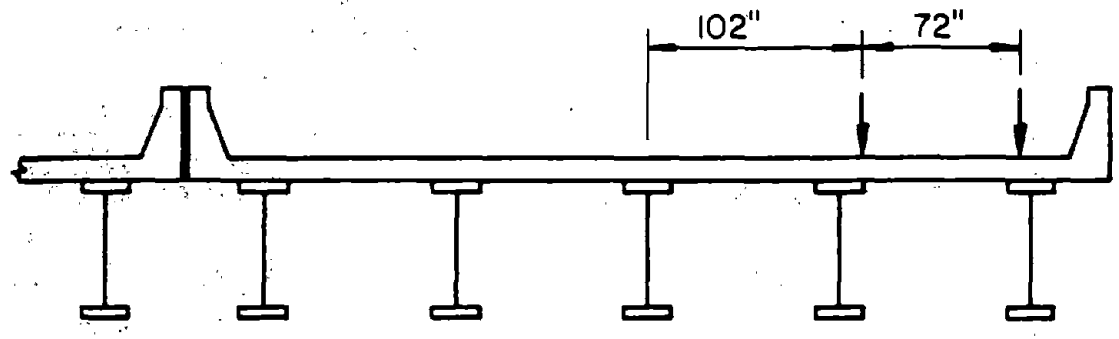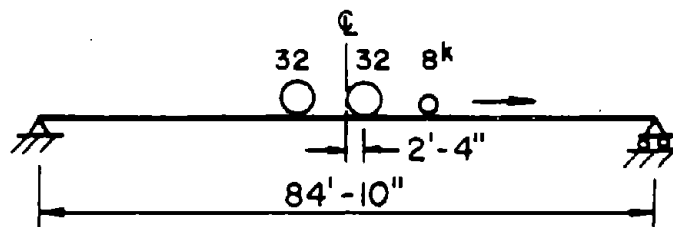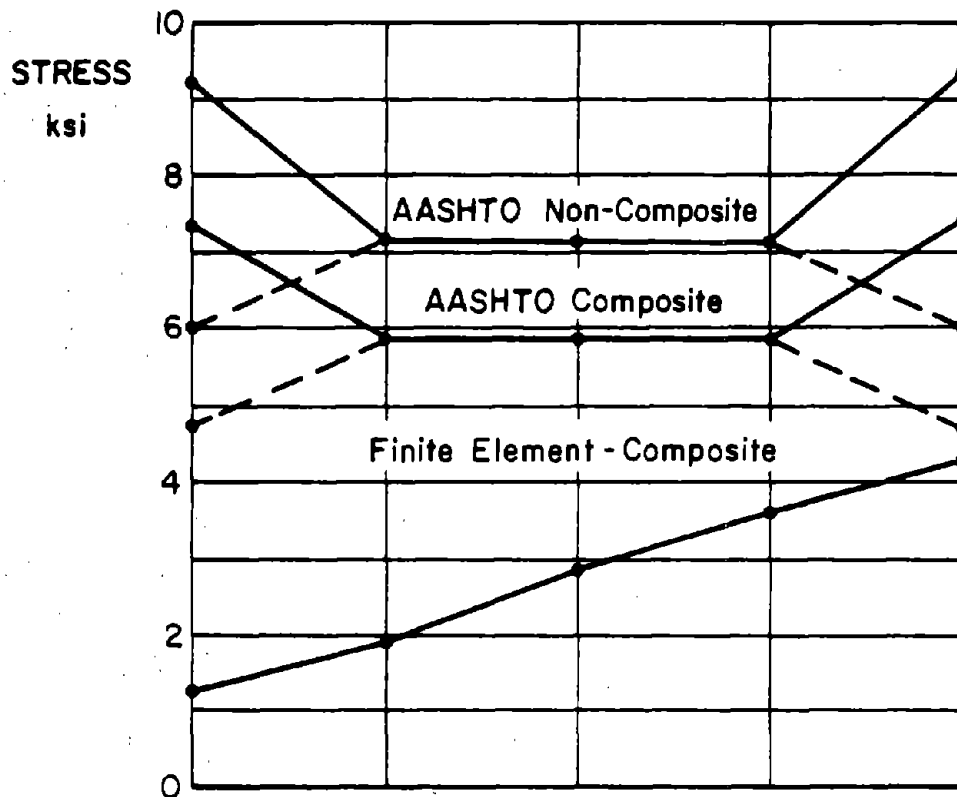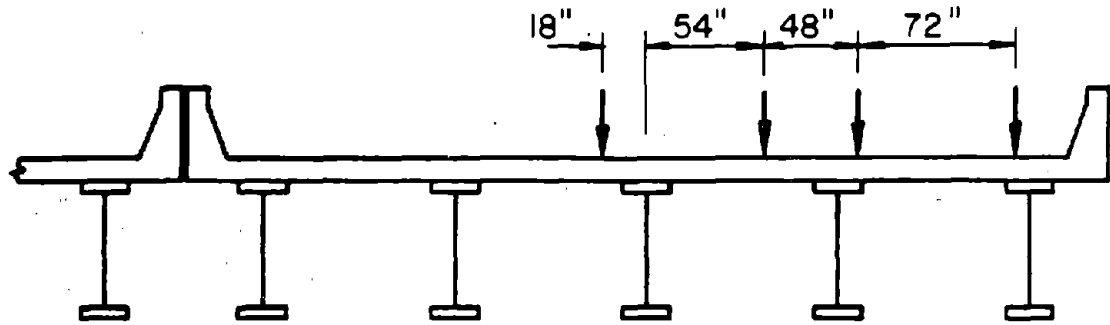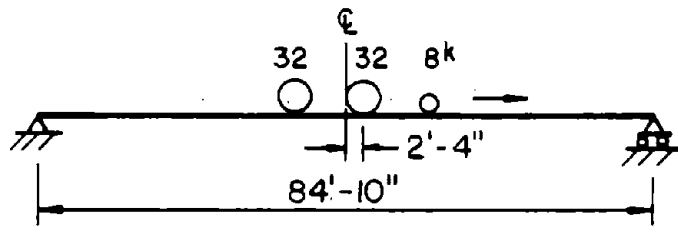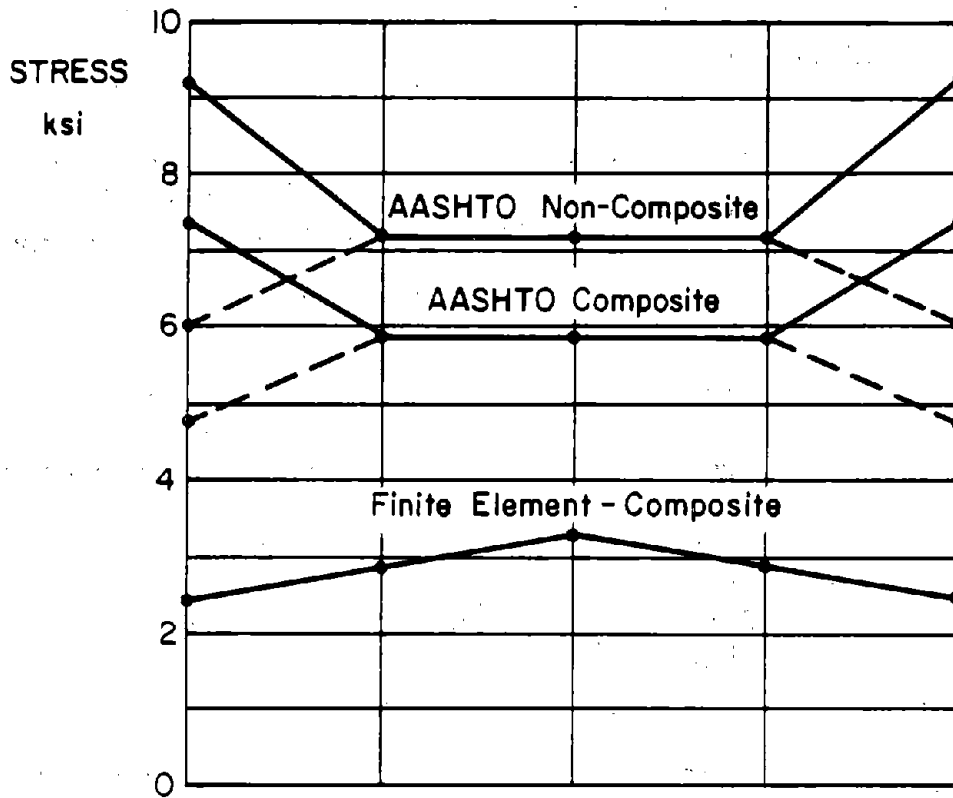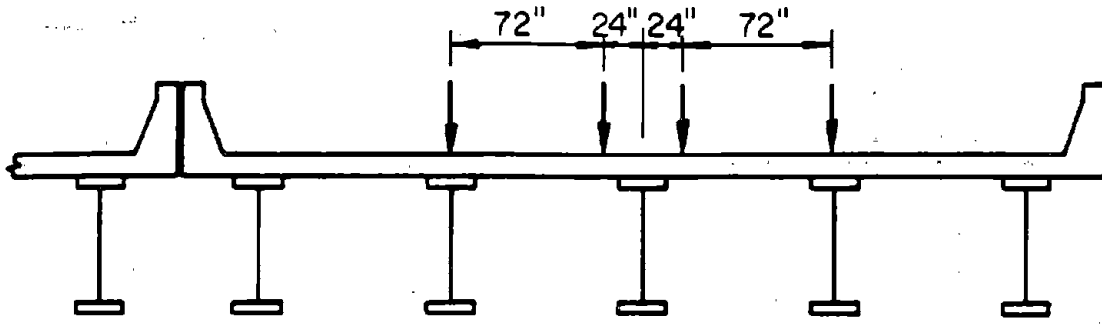(MS 18) trucks are also shown for comparison.

1 ft. = 0.3048 m
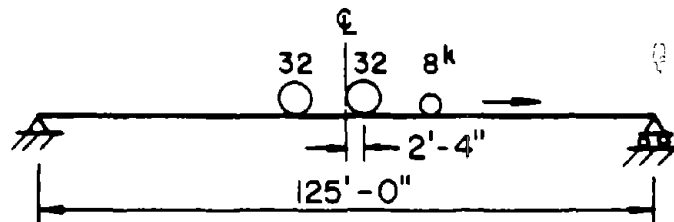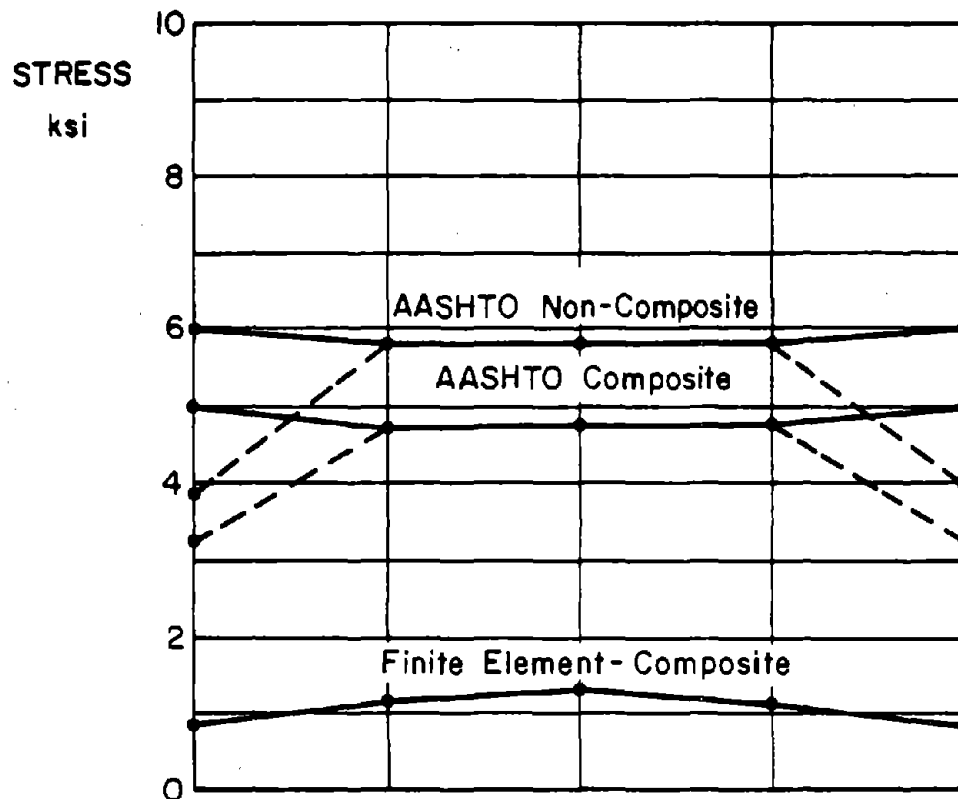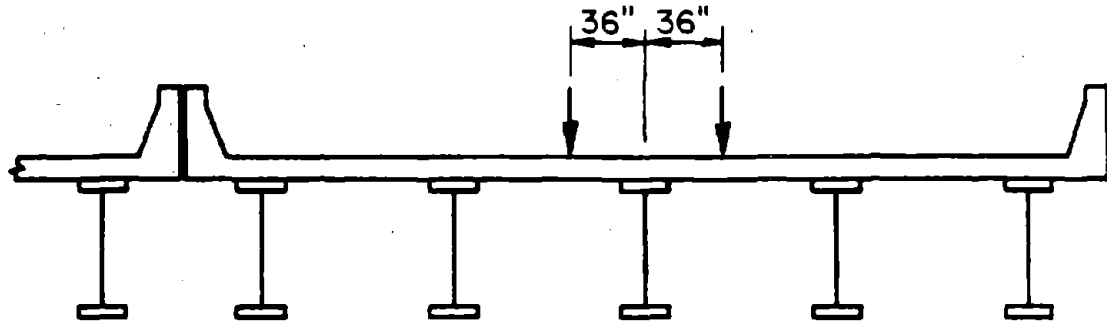
Figure 153. Comparison of girder flexural stresses--span 2 WB Route 22 over 19th Street--AASHTO HS 20 (MS 18) vs. FE analysis.
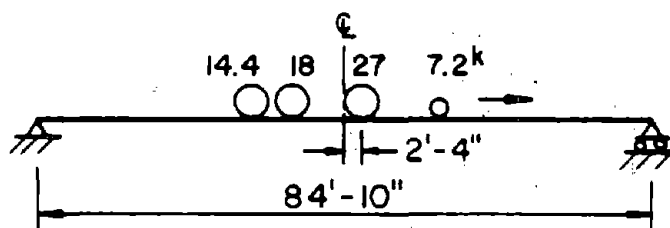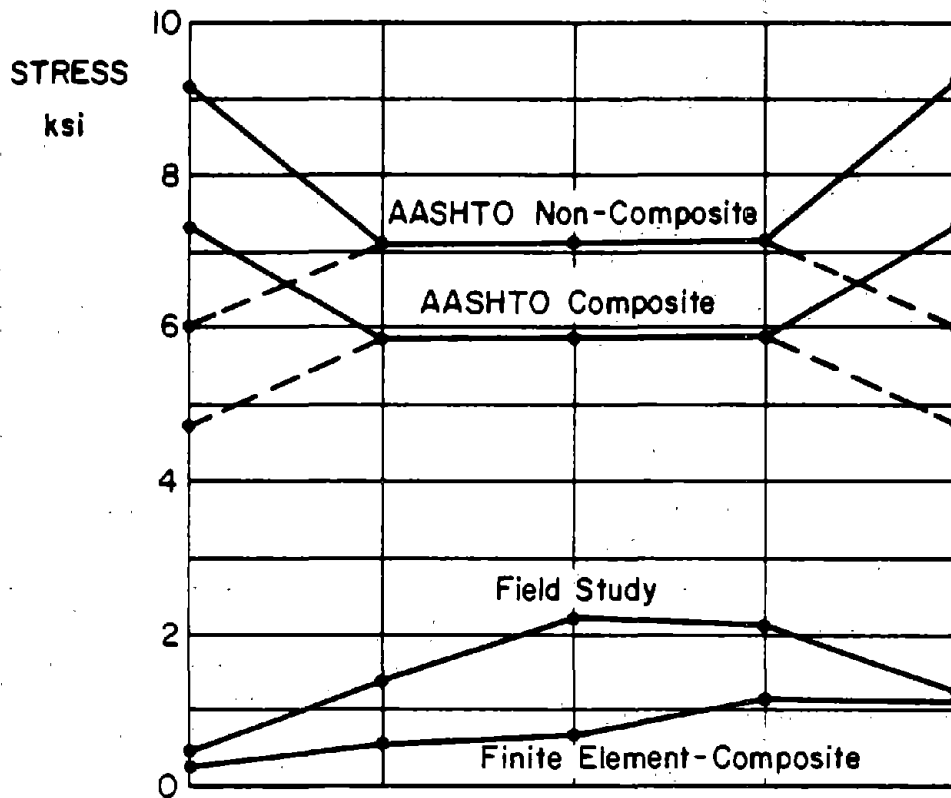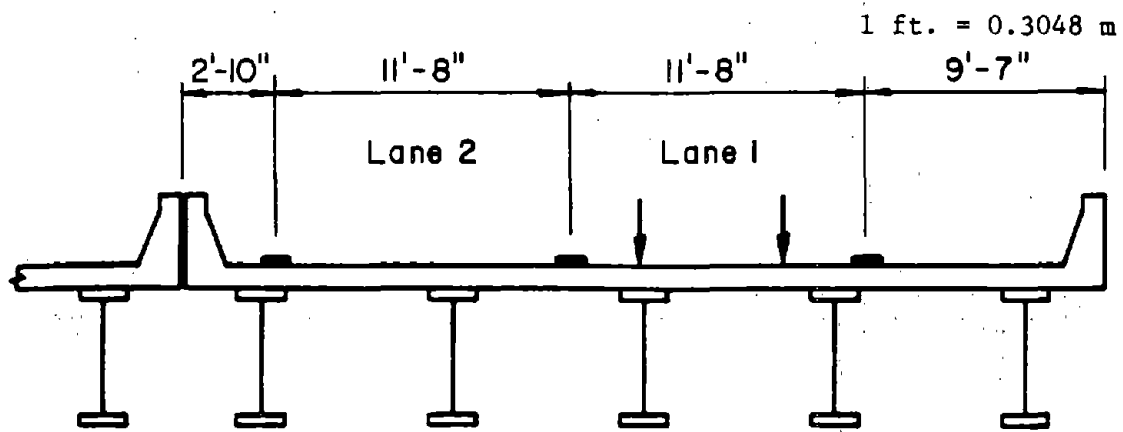
148

1 ft. = 0.3048 m
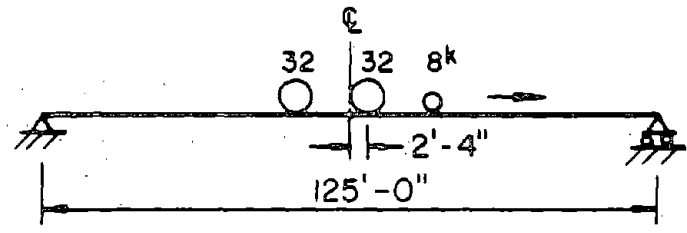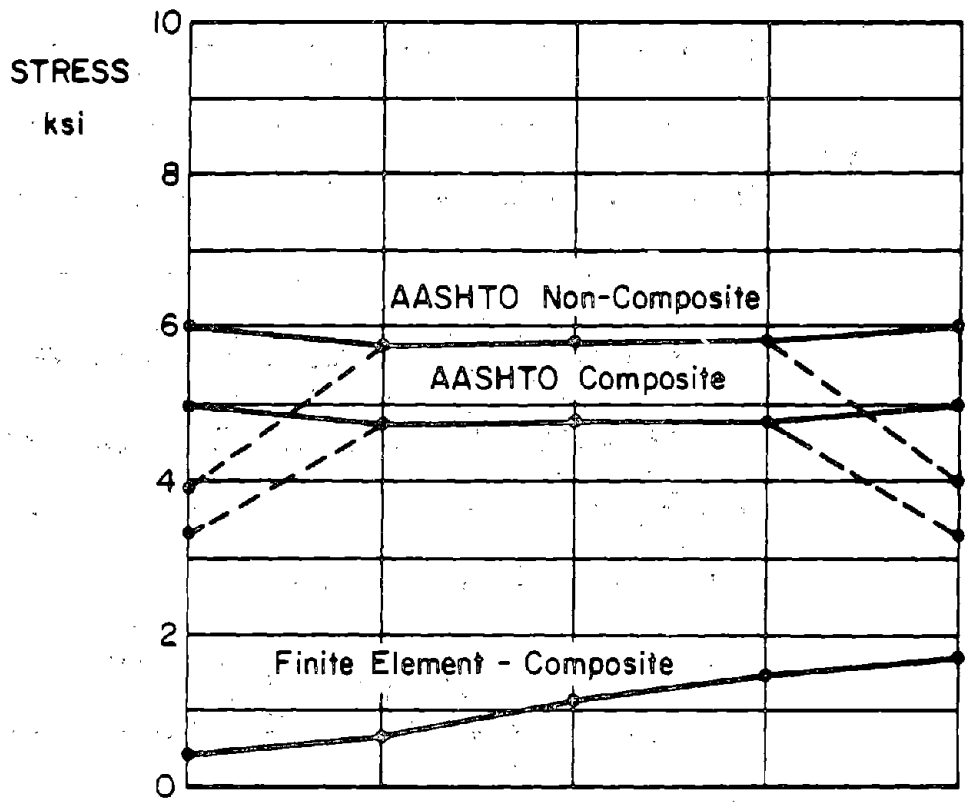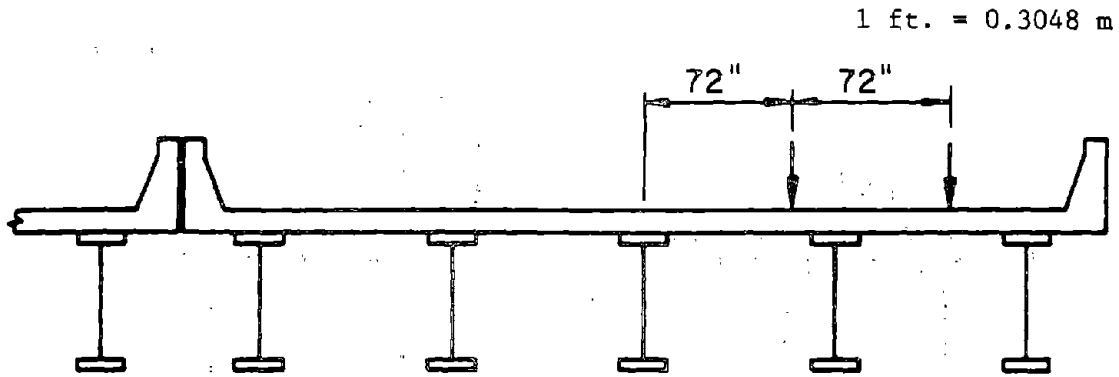
Figure 154. Comparison of girder flexural stresses--span 2 WB Route 22 over 19th Street--AASHTO HS 20 (MS 18) vs. FE analysis.

149

1 ft. = 0.3048 m

STRESS
ksi

AASHTO Non-Composite

AASHTO Composite

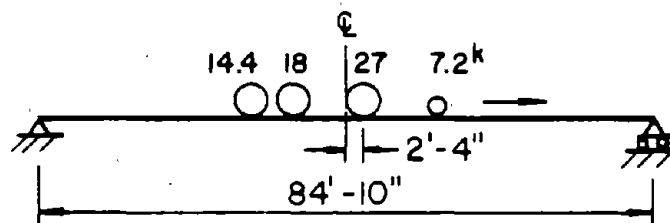Finite Element-Composite

102"   72"

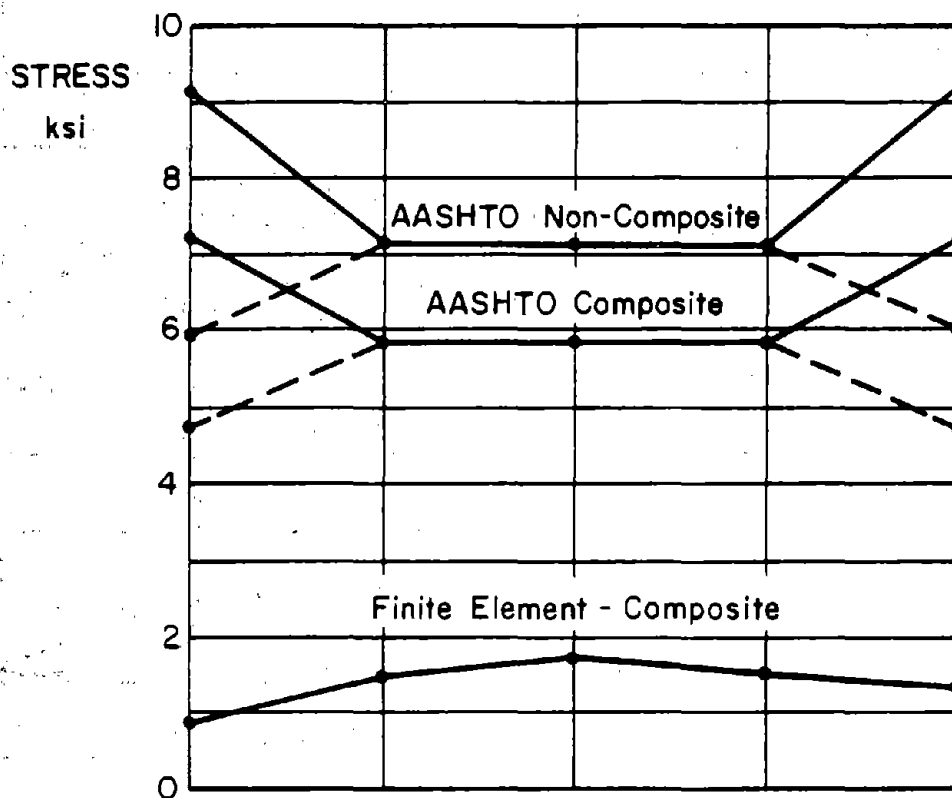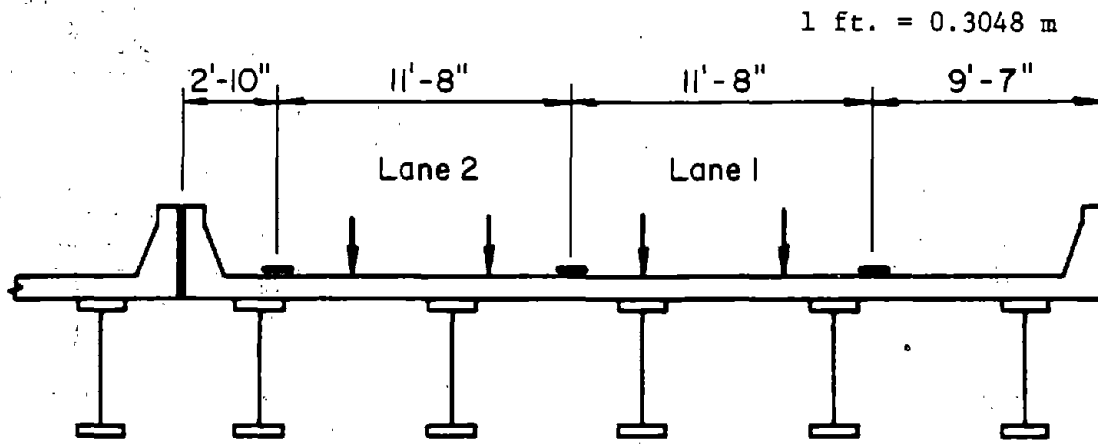32 32 8ᵏ

2'-4"

125'-0"
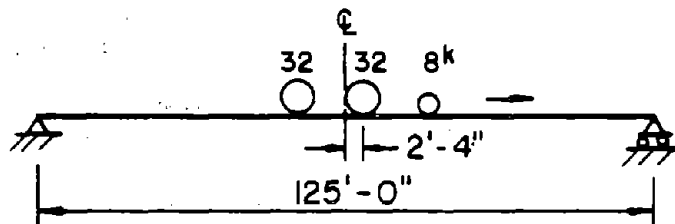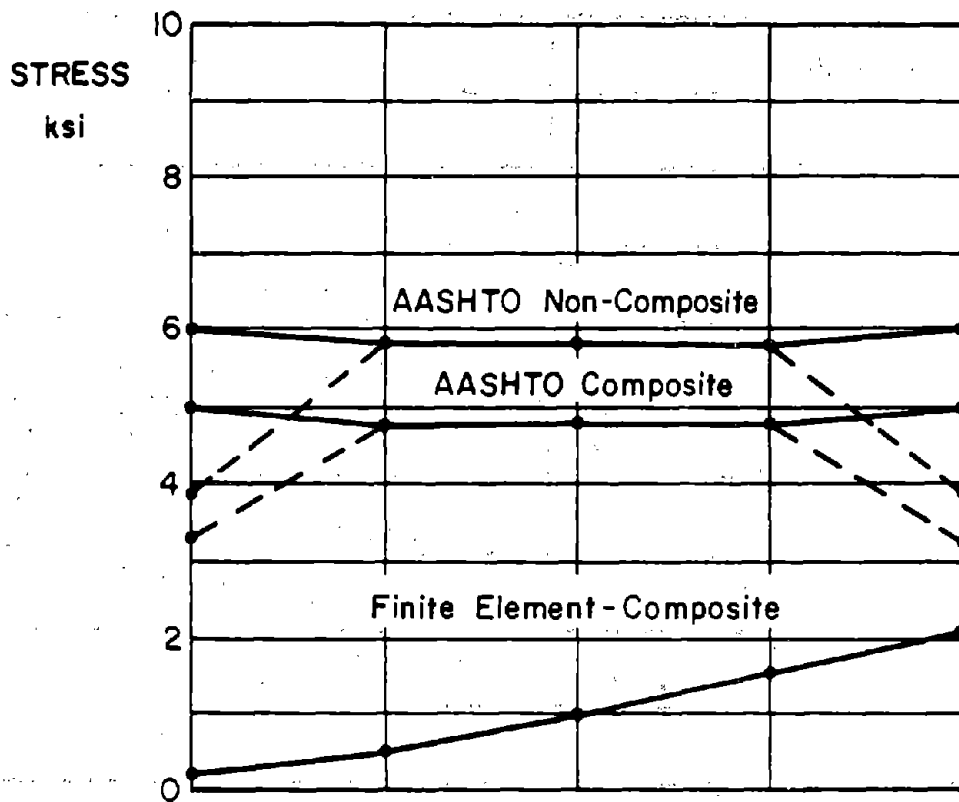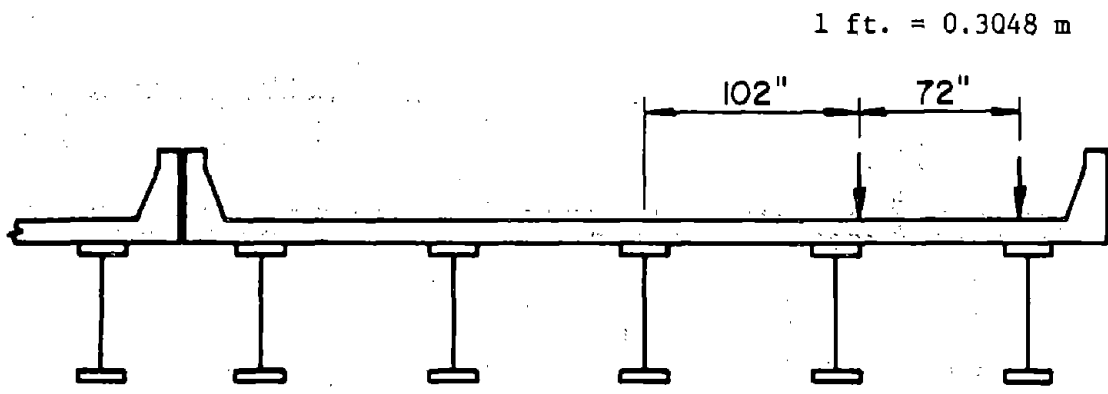
Axle Spacing : 14' - 14'

Figure 155.   Comparison of girder flexural stresses--span 2 WB Route 22 over
19th Street--AASHTO HS 20 (MS 18) vs. FE analysis.

150
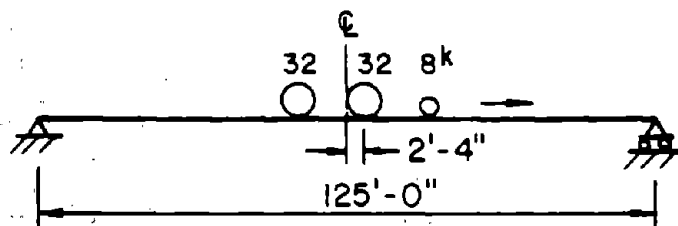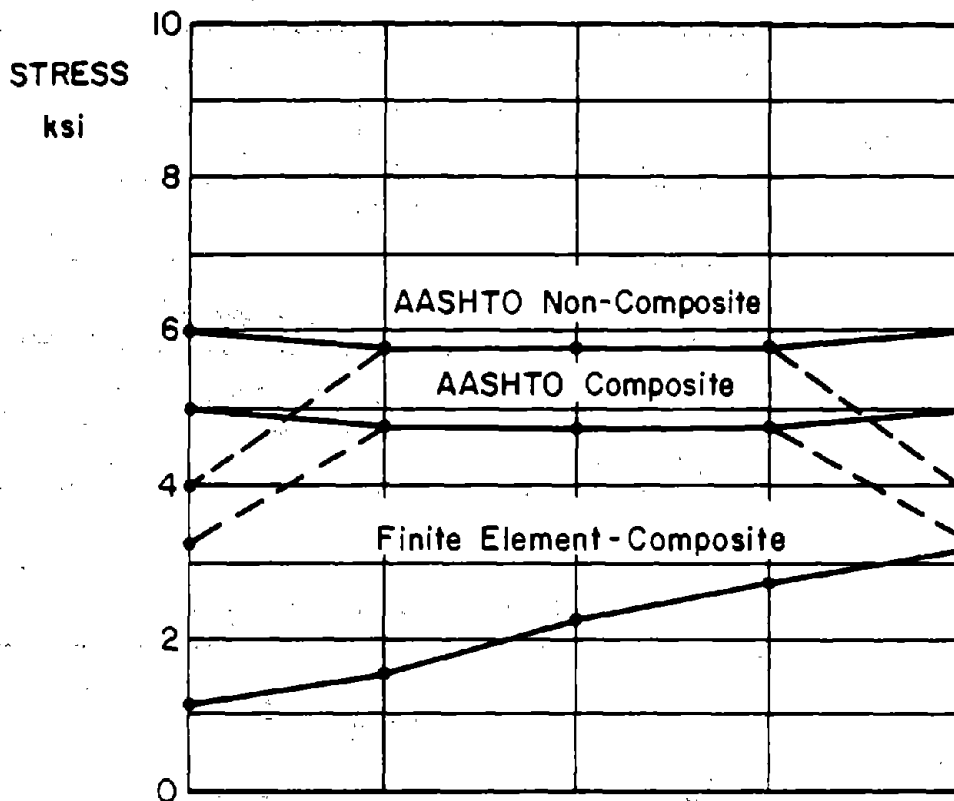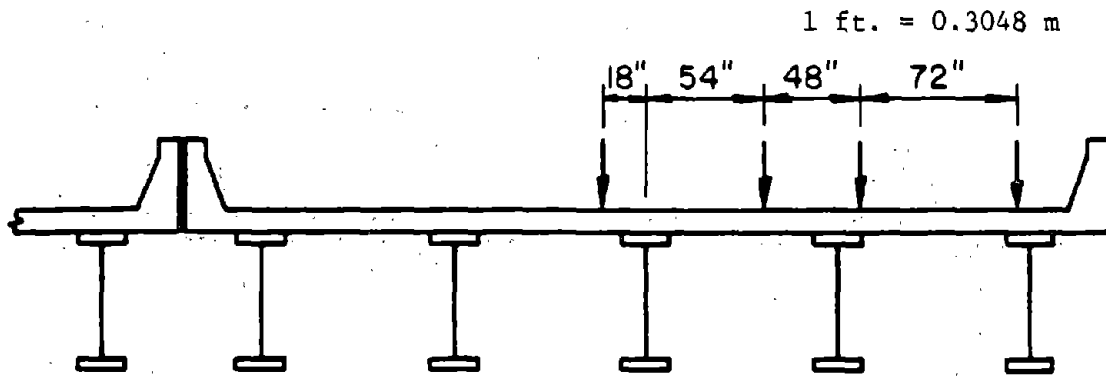
Figure 156. Comparison of girder flexural stresses--span 2 WB Route 22 over 19th Street--AASHTO HS 20 (MS 18) vs. FE analysis.

151

1 ft. = 0.3048 m
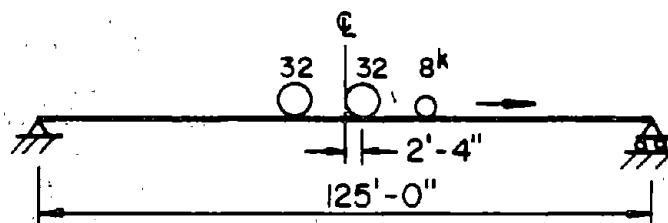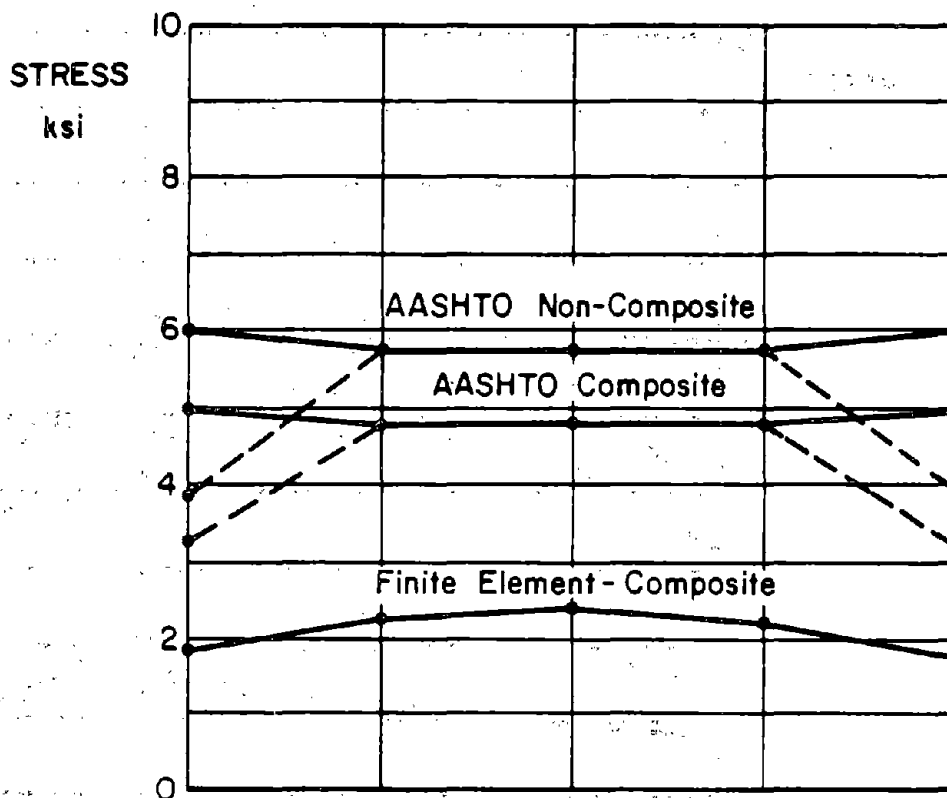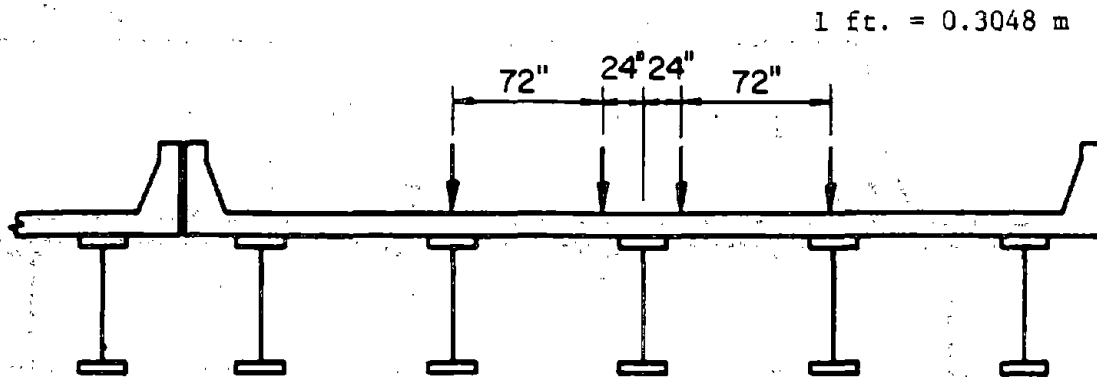
Figure 157. Comparison of girder flexural stresses--span 2 WB Route 22 over 19th Street--AASHTO HS 20 (MS 18) vs. FE analysis.

152

1 ft. = 0.3048 m
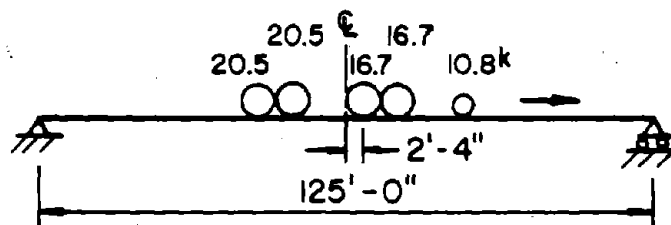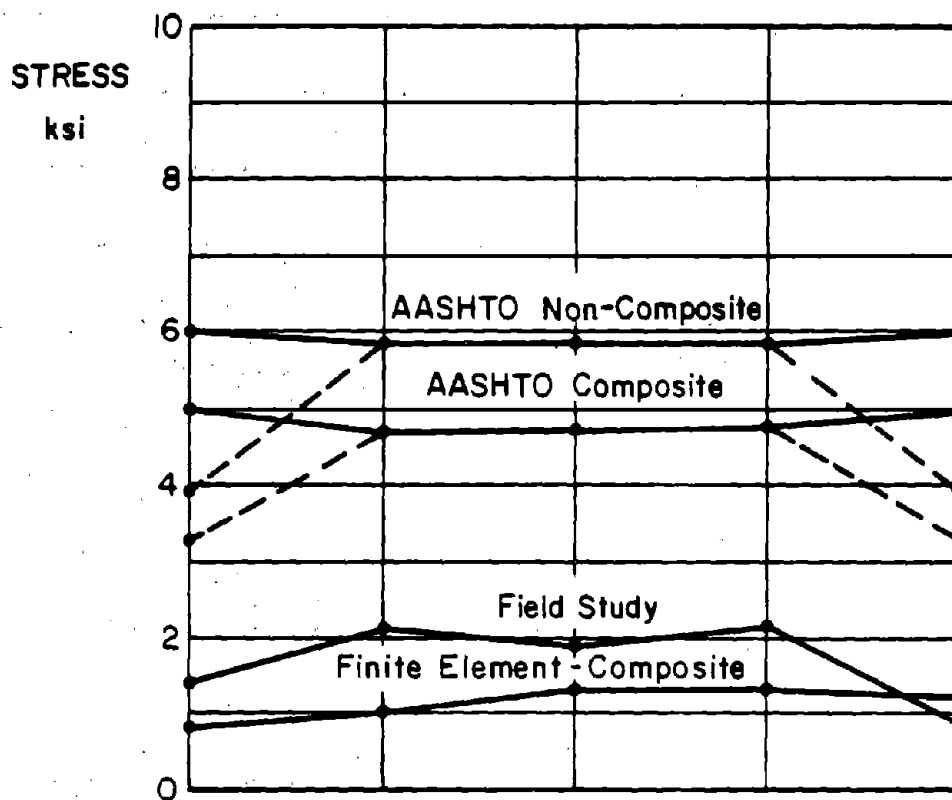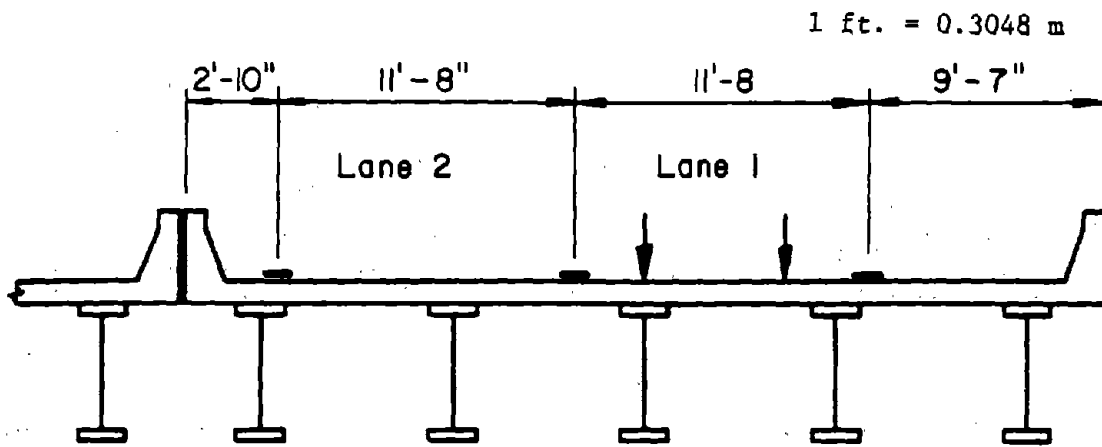
Figure 158. Comparison of girder flexural stresses--span 2 WB Route 22 over 19th Street--AASHTO HS 20 (MS 18) vs. FE analysis.

153
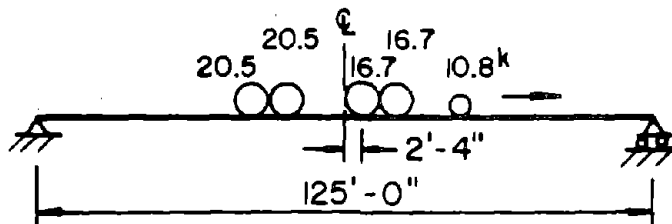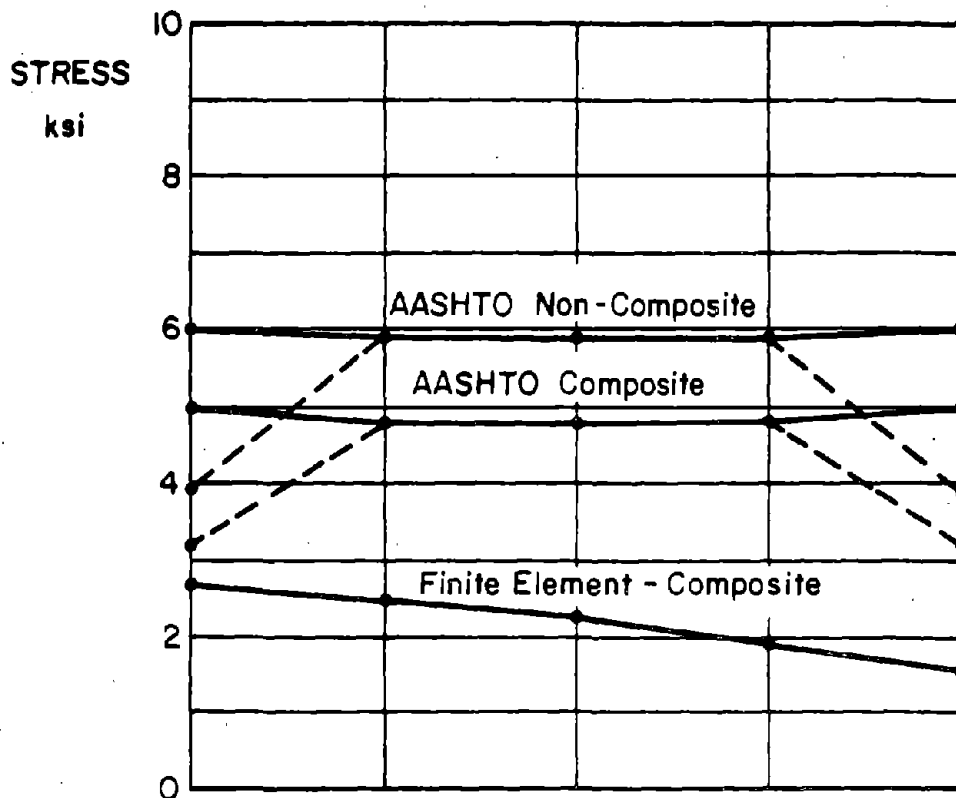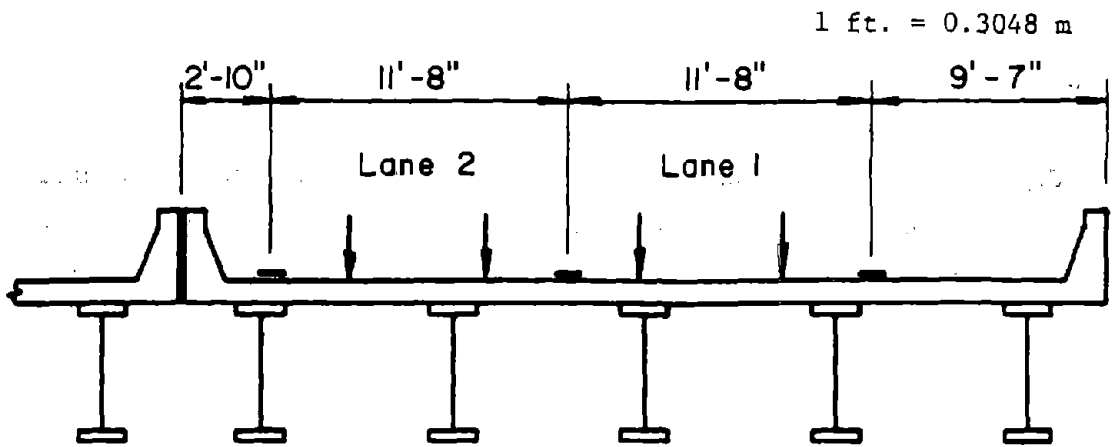
Figure 159.   Comparison of girder flexural stresses--span 2 WB Route 22 over 19th Street--AASHTO HS 20 (MS 18) vs. FE analysis.

154

4. NB Route 33 Over Van Buren Road

Figures 160 and 161 compares girder live-load-plus-impact flexural steel stresses computed in accordance with the 1983 AASHTO specifications with flexural stresses obtained from finite element analyses of span 2. AASHTO HS 20 (MS 18) truck loading is used. The girder spacing and deck width are provided on page 43.

In each figure, values of girder stresses located on the upper solid line labelled "AASHTO--Composite" are computed using the AASHTO specifications. Although the deck width is 40 ft (12.19 m) it is common practice not to use the reduction in load intensity provision of AASHTO (article 3.12 of the 13th Edition) for more than 2 design traffic lanes when designing individual girders of multiple girder bridges and none was used here.

Values of girder live-load-plus-impact stresses on the lower solid line, labelled "Field Study", of each figure were obtained from finite element analysis of the actual composite superstructure. In these analyses two design traffic lanes of HS 20 (MS 18) trucks are used and placed in the transverse locations shown at the top of each figure. The position of each AASHTO truck on the span is shown at the bottom of each figure. The arrow indicates the direction of travel for the trucks.

Figure 162 compares stresses in the three instrumented girders of span 2 (figure 16) resulting from the field study with the stresses computed using AASHTO specifications. Points on the solid line labelled "Field Study" are the maximum measured girder stresses as a random heavy truck travelled across the span in lane 1, as as shown at the top of the figure. The random truck selected is truck No. 43, disk No. 20. The transverse position of the truck in lane 1 is unknown. The longitudinal position of the truck corresponding to each maximum girder stress is also unknown. As before, however, a single truck location would not likely produce simultaneous maximum stress in each girder. The axle spacings and axle weights of this truck are shown at the bottom of the figure.

155

No finite element analysis was made of span 2 to determine girder stresses for the above truck. Figure 163 compares girder live-load-plus-impact stresses computed in accordance with the 1983 AASHTO specifications with stresses obtained from the field study for span 1. The girder spacing and deck width are provided on page 43.

In the figure, values of girder stresses located on the upper solid line labelled "AASHTO Noncomposite" are computed using AASHTO HS 20 (MS 18) truck loading. As before the provisions of AASHTO article 3.12 are not used.

Values of girder live-load-plus-impact stresses on the lower solid line of figure 163 labelled "Field Study" are the maximum measured girder stresses as truck No. 43, disk No. 20 travelled across the span in lane 1 as shown at the top of the figure. No data was obtained for the left fascia girder (gauge 6, figure 16). As before the transverse position of the truck in lane 1 and the longitudinal position of the truck corresponding to each maximum girder stress are unknown. As shown at the bottom of the figure the truck length exceeds the span length.

No finite element analysis was made of span 1 to determine girder stresses for the above truck.

156

1 ft. = 0.3048 m
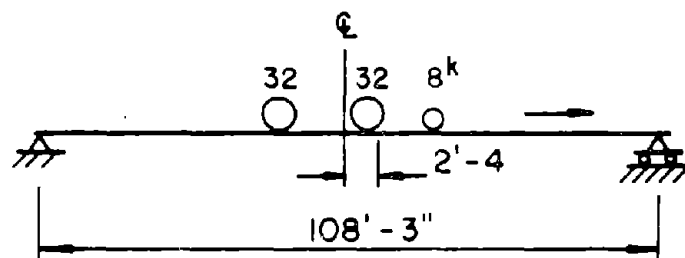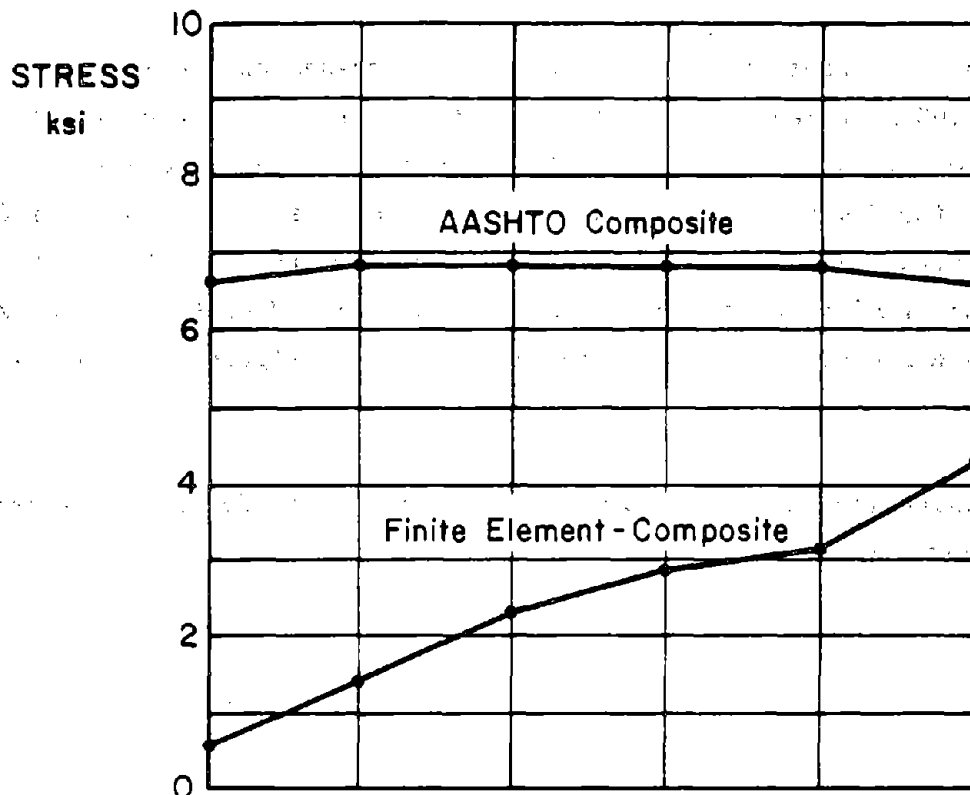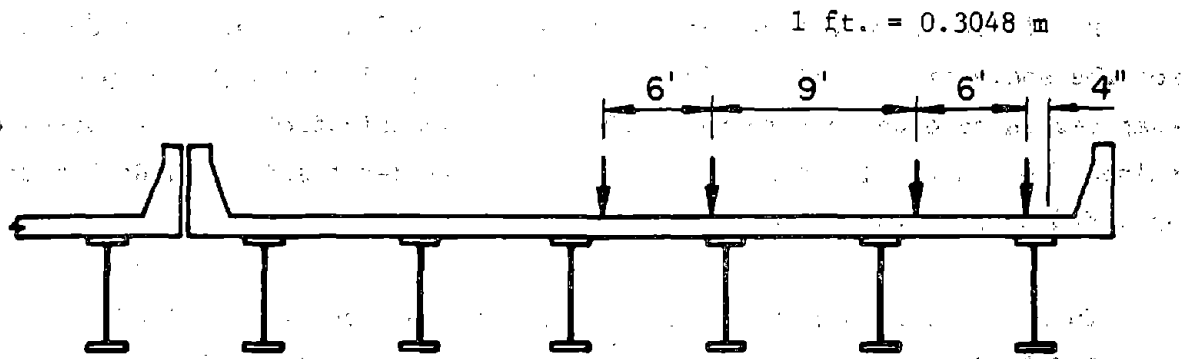
Figure 160. Comparison of girder flexural stresses--span 2 NB Route 33 over Van Buren Road --AASHTO HS 20 (MS 18) vs. FE analysis.

157

1 ft. = 0.3048 m
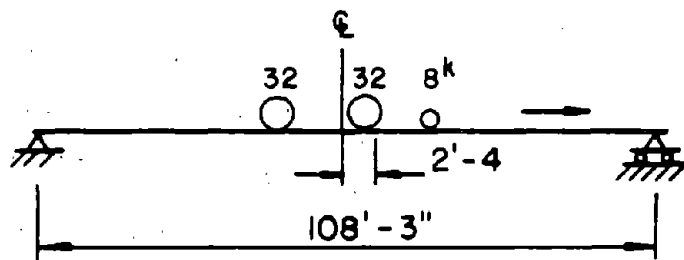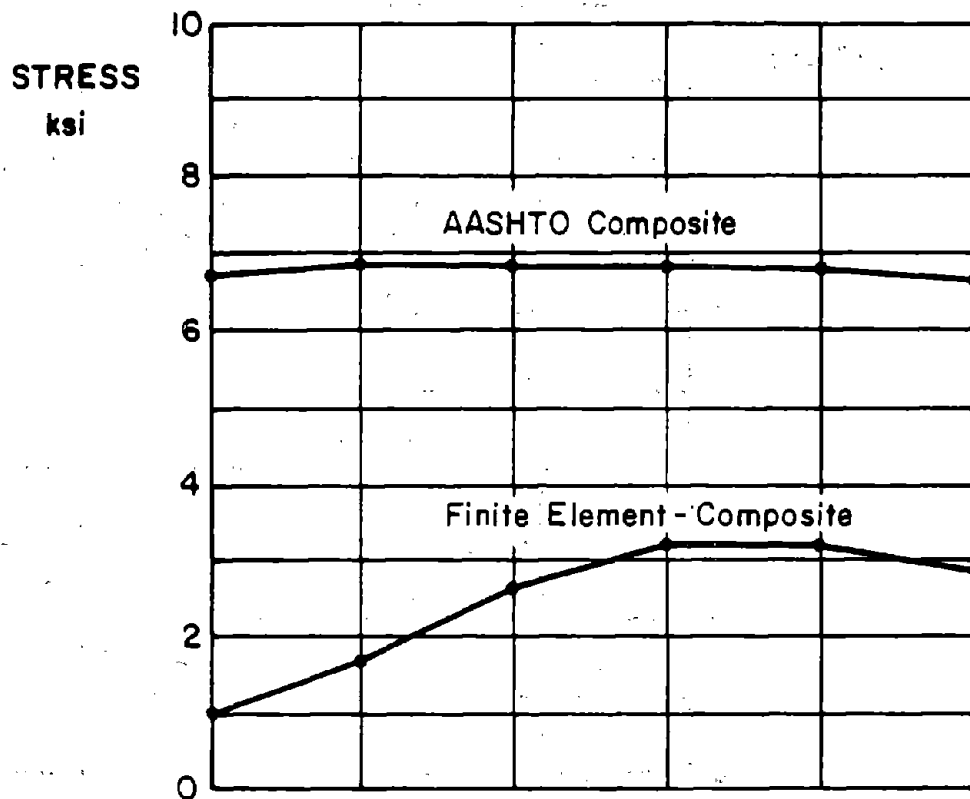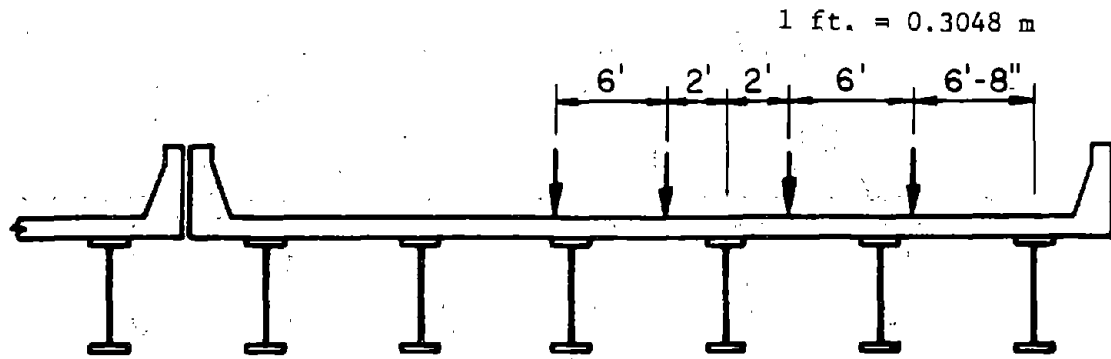
Figure 161. Comparison of girder flexural stresses--span 2 NB Route 33 over Van Buren Road--AASHTO HS 20 (MS 18) vs. FE analysis.

158
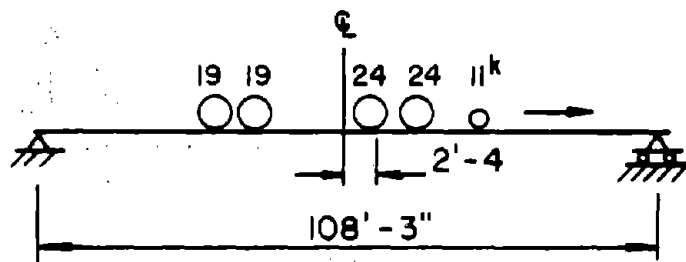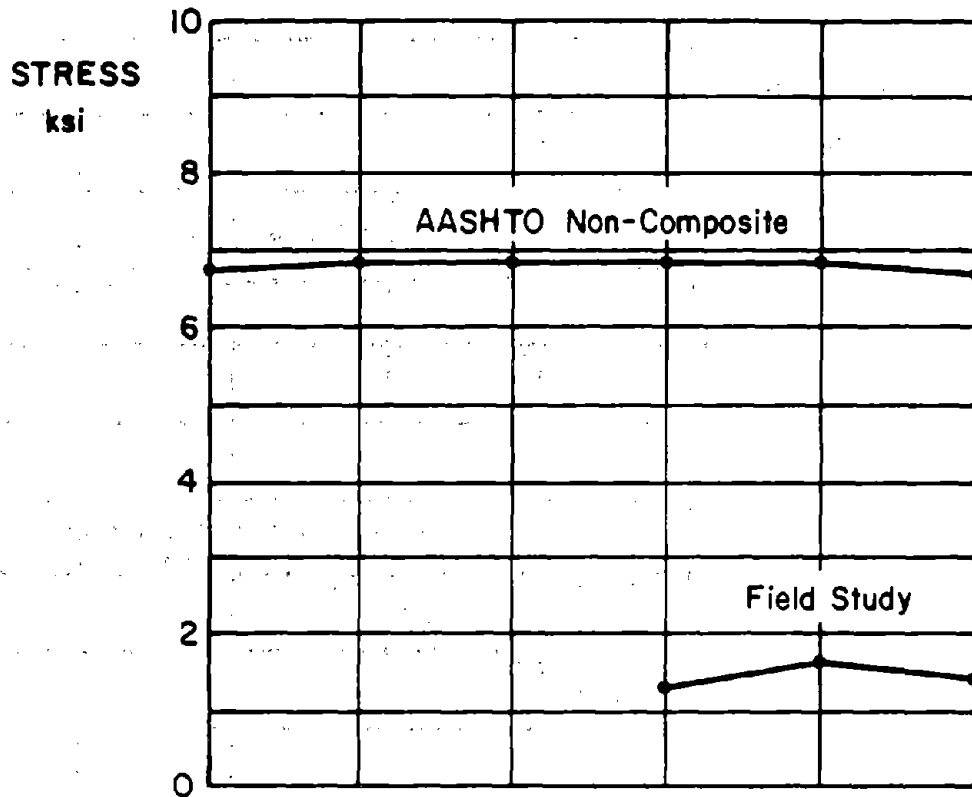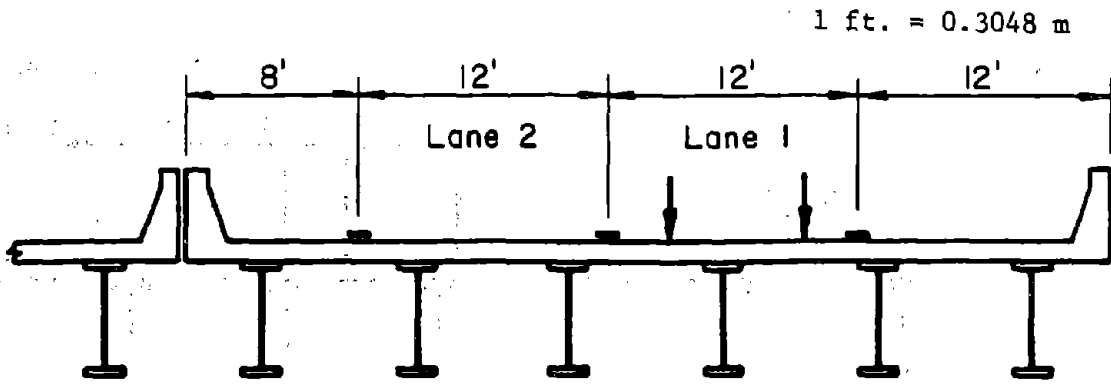
Figure 162. Comparison of girder flexural stresses--span 2 NB Route 33 over Van Buren Road--AASHTO HS 20 (MS 18) vs. field study.
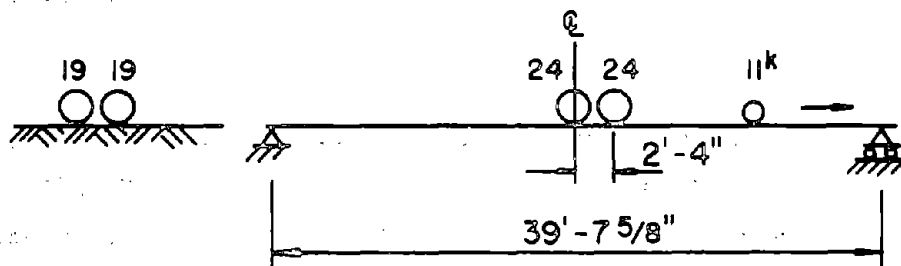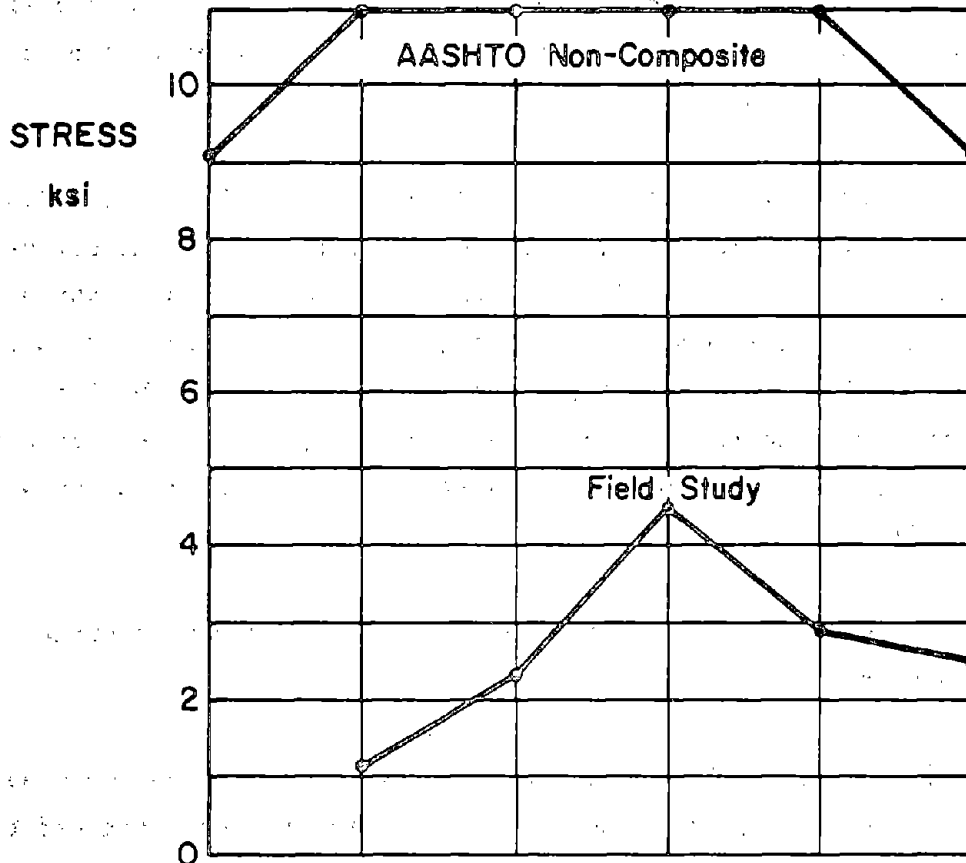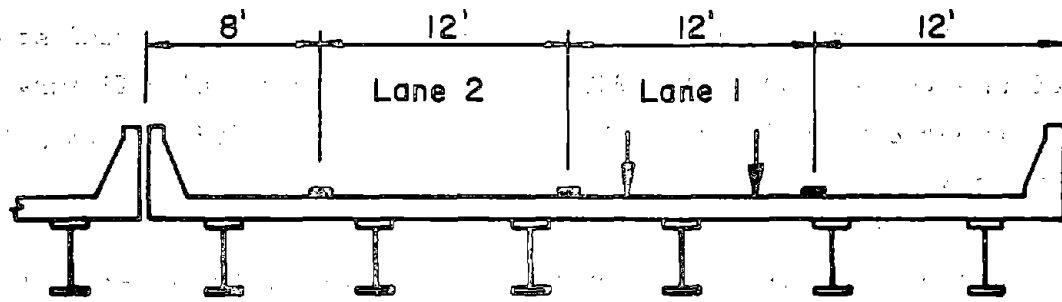
Figure 163. Comparison of girder flexural stresses--span 1 NB Route 33 over Van Buren Road--AASHTO HS 20 (MS 18) vs. field study.

160

5. NB Route 33 Over State Park Road

Figure 164 compares girder live-load-plus-impact flexural steel stresses computed in accordance with the 1983 AASHTO specifications with flexural stresses obtained from the field study for span 2. The girder spacing and deck width are provided on page 51.

In the figure, values of girder stresses located on the upper solid line labelled "AASHTO--Composite" are computed using AASHTO HS 20 (MS 18) truck loading. As for the Van Buren Road Bridge (page 155) the provisions of AASHTO article 3.12 are not used.

Values of girder live-load-plus-impact stresses on the lower solid line of figure 164 labelled "Field Study" are the maximum measured girder stresses as a random heavy truck travelled across the span in lane 1 as shown at the top of the figure. The random truck selected is truck No. 23, disk No. 22. The transverse position of this truck in lane 1 is unknown. The longitudinal position of the truck corresponding to each maximum girder stress is also unknown. The axle spacings and axle weights of this truck are shown at the bottom of the figure.

No finite element analysis was made of span 2 to determine girder stresses for the above truck.

Figure 165 compares girder live-load-plus-impact stresses computed in accordance with the 1983 AASHTO specifications with stresses obtained from the field study for span 3. The girder spacing and deck with are provided on page 51.

In the figure, values of girder stresses located on the upper solid line labelled "AASHTO--Composite" are computed using AASHTO HS 20 (MS 18) truck loading. As before the provisions of AASHTO article 3.12 are not used.

Values of girder live-load-plus-impact stresses on the lower solid and dashed line of figure 165 labelled "Field Study" are the maximum measured

girder stresses as truck No. 23, disk No. 22 travelled across the span in lane 1 as shown at the top of the figure. No data was obtained from gauges 5 and 16, figure 25. As before the transverse position of the truck in lane 1 and the longitudinal position of the truck corresponding to each maximum girder stress are unknown. As shown at the bottom of the figure the truck length exceeds the span length.

No finite element analysis was made of span 3 to determine the girder stresses for the above truck.
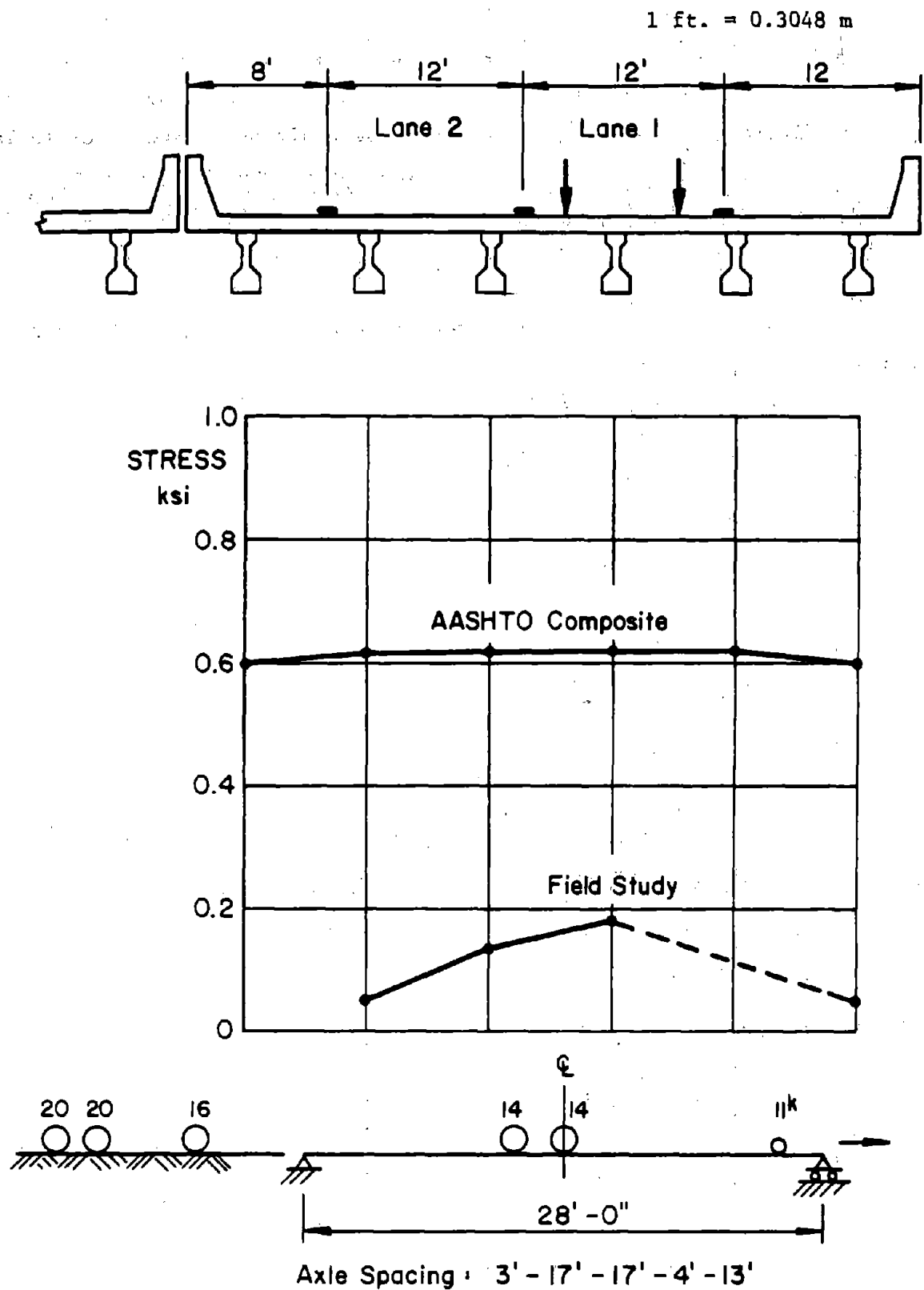
Figure 164. Comparison of girder flexural stresses—span 2 NB Route 33 over
State Park Road—AASHTO HS 20 (MS 18) vs. field study.
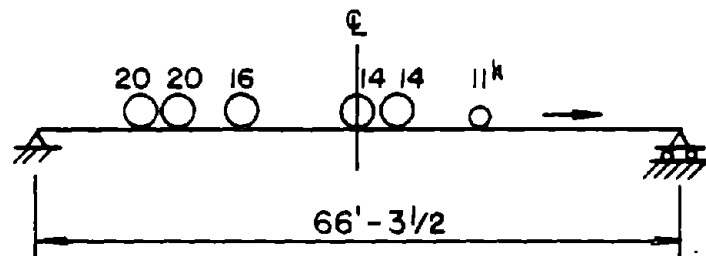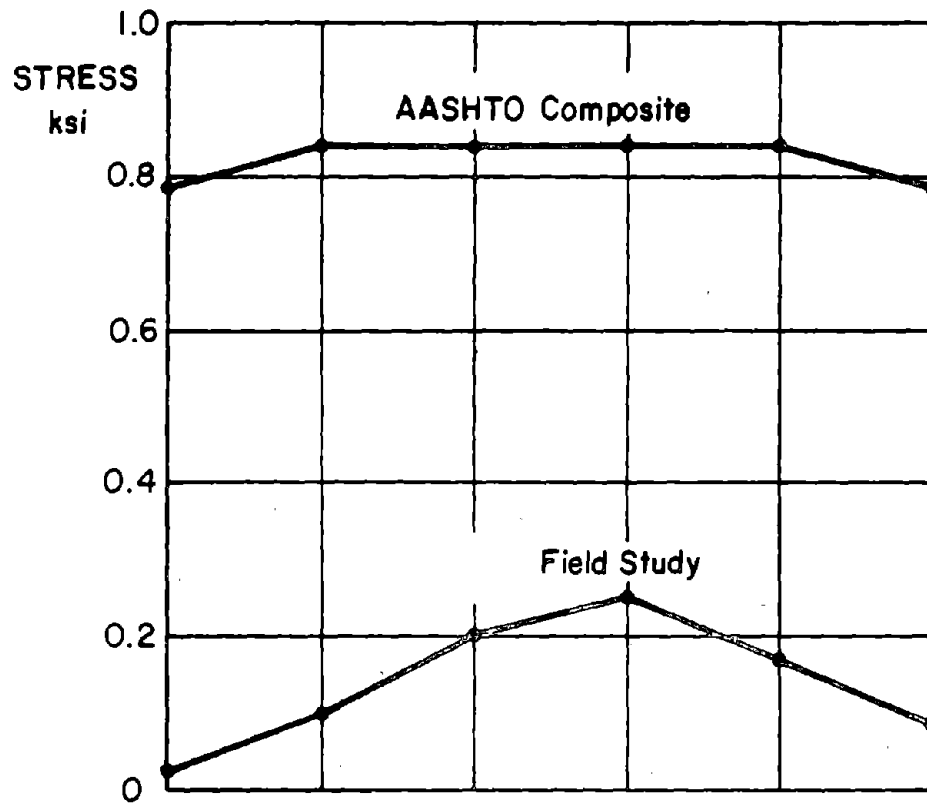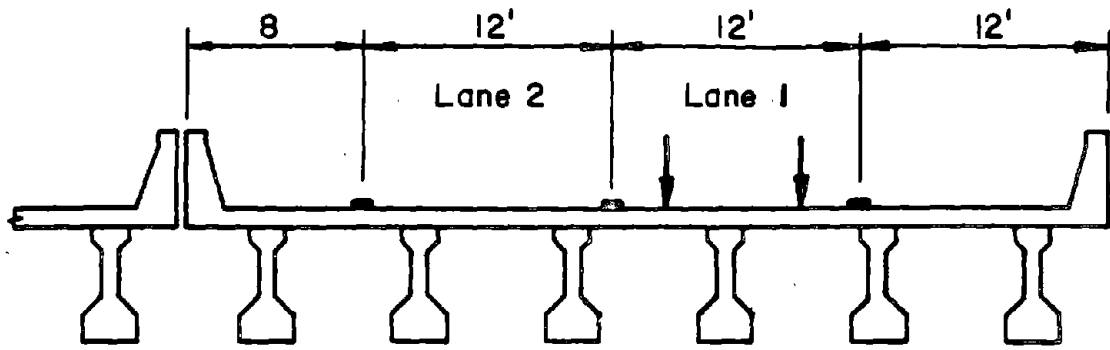
Figure 165. Comparison of girder flexural stresses—span 3 NB Route 33 over
State Park Road—AASHTO HS 20 (MS 18) vs. field study.

6.   Discussion of Analytical Results

a.   Stress Range Ratios (α Ratios)

One assumption used to develop the 1983 AASHTO stress cycle table (reference 21 - article 10.3.2) for use in design against fatigue damage is that the actual stress range produced by vehicles similar to the design truck is a factor α times the design stress range.[6] Previous stress history studies have indicated that this factor could be expected to be less than one.[57] That is, the measured stress ranges would likely be less than the design stress range, due to such factors as difference in load distribution, impact, actual truck loadings, etc.[6] The AASHTO stress cycle table assumes values of α of 0.8 for transverse members and 0.7 for longitudinal members.

Table 3 shows the average α ratios computed from the results of the field and analytical studies. For a particular interior or fascia girder α was calculated as the ratio of the actual maximum stress range reported on page for the gauge nearest midspan to the AASHTO design HS 20 (MS 18) live-load-plus-impact stress reported in this chapter.

Table 3 - Average α Ratios Computed from Results
of Field and Analytical Studies

Location	EB Span 2	WB Span 2	Van Buren Road Span 1	Span 2
Interior Girders	0.96	1.29	0.44	0.34
Fascia Girders	0.45	0.95	0.38	0.87

In calculating the α ratio it is assumed that, for simple spans, the design maximum stress range equals the design maximum stress. Care was taken not to use the reported maximum stress range if a spike in the strain-vs.-time response was suspected (page 123).

For example, for the interior girders of the EB bridge since the absolute maximum stress somewhat exceeds the maximum stress range for strain gauge

transducers 1 and 3, only gauge 3 was used to calculate $\alpha = 0.96$ in the table. For the fascia girders, no spike is suspected and gauges 8 and 15 were used to compute the average value, $\alpha = 0.45$, shown in the table. The largest ratio of 1.29 was computed using only data from gauge 2 of the WB bridge since spikes are suspected in the data from gauges 1 and 3.

Three of the eight α ratios are somewhat larger than the assumed ratio of 0.7 in developing the AASHTO stress cycle tables. Interestingly, the average of all ratios shown in table 3 is 0.71 which compares favorably with the assumed ratio.

The presence of large α ratios, even those exceeding 1.0, was not unexpected for the following reasons:

o From information provided by PA District 5-0 AASHTO HS 20 (MS 18) live-load-plus-impact steel stresses used in the 1983 retrofit of the EB and WB bridges on PA Route 22 over 19th Street to composite girders were checked. These stresses were consistently about 1 ksi higher than the corresponding stresses calculated in this investigation, and are as follows:

    EB Interior: 6.76 ksi   WB Interior: 5.39 ksi
    EB Fascia : 8.60 ksi   WB Fascia : 5.67 ksi

The live-load-plus-impact moments calculated herein agreed with those used by PADOT. However the composite section modulus apparently used by PADOT was consistently about 10 percent less than that used in this investigation which assumed complete interaction. Larger α ratios therefore will result from the use of the lower live-load-plus-impact stresses shown in this chapter. The live-load-plus-impact moments and steel stresses calculated by PADOT for the two NB bridges on PA Route 33 agreed favorably with those shown in this chapter. As is the usual custom in designing multiple girder bridges, no live load intensity reduction was taken by PADOT or herein for the two NB bridges which have 3 design traffic lanes.

o During the field study response data was obtained from as many multiple truck events as possible in order to capture maximum response data. The resulting higher maximum stress ranges will lead to some higher than assumed α ratios.

o As shown on page 27, a significant number of trucks were substantially heavier than the AASHTO HS 20 (MS 18) design truck, which would account for some higher than assumed α ratios. If one of these very heavy trucks were one of several heavy trucks crossing the bridge at the same time, the

166

α ratio would again be higher than assumed.

b. Comparison of Field Study and FE Stresses

In figures 151 and 158 the field study girder stresses are usually higher than the stresses obtained from the finite element analysis of the complete superstructure. Although the relative differences are large the absolute differences are quite small since the girder stresses are very low. Stresses resulting from a FE analysis of the superstructure are expected to be a little lower than the measured stresses for the following reason.

The FE results were obtained using the SAP IV program (library of elements) which is based on the principle of minimum potential energy. Utilizing the stiffness method of analysis (displacement method) this numerical solution will underestimate the value of strain energy, U. The resulting displacement solution is therefore often referred to as a lower bound solution. Practically speaking, this means that the discrete finite elements used to model the superstructure are more stiff than the actual components. This in turn means that the deflections, and hence the stresses, are underestimated by the FE techniques employed in this comparative study.

c. Comparison of Field Study and AASHTO Stresses

Although no field study stresses are available for the assumed case shown in figure 159, based on the above discussion, actual stresses would likely be a little larger than the FE results shown in the figure, but somewhat less than the AASHTO design live-load-plus-impact stresses. Stress history studies have consistently shown that for most truck traffic measured stresses are below AASHTO stresses, considerably so for some bridges. Only a small portion of the truck traffic, that associated with very high GVW and with multiple truck events, will produce extreme values (as shown on page 27) which may equal or exceed the design stress.

167

SUMMARY AND CONCLUSIONS

Highway bridges sustain vehicular traffic which varies in weight, overall length, number of axles, axle spacing, speed, and dynamic characteristics. The volume and conditions of traffic such as headway and multiple presence, as well as the correlation of traffic with bridge type, geometry, configuration, and other factors, such as maintenance, determine the integrity and life expectancy of highway bridges and their components.

For any particular bridge the static and dynamic response to a vehicle can be accurately monitored and evaluated if the geometrical and loading characteristics of the vehicle are known. Until recently it has not been possible to determine, to a reasonable degree of accuracy, the characteristics of vehicles crossing a bridge under actual highway conditions. Consequently, expected damages, if any, by vehicular traffic could not be accurately estimated.

In recent years significant advances have been made in the development of weigh-in-motion (WIM) systems. A typical FHWA WIM system is portable and utilizes an existing bridge to serve as an equivalent weigh scale to obtain not only gross vehicle weights (GVW) but also axle weights and spacings, as well as speeds of vehicles as they cross the bridge at normal highway speeds. Since the weighing operation cannot easily be detected by truck drivers the results are not subject to the usual bias associated with traditional truck weighing methods. Both loadometer surveys and weight data from weigh stations are subject to bias because illegal trucks can easily avoid an operating weigh station with the aid of CB radios.

Current analysis and design of highway bridges in the U.S. is based on the AASHTO H (M) and HS (MS) truck and lane loads. These "standard" AASHTO live loads have remained basically unchanged for over 40 years. These live loads do not represent the majority of modern trucks using today's highway system. In the intervening years the weights of trucks and their frequency of occurence have increased significantly. With the development of the FHWA WIM

168

system it is now possible to obtain relatively unbiased statistical data on truck speed, configuration, loading and frequency of occurence, and to update that data.

Much more can be done, however, with the WIM system. By coupling the WIM system with a system for measuring strains in bridge components, data on bridge response can be achieved at the same time that loading data is being obtained from all the vehicles crossing the bridge within an arbitrary period of time. For an evaluation of bridge response the primary information required is the magnitude and variation of stress in bridge components during passage of vehicles over the bridge. The correlation of gross vehicle weight (GVW), axle weights and frequency with sress range, and induced maximum stress is the foundation of simple bridge design procedures and specifications based on strength and serviceability (such as fatigue) requirements.

This report presents the results of a 30 month research investigation conducted at Lehigh University, Bethlehem, PA, during which one of the FHWA WIM systems was redesigned and used to obtain simultaneous load and response data from 19,402 trucks crossing four in-service bridges. The redesigned system is designated the WIM+RESPONSE system throughout the report.

A prototype WIM+RESPONSE system was designed to obtain simultaneous data on truck weight and bridge response which can be used for a detailed evaluation of the structural performance of bridges. The information obtained from such an evaluation is needed for continuing improvements in bridge design procedures and specifications, for improved evaluations of inservice bridges (inventory and operating ratings), for a better understanding of bridge redundancy, and for continuing improvements of the bridge formula. Specific needs which can be addressed by the WIM+RESPONSE system include GVW distributions, stress range distributions, strain rates, maximum stresses, load distribution, and dynamic effects. It was not the intent of this study to exhaustively acquire and evaluate load and response data for the purpose of providing definitive solutions to all of these needs. Rather the objective is to determine what load and response information is needed for a detailed evaluation of

169

structural performance and to develop methods for using WIM technology to
obtain the required data. Of necessity the prototype WIM system was designed
to acquire response data from a limited number of points on a bridge super-
structure. Future improvements to the system will enable it to acquire data
from a larger number of points.

The WIM+RESPONSE system was used to obtain simultaneous truck weight plus
bridge response information from 19,402 trucks crossing six spans of four
inservice HS 20 (MS 18) bridges in Pennsylvania. Three bridges have steel
(rolled, riveted, or welded) multiple girder, simple spans and include
composite and noncomposite construction, both right and skew. The fourth has
composite, prestressed, multiple I-girder, simple spans with skew. Information
obtained from the four inservice bridges was evaluated with respect to GVW
distributions, stress range distributions, strain rates, and maximum stresses.

The GVW distributions obtained in this study closely resembles that from
the 1970 FHWA Nationwide Loadometer Survey and distributions obtained from
other WIM studies. The stress range distributions computed for the three
steel field study bridges are typical of those from other stress history
studies of bridges. All studies indicate that the peak values of maximum
stress range at a particular location usually exceed the peak values of maxi-
mum stress. This study indicates that the highest strain rates are not
associated with the highest stress range.

Analyses of the four inservice bridges were also performed. For the steel
bridges, girder live-load-plus-impact flexural stresses, computed by the AASHTO
specification procedures, are compared with stresses obtained from detailed
finite element analyses of each three-dimensional superstructure. For the pre-
stressed concrete bridge girder stresses are computed by the AASHTO specifica-
tion procedures. Analytically obtained stresses (AASHTO and finite element
methods) are compared with the stresses obtained from the field studies of the
four bridges.

One assumption used to develop the 1983 AASHTO stress cycle table for use in design against fatigue damage is that the actual stress range produced by vehicles similar to the design truck is a factor α times the design stress range. Previous stress history studies have indicated that this factor could be expected to be less than one. That is, the measured stress ranges would likely be less than the design stress range, due to such factors as differences in load distribution, impact, actual truck loadings, etc. The AASHTO stress cycle table assumes values of α of 0.8 for transverse members and 0.7 for longitudinal members. The average value of α obtained from this study for the longitudinal interior and fascia girders is 0.71 although actual values varied from 0.34 to 1.29.

Measured girder flexural stresses are comparable with stresses obtained from the finite element analyses. However, as expected, these flexural stresses are somewhat lower than those computed by the ASSHTO specification procedures.

This report is accompanied by six other reports which completely document the use of the WIM+RESPONSE system and the processing of the data obtained. These six reports are listed in references 25 through 30.

ALLENTOWN — BETHLEHEM — EASTON
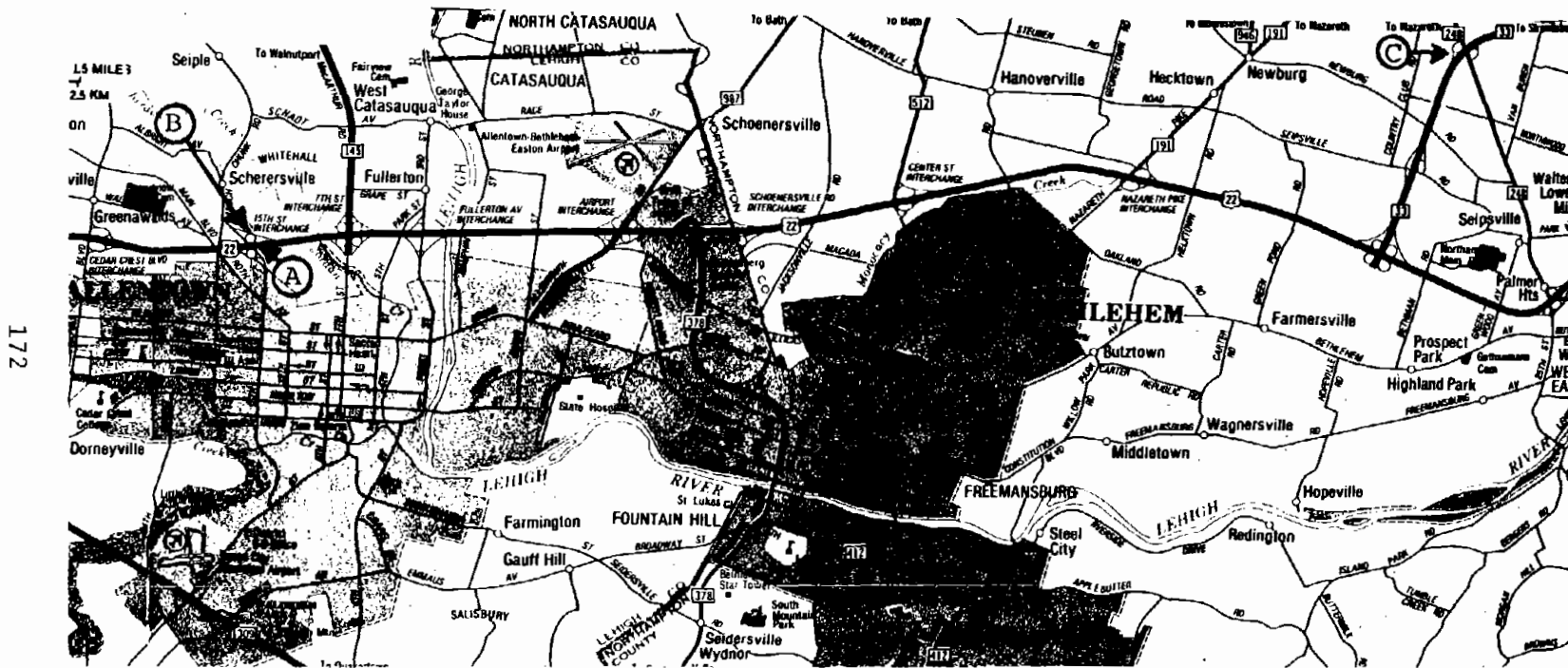
Figure 166. Locations of field study bridges in the Commonwealth of Pennsylvania.

REFERENCES

(1) J. W. Fisher, A. W. Pense, H. Hausammann, and G. R. Irwin, "Quinnipiac River Bridge Cracking", Journal of the Structural Division, Proceedings of ASCE, Vol. 106, ST4, April 1980.

(2) D. G. Bower, "Loading History--Span No. 10, Yellow Mill Pond Bridge, 195, Bridgeport, Connecticut", Highway Research Record 428, Transportation Research Board, 1973.

(3) J. W. Fisher and A. W. Pense, "Evaluation of Fracture of Lafayette Street Bridge", Proceedings of ASCE, Vol. 103, No. ST7, July 1977.

(4) J. W. Fisher, J. H. Daniels, B. T. Yen, et al, "An Evaluation of the Fracture of the I-79 Back Channel Girder and the Electroslag Welds in the I-79 Complex", Fritz Engineering Laboratory Report No. 425-1(80), Lehigh University, Bethlehem, Pennsylvania.

(5) J. W. Fisher, B. T. Yen, and J. H. Daniels, "Fatigue Damage in the Lehigh Canal Bridge From Displacement Induced Secondary Stresses", Transportation Research Record 607, TRB, 1977.

(6) J. W. Fisher, "Bridge Fatigue Guide--Design and Details", American Institute of Steel Construction, 1977.

(7) J. W. Fisher and B. T. Yen, "Design, Structural Details, and Discontinuities in Steel", Proceedings of ASCE Specialty Conference on the Safety and Reliability of Metal Structures, November 1972.

(8) J. W. Fisher and B. T. Yen, "Fatigue Strength of Steel Members With Welded Details", American Institute of Steel Construction, Engineering Journal, No. 4, November 14, 1977.

(9) J. W. Fisher, B. T. Yen, and K. H. Frank, "Minimizing Fatigue and Fracture in Steel Bridges", Journal of Engineering Materials and Technology, Transportation ASME, Vol. 102, January 1980.

(10) S. T. Rolfe and J. M. Barsom, "Fracture and Fatigue Control in Structures--Applications of Fracture Mechanics", Prentice-Hall, Englewood Cliffs, New Jersey, 1977.

(11) J. W. Fisher, J. R. Bellenoit, J. H. Daniels, and B. T. Yen, "High Cycle Fatigue Behavior of Steel Bridge Details--A Final Report", Fritz Engineering Laboratory Report No. 386-13(82), Lehigh University, Bethlehem, Pennsylvania, December 1982.

(12) J. W. Fisher, B. T. Yen, et al, "An Assessment of the Blue Route Bridge Electroslag Weldement", Fritz Engineering Laboratory Report No. 457.1, Lenigh University, Bethlehem, Pennsylvania, December 1981.

(13) J. W. Fisher, B. T. Yen, et al, "Fatigue and Fracture Resistance of Liberty Bridge Members", Fritz Engineering Laboratory Report No. 420.2, Lehigh University, Bethlehem, Pennsylvanie, May 1981.

(14) J. R. Bellenoit, B. T. Yen, J. W. Fisher, and R. Roberts, "A Fatigue and Fracture Investigation of Suspended Span Bridge Components", Fritz Engineering Laboratory Report No. 449.2, Lehigh University, Bethlehem, Pennsylvania, June 1982.

(15) J. W. Fisher, et al, "Detection and Repair of Fatigue Damage in Welded Highway Bridges", NCHRP Report 206, 1979.

(16) J. H. Daniels, "Use of Bartonsville Bridge to Weigh Trucks in Motion", Fritz Engineering Laboratory Report No. 415.1, Lehigh University, Bethlehem, Pennsylvania, April 1977.

(17) F. Moses and M. Kriss, "Weigh in Motion Instrumentation", Final Report to FHWA, Federal Highway Administration, Washington, DC, Report No. FHWA-RD-78-81, June 1978.

(18) F. Moses and M. Ghosn, "Weighing Trucks-in-Motion Using Instrumented Highway Bridges", Department of Civil Engineering Report, Case Western Reserve University, Cleveland, Ohio, December 1981.

(19) Richard E. Synder, E. Garland, Jr., and Fred Moses, "Loading Spectrum Experienced by Bridge Structures in the United States", Final Report to FHWA, Federal Highway Administration, Washington, DC, Report No. FHWA/RD-82/107, September 1982.

(20) Fred Moses and Michel Ghosn, "Instrumentation For Weighing Trucks-in-Motion For Highway Bridge Loads", Final Report to FHWA, Federal Highway Administration, Washington, DC, Report No. FHWA/RD-83/001, March 1983.

(21) American Association of State Highway and Transportation Officials, "Standard Specifications for Highway Bridges", AASHTO 13th Ed., 1983.

(22) L. Tall, et al, "Structural Steel Design", Ronald Press, New York City, Second Edition, 1974.

(23) American Association of State Highway and Transportation Officials, "Manual For Maintenance Inspection of Bridges", AASHTO, 1983.

(24) J. H. Daniels, et al, "Structural Evaluation of In-Service Bridges Using WIM Technology--Briefing Report for Oral Presentation No. 1", Prepared for the FHWA, Washington, DC, Fritz Engineering Laboratory Report No. 490.1, February 1985.

(25) J. H. Daniels, J. L. Wilson, L. Y. Lai, R. Abbaszadeh, and B. T. Yen, "WIM+RESPONSE System Overview", Documentation Report to FHWA, Federal Highway Administration, Washington, DC, Report No. FHWA/RD-86/046, March 1986.

174

(26) J. L. Wilson, J. H. Daniels, and R. Abbaszadeh, "WIM+RESPONSE Training Guide", Documentation Report to Federal Highway Administration, Washington, DC, Report No. FHWA/RD-86/047, March 1986.

(27) J. L. Wilson, R. Abbaszadeh, L. Y. Lai, and J. H. Daniels, "WIM+RESPONSE System User's Guide", Documentation Report to Federal Highway Administration, Washington, DC, Report No. FHWA/RD-86/048, March 1986.

(28) J. L. Wilson, J. H. Daniels, L. Y. Lai, and R. Abbaszadeh, "WIM+RESPONSE Hardware Reference Manual", Documentation Report to Federal Highway Administration, Washington, DC, Report No. FHWA/RD-86/049, March 1986.

(29) J. L. Wilson, L. Y. Lai, R. Abbaszadeh, and J. H. Daniels, "WIM+RESPONSE Software Reference Manual", Documentation Report to Federal Highway Administration, Washington, DC, Report No. FHWA/RD-86/050, March 1986.

(30) J. L. Wilson, J. H. Daniels, L. Y. Lai, R. Abbaszadeh, and B. T. Yen, "WIM+RESPONSE Appendices", Documentation Report to Federal Highway Administration, Washington, DC, Report No. FHWA/RD-86/051, March 1986.

(31) R. F. Varney and C. F. Galambos, "Field Dynamic Loading Studies of Highway Bridges in the U.S., 1948-1965", Highway Research Record No. 76, 1965, pp. 285-305.

(32) C. F. Galambos and W. L. Armstrong, "Loading History of Highway Bridges", Highway Research Record 295, Highway Research Board, Washington, DC, 1969.

(33) Charles F. Galambos, "Highway Bridge Loadings", Public Roads" A Journal of Highway Research and Development, U.S. Department of Transportation, FHWA, Vol. 43, No. 2, September 1979.

(34) Clyde E. Lee and Randy B. Machemehl, "Traffic Control and Geometrics For Weigh-in-Motion Enforcement Stations", Center for Transportation Research, Bureau of Engineering Research, The University of Texas at Austin; Paper Presented at the 60th Annual Meeting of the TRB, Washington, DC, January 1981.

(35) J. W. Fisher, "Fatigue and Fracture in Steel Bridges--Case Studies", John Wiley & Sons, 1984.

(36) S. Shore, J. L. Wilson, and G. Semsarzadeh, "Interactive Modeling System For Bridges", Journal of Computers and Graphics, Vol. 1, 1975, pp. 1-9.

(37) S. Shore, J. L. Wilson, and G. Semsarzadeh, "Interactive Techniques With Graphical Output For Bridge Analyses", International Journal of Computer Methods in Applied Mechanics and Engineering, Vol. 5, No. 3, March 1975, pp. 197-209.

175

(38) D. Motarjemi and D. A. VanHorn, "Theoretical Analysis of Load Distribution in Prestressed Concrete Box-Beam Bridges", Fritz Engineering Laboratory Report No. 315.9, Lehigh University, Bethlehem, Pennsylvania, October 1969.

(39) Task Committee on Redundancy of Flexural Systems, "State of the Art on Redundant Bridge Systems", ASCE-AASHTO Committee on Flexural Members of the Committee on Metals of the Structural Division, Journal of the Structural Division, Proceedings of the ASCE, Vol. 111, No. 12, December 1985.

(40) James S. Noel, Ray W. James, Howard L. Furr, and Francisco E. Bonilla, "Bridge Formula Development--A Final Report", Final Report to FHWA, Federal Highway Administration, Washington, DC, Report No. FHWA/RD-85-088, June 1985.

(41) S. B. Johnston and A. H. Mattock, "Lateral Distribution of Load in Composite Box Girder Bridges", Highway Research Record No. 167, 1967, pp. 25-33.

(42) A. H. Mattock, "Development of Design Criteria For Composite Box Girder Bridges", Development of Bridge Design and Construction Procedures, Cardiff, Wales, 1971, pp. 371-386.

(43) National Cooperative Highway Research Program, "Distribution of Wheel Loads on Highway Bridges--Final Report", NCHRP Project 20-5, Topic 14-22, February 1984.

(44) W. H. Walker, "Final Report of the Investigation of Impact on Highway Bridges", NTIS Report PB 189908, Engineering Experiment Station, University of Illinois, Urbana, Illinois, June 1969.

(45) J. W. Fothergill, H. D. Childers, and M. A. Johnson, "Feasibility of Utilizing Highway Bridges to Weigh Vehicles in Motion, Vol. I, Exotic Sensors on the Bridge Deck", Report to FHWA, May 1975.

(46) F. Moses and G. G. Goble, "Feasibility of Utilizing Highway Bridges to Weigh Vehicles in Motion, Vol. II, Strain Gauges on Main Longitudinal Girders", Report No. FHWA-RD-75-34, October 1974.

(47) H. J. Siegel, "Feasibility of Utilizing Highway Bridges to Weigh Vehicles in Motion, Vol. III, Strain Gauges at Bridge Bearings", Report No. FHWA-RD-75-35, November 1974.

(48) Bridge Weighing Systems, Inc., "Draft Software Users Manual For Bridge Weigh-in-Motion System", Prepared for the FHWA by Bridge Weighing Systems, Inc., 4423 Emery Industrial Parkway, Warrensville Heights, Ohio, 44128, November 1982.

(49) A. Ostapenko, D. H. DePaoli, J. H. Daniels, J. E. Obrien, B. T. Yen, M. E. Bhotti, and J. W. Sifher, "A Study of the President Costa e Silva Bridge During Construction and Service (Steel Structure)", Submitted to Empresa de Engenhoria e Construcao de Obras Especiois (ECEX), Rio de Janerio, Brazil, Fritz Engineering Laboratory Report No. 397.6, March 1976.

(50) Minutes of Meeting with Mr. Harold Bosch, on USDOT/FHWA Contract-DTFH 61-83-C-00091, "Structural Evaluation of Inservice Bridges Using WIM Technology", Meeting held at Turner-Fairbank Highway Research Center, McLean, Virginia, November 8, 1984.

(51) Letter from Karen R. Smith, Contract Administrator, Research and Equipment Administration Branch, Offices of Contracts and Procurement, USDOT/ FHWA, to Mr. J. M. Cheezum, Jr., Research Administrator, Lehigh University, February 12, 1985.

(52) Letter to Mr. Harold Bosch, Research Structural Engineer, Contracting Officer's Structural Representative (COTR), FHWA from Dr. J. H. Daniels, confirming Completion of Work Plan and Task D--Conduct Field Studies.

(53) Commonwealth of Pennsylvania, Department of Transportation, "Standards For Bridge Design" (Prestressed Concrete Structures), Bureau of Design, BD-201, March 1973.

(54) N. E. Dowling, "Fatigue Failure Predictions For Complicated Stress-Strain Histories", Journal of Materials, JMLSA, Vol. 7, No. 1, March 1972, pp. 71-87, (published quarterly by ASTM).

(55) J. W. Fisher, D. R. Mertz, and A. Zhong, "Steel Bridge Members Under Variable Amplitude, Long Life Fatigue Loading--Final Report", Fritz Engineering Laboratory Report No. 463-1(83), Lehigh University, Bethlehem, Pennsylvania, September 1983.

(56) J. W. Fisher and A. W. Pense, "Analysis of Cracking of I79 Bridge at Neville Island", Proceedings, Fracture Problems in the Transportation Industry Fall Convention, Detroit, Michigan, October 1985.

(57) C. F. Galambos and C. P. Heins, "Loading History of Highway Bridges: Comparison of Stress-Range Histograms", Highway Research Board, Highway Research Record No. 354, 1971.

(58) C. G. Schilling, "Stress Cycles For Fatigue Design of Steel Bridges", Journal of Structural Engineering, ASCE, Vol. 110, No. 6, June 1984.

(59) R. L. Khosa and C. P. Heins, "Study of Truck Weights and the Corresponding Induced Bridge Girder Stresses", Prepared for Maryland State Road Commission and U.S. Bureau of Public Roads, University of Maryland at College Park, Maryland, Progress Report No. 40, February 1971.

(60) Richard W. Hertzberg, "Deformation and Fracture Mechanics of Engineering
      Materials", John Wiley and Sons, 2nd Ed., 1983.

(61) K. J. Bathe, E. L. Wilson, and E. E. Peterson, "SAP IV--A Structural
      Analysis Program for Static and Dynamic Response of Linear Systems",
      Earthquake Engineering Research Center Report No. EERC 73-11, University
      of California, Berkeley, California, June 1973 (revised April 1974).